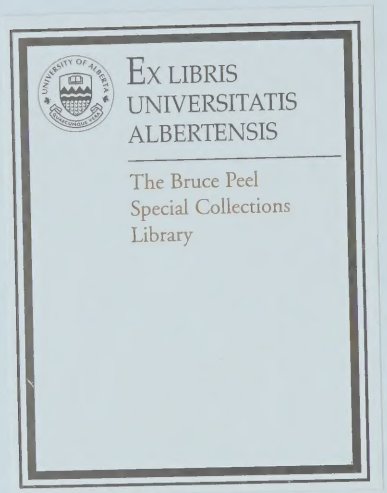
EX LIBRIS
UNIVERSITATIS
ALBERTENSIS
The Bruce Peel
Special Collections
Library

JUN 1 5 2005

Digitized by the Internet Archive
in 2026 with funding from
University of Alberta Library

https://archive.org/details/0162020418545

University of Alberta

Library Release Form

Name of Author: *Melissa Lai Tee Teoh*

Title of Thesis: *Characterization and Functional Analysis of Leporipoxvirus Copper-Zinc Superoxide Dismutase Homologs*

Degree: *Doctor of Philosophy*

Year this Degree Granted: *2005*

Permission is hereby granted to the University of Alberta Library to reproduce single copies of this thesis and to lend or sell such copies for private, scholarly or scientific research purposes only.

The author reserves all other publication and other rights in association with the copyright in the thesis, and except as herein before provided, neither the thesis nor any substantial portion thereof may be printed or otherwise reproduced in any material form whatsoever without the author's prior written permission.

Characterization and Functional Analysis of Leporipoxvirus Copper-Zinc Superoxide Dismutase Homologs

By

Melissa Lai Tee Teoh

A thesis submitted to the Faculty of Graduate Studies and Research in partial fulfillment of the requirement for the degree of

Doctor of Philosophy

In

Virology

Department of Medical Microbiology and Immunology

University of Alberta

Edmonton, Alberta

Canada

Spring, 2005

Characterization and Functional Analysis of *Leptospira* Copper-Zinc Superoxide Dismutase Homologs

by

Melissa Lee Tseng

A thesis submitted to the Faculty of Graduate Studies and Research in partial fulfillment of the requirements for the degree of

Doctor of Philosophy

in

Virology

Department of Medical Microbiology and Immunology

University of Alberta

Edmonton, Alberta

Canada

Spring 2005

University of Alberta

Faculty of Graduate Studies and Research

The undersigned certify that they have read, and recommend to the Faculty of Graduate Studies and Research for acceptance, a thesis entitled **Characterization and Functional Analysis of Leporipoxvirus Copper-Zinc Superoxide Dismutase Homologs** submitted by **Melissa Lai Tee Teoh** in partial fulfillment of the requirements for the degree of **Doctor of Philosophy** in **Virology**.

DEDICATION

To my dearest parents, Peng Tiong Teoh and Siew Ying Wong.

ABSTRACT

Paradoxically, the "vital air" required for sustenance of aerobic life possesses a toxic threat. Normal cellular metabolism accidentally produces reactive oxygen species (ROS-superoxides, hydrogen peroxides, and hydroxyl radicals), leading to oxidative damage to DNAs, lipids, and proteins. The deleterious potential of these ROS can be counterbalanced by antioxidant enzymes such as superoxide dismutase (SOD). This regulation of redox balance in cell is very important since ROS produced in a regulated fashion, on the other hand, are required participants in signalling pathways, influencing central cellular functions such as proliferation, apoptosis, and necrosis.

Interestingly, tumourigenic Leporipoxviruses, Shope fibroma virus and myxoma virus encode homologs of copper and zinc containing SODs (SOD1). We have shown that the Leporipoxviral SOD1 homologs (M/S131R) are abundantly expressed late gene products which are catalytically inactive but downregulate the dismutase activity of the cellular SOD1. One probable route by which the Leporipoxvirus proteins cause this inhibition is by targeting cellular proteins, its counterpart, cellular SOD1 as well as the copper chaperone for SOD1, CCS. By forming complexes with these proteins, hence inactivate them, M/S131R promote a mild intracellular oxidative stress which enhances the tumourigenic phenotype in an animal model. Besides inducing cellular proliferation, M/S131R also protect cells from undergoing apoptosis.

We have shown, through this project that Leporipoxviruses have acquired a defence to disarm host anti-viral immune system by deploying their SOD1 mimics to modulate the redox status of infected cells, thereby altering cell signalling events in favour of virus survival and pathogenesis.

AKNOWLEDGEMENTS

I would like to sincerely thank my supervisor, Dr. David H. Evans, who has been a superior mentor throughout my study. My work was a result of his excellent guidance and advice. He has provided a great training environment for his students and I am truly blessed to have been one of his trainees. I would also like to thank past and present members of the Evans' lab: Mijin, Melissa W, Alicia, Li, Kathleen, Wendy, Michael, Janna, Don, especially Xiaodan, Jim, and Paula for their friendship and support. My thanks also to Dr. Mary Hitt and her group for all those fun times.

I would like to express my deepest gratitude to my family in Malaysia for their continuing love and support. In particular, my dad, mom, grandpa, grandma, sisters and brothers. I have to acknowledge my grandpa, who sadly passed away before the completion of my programme, for encouraging and inspiring me to pursue a Ph.D. study. I owe a great deal to my cat, Pepper, for always being there for me. Lastly, I would like to thank Austin for his love and encouragement especially during the first year of my study.

This study was supported by operating and equipment funding from Natural Sciences and Engineering Research Council of Canada, Canadian Institutes of Health Research, and Alberta Heritage Foundation for Medical Research for Dr. David H. Evans. My study was partially supported by Alberta Heritage Foundation for Medical Research Studentship.

TABLE OF CONTENTS

DEDICATION

ABSTRACT

ACKNOWLEDGEMENTS

TABLE OF CONTENTS

LIST OF TABLES

LIST OF FIGURES

LIST OF ABBREVATIONS

CHAPTER 1 – GENERAL INTRODUCTION

1.1 Properties of poxviruses **1**

1.1.1. Classification **1**

1.1.2. Poxvirus genome **3**

1.1.3. Poxvirus life cycle **5**

1.1.4. Virion morphology **8**

1.2 Leporipoxviruses **9**

1.2.1. Myxoma virus **9**

1.2.2. Shope fibroma virus **10**

1.3 Poxvirus interaction with the host **10**

1.3.1. Myxoma virus immuno-modulatory genes **11**

1.4 Free radical biology **14**

1.5 The toxicity of superoxide radical and its reactive progenies 16

1.6 Superoxide dismutases 20

1.6.1. Properties of SOD1 21

1.7 Copper chaperone for SOD1 23

1.8 Activation of SOD1 by CCS 25

1.9 Leporipoxviral SOD1 homologs 30

1.10 Biological significance of SOD1 33

1.11 Oxidative stress and related pathologies 34

1.12 Regulatory functions of superoxide 35

1.12.1. Anti-microbial agent 35

1.12.2. Stimulation of cellular proliferation 36

1.12.2.1. Growth factor signalling pathway 36

1.12.2.2. ROS and cell proliferation 40

1.12.2.3. ROS and tumor growth 41

1.12.2.4. Mechanisms of ROS-mediated cell signalling 42

1.12.3. Regulation of apoptosis 45

1.12.3.1. Apoptosis pathways 45

1.12.3.2. ROS in induction of apoptosis 48

1.12.3.3. ROS in prevention of apoptosis 49

1.13 Redox balance and cell signalling 51

1.14 Leporipoxviruses and cellular proliferation 54

1.15 Hypothesis and experimental rational 55

1.16 References 57

CHAPTER 2 – LEPORIPOXVIRUS M/S131R INHIBIT CELLULAR SOD1 BUT ARE NOT ESSENTIAL FOR VIRUS REPLICATION OR VIRULENCE 69

2.1 Introduction 71

2.2 Methods and materials 74

2.3 Results 80

2.4 Discussion 99

2.5 References 104

CHAPTER 3 – LEPORIPOXVIRUS SOD1 HOMOLOGS ARE CATALYTICALLY INERT DECOY PROTEINS THAT BIND COPPER CHAPERONE FOR SOD1 (CCS) 107

3.1 Introduction 109

3.2 Methods and materials 112

3.3 Results 118

3.4 Discussion 141

3.5 References 146

CHAPTER 4 – TUMORIGENIC LEPORIPOXVIRUSES UPREGULATE INTRACELLULAR SUPEROXIDE TO INHIBIT APOPTOSIS AND PROMOTE CELL PROLIFERATION 148

4.1 Introduction 150

4.2 Materials and methods 153

4.3 Results 161

4.4 Discussion 187

4.5 References 192

CHAPTER 5 – DICUSSION AND FUTURE DIRECTIONS 196

5.1 Discussion 196

5.2 Future directions 210

5.3 References 213

APPENDIX A- SUPPORTING METHODS AND DATA

A.1 SFV S131R is regulated as a late gene product 217

A.2 Leporipoxviral M/S131R are virion structural components 219

A.3 S131R interacts with cellular SOD1 221

A.4 References 224

LIST OF TABLES

Table 1.1. *Poxviridae* Family Taxonomy.....2

Table 1.2. Immuno-modulatory genes of myxoma virus and SFV 12

Table 2.1. Pathogenicity of M131R-deficient viruses in European rabbits 98

Table 3.1. Mutant forms of S131R proteins generated by sequential rounds of site directed mutagenesis 123

Table 4.1. Sequences of the oligonucleotides used in the study 155

LIST OF FIGURES

Figure 1.1. Genome organization of poxviruses showing terminal inverted repeats (TIR).....4

Figure 1.2. Schematic representation of the poxviral replication cycle.....7

Figure 1.3. Structural morphology of a poxvirus virion.....8

Figure 1.4. Primary antioxidant defence mechanisms against reactive oxygen species 19

Figure 1.5. Structural features of SOD1.....22

Figure 1.6. Ribbon diagrams showing human CCS interacting with a copper-free human SOD1 subunit 25

Figure 1.7. Proposed models for activation of SOD1 though an interaction with copper CCS.....26

Figure 1.8. Formation of an intermolecular disulfide bond between the SOD1 S-S subloop and yCCS domain III.....29

Figure 1.9. Amino acid sequence alignment of SOD1 homologs encoded by Leporipoxviruses and Orthopoxviruses in comparison to rabbit and bovine SOD1s.....30

Figure 1.10. The major signalling pathways activated by the epidermal growth factor receptor (EGFR), leading to cell proliferation, apoptosis, and/or survival.....39

Figure 1.11. Extrinsic (receptor-mediated) and intrinsic (mitochondrial-mediated) apoptosis pathways.....47

Figure 1.12. A general schematic showing the regulation of cell death and signal transduction pathways in response to reactive oxygen species 53

Figure 2.1. Multiple sequence alignment illustrating viral and cellular SOD1 homologs 81

Figure 2.2. Insertional inactivation of myxoma virus M131R.....83

Figure 2.3. Effect of an M131R deletion mutation on virus growth.....84

Figure 2.4. Kinetics of M131R protein expression determined by ^{35}S-labeling and western blot analysis 86

Figure 2.5. Recombinant sfvSOD does not catalyze superoxide dismutase reactions ...89

Figure 2.6. SfvSOD can form disulfide-crosslinked dimers 92

Figure 2.7. Cellular SOD1 activity declines during SFV infection 94

Figure 2.8. Changes in cellular SOD1 activity monitored by hydroxydopamine assays 96

Figure 3.1. Multiple sequence alignment of cellular and viral SOD1 homologs 121

Figure 3.2. SDS-PAGE analysis of recombinant forms of SFV SOD protein 124

Figure 3.3. Superoxide dismutase activity of wild-type and mutant forms of S131R protein 126

Figure 3.4. Metal content of wild-type and mutant forms of SFV SOD 129

Figure 3.5. *In vitro* interactions between SFV SOD and human CCS 131

Figure 3.6. Co-immunoprecipitation of SFV SOD1 and cellular CCS 133

Figure 3.7. Co-immunoprecipitation of MYX SOD1 and cellular CCS in myxoma-infected cells 135

Figure 3.8. Stability of cellular SOD1 in virus-infected cells 136

Figure 3.9. Intracellular localization of myxoma virus SOD1 138

Figure 3.10. Density gradient fractionation of mitochondria from virus-infected cells 140

Figure 4.1. Construction and characterization of recombinant SFV strains 162

Figure 4.2. Single-step growth properties of an S131R-deficient SFV strain 164

Figure 4.3. The S131R gene promotes an increase in the level of intracellular superoxide radical in SFV-infected cells 167

Figure 4.4. Detection of intracellular superoxide using an aconitase inhibition assay 169

Figure 4.5. Deleting the S131R gene attenuates SFV-induced disease in rabbits 174

Figure 4.6. Histologic analysis of tumours induced by wild type, VMLT1.6, and R-S131R viruses 178

Figure 4.7. The MYX M131R gene product protects infected cells from Fas- and staurosporine-induced apoptosis 181

Figure 4.8. FACS detection of apoptosis in MYX-infected cells 183

Figure 4.9. Distribution of EGFP-tagged M131R protein in virus-infected cells 186

Figure 5.1. Postulated impact of varying net cellular redox status on progressive behavior from proliferation to apoptosis to necrosis 204

Figure 5.2. A proposed model by which Leporipoxviral M/S131R could promote cell proliferation and survival 206

Figure A.1. Northern blot analysis of S131R transcription 218

Figure A.2. M131R is packaged into myxoma virion particles 220

Figure A.3. GST-S131R forms complex with cellular SOD1 223

LIST OF ABBREVATIONS

AIF	Apoptosis Inducing Factor
Ang II	Angiotensin II
Bcl-2	B-cell lymphoma/leukemia-2
BGMK	Baby Green Monkey Kidney
Bid	Bcl-2 Interacting Domain
bSOD1	Bovine SOD1
CAT	Catalase
cCCS	Cellular CCS
CCS	Copper Chaperone for SOD1
CEV	Cellular Associated Enveloped Virus
cSOD1	Cellular SOD1
EEV	Extracellular Enveloped Virus
EGFP	Enhanced Green Fluorescent Protein
EGFR	Extracellular GFR
ERK	Extracellular signal-Regulated Protein Kinase
FALS	Familial form of Amyotrophic Lateral Sclerosis
FeSOD	Iron containing SOD
GFR	Growth Factor Receptor
gpt	Guanine Phophoribosyl Transferase
GSH	Glutathione
GSH-Px	Glutathione Peroxidase
GSSG	Reduced-Glutathione
GSSG-Rx	GSSG Reductase

GST	Glutathione-S-Transferase
hCCS	Human CCS
HE	Hydroethidine
4-HNE	4-hydroxynonenal
H_2O_2	Hydrogen Peroxide
IAP	Inhibitor of Apoptosis
IFN	Interferon
IκB	Inhibitor of NFκB
IKK	I kappa kinase
IMV	Intracellular Mature Virus
JNK	c-Jun N-terminal Kinase
MAPK	Mitogen Activated Protein Kinase
MFV	Malignant Fibroma Virus
MGF	Myxoma Virus Growth Factor
MPT	Mitochondria Permeability Transition
MYX	Myxoma Virus
NFκB	Nuclear Factor kappa B
NiSOD	Nickel containing SOD
NO	Nitric Oxide
O_2^{*-}	Superoxide Radical
$^{*}OH$	Hydroxyl Radical
$ONOO^-$	Peroxynitrite
ORF	Open Reading Frame
PI3-K	Phosphatidylinositol 3-Kinase

RNS	Reactive Nitrogen Species
ROS	Reactive Oxygen Species
RTK	Receptor Tyrosine Kinase
SAPK	Stress-Activated Protein Kinases
SFV	Shope Fibroma Virus
SFGF	Shope Fibroma Virus Epidermal Growth Factor
SIRC	Spontaneously Immortalized Rabbit Corneal Fibroblast
SOD	Superoxide Dismutase
SOD1	Copper and Zinc containing SOD or Cu-Zn SOD
SOD2	Manganese containing SOD or MnSOD
SOD3	Extracellular Copper and Zinc containing SOD or EcSOD
TF	Transcription Factor
TGFα	Transforming Growth Factor Alpha
TIR	Terminal Inverted Repeat
TNF	Tumor Necrosis Factor
TUNEL	Terminal Transferase-mediated dUTP-fluorescein Nick End Labeling
VGF	Vaccinia Virus Growth Factor
VV	Vaccinia Virus

CHAPTER 1 – GENERAL INTRODUCTION

1.1. Properties of Poxviruses

Poxviruses are among the largest and the most complex mammalian viruses. Unlike most other DNA viruses, they replicate in the cytoplasm and encode many proteins that permit transcription and replication to occur outside of the nucleus. More than 150 virion proteins have been found in poxviruses but the functions of these various proteins are mostly unknown. These viruses are of special interest due to the impact of smallpox on human history. Smallpox, caused by variola virus is once a common and devastating infectious disease since its emergence some 5,000 years ago [55]. Although smallpox was eradicated in 1977 after a widely applied vaccination program [55], poxviruses still draw huge attention, due to recent concerns of them being used as a potential biological weapon. In addition, vaccinia virus possesses useful characteristics as a powerful recombinant expression vector [121], which can also be applied in the development of therapeutic vaccines against various diseases [181]. Furthermore, since several chordopoxviruses encode a wide array of genes to counteract the host defence responses, studying the intricate relationship between poxviruses and their host provide a powerful tool in understanding detail mechanisms of both the innate and adaptive cellular immune response [156].

1.1.1 Classification

The Poxviridae comprise a diverse group of viral species that infect a wide range of hosts. The virus family is classified principally by the host range, *Entomopoxviririnae*

Table 1.1 *Poxviridae* Family Taxonomy

Subfamilies	Genera	Members
Chordopoxvirinae (Vertebrate poxviruses)	*Orthopoxvirus*	Buffalopox, camelpox, cowpox, ectromelia, monkeypox, rabbitpox, racoonpox, skunkpox, terapox, vaccinia, variola, volepox
	Parapoxvirus	Deerpox, orf virus, pseudocowpox
	Avipoxvirus	Canarypox, fowlpox, juncopox, mynahpox, pigeonpox, psittacinepox, quailpox, sparrowpox, starlingpox, turkeypox
	Capripoxvirus	goatpox, lumpyskin disease, sheeppox
	Leporipoxvirus	Hare fibroma virus, myxoma, Shope fibroma (rabbit fibroma), Squirrel fibroma
	Suipoxvirus	Swinepox
	Mulluscipoxvirus	Molluscum contagiosum
	Yatapoxvirus	Tanapox, Yaba monkey tumour
Entomopoxvirinae	A	*Melanotha mlolontha*
(Insect poxviruses)	B	*Amsacta moorei*
	C	*Chironimus luridus*

Adapted from Moss, 1996 [122]

(poxvirus of the insects) and *Chordopoxvirinae* (poxvirus of the vertebrates) [122]. They are further classified into genera, as shown on Table 1.1, by comparing cross-protection in animal studies, crossing neutralization of infectivity in tissue culture, and cross hybridization of genomic DNA from virions. In general, members of the same genus have similar morphology, biological properties, and host range [122]. The *Chordopoxvirinae* consist of eight genera: *Orthopoxvirus, Parapoxvirus, Avipoxvirus, Capripoxvirus, Leporipoxvirus, Suipoxvirus, Molluscipoxvirus,* and *Yatapoxvirus.* Two examples of the vertebrate poxviruses that are relevant to human health are: variola virus, the causative agent of smallpox; and molluscum contagiosum virus, which produces skin lesions in children and immuno-compromised patients. The most comprehensively studied member is vaccinia virus which belongs to the *Orthopoxvirus* [55]. As the name implies, vaccinia virus was the vaccination agent that conferred immunity against smallpox infection. The eradication of smallpox marks the first successful human combat against a deadly infectious agent [55].

1.1.2 Poxvirus Genome

The poxvirus virion contains a noninfectious, linear, A + T rich, double stranded DNA genome that can vary from 135 kb in Yaba monkey tumour virus to 365 kb in canarypox virus, and encode between 136 and 328 open reading frames (ORF) respectively [122, 155, 184]. The virus genome contains covalently closed hairpin loops at both ends and the extreme left and right termini consist of identical but oppositely oriented terminal inverted repeats (TIR) (Figure 1.1). TIRs range in length from 58 bp in variola virus [161] to 12.4 kb in Shope fibroma virus [196]. The viral genes are separated

into early, intermediate, and late genes. Gene expression is stringently regulated by a cascade mechanism, where the products of earlier genes regulate the expression of the later genes. The genome organization and direction of transcription are very similar among *Chordopoxviruses*. The central region of approximately 100 kbp comprises of the so-called "house-keeping" genes with essential transcription and replication regulatory genes and structural genes, whereas the flanking ends of the genome are enriched with genes that function to promote virus survival in infected host, including proteins that determine host range, inhibit apoptosis, or subvert the host immune system [66, 111, 131]. The central core region is highly conserved among poxviruses while the flanking regions are more specific to virus species.

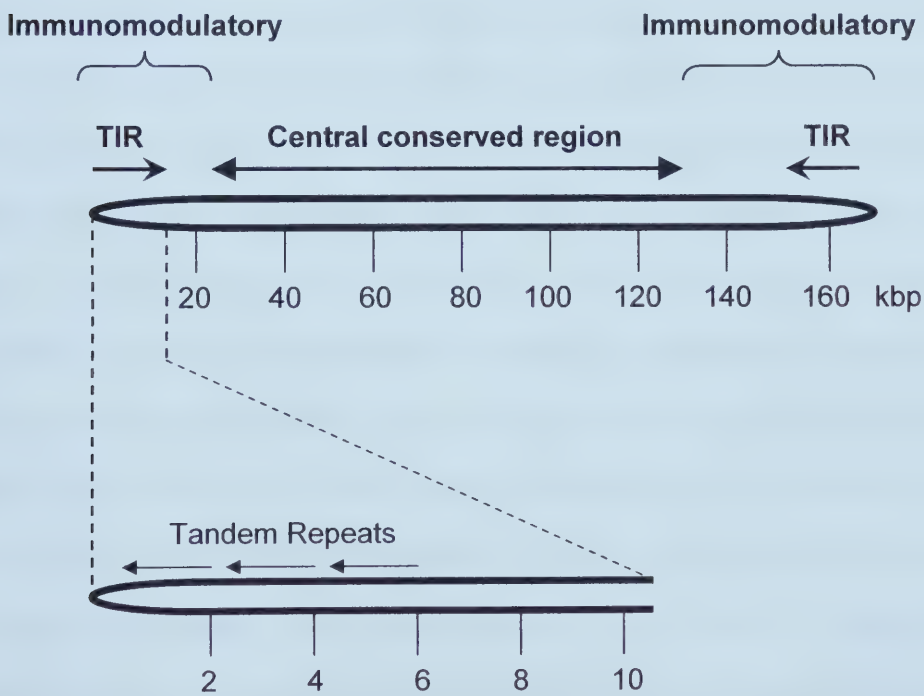

Figure 1.1. Genome organization of poxviruses showing terminal inverted repeats (TIR).

1.1.3 Poxvirus Life Cycle

Poxviruses exist in multiple infectious forms due to their complicated life cycles (Figure 1.2). Virus entry into a cell involves intracellular mature virion (IMV) fusion with plasma membrane following attachment. Due to the fact that poxviruses infect a wide host range and no receptor has been identified for any poxviruses, it is suggested that many receptors are involved or the receptor must be ubiquitous [123]. Infectious virus particles carry with them a large number of virus-encoded enzymes and factors to prime-start their gene expression such as RNA polymerase and early transcription factors [122]. Immediately after fusion and entry, the virus core is released into the cytoplasmic region where early mRNA is synthesized. The early mRNAs are translated into a variety of proteins, including immuno-modulatory proteins, enzymes required for DNA replication and intermediate transcription factors. Uncoating is then taken place to allow for viral DNA replication. There is no evidence suggesting a discrete origin of poxvirus DNA replication and that progeny DNA appear to be synthesized through the generation and resolution of large concatemeric molecules [122]. Recombination occurs at high levels in poxvirus-infected cells, tightly linked to DNA replication due to the activity of viral DNA polymerase. Recombination has apparently occurred naturally between two Leporipoxviruses, Shope fibroma virus and myxoma virus, giving rise to malignant fibroma virus (MFV) [175]. The sites of virus replication are often referred to as the "viral factories". Intermediate genes are then transcribed and translated to serve as late gene transcription factors. The late mRNAs are then translated to produce virion structural proteins, enzymes, and early transcription factors, which comprised the mature virion. During assembly, immature virion acquires two layers of membranes from

cellular compartments to form infectious intracellular mature virion (IMV). The IMV is further wrapped by additional membranes derived from the trans-Golgi or endosomal network to become intracellular enveloped virion (IEV). IEV is then transported to the periphery of the cell where it fuses with plasma membrane to form cell-associated enveloped virion (CEV). CEV can mediate cell to cell spread by inducing actin-tail formation. In the case where the virion is externalized, it is designated extracellular enveloped virion (EEV), which provides longer range of virus dissemination.

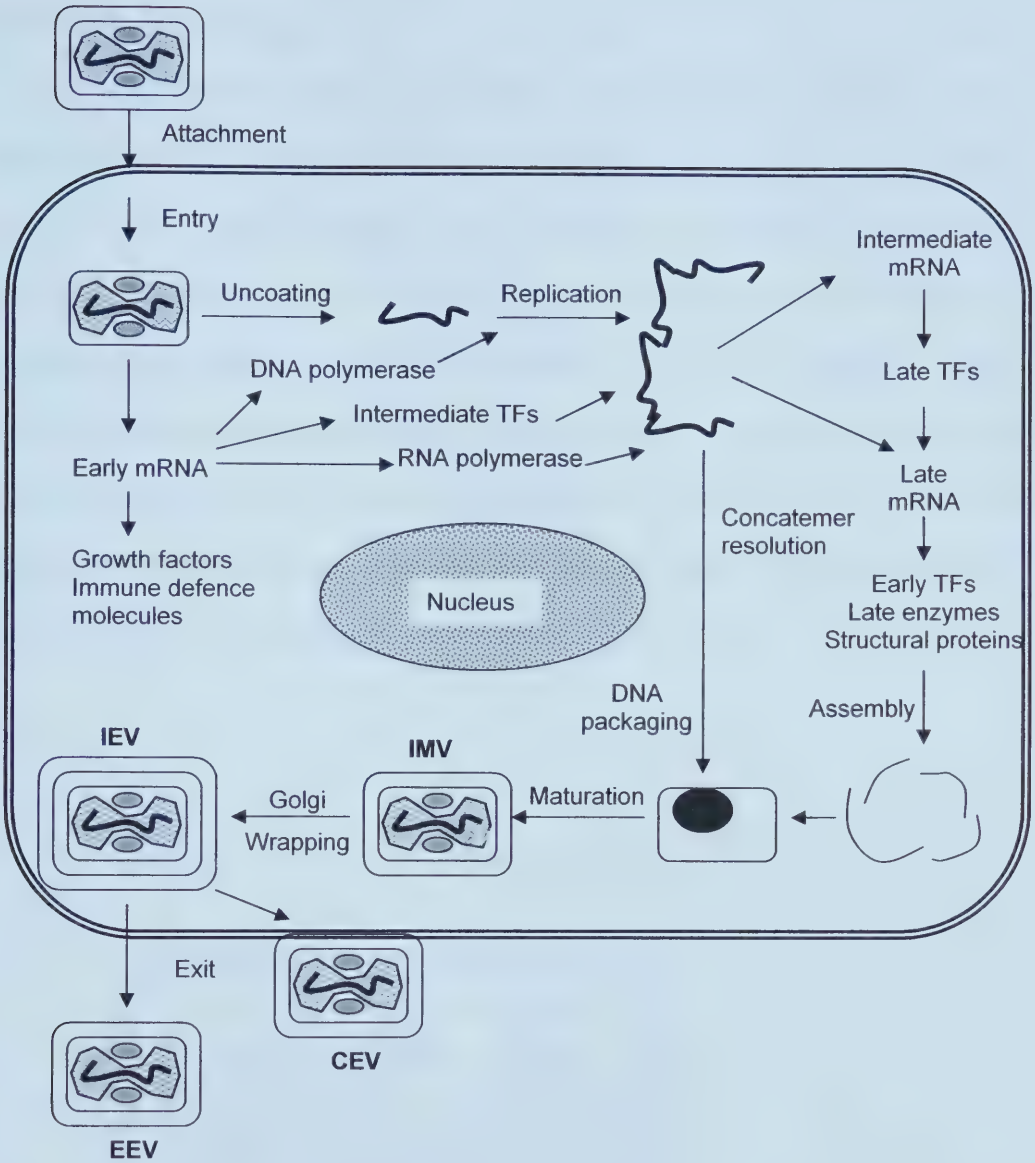

Figure 1.2. Schematic representation of the poxviral replication cycle. Modified from Moss [122].

1.1.4 Virion morphology

Poxvirus virions visualized using electron microscopy appear to be oval or brick shaped structures of approximately 200nm to 350nm in length [122]. There are more than 100 virus proteins arranged in four distinct structures: core, lateral body, membrane, and envelope, as revealed by electron microscopy of thin sections and negatively stained preparations of purified virions [51]. The lateral bodies are readily seen in traditional electron microscopy images but could very well be an artifact of specimen preparation [49]. There are two forms of enveloped viruses: the intact M (mulberry) form appears bumpy or beaded, whereas the C (capsule) form is smooth [20]. Treatment with non-ionic detergent can convert M to C forms [50].

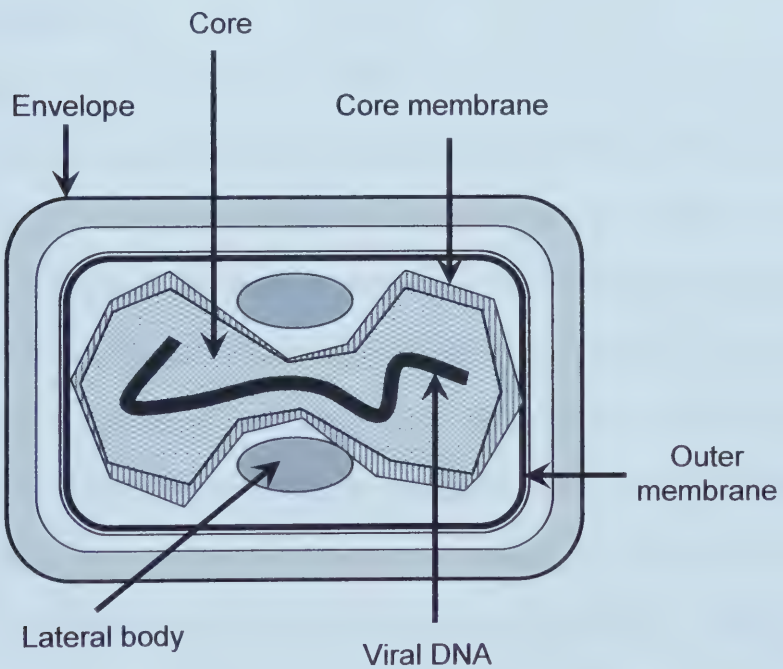

Figure 1.3. Structural morphology of a poxvirus virion.

As illustrated on Figure 1.3, the virus nucleosome is housed in a membraneous core region. A second layer of membrane encases the core along with two lateral bodies. This is the structure of the infectious form of IMV particle. In the case of EEV, there is an outer envelope wrapping the IMV.

1.2 Leporipoxviruses

Leporipoxviruses contains four species: myxoma virus, Shope fibroma virus, hare fibroma virus, and squirrel fibroma virus, whose host ranges include rabbits, hares and squirrels [47]. Virus transmission from host to host is thought to be mediated through arthropod vectors.

1.2.1 Myxoma Virus

Myxoma virus genome is about 160 kb in size, with approximately 170 ORFs [28]. Myxoma virus causes a localized benign cutaneous fibroma in its natural hosts, the North American brush rabbits (*Sylvilagus californicus*) and the South American tapeti (*Sylvilagus brasiliensis*). However, it can cause a rapid systemic and lethal infection, myxomatosis (hence it's named) in European rabbits (*Oryctalagus cuniculus*) [122]. In European rabbits, myxoma virus can inhibit an apoptotic response in rabbit T lymphocytes and spread through the lymphatic system [147]. Thus, the virus induced tumours disseminate rapidly and the infected animals die within a few weeks of inoculation. It is unclear why myxoma virus infection causes such striking differences seen in *Sylvilagus sp.* and in *O. cuniculus*. The genotype of the host probably defines the severity of the effects of viral immuno-modulatory proteins. Due to the severe mortality

rates of myxomatosis, which is up to virtually 100%, myxoma virus was deliberately introduced to Australia and Europe during the 1950s in an effort to control the population of European rabbits in these continents [55]. During the first year of introduction, about 99% of rabbits died but later, attenuated strains emerged, giving rise to resistant rabbit progeny [7, 148]. Since myxomatosis is an extensively characterized veterinary disease, it provides a well-defined model for the study of virus-encoded virulence factors.

1.2.2 Shope Fibroma Virus

Shope fibroma virus is closely related to myxoma virus based on the immunological studies [166] and subsequent DNA sequence analyses [28, 196]. The SFV genome spans approximately 160 kbp and encodes 165 putative genes [196]. In its natural host, the eastern cottontail rabbit (*Sylvilagus floridanus*), SFV induces fibroxantosarcoma-like tumours. Healthy adult rabbits will mount an effective cell-mediated immune response to clear the infection [154, 157], but SFV can sometimes cause a lethal infection in newborn rabbits and immuno-compromised adults. Unlike myxoma virus infection, SFV-induced disease in European rabbits closely resembles the disease in cottontail rabbits. While myxoma virus is of veterinary importance due to the serious risk possess to farm European rabbits, SFV has been used to immunize rabbits (both farmed and pet rabbits) against myxomatosis.

1.3 Poxvirus interactions with the host

When viruses interact with an animal host, a variety of specific and nonspecific components are involved in the defence against the virus. In the response to viral

infection, most cells will secrete the anti-viral cytokines interferon (IFN-α/β). These IFNs will in turn activate multiple intracellular pathways that limit the viral replication and spread. Despite these features, poxviruses are relatively successful animal pathogens, perhaps due in part to a growing list of virus-encoded proteins that have been shown to subvert the host defence mechanisms.

Poxviruses encode a considerable amount of genes which appear to be nonessential for replication in tissue culture cells, but are thought to be important during in vivo infections of the natural hosts. Although the biological functions are not clearly defined, these proteins have been shown to be important players in immunomodulatory mechanisms of poxviruses and the loss of these molecules influences the pathogenicity in vivo [156]. Examples include cytokine receptor homologs, complement regulators, and apoptosis inhibitors. However, no single common immuno-modulatory gene can be found in all poxvirus genomes, reflecting the differences in host and tissue tropism, hence the diverse clinical manifestations of poxvirus diseases.

1.3.1 Leporipoxviruses immuno-modulatory genes

The ability of myxoma virus to induce myxomatosis, which is characterized by skin lesions, systemic immunosupression, and a high mortality rate in European rabbits, provides an ideal poxvirus-host system to study the effect of virus-encoded immuno-modulatory proteins. Hence, the immuno-modulatory mechanisms of poxviruses have been elucidated chiefly from the studies of gene knockout variants of myxoma virus in common laboratory rabbits.

Table 1.2. Immuno-modulatory genes of myxoma virus and SFV

	Myxoma virus	SFV
Chemokine pathway		
Chemokine binding protein	M001R/L	S001L/R
TNF receptor	M002R/L	S002L/R
eIF2α homolog	M007R/L	S007R/L
IFNα/β receptors	M135R	deleted
dsRNA-binding protein	M029L	S029L
OX-2 homolog	M141R	S141R
MHC pathway		
LAP domain	M153R	S153R
Anti-apoptotic molecules		
Ankyrin repeat	M005L/R	S005L/R
dsRNA binding protein	M029L	S029L
eIF2α homolog	M156R	S156R
M-T4	M004L/R	S004L/R
Inhibition of apoptosis	M011L	S011L
M-T2	M002L/R	S002L/R
RING finger	M143R	S143R
SP-1	M008.1L	fragmented
SPI-2/CrmA	M151R	S151R
Other poxvirus immuno-modulators		
Viral growth factor	M010L	S010L
Complement inhibition	M144R	S144R
CD47-like protein	M128L	S128L

The immuno-modulatory molecules that have been characterized in myxoma virus and SFV are listed in Table 1.2. In general, these molecules can be divided into modulators of complement pathway, inhibitors of interferon system, modulators of TNF and chemokines, growth factor homologs, anti-inflammatory serpins, and anti-apoptosis regulators. Homologs of these genes are also found in other *Chordopoxviruses* [156]. These wide arrays of gene targeting the host anti-viral defence system at both extracellular and intracellular environment, at multiple pathways signify the complexity of poxviruses, which make them such successful pathogens. When both genomes of SFV and myxoma virus were sequenced and compared [28, 196], there are only limited insights into the altered virulence of the viruses in the European rabbits. The most obvious difference is the fragmentation in SFV of two serpin-like genes, M008.1L/R and M152R encoded by myxoma virus. M008.1, a secreted serine protease inhibitor, has been shown to be an important virulence factor with a potent anti-inflammatory action [187]. Other predicted myxoma virus immuno-modulatory molecules are discussed by Barrett *et al.* [10].

Besides those genes with predicted immuno-modulatory functions presented in Table 1.2, there is a gene with potential regulatory role in modulating the redox status of infected cells. The gene is homologous to cellular SOD1 and is named M131R in myxoma virus (S131R in SFV) [28, 196]. Cellular SOD1 is an antioxidant that catalyzes dismutation of superoxide radicals. These Leporipoxviral genes are of particular interest since they are highly conserved, with ~96% amino acid identity, which suggest a function retained by selection. Homologs of SOD1 are also found within the *Poxviridae*, including the *Orthopoxviruses* vaccinia [170] and variola [2], [162], *Entomopoxviruses* B

Amsacta moorei [11], and in molluscipoxvirus molluscum contagiosum virus [160]. Sequence analysis revealed that all these genes are unlikely to function as dismutases due to deletions and/or substitutions within the coding region, with the exception of *Amsacta moorei*, where the SOD1 protein appears to be intact. Interestingly, other DNA viruses with different replication strategies also encode SOD1-like proteins, such as baculovirus [183] and *Paramecium bursaria* chlorella virus PBCV-1 [108]. More information on poxviruses SOD1 genes will be discussed later in this chapter.

1.4 Free radical biology

The presence of free radicals in biological system and oxygen toxicity-related damage were not generally appreciated until the discovery of copper and zinc containing superoxide dismutase (SOD1) in 1969 by McCord and Fridovich [112]. SOD1 has an interesting discovery history in that it was accidentally recognized by its inhibitory action upon the reduction of cytochrome c by xanthine oxidase. McCord and Fridovich investigated the ability of cytochrome c to be readily reduced, from a number of different preparations, but suffered from a consistency issue. Later, they discovered a contaminating enzyme in their preparations, SOD1, which inhibited the reduction of cytochrome c by competing with it for superoxide radical produced by xanthine oxidase. As complicated as is the free radical field, understanding the biological significance of these molecules is important in appreciating how evolutionary pressure has shaped aerobic organisms to adapt to oxygen toxicity. These molecules are also important mediators in cellular signalling pathways.

Life on earth first evolved in a reducing atmosphere and the environment shifted to an oxidizing one following the appearance of photosynthetic algae. This change resulted in some serious evolutionary pressures. Although aerobic organisms have been utilizing oxygen for millions of years, it is difficult to handle biologically. This is because oxygen is capable of stealing electrons from other molecules by nonenzymatic autoxidation. Oxygen is a diradical, which contains two electrons that are not spin paired. In order to be converted into a lower free energy water molecule, oxygen must acquire additional electrons (two per atom and four per molecule). Due to its unconventional distribution of electrons (parallel spin-state instead of anti-parallel spin-state), it is impossible for the oxygen to accept a spin-matched pair of electrons, but must take on the electrons one at a time [114]. This breaking up of electron pairs results in free radical formation [115]. The one electron reduction product of oxygen is the superoxide radical (O_2^{-*}). If two electrons are accepted, the product is hydrogen peroxide (H_2O_2). Hydrogen peroxide is not a radical but a cytotoxic oxidant since it is capable of stealing two electrons. If a third electron is transferred to the hydrogen peroxide, a highly reactive oxidant, hydroxyl radical ($^*OH$) is formed. The resulting products of the incomplete reduction of oxygen are also known as reactive oxygen species (ROS).

It has been estimated that ~98% of the oxygen we metabolized is handled by cytochrome oxidase in the mitochondria [115]. This enzyme contains four redox centers, which can transfer four electrons simultaneously to an oxygen molecule via the reaction:

$$O_2 + 4H^+ + 4e^- \rightarrow 2H_2O$$

This electron transport through the mitochondrial respiratory chain is extremely efficient. However, as advanced as we would like to think the human species is, our system is not

perfect when dealing with oxygen reduction. At least two sites have been identified in the electron-transport chain of mitochondria where problems can arise, the NADH dehydrogenase and ubisemiquinone [116]. Electrons leaking out from these sites could form superoxide radicals upon encountering oxygen molecules. This leakage has been estimated to account for 1-2% of total electron flux through the mitochondria [116]. Hence, mitochondria are the major source of accidental free radical production. In addition, ROS can also be produced from activation of membrane bound system enzymes in response to exogeneous stimuli such as the NADPH oxidase complex well characterized in phagocytic cells [90]. Non-phagocytic NADPH oxidases have also been identified in other cell type in production of ROS [87]. Furthermore, superoxide radical is also generated by cellular enzymes such as xanthine oxidase [78].

1.5 The toxicity of superoxide radical and its reactive progenies

Superoxide can act both as a reductant and as an oxidant, but it is primarily an oxidant in the reducing environment of a cell. Although it contains only one free electron and is less reactive than other radicals such as hydroxyl radical, superoxide is considered potentially more damaging. Due to its small size, superoxide radical can diffuse a considerable distance before it encounters a suitable and possibly, critical target. More importantly, it can rapidly inactivate dehydratases containing [4Fe-4S] cluster, such as aconitase (thus interrupting the Kreb cycle pathway), resulting in the release of Fe(II) [61, 62]. The metal in turn mediates production of hydroxyl radical via the Fenton reaction. Hydroxyl radical is one of the most potent oxidants known. In fact, as soon as it is produced, hydroxyl radical reacts with a substrate in its close proximity. This highly

reactive radical can initiate lipid peroxidation, cause DNA strand breaks, and indiscriminately oxidize virtually any organic molecule. Another means by which superoxide can damage cells is by forming peroxynitrite ($ONOO^-$) and subsequently other reactive nitrogen species (RNS) by reacting with nitric oxide (NO). RNS can cause DNA deamination and modification of amino acid residues, such as nitrating tyrosine residue. In addition, superoxide radical also causes the indirect formation of hydrogen peroxide, from the dismutation reaction. Hydrogen peroxide is considered weakly reactive, although at high level, it can be used as a disinfectant. It causes direct damage to some enzymes by oxidizing labile thiol group at active site. Similar to superoxide, the most damaging effect of hydrogen peroxide is caused by its reduction into hydroxyl radical via the Fenton reaction. Thus, the toxicity of superoxide is not seen in its own reactivity, but its potential to generate other more toxic and reactive compounds.

The overall damage of ROS involves DNA damage: single or double strand breaks, depurination/depyrimination, base mutations, blocks in DNA replication, transcription, and repair; causes protein malfunction, aggregation, and even triggers auto immune response; induces lipid peroxidation, which results in loss of membrane fluidity or integrity and imbalance of permeability, causing pore opening and activates Ca^{2+} dependant endonucleases which attack DNA residues [79]. The list in fact keeps growing since when a free radical reacts with a non radical, a new radical product forms and could in turn set the stage for further reactions. This is known as free radical propagation. The most efficient way to eliminate these toxic effects caused by ROS is by means of catalysis. Families of anti-oxidant enzymes have thus evolved. Of these enzymes, SODs provide the first line of defence by eliminating the superoxide radical,

hence blocking the initiation of any chain reaction (Figure 1.4). SOD scavenges superoxide by converting it into a more stable species, hydrogen peroxide, which is then degraded to water molecules by several cellular enzymes. The most important is the glutathione peroxidase that reduces hydrogen peroxide using reduced glutathione (GSH) as a substrate [119] (Figure 1.4). As a result of this reaction, oxidized glutathione (GSSG) is formed which can be restored to GSH by GSSG reductase [46]. Catalase provides further protection by eliminating hydrogen peroxide and organic peroxide (Figure 1.4).

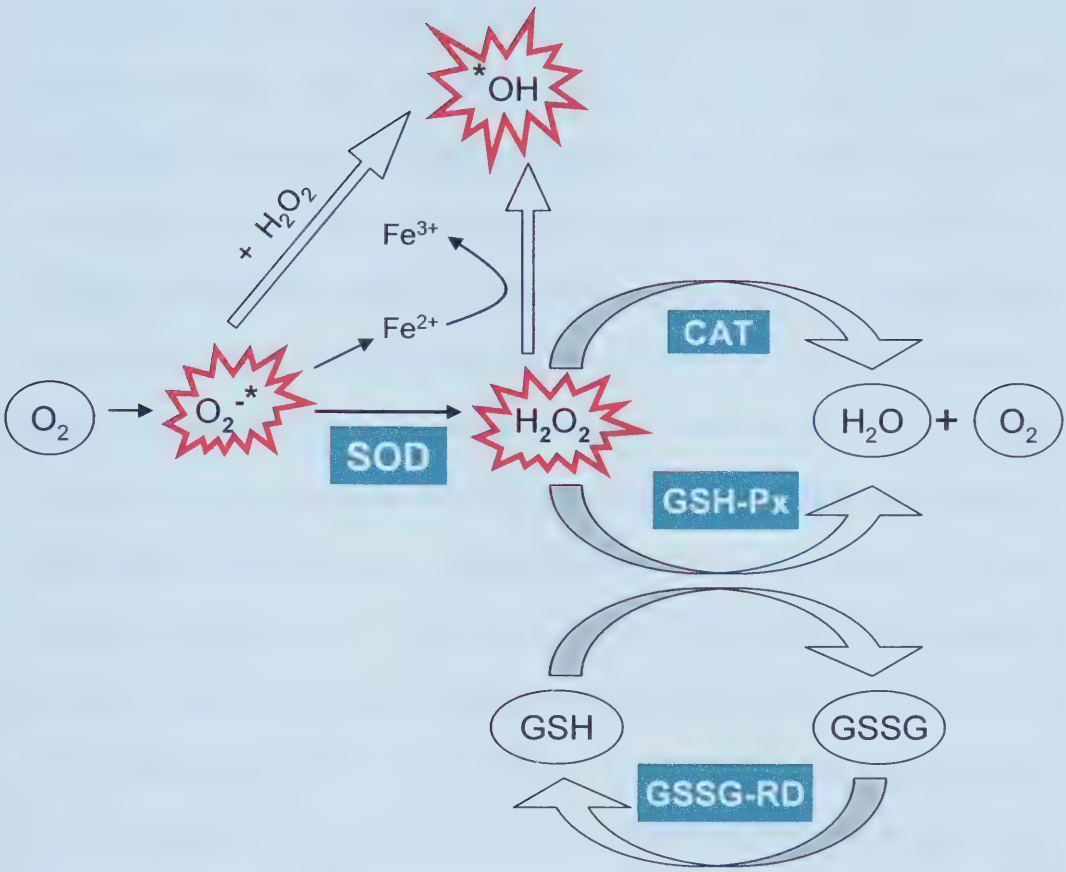

Figure 1.4. Primary antioxidant defence mechanisms against reactive oxygen species. Superoxide dismutase (SOD) converts superoxide (O_2^{-*}) into hydrogen peroxide (H_2O_2), which is further reduced by catalase (CAT) or glutathione peroxide (GSH-Px) into water molecule plus oxygen. GSH-Px uses reduced glutathione (GSH) as a substrate. As a result of this reaction, oxidized glutathione (GSSG) is formed which can be restored to GSH by glutathione reductase (GSSG-RD). These antioxidants also prevent the formation of highly cytotoxic radical, the hydroxyl radical ($^*OH$) from O_2^{-*} and H_2O_2 catalyzed Fenton reaction (by using transition metal ion such as Fe^{2+}) or Harber/Weiss reaction.

1.6 Superoxide dismutases

The importance of this antioxidant enzyme is seen in the variety of enzyme families that exist, as well as in the distribution of these enzymes in the cellular compartments, protecting cells against all possible sources of superoxide generation. In eukaryotes, there are: a copper and zinc containing enzyme (Cu-Zn SOD or SOD1) that localizes primarily in the cytosol, a manganese containing enzyme (MnSOD or SOD2) which is found solely in the mitochondria, and a different copper and zinc containing enzyme (EcSOD or SOD3) in the extracellular space. SOD1 comprises ~ 90% of total SOD activities in an eukaryotic cell [40]. Besides its primary distribution in cytosol, a small fraction of this enzyme has been found in cellular organelles such as lysosomes, peroxisomes, and nucleus. In contrast to the "wide-spread" SOD1 antioxidant protection, SOD2 is limited to the matrix of mitochondria [195]. Since the mitochondria are the major sources of ROS, SOD2, although exists in much lower concentration and won't protect against the cytosolic superoxide, is considered the most important SOD. Recently, there are also some evidences showing the presence of ~2% of SOD1 in the intermembrane space (IMS) of mitochondria [127, 176] and this localization was suggested to be important in providing further protection against ROS and in preventing superoxide radicals from leaking out of mitochondria. The expression of SOD3 is highly restricted to specific cell type and tissues such as plasma, lymph, ascites, and cerebrospinal fluids [110]. Plants have a SOD1, a SOD2, and also an iron containing FeSOD. In prokaryotes, there is a FeSOD and SOD2, as well as a SOD1 in the periplasmic region of Gram negative bacteria. Recently, a nickel containing SOD (NiSOD) has been found in some fungi. The metal in the active sites of all the SODs is

reduced by one superoxide and then reoxidized by the next during the enzymatic catalysis. Since the poxvirus genes I studied are homologs of SOD1, this enzyme will be the focus of this thesis.

1.6.1 Properties of SOD1

The most well characterized SOD1 is the bovine enzyme. This enzyme is a homodimer of approximately 31-33 kDa [172]. Each SOD1 monomer folds into a Greek-key β barrel made of eight anti-parallel strands connected by seven turns and loops (Figure 1.5A). The active site of each monomer contains one copper and one zinc ion. X-ray diffraction studies [144] combined with amino acid sequence analysis [52] indicate that the imidazole rings of histidines 46, 48, 63, and 120 are coordinated to Cu(II) in yeast SOD1. Histidine 63 bridges copper and zinc, which are 6 Å apart and co-ordination of zinc is completed by two other histidine residues and an aspartate residue in a tetrahedral geometry [99, 144, 149] (Figure 1.5B). An arginine residue (Arg-143 in human and yeast; and Arg-142 in bovine) are located adjacent to the active site copper ion. Chemical modification and site-directed mutagenesis studies have shown the importance of this arginine for catalysis [57, 109]. Another unique and important feature of SOD1 is the presence of an electrostatic channel loop, which is comprised of positively charged residues such as Lys 122, Lys 128, and Lys 136 [57, 64]. This channel serves as a guide to drive the negatively charged superoxide radical towards the active site, where the Arg 143 residue will hold the substrate in position against the copper ion for catalysis. The Cu(II) form of this enzyme is reduced by a superoxide to produce dioxygen and the reduced Cu(I) enzyme is then oxidized by another superoxide

molecule to yield hydrogen peroxide at a rate constant of 2 x 10^9 M^{-1} S^{-1} [94] by the following reaction equations:

$$\text{E-Cu(II)} + O_2^{-\cdot} + H^+ \rightarrow \text{E-Cu(I)} + O_2$$
$$\text{E-Cu(I)} + O_2^{-\cdot} + H^+ \rightarrow \text{E-Cu(II)} + H_2O_2$$
$$2\,O_2^{-\cdot} + 2H^+ \rightarrow O_2 + H_2O_2$$

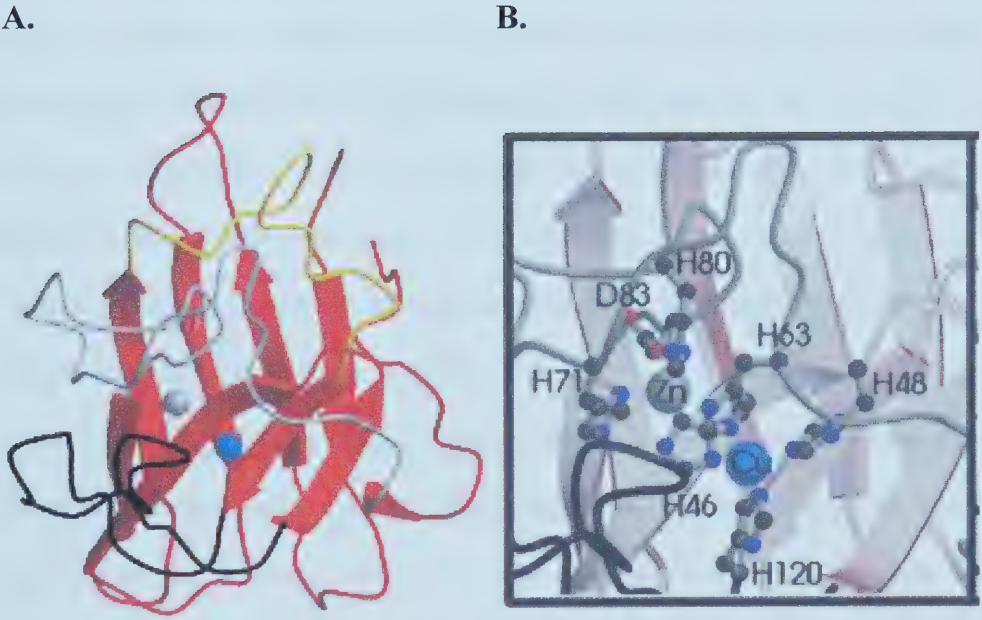

Figure 1.5. Structural features of SOD1. (A) Ribbon model of human SOD1 in Greek-key β barrel motif. The copper and zinc cofactors in the active site are represented as blue and silver spheres, respectively. The positively charged electrostatic channel loop is shown in black. (B) The metal coordinating residues are shown in a stick model, including the H63, which bridges both the copper and zinc ions. Adapted from Lamb *et al.* [99].

1.7 Copper chaperone for SOD1

Although copper is a very important cofactor for many enzymes, including SOD1, it can be toxic even at low concentration (copper, like iron can participate in Fenton chemistry as mentioned in Chapter 1. 5) and all organisms have developed various metal-homeostasis factors to properly control the cellular accumulation, distribution , and detoxification of this metal [94]. Copper is maintained at a total intracellular concentration in the 10^{-4} to 10^{-5} M range [141]. In spite of that abundance, many studies have shown that this metal ion is typically unavailable in the cytoplasm for direct substitution into metallo-enzymes [141]. In fact, Rae *et al.* [140] showed that the steady state concentration of free/labile form of copper ion in the cytoplasm of yeast is far less than 1 ion per yeast cell. Cells are also armed with a variety of proteins such as metallothioneins that scavenge free copper ions. Therefore, proteins that use copper as a cofactor must acquire it from those scavenging molecules. This raises the issue of how apo-enzymes might acquire the correct metal cofactors.

The discovery of copper chaperones has opened the door towards understanding the cellular trafficking of these cofactors. These chaperones acquire copper either directly or indirectly from the membrane transporter, protect it from scavenging molecules and deliver and insert the ion into specific target proteins [190]. Several copper chaperones have been identified in eukaryotes, including Cox17 which delivers copper to cytochrome c oxidase in mitochondria [65], Atxl which delivers the metal ion to vesicular transport ATPase [106] and human copper chaperone for SOD1 (hCCS) or the yeast CCS which delivers copper to cytoplasmic human and yeast SOD1 respectively [42].

Amino acid sequence comparison revealed striking homology between SOD1 and CCS, including residues involved in forming the SOD1 homodimers [32, 42]. This suggests a mechanism by which copper can be delivered to SOD1 by CCS through a direct protein-protein interaction. The crystal structure of hCCS revealed a homodimer (~60kDa), with each monomer comprising three domains: Domain I (N-terminal, Atx1-like), Domain II (SOD1-like), and Domain III (C-terminal, unique to CCS sequences) [141] (Figure 1.5). It is suggested that Domain I and III function in metal uptake and delivery because they contain a MXCXXC and CXC metal-binding motifs, respectively [152]. Domain II folds in a Greek key β-barrel conformation that is very similar to its binding target, SOD1. SOD1 and this portion of CCS share ~50% amino acid identity, which includes the residues involved in the formation of a SOD1 dimer interface and which could be expected to play a role in target recognition [77, 98, 99]. Based on this information, it has been proposed that the copper transfer process occurs through the cysteine pair of Domain III via ligand exchange with Cu-binding residues of SOD active site. Since the metal-binding motif of Domain I can bind copper, it is feasible that Domain III can actually interact alternatively with Domain I or the SOD1 target site in a switch–like translocation of metal transfer [77] (Figure 1.6).

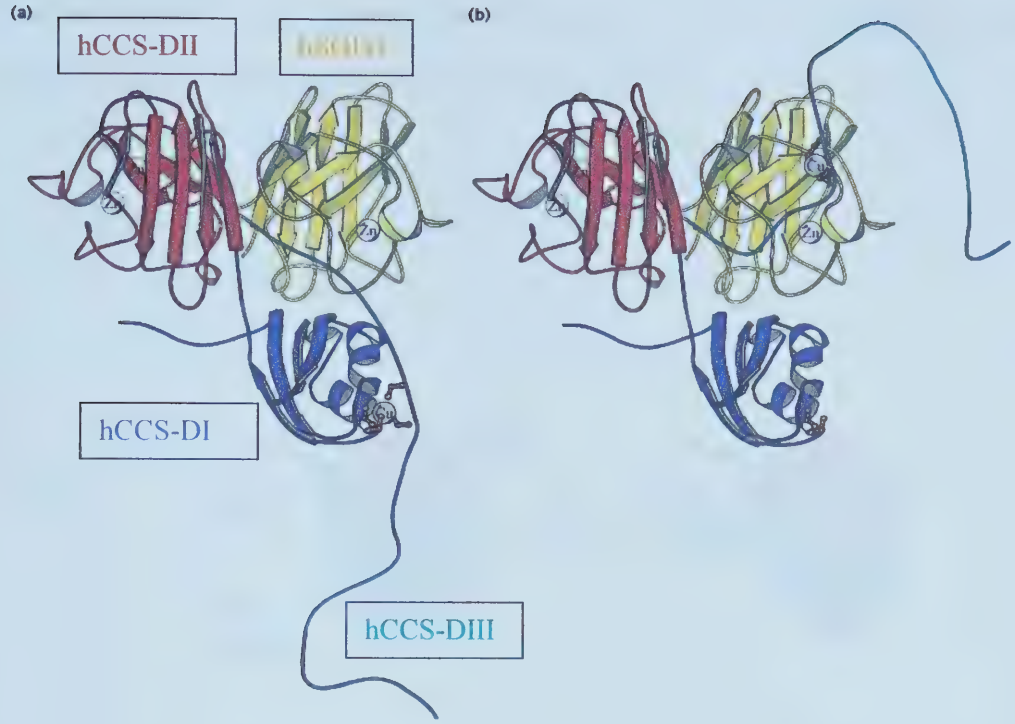

Figure 1.6. Ribbon diagrams showing human CCS interacting with a copper-free human SOD1 subunit. (a) The delivery region is modeled like a random coil in which the two cycteines of the CXC sequence are within interacting distance of the copper-binding site of the Atx1-like Domain I. (b) Copper transferring from Domain III of hCCS to a target site within hSOD1. Adapted from Falconi *et al.* [53].

1.8 Activation of SOD1 by CCS

Although the crystal structures of both SOD1 and CCS have long been available, the details of chaperone-target protein recognition and docking for metal transfer were not clear until Lamb and her colleagues [97] solved the crystal structure of the heterodimeric complex between SOD1 and CCS. Two models have been previously proposed for the activation of SOD1 by CCS. In the first model, SOD1 dimer and its CCS dimer "swap" monomers to yield a pair of heterodimers prior to metal transfer. In

the second model, it was suggested that CCS simply activates apo-SOD through a dimer to dimer transfer of copper ion [77, 98, 99] (Figure 1.7).

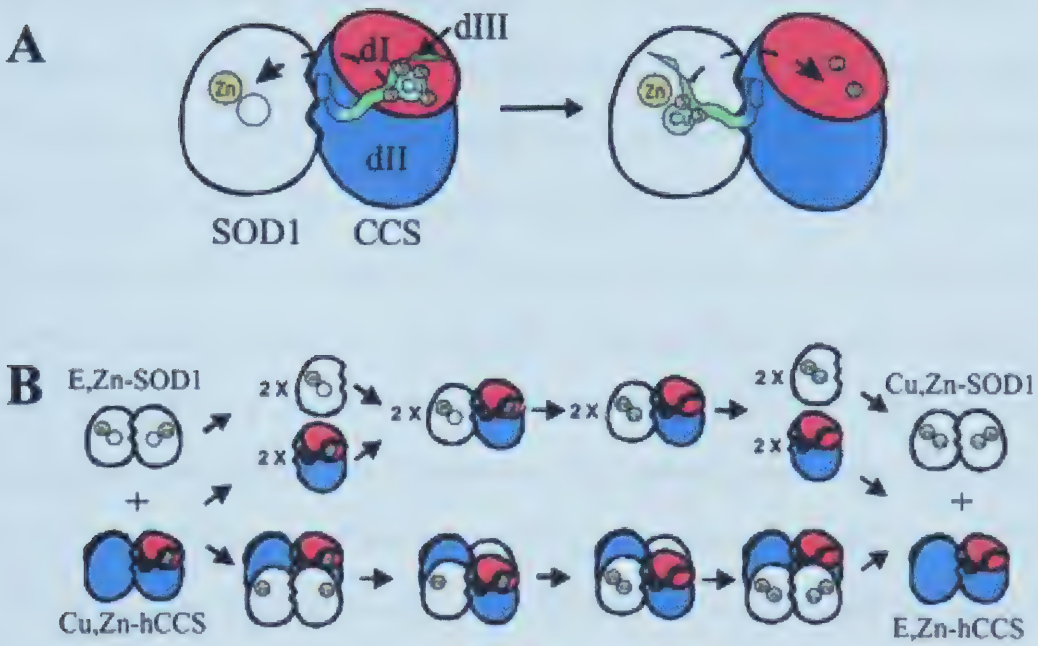

Figure 1.7. Proposed models for activation of SOD1 though an interaction with copper CCS. A. General method of copper transfer from Domain III of CCS to a target site on SOD1. B. The top row shows a suggested scheme involving an interaction between monomers of SOD1 and CCS. The bottom row shows a hypothesized dimer-dimer mode of interaction between the two proteins. In both models, after CCS recognizes its target and docks with SOD1, copper transfer is triggered through conformational changes, which will then create a signal for dissociation of the complex formation. This then allows copper-loaded SOD1 to form an active homodimeric enzyme. Adapted from Rae *et al.* [141].

There has been a lot of debate upon which, or both models are feasible *in vivo*. Due to the thermodynamic stability of SOD1 homodimers, and the lower abundance of CCS compared to SOD1, Hall *et al.* [77] prefer the dimer-dimer mode of interaction. However, heterodimer formation between different SOD isozymes and SODs from different organisms has been observed [141]. In fact, Lamb *et al.* [96] have shown that *in vivo* copper loading of yeast SOD1 occurs via a heterodimeric intermediate and could not detect dimer-dimer or higher oligomers. The main reason for questioning the heterodimeric mode of interaction is due to difficulties crystallizing a complex formed by SOD1 and CCS. The interaction is transient, since soon after metal delivery, the complex has to be dissociated for SOD1 to reach its fully active homodimeric state [96]. However, Lamb and her colleagues [97] overcame the problem by mutating one of the copper coordinating residues, H48F in yeast SOD1, rendering the protein unable to accept the metal ion. This loss of metal binding ability interferes with copper transport and results in the formation of a stronger and more stable complex. Most surprisingly, they observed formation of an intermolecular disulphide between C57 of SOD1 and C229 of CCS (at DIII), which suggested that the oxidation of the cysteine residues might be important in facilitating metal ion insertion, hence the activation of SOD1 (Figure 1.8). These reaction features have important implications for how Leporipoxvirus SOD1 homologs might interact with CCS and inactivate the cellular SOD1, which are presented in Chapter 3. The evidence favouring heterodimer formation, however still does not rule out the possibility of a dimer-dimer mode of interaction and metal transfer.

Since copper is the core metal that activates SOD1, a lot of attention has been focused on its involvement in SOD1-CCS interaction and hence, the role played by zinc

has been overlooked. To address that concern, Lamb *et al.* [96] investigated the issue and showed that heterodimer formation is actually facilitated by zinc but does not depend on copper loading of yeast CCS. Zinc binding is known to cause conformational changes in loop regions of SOD1 and likely stabilizes the zinc and S-S subloops, which are involved in forming the dimer interface [189]. Therefore, it has been suggested that the affinity of SOD1 for CCS might depend on conformational priming of a SOD1:CCS dimer interface by zinc binding. It is also possible that yeast CCS assists in zinc loading of SOD1 either directly or as a molecular chaperone. However, the transition of SOD1 from a metal free to fully active state requires the presence of both metal ions [189].

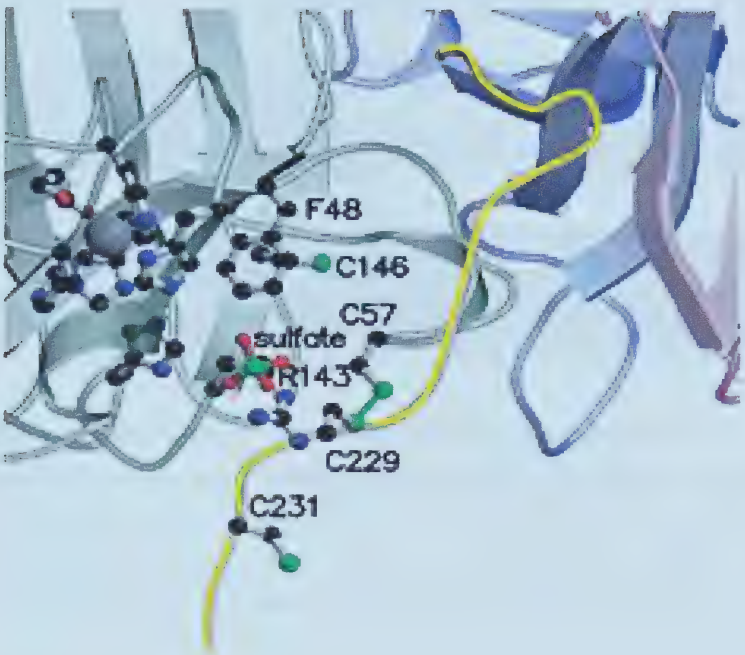

Figure 1.8. Formation of an intermolecular disulphide bond between the SOD1 S-S subloop and yCCS domain III. In the heterodimer complex, a previously formed intradisulphide bond between C146 and C57 in SOD1 S-S subloop is broken, allowing C57 to form a new intermolecular disulphide bond with C229 on yCCS domain III (highlighted in yellow). This new conformation, upon CCS-SOD1 interaction, opens up the SOD1 active site, and mediates copper ion insertion. The zinc ion is shown as a grey sphere, and key residues are shown as ball-and-stick representations. Modified from Lamb *et al.* [97].

1.9 Leporipoxviral SOD1 homologs

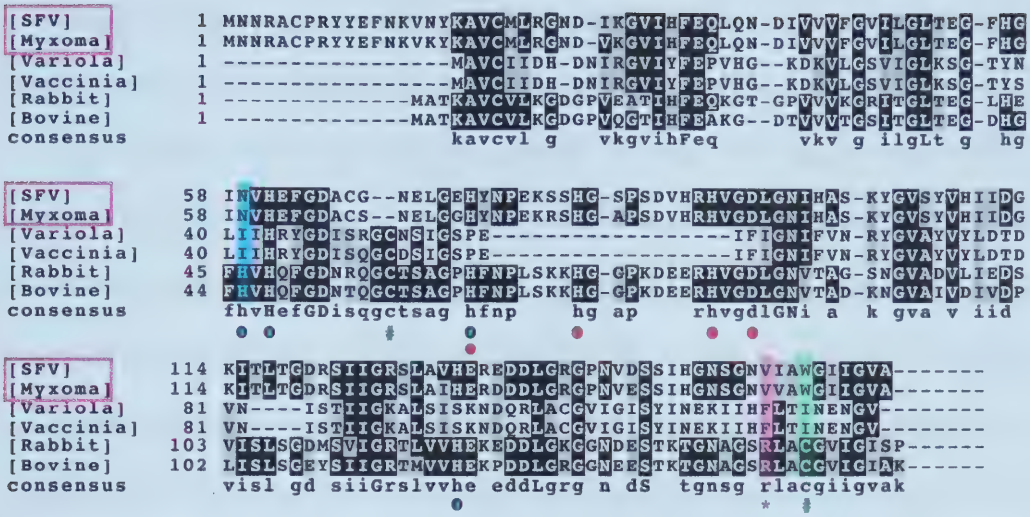
[SFV] 1 MNNRACPRYYEFNKVNYKAVCMLRGND-IKGVIHFEQLQN-DIVVVFGVILGLTEG-FHG
[Myxoma] 1 MNNRACPRYYEFNKVKYKAVCMLRGND-VKGVIHFEQLQN-DIVVVFGVILGLTEG-FHG
[Variola] 1 ----------MAVCIIDH-DNIRGVIYFEPVHG--KDKVLGSVIGLKSG-TYN
[Vaccinia] 1 ----------MAVCIIDH-DNIRGVIYFEPVHG--KDKVLGSVIGLKSG-TYS
[Rabbit] 1 ----------MATKAVCVLKGDGPVEATIHFEQKGT-GPVVVKGRITGLTEG-LHE
[Bovine] 1 ----------MATKAVCVLKGDGPVQGTIHFEAKG--DTVVVTGSITGLTEG-DHG
consensus kavcvl g vkgvihFeq vkv g ilgLt g hg
[SFV] 58 INVHEFGDACG--NELGEHYNPEKSSHG-SPSDVHRHVGDLGNIHAS-KYGVSYVHIIDG
[Myxoma] 58 INVHEFGDACS--NELGGHYNPEKRSHG-APSDVHRHVGDLGNIHAS-KYGVSYVHIIDG
[Variola] 40 LIIHRYGDISRGCNSIGSPE----------IFIGNIFVN-RYGVAYVYLDTD
[Vaccinia] 40 LIIHRYGDISQGCDSIGSPE----------IFIGNIFVN-RYGVAYVYLDTD
[Rabbit] 45 FHVHQFGDNRQGCTSAGPHFNPLSKKHG-GPKDEERHVGDLGNVTAG-SNGVADVLIEDS
[Bovine] 44 FHVHQFGDNTQGCTSAGPHFNPLSKKHG-GPKDEERHVGDLGNVTAD-KNGVAIVDIVDP
consensus fhvHefGDisqgctsag hfnp hg ap rhvgdlGNi a k gva v iid
[SFV] 114 KITLTGDRSIIGRSLAVHERDDDLGRGPNVDSSIHGNSGNVIAWGIIGVA-------
[Myxoma] 114 KITLTGDRSIIGRSLAIHERDDDLGRGPNVESSIHGNSGNVVAWGIIGVA-------
[Variola] 81 VN----ISTIIGKALSISKNDQRLACGVIGISYINEKIIHFLTINENGV--------
[Vaccinia] 81 VN----ISTIIGKALSISKNDQRLACGVIGISYINEKIIHFLTINENGV--------
[Rabbit] 103 VISLSGDMSVIGRTLVVHEKEDDLGKGGNDESTKTGNAGSRLACGVIGISP------
[Bovine] 102 LISLSGEYSIIGRTMVVHEKPDDLGRGGNEESTKTGNAGSRLACGVIGIAK------
consensus visl gd siiGrslvvhe eddLgrg n dS tgnsg rlacgiigvak

Figure 1.9. Amino acid sequence alignment of SOD1 homologs encoded by Leporipoxviruses and Orthopoxviruses in comparison to rabbit and bovine SOD1s. The active site arginine (★) in bSOD at position 142 is replaced by a valine (V) in Leporipoxvirus SOD1 homologs, but most metal-binding residues are retained. Copper and zinc coordinating residues are represented as ● and ● respectively. The cysteine residues that form an intrastrand disulphide bond in the cellular SOD1 protein are also marked #.

At first, SOD1 was believed to be exclusively an eukaryotic enzyme, but then several bacterial species turned out to possess this enzyme including *Caulobacter crescentus*, *Brucella abortus*, and the human pathogens, *Leionella pneumophila* and *E. coli* [172]. In 1974, a homolog of the enzyme was discovered in the luminescent marine bacterium, *Photobacterium leiohnathi*, which occurs in nature as a symbiont in leiognathid fishes (pony fish) [81]. The long-standing symbiotic relationship between the fish and bacterium, plus the similarities between their two SOD1 homologs, has led to the

suggestion that the bacterial gene for the dismutase may have been acquired by natural gene transfer from the pony fish host [172]. The bacterial SOD1s have been well documented to be important virulence factors in protecting these pathogens against exogeneous superoxide radicals generated by host phagocytes [54, 95, 101].

Intriguingly, homologs of SOD1 are also encoded by complex DNA viruses, including the *Poxviridae* [2, 11, 28, 160, 162, 170, 196], baculoviruses [183] and chlorella virus PBCV-1 [108]. The amino acid alignment of SFV, myxoma virus, and two of the Orthopoxviruses (vaccinia and variola) are shown in Figure 1.9 in comparison to the SOD1 genes of rabbits and cows. The alignment reveals some mutations and deletions in poxviral homologs relative to the cellular SOD1s. Most critically, the active site arginine in bovine SOD1 (R142) is replaced by a valine in Leporipoxviral SOD1 homologs. Recall that this arginine residue serves an essential role in catalysis in SOD1 by "holding" a superoxide radical in position next to the catalytic copper ion at the active site. Thus, replacing the residue with a hydrophobic valine is expected to reduce dismutase activity. In addition, one of the four copper coordinating residues, H46, has been replaced with an asparagine residue in Leporipoxviral proteins. These two mutations should together be sufficient to render poxviral SOD1 homologs inactive as dismutases. Furthermore, an intrastrand disulphide interaction between two cysteines that forms the S-S subloop in the bovine SOD1 is disrupted in the viral proteins. One of the cysteine residues (C157) in bovine SOD1 is mutated to tryptophan while C56 is deleted in Leporipoxviral homologs. However, all four of the zinc coordinating residues are retained in Leporipoxvirus genes and most of the hydrophobic residues comprising the bovine SOD1 dimer interface are well conserved. Despite these mutations, SFV

S131R and myxoma virus M131R still share ~53% amino acid identity with rabbit cellular SOD1 [29].

In contrast, the Orthopoxviral SOD1 homologs show evidence of a greater degree of divergence from their eukaryotic SOD1 homologs [4]. There are more mutations in Orthopoxviral homologs, besides the ones already mentioned, and the overall amino acid identity is only 39% [4]. Both vaccinia and variola virus SOD1 proteins are also much smaller because of many in-frame deletions. Of all the metal binding residues, only the homolog of H47 is retained, indicating that these proteins are also unlikely to be active. They would also be predicted to not bind zinc which may also affect the structural stability of the Orthopoxviral proteins.

A unique feature of Leporipoxviral SOD1 homologs (Figure 1.9) is the presence of a 16 amino acid N-terminal extension not detected in either mammalian SOD1 or homologs encoded by other poxviruses. We do not know much about these amino acids except that protein modeling software predicted it to fold in a random coil structure. Another graduate student (A. Zachertowska) from Dr. David Evans's lab has shown that this N-terminal peptide is very accessible to trypsin with purified virus particles [199]. Molecular modeling of S131R, using the known structure of bSOD1, also predicted that the Leporipoxviral SOD1 homologs fold in a similar confirmation to the cellular SOD1.

1.10 Biological significance of SOD1

Information on the biological importance of SOD1 enzyme has been derived primarily from the studies of mutant mice and in the fruit fly *Drosophila*. Knockout mice, missing the cytosolic SOD1, showed increased neurologic and histologic damage after focal cerebral ischemia and reperfusion, and increased motor neuron death after axonal injury [142]. They also exhibited a shortened lifespan and could not reproduce successfully. In *Drosophila*, strains carrying the SOD1-null mutation $cSOD^{n108}$ show hypersensitivity to the superoxide generator paraquat and the Fenton catalyst Cu(I), male infertility, and reduced longevity [136]. Most importantly, mutations in this enzyme in humans have been linked to familial amyotrophic lateral sclerosis (FALS), a dominantly inherited motor neuron disorder of midlife [3]. More than 90 SOD1 mutations have been identified and account for approximately 20% of cases of FALS [63]. Although some SOD1 mutants show reduced antioxidant activities, a loss of function of SOD1 is not sufficient to explain the FALS phenotype since mice in which SOD1 has been deleted do not develop motor neuron disease [142]. In addition, some of the mutant SOD1 forms retain full or even elevated SOD1 activity [70]. A more plausible explanation is that SOD1 mutation causes cell death through a gain of some toxic function, since this is a property commonly observed in diseases inherited in an autosomal dominant pattern. Although the precise mechanisms whereby mutations in SOD1 (including several that involve copper binding residues), produce neuronal injury remain unclear, current evidence suggest that FALS is likely to be multifactorial in origin [39]. Among those factors, aberrant protein aggregation induced toxicity seems to be the most commonly reported feature. This has been seen in both mice and cell culture models of FALS [19,

89] and the presence of protein aggregates in brain tissue is a common feature of many neurodegenerative diseases [171]. However, how the many different SOD1 single-site mutations, dispersed throughout the protein sequence, can give rise to the same FALS pathology is still an enigma.

1.11 Oxidative stress and related pathologies

During lifetime, an antioxidant network counteracts the deleterious actions of ROS in biological system. Cells synthesize antioxidants, such as superoxide dismutases, catalase, glutathione peroxidase, as well as peptide with thiol group (glutathione), while nonenzymatic antioxidants are obtained through nutrition, including vitamin C, vitamin E, and carotenoids. Together, these antioxidants play an important role in the ability of the body to respond to the oxidant challenge, a consequence of utilizing molecular oxygen to drive the necessary life processes. Oxidative stress is classically defined as a redox (reduction/oxidation) unbalance with an access of oxidants or a defect in antioxidant capacities [167]. Oxidative stress caused by ROS damage has been implicated in an enormous variety of natural and pathological inflammatory diseases, including aging, cancer, diabetes, atherosclerosis, neurological degeneration such as Alzeimer's disease and Parkinson disease, and autoimmune disorders such as arthritis [6, 44, 58, 80, 88]. Although overproduction of ROS is a feature of such a broad spectrum of diseases, the molecular mechanism of the contribution of each component of oxidative stress to human diseases has not yet been elucidated. However, the correlation of oxidative stress on diseases does suggest that ROS may mediate specific signalling

pathways in the cell and these pathways lead to the modulation of gene expression through regulation of transcription factors.

1.12 Regulatory functions of superoxide

All cells rely on a complex interplay of both extracellular and intracellular signals to control their metabolism, growth, differentiation, and death. As damaging as superoxide radical and its reactive derivatives are at high levels, there is another side to the story. Superoxide radical is not simply a noxious cytotoxic byproduct, but has long been recognized to work as physiological mediator and signalling molecule in regulating inflammation, stimulating cell proliferation, and regulating apoptosis [13, 14, 115].

1.12.1 Anti-microbial agent

The destructive power of superoxide radical can be harnessed and used by organisms to destroy both invading pathogens and tumour cells. Phagocytic leukocytes, when activated, increase their oxygen consumption 15- to 20-fold in what is known as the respiratory burst. This is due to the activation of membrane-bound NADPH oxidases which reduce oxygen to superoxide radical using NADPH as an electron donor [8]. This production of superoxide radical is an essential anti-microbial [8] and anti-viral [85] defence which helps phagocytes chemically destroy ingested pathogens. As a side effect, the neutrophil is often destroyed in the process and the surrounding healthy host cells may also be injured or even killed. In effect, superoxide serves as an extremely broad spectrum antibiotic and a mediator of inflammation. Because SOD1 breaks down this superoxide, it can serve a role in suppressing inflammation [113, 135].

1.12.2 Stimulation of cellular proliferation

Superoxide radicals are also believed to play another constructive role in promoting or regulating cellular proliferation. Cellular proliferation is a tightly controlled process involving a variety of genetic and biochemical factors. Basically, growth factors, cytokines, and hormones interact with specific cell surface receptors and trigger intracellular signals. This in turn, can activate specific genes, including protooncogenes, and initiate a series of events leading to cell division. Faulty regulation of these processes leads to the deregulation of growth, a characteristic feature of cancer cells. One such cell membrane receptor often modified in cancer cells is the epidermal growth factor receptor (EGFR) [1]. Growth factors are known to play an important role in regulating tumour growth and survival, predominantly via their effects on mitogenesis.

1.12.2.1 Growth factor signalling pathway

The EGFR belongs to a large family of cell surface receptors with intrinsic receptor tyrosine kinase (RTK) activity. In vertebrates, there are four closely related EGFR members: ErbB1, ErbB2, ErbB3, and ErbB4. At the plasma membrane the unstimulated EGFR is present as a monomer, which upon interaction with a ligand such as epidermal growth factor (EGF), will undergo dimerization resulting in transautophosphorylation of its cytoplasmic domain [151]. These events lead to the recruitment and phosphorylation of several intracellular substrates, leading to mitogenic l and other cellular activities [5, 145]. A major signalling route of the ErbB family appears to be via the mitogen-activated protein kinase (MAPK) pathway [5]. Phosphorylated

tyrosine residues are docking sites for the adaptor proteins Grb2, which then recruits SOS guanine nucleotide exchange factor to the plasma membrane. The complex then activates Ras to stimulate the MAPK cascade. There are three subfamilies of MAPKs, which include the extracellular signal-regulated protein kinase (ERK), c-Jun N-terminal kinase (JNK), and p38. These subfamilies are differentially affected by particular stimuli. In general, ERK shows greater activation in response to mitogenic stimuli, whereas JNK and p38 are activated to a much greater extent by stress stimuli [146, 194]. JNK signalling causes opposite responses depending on the cellular state [14]. Signalling through JNK pathway has been shown to mediate oncogenic signals and supports cell proliferation in the absence of stress, but on the other hand this signalling pathway can promote apoptosis in many cell types under stress. High levels of JNK activity have also been correlated in many instances with the induction of apoptosis [197]. ERK activity is often suppressed in many conditions of stress-related apoptosis, leading to suggestion that the balance between JNK and ERK activities is the key factor in regulating apoptosis [197]. ERK activation leads to the cell proliferation through the activation of a number of nuclear targets, including activation protein-1 (AP-1) formed by c-jun and c-fos, nuclear factor kappa B (NFκB), zinc finger transcription factor Sp1, and c-myc oncoprotein [5]. Another important pathway in ErbB signalling pathway is the one constituted by phosphatidylinositol 3-kinase (PI3-K) and the downstream protein kinase Akt [25]. After its activation, Akt transduces signals that regulate multiple biological processes including apoptosis, gene expression, and cellular proliferation [35]. Akt is likely to send survival (antiapoptotic) signals by phosphorylating multiple targets, including a proapoptotic factor BAD of the Bcl-2 family member [45] and a key

apoptotic executioner caspase 9 [30]. A signal transducer and activator of transcription (STAT) is also activated by ErbB pathway, which is then translocated to nucleus, resulting in enhancement of transcription leading to cell proliferation. These major signalling pathways activated by the EGFR are illustrated in Figure 1.10. These signalling pathways do not simply direct linear signals from the cell surface to the nucleus but several forms of crosstalk also connect the pathways [120]. Through these transcriptional programs, the ErbB signalling network controls a wide spectrum of biological outcomes, including cell proliferation, differentiation, survival, adhesion, and migration.

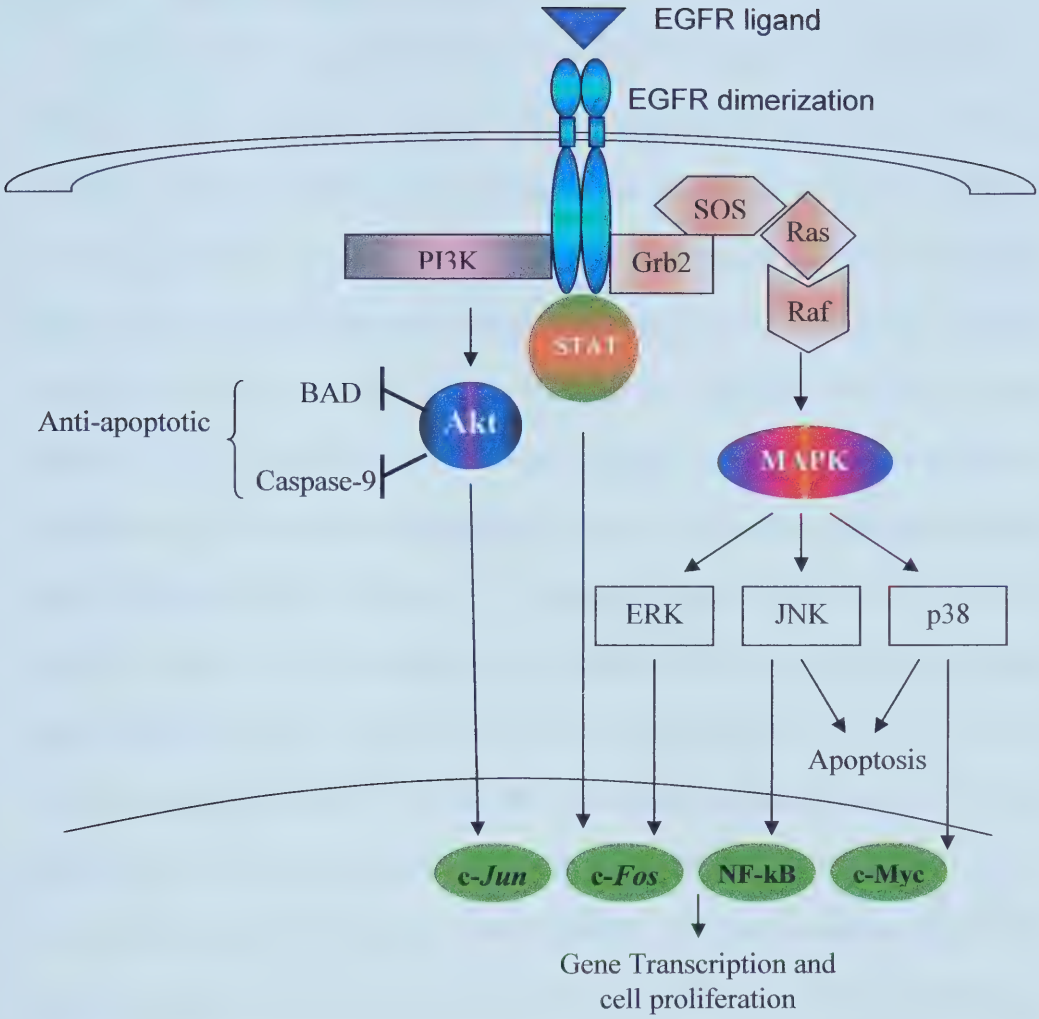

Figure 1.10. The major signalling pathways activated by the epidermal growth factor receptor (EGFR), leading to cell proliferation, apoptosis, and/or survival. ERK activation by the Ras-Raf family leads to cell proliferation through the activation of a number of nuclear targets such as c-Myc, which is a major transcription factor and regulator of cell cycle progression. The PI3K-Akt pathway results in enhancement of antiapoptotic and prosurvival signals, through inhibition of the proapoptotic proteins Bad and caspase-9. In addition, the STAT pathway also leads to enhancement of transcription leading to cell proliferation. JNK and p38 are also known as stress-activated protein kinases (SAPK), which upon exposure to stress stimuli, will cause cell death via apoptosis.

1.12.2.2 ROS and cell proliferation

There is now a growing body of evidence to suggest that superoxide and hydrogen peroxide may play a crucial role in regulating the mechanisms underlying proliferative responses. Phagocyte-generated superoxide serves to stimulate fibroblasts to enter a proliferative mode [124], forming scar tissue to close up the wound. The generation of superoxide was also associated with triggering the proliferation of cultured keratinocytes, while cells decreased their release of superoxide when they reached confluence [60]. In other studies, Burbon *et al.* [22-24] observed that adding low concentrations of superoxide and hydrogen peroxide to cell culture media stimulated the growth of hamster and rat fibroblasts. Exogenously added superoxide has also been shown to stimulate a growth response in other cultured mammalian cell types, including human fibroblasts [125], Balb/3T3 cells [163, 165, 173], human amnion cells [86], mouse epidermal cells (JB6) [41], and human histiocytic leukemia cells (U937) [164]. Growth responses are also elicited by hydrogen peroxide in hamster (BHK-21) [22, 24] and rat fibroblasts (208F) [23], as well as in Balb/3T3 [165] and mouse osteoblastic cells (MC3T3) [126]. In JB6, Balb/3T3, and MC3T3 cells, these ROS stimulate the expression of early growth related genes such as *c-fos* and *c-jun* [41, 126, 163, 165], suggested that superoxide and hydrogen peroxide might function as mitogenic stimuli through biochemical processes common to natural growth factors.

1.12.2.3 ROS and tumour growth

Since uncontrolled cell proliferation is a feature of tumour growth, it is not surprising that a growing body of evidence also suggests that ROS are involved in tumour promotion. Zimmerman and Cerutti [200] have shown that the superoxide generated by xanthine/xanthine-oxidase acted like a weak complete carcinogen in promoting transformation in mouse embryo fibroblasts, and that a scavenger of superoxide (SOD enzyme) reduced the frequency of appearance of transformed foci 3- to 25- fold. As well, there have been many reports of aberrant antioxidant defence levels in tumour cells [15, 93, 177], where the activities of both SOD1 and SOD2 are seen to be relatively low as compared with the normal cellular counterparts. Some tumours have also been shown to express elevated levels of SODs, but this is often associated with other aggressive tumour characteristics in the case of malignant tumours [93]. The importance of the loss of SOD activities in most tumour cells is not well understood, except that all tumour cells examined to date clearly demonstrate an altered redox balance, with most studies suggest a more oxidative state [93], characterized by elevated intracellular ROS, and more specifically, superoxide level [33]. Although exceptions can be found, in general, augmenting antioxidant levels (by either genetic or pharmacologic mean) has been shown to inhibit tumour growth and/or differentiation [93]. In contrast, down-regulation of SOD expression or chemically promoting a prooxidant state induces cellular proliferation [93, 107].

1.12.2.4 Mechanisms of ROS-mediated cell signalling

What are the molecular mechanisms by which superoxide and hydrogen peroxide can induce cellular proliferation or disrupt the normal cellular control of this process? Ligand-receptor binding has been shown to trigger the production of ROS [56] and antioxidants can block some aspects of receptor-coupled signal transduction [178]. This suggests that ROS participate in the transmission of a receptor signal, probably by modulating the activities of kinases and phosphatases, redox-sensitive transcription factors, and genes. Many studies have now detected ROS production in non-phagocytic cells in response to the activation of growth-receptor signalling cascades, including activation triggered by platelet-derived growth factor, basic-fibroblast growth factor, or EGF [138]. More recently, angiotensin II (Ang II) has also been shown to produce superoxide radical mediated by NADPH oxidase in vascular smooth muscle cell as well as in epithelial cells [68, 100]. This Ang II signalling pathway stimulates a variety of important intracellular signals such as EGFR transactivation, p38 MAPK, and Akt [67]. In addition, cytokines such as tumour necrosis factor-alpha (TNF-α), gamma interferon (γ-IFN), and interleukin-1beta (IL-1β) are also known inducers of superoxide [138].

There are many places in these cascades where ROS can target. For example, upon growth factor stimulation, ROS have been shown to act both upstream and downstream of the RTK and Ras. ROS also modulate the activity of some members of the MAPK family. In transformed fibroblasts, Ras activity appears to be directly linked to the production of superoxide, and in turn, transformation of the cells depends on this ROS [87]. Ras is activated by ROS via oxidative modification of a cysteine residue at position 118, and this oxidized formed of Ras then recruits PI-3K, an event that is

required for activation of downstream signalling such as Akt and MAPK [67]. Therefore, the outcome of ROS production in growth factor receptor signalling is the activation of the downstream effector kinases of the MAPK family. Depending on the cellular system, different MAPK family members, such as p38, ERK, and JNK have been shown to possess ROS-sensitive kinase activity [138].

The signal transduction cascade elicited by ROS culminates in the activation by phosphorylation of transcription factors, which in turn activates genes involved in cellular proliferation. At least two well-defined transcription factors, NFκB and AP-1 have been shown to be regulated by the intracellular redox state [69, 74, 75, 118, 153]. NFκB is sequestered in the cytoplasm by its inhibitory protein, IκB, until I kappa kinase (IKK) releases the inhibition by phosphorylating two serine residues on IκB. Once phosphorylated, IκB is polyubiquitinylated and rapidly degraded, allowing NFκB to translocate to the nucleus. There, it regulates the transcription of a large number of genes that control various aspects of the immune and inflammatory response [9]. A wide array of antioxidants that can detoxify ROS have been reported to suppress the activation of NFκB [72]. Conversely, IKK phosphorylation [138] and protease degradation [34] can both be stimulated by ROS and results in NFκB activation. Interestingly, NFκB has been proposed to serve as an intracellular "redox sensor" in mammalian cells since its activation is sensitive to oxidative modification [72]. In this regard it is notable that SOD is one of the genes activated by NFκB (SOD2 in general but also SOD1 in some cell types) suggesting that feed back loops exist in cells to regulate the superoxide level [14].

Another transcription factor that is sensitive to ROS is AP-1. AP-1 is a dimer composed of *c-Fos* and *c-Jun* subunits that regulates many kinds of early response genes. Overexpression of this heterodimeric complex is often associated with tumour progression whereas inhibiting AP-1 activity blocks cellular transformation and attenuates a malignant phenotype [69]. Not much is known about the exact mechanisms of oxidant-induced AP-1 activation, but superoxide has been shown to induce c-*Fos* expression. Since antioxidants can attenuate MAPK activation [193], ROS-mediated AP-1 activation likely results from changes in MAPK signalling cascades that ultimately control the phosphorylation of Fos and Jun [69].

Since superoxide and hydrogen peroxide are known to cause membrane lipid peroxidation, it is conceivable that the ROS mediated cellular signalling may indeed be transduced at least in part, through lipid peroxidation products. In particular, 4-HNE (4-hydroxynonenal) and lipid hydroperoxides can modify the activity of membrane associated enzymes that play key roles in proliferative signal transduction [103, 186].

Although the importance of ROS in transducing proliferative stimuli has been studied extensively and has become clearer in recent years, many important details remain to be elucidated. One general conclusion is that superoxide radical and hydrogen peroxide may affect signalling molecules through the oxidative modification of redox-sensitive proteins. Such modifications of critical amino acids within the functional domain of proteins may occur in several ways, including the oxidation of cysteine residues, rearrangement of intramolecular disulphide linkages, and adduct formation. Another speculation is that low levels of superoxide and hydrogen peroxide, added exogeneously or generated endogenously, could exert their pro-proliferative effects

through causing alterations in the intracellular ratios of reduced-to-oxidized glutathione. In this model, changing these ratios might then alter the thiol/disulphide balance in a diversity of enzymes, regulating in the signalling cascades [21]. However, what remains to be determined is what specific changes and in what key proteins are exactly responsible for many of these effects.

1.12.3 Regulation of apoptosis

Although low levels of ROS can stimulate the growth of many cell lines, high levels of superoxide and hydrogen peroxide can have deleterious effects on mammalian cells and lead to cell death. Many of the chemical treatments that are known to evoke oxidative stress, are capable of inducing apoptosis [26, 91, 105, 180]. Conversely, many studies have shown that protection from apoptosis can be achieved by adding SOD, catalase, and/or hydroxyl radical scavenger [78]. These and previous observations make one ponder how ROS can affect signal cascades that lead to two opposite events, cellular proliferation and programmed cell death. The answer to this question is only partially known, but is addressed in the following sections.

1.12.3.1 Apoptosis pathways

Apoptosis or programmed cell death is a complex and multi-faced process that involves a plethora of signalling pathways which lead from the cell membrane all the way down to the nucleus. Not only is apoptosis required for eliminating redundant cells during development, but multicellular organisms destroy damaged, transformed, or infected cells by committing this "programmed suicide" [16, 104]. This process is

characterized by a variety of cellular changes, including loss of membrane phospholipids asymmetry, chromatin condensation, loss of mitochondrial integrity, and DNA cleavage. Apoptosis can be executed through two main pathways, the intrinsic (mitochondria) and the extrinsic (receptor-mediated) pathways [48], through the cascaded activation of caspases as shown in Figure 1.11. Caspases, a family of cysteine proteases, are central regulators of apoptosis. Initiator caspases, including caspases-8, -9, -10, and -12, are coupled to pro-apoptotic signals. Once activated, these caspases cleave and activate downstream effector caspases such as caspase-3, -6, and -7, which in turn cleave cytoskeletal and nuclear proteins leading to the induction of apoptosis. TNF-α and Fas ligand can both trigger the receptor-mediated pathway by interacting with TNF receptor and Fas receptor, respectively, while stimulation of the intracellular pathway is often caused by physiological changes such as virus infection, organelle malfunction, and DNA damage [143]. There is a cross talk between the two apoptosis pathways in which activated caspase-8 can cleave a Bcl-2 family member, the Bcl-2 interacting domain (Bid), which then translocates to the mitochondria. This leads to release of cytochrome c which amplifies the apoptotic signal by activating caspase-9.

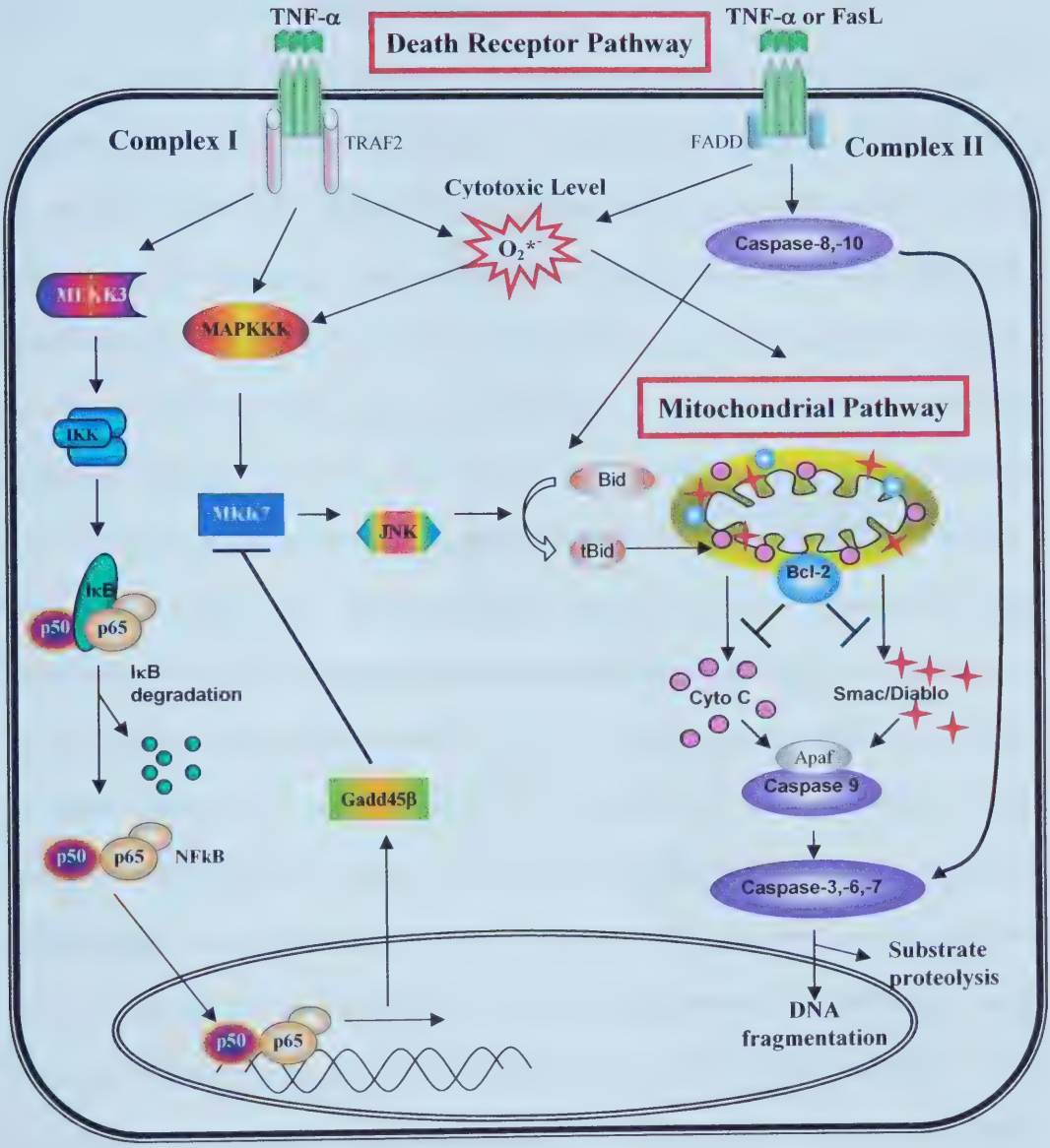

Figure 1.11. Extrinsic (receptor-mediated) and intrinsic (mitochondrial-mediated) apoptosis pathways. TNF-α engagement can lead to two separate events. Formation of complex I leads to NF-κB activation, Gadd45β induction, JNK inhibition and cell survival. Formation of complex II leads to caspase-8 or -10 mediated cleavage of Bid into tBid, which then targets mitochondria to induce cytochrome c release, and ultimately, activation of effector caspases (caspase-3, -6, or -7) resulting in cell death. Superoxide radical induced by receptor-mediated pathway can also trigger apoptosis. At cytotoxic level, this superoxide has been shown to target the mitochondrial- and JNK-mediated cell death. Adapted from Papa *et al.* [130].

1.12.3.2 ROS in induction of apoptosis

Apoptosis may be induced by stimuli as diverse as growth factor depletion, hyperthermia, chemotherapeutic agents, irradiation, and cytokines [16, 92, 174]. Recently, ROS have been proposed to be a common mediator for apoptosis [31, 73] since many agents that induce apoptosis are either oxidants or stimulators of cellular oxidative metabolism [26, 91, 180]. This role of ROS during apoptosis was initially proposed based upon the observation that a general inhibitor of apoptosis, a protein called B-cell lymphoma/leukemia-2 (Bcl-2), seems to have antioxidant activity [84]. Bcl-2 deleted mice showed symptoms related to oxygen-generated radical damage and eventually died [192]. Hockenberry *et al.* [83] subsequently showed that Bcl-2 protein does indeed protect from oxidative damage and further suggested that its membrane localization may not be necessary for the activity of Bcl-2 but rather, may serve to concentrate it at sites of oxidative damage. This would likely be the mitochondrial outer membrane. As the cytotoxic effects of high level of ROS are well documented, it is not surprising that manipulating the cellular redox status to create severe oxidative stress will cause oxidative damage and lead to cell death rather than proliferation. Furthermore, a variety of mitochondrial damaging agents are well known to stimulate superoxide generation, due to a switch from the normal 4-electron reduction of oxygen to a 1-electron reduction when cytochrome c is released from mitochondria [27]. Another superoxide-dependent targeting mechanism could also involve the activation of the mitochondrial permeability transition pore (MPT pore). MPT pore proteins contain critical thiols, which upon oxidation, can trigger pore opening and leads to the release of apoptosis inducing factors [82, 179, 201]. As shown on Figure 1.11, triggering of both TNF and Fas mediated

apoptosis pathways can induce high levels of production of superoxide radical, which can trigger JNK-mediated apoptosis as well as mitochondrial-mediated apoptosis [130]. Superoxide at high levels, besides being converted into hydrogen peroxide by SOD, can also spontaneously auto-dismutate into hydrogen peroxide. This hydrogen peroxide can trigger activation of caspases -3 and -9 [198] by damaging mitochondrial membranes, and thus releasing proapoptotic factors like cytochrome c, apoptosis inducing factors (AIF), and Smac/DIABLO [132]. Perhaps not surprisingly, adding catalase to break down the hydrogen peroxide prevents apoptosis [168], further suggesting that this oxidant plays a key role in mediating cell death.

1.12.3.3 ROS in prevention of apoptosis

At high levels it is clear that ROS can trigger apoptosis. However, at lower levels, molecules like superoxide seems to play an anti-apoptotic role more compatible with the pro-proliferative function described previously. For instance, overexpressing SOD1 in melanoma cells caused a significant increase in caspase activity and cell death upon exposure to a variety of anti-cancer agents [133]. This led the authors to suggest that superoxide had anti-apoptotic functions, and that depleting a cell of this radical created a pro-apoptotic environment. Conversely, inducing a prooxidant state using anti-sense SOD1 mRNA led to inhibition of caspase activity. It has also been noted that low levels of hydrogen peroxide protect human lymphoma cells from chemotherapy drug-induced apoptosis [102]. The role of ROS in regulating cell sensitivity to apoptosis thus appears to be common in a number of cells. More specifically, oxidative stress induced by increasing superoxide level has been shown to abrogate Fas-mediated apoptosis in

cells which are constitutively sensitive to Fas [38]. Conversely, overexpression of SOD1 increased tumour cell sensitivity to drug-induced cell death via caspase 3 activated pathway [134].

One pathway targeted by superoxide which might be responsible for these effects is that regulated by NFκB. Hyperoxia has been reported to inhibit apoptosis by a process that is mediated through degradation of IκB. This frees and activates NFκB [59]. Furthermore, TNF induced activation of NFκB is known to induce the expression of Gadd45β, an inhibitor of JNK-mediated apoptosis as shown in Figure 1.11 [130]. Inhibitor of apoptosis proteins (IAP), which can inhibit the activities of caspases -3, -7, and -9, have also been shown to be activated by NFκB [37, 191]. Superoxide has been shown to directly modulate the activity of caspases. All members of caspases incorporate the sequence QACXG. This motif contains the active site cysteine, which is sensitive to redox changes [182], and which can be oxidized to form a mixed disulphide. This impedes enzymatic activity and blocks the death signalling function [158]. These data suggest that irrespective of the trigger, caspase function could be modulated by changes in the intracellular redox state. This is supported by recent observations showing that caspase activity is optimal under reducing conditions [76]. For example, caspase-3 dependent apoptosis has been shown to require the reductive activity of both thioredoxin and glutathione [159, 169]. This reducing environment is also required by apoptosis signal-regulating kinase-1 (ASK-1), a MAPK that regulates the activation of kinases involved in mediating apoptosis signalling [71, 150].

A contrary view has been suggested by Pervaiz and Clement [132] who have hypothesized that superoxide could inhibit apoptosis signalling not by affecting redox

state, but rather by affecting intracellular pH. The reduction of molecular oxygen by the NADPH oxidase complex not only produces superoxide radical, but NADPH is oxidized into $NADP^+$ along with a proton (H^+), which is extruded from cell into extracellular space. This in turn favours an increase in cytosolic pH towards a more basic environment [164]. An increase in pH has also been shown to stimulate cells to divide [21]. Conversely, SOD was found to inhibit the increase in pH [164]. Hence, it can be generalized that survival is favoured with a mild sustainable increase in intracellular superoxide, whereas a decrease in superoxide and the accompanying cytosolic acidification create an environment permissible for efficient activation and execution of the apoptotic signal. Pervaiz and Clement [132] further proposed to use "reductive stress" when referring to ROS-mediated apoptosis.

1.13 Redox balance and cell signalling

What can be concluded from the above evidence is that changing the levels of ROS can have complex and pleiotropic effects on cell signalling. A mild prooxidant state seems to promote cellular proliferation while also suppress apoptosis. However, as the ROS levels further increase, the concentration of hydrogen peroxide will reach a level sufficient to activate apoptosis signals via ROS-mediated oxidative stress. This can induce programmed cell death. The exposure to even more severe oxidative stress, caused by even higher levels of ROS (especially hydroxyl radicals), will ultimately lead to necrotic death as a result of oxidative damage to biological molecules. However, the molecular mechanisms that underlie these effects are not yet clear and may even differ in different cell types. It is noteworthy that most studies concerning the effects of

superoxide and hydrogen peroxide have only examined cells and cellular responses *in vitro*. The effects may not necessarily be similar to the effects of ROS on cells *in vivo* or indeed the effects on multicellular organism. Moreover, the outcome of such experimental approaches will depend on the relative steady state levels of superoxide and/or hydrogen peroxide as well as to the relative cellular activities of antioxidant defence such as SODs, catalase, and/or glutathione redox systems. These interacting factors could explain, at least in part, the sometimes contradictory reports on the effects of ROS found in the literature. What is clear is that the survival of a cell requires an optimum balance of oxidants and antioxidants. As depicted in Figure 1.12, over the lifetime of a cell, ROS levels will fluctuate in response to intracellular as well as extracellular signals and this in turn, stimulates specific signalling cascades that regulate cell growth and cell death.

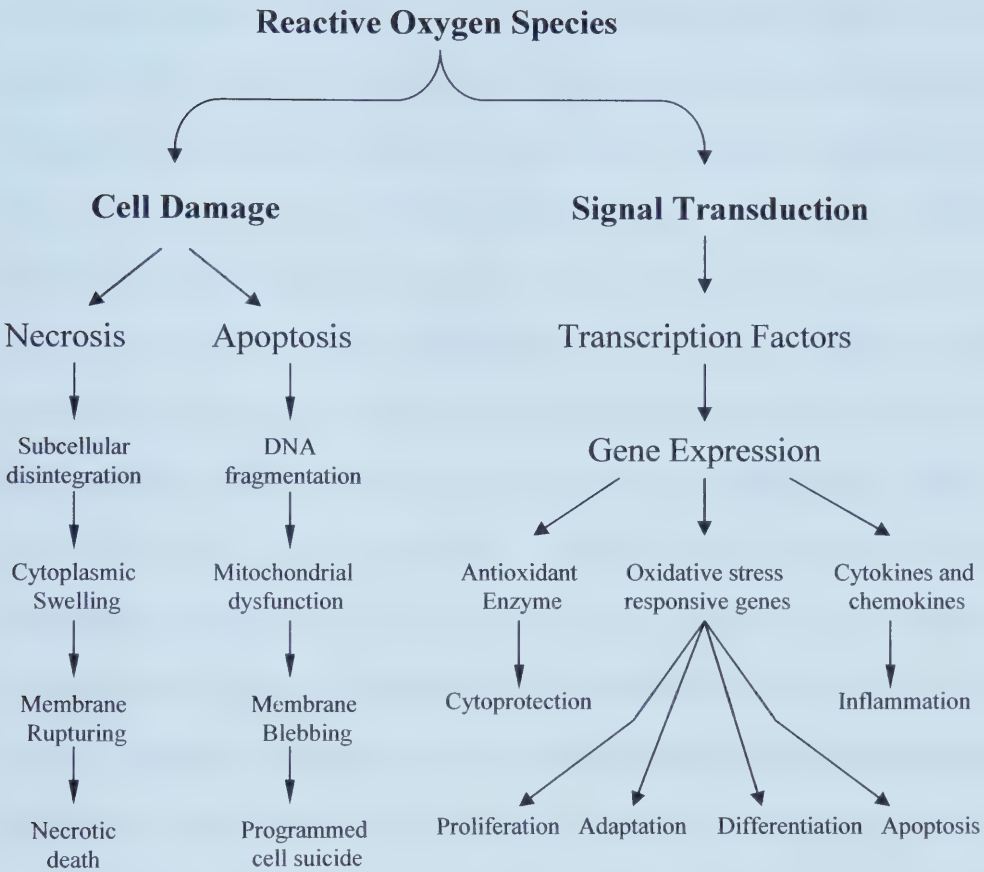

Figure 1.12. A general schematic showing the regulation of cell death and signal transduction pathways in response to reactive oxygen species. ROS may induce cell damage or initiate a cascade of signalling mechanisms that ultimately lead to proliferation, adaptation, differentiation, or apoptosis. The level of ROS in relation to the antioxidants will likely be a major factor in activating each pathway.

1.14 Leporipoxviruses and cellular proliferation

In view of the importance of regulation of cellular redox status in maintaining cellular homeostasis, is there any relevance of these redox regulation issues to Leporipoxvirus infections? Recall that both myxoma and Shope fibroma virus are tumourigenic poxviruses and they, like several other poxviruses, are well known to induce proliferative diseases. Besides Leporipoxviruses, Yaba tumour virus causes subcutaneous histocytomas in monkeys and humans [12] and molluscum contagiosum virus causes benign tumourlike epidermal lesions in humans [18]. To date, it is still not entirely clear how Leporipoxviruses induce cellular proliferation at the molecular level. Many poxviruses encode homologs of cellular epidermal growth factors (EGF) and transforming growth factor alpha (TGFα). This may be one factor that explains the proliferative phenotype [17, 36, 139, 185, 188]. However, what differentiates Leporipoxviruses, mollucum contagiosum, and Yaba tumour virus from other poxviruses is unclear. It has been suggested to be due to some unique property of their respective growth factors which differentiates them from the growth factor homologs encoded by cytolytic poxviruses [43, 117, 137]. The Shope fibroma virus epidermal growth factor (SFGF) and myxoma virus growth factor (MGF) share about 80% amino acid identity, but they are quite different from other members of the EGF family (less than 40% identity) [188]. In addition, there are no obvious putative membrane spanning hydrophobic regions located near the C termini in SFGF or MGF in comparison with vaccinia growth factor (VGF), TGFα, and cellular EGF precursors. This suggests that the biological activities of Leporipoxviral growth factors might be unique [129]. However, recombinant myxoma virus strains expressing heterologous growth factors

(SFGF, VGF, or rat TGFα) cause infections with clinical and histopathological disease features similar to that of wild type myxomatosis [129]. These observations imply that the proliferative features of Leporipoxvirus infections are not entirely due to characteristic properties of MGF and SFGF themselves. Moreover, mutant myxoma viruses lacking MGF are still able to induce tumour-like lesion in European rabbits although the animals showed marked attenuation of the disease syndrome [128, 129]. If the pro-proliferative effects of mild oxidative stress that are seen *in vitro* also hold true for the *in vivo* state, it raises the interesting question of whether Leporipoxvirus SOD1 homologs might serve some roles in modulating the redox state of infected cells and thus partially explain the tumourigenic phenotype characteristic of Leporipoxvirus infections.

1.15 Hypothesis and experimental rational

Based on what is known about bacterial SOD1s, one might predict that the primary role of Leporipoxviral SOD1 homologs is to protect viruses against the host anti-viral ROS systems. However, the viral enzymes are predicted to be inactive as dismutases based on amino acid sequence analysis. It seems very unlikely that these are just remnant genes which no longer serve any biological purpose. Closer examination of the sequences suggests that these viral proteins should still be able to form heterodimers with cellular SOD1 as well as with CCS due to the conservation of the residues involved in dimer/heterodimer interactions. Furthermore, most of the poxviruses sequenced to date encode some form of SOD1-like gene, implying that there exists a beneficial function of these genes which is retained by natural selection. In this regard it is striking that while they have clearly evolved substantially from some distant common ancestors,

both myxoma virus and SFV possess SOD1 homologs, that have retained 94% amino acid identity. This is not a degree of stability that would be expected of non-functional genes.

The diverse effects of ROS on cellular metabolism, discussed in the previous sections, have highlighted the crucial role played by SOD1 in regulating cellular homeostasis and in determining the ultimate fate of the cell. It is my *hypothesis* that these tightly regulated processes could serve as an ideal targeting point for Leporipoxvirus SOD1-like gene products, helping the virus to evade host defence mechanism by interfering with reactions catalyzed by cellular SOD1. In the following chapters I will present data illustrating that, this is, in fact, the case. In particular this research was intended to

- Study the physical and biochemical properties of the myxoma (M131R) and SFV (S131R) SOD1 homologs [these are collectively referred to as M/S131R];
- Investigate the effects of M/S131R on cellular SOD1 dismutation activity;
- Search for interactions between M/S131R and the cellular targets, SOD1 and CCS;
- Determine the intracellular distribution of M/S131R in infected cells;
- Perform structure/function studies on M/S131R using site-directed mutagenesis;
- Study the role served by S131R in promoting infection in rabbits; and
- Investigate a possible regulatory role for M/S131R in regulating cellular signalling, especially as it concerns apoptosis.

1.16 References

1. Aaronson SA (1991) Growth factors and cancer. Science 254: 1146-1153

2. Aguado B, Selmes IP, Smith GL (1992) Nucleotide sequence of 21.8 kbp of variola major virus strain Harvey and comparison with vaccinia virus. J Gen Virol 73 (Pt 11): 2887-902

3. Aguirre T, Matthjs G, Robberecht W, Tilkin P, and Cassiman IJ (1999) Mutational analysis of the Cu/Zn superoxide dismutase gene in 23 familial and 69 sporadic cases of amyotrophic lateral sclerosis in Belgium. Eur J Hum Genet 7: 599-602

4. Almazan F, Tscharke DC, Smith GL (2001) The vaccinia virus superoxide dismutase-like protein (A45R) is a virion component that is nonessential for virus replication. J Virol 75: 7018-29

5. Alroy I, Yarden Y (1997) The ErbB signalling network in embryogenesis and oncogenesis: signal diversification through combinatorial ligand-receptor interactions. FEBS Lett 410: 83-86

6. Ames BN, Shigenaga MK (1992) Oxidants are a major contributor to aging. Ann N Y Acad Sci 663: 85-96

7. Anderson RM, May RM (1982) Coevolution of hosts and parasites. Parasitology 85 (Pt 2): 411-26

8. Babior BM (1978) Oxygen-dependent microbial killing by phagocytes. N Engl J Med 298: 659-668

9. Baeuerle PA, Baltimore D (1996) NFkB: ten years after. Cell 87: 13-20

10. Barrett JW, Cao JJ, Hota-Mitchell S, McFadden G (2001) Immunomodulatory proteins of poxviruses. Seminar in Immunol. 13: 73-84

11. Bawden AL, Glassberg KJ, Diggans J, Shaw R, Farmerie W, Moyer RW (2000) Complete genomic sequence of the Amsacta moorei entomopoxvirus: analysis and comparison with other poxviruses. Virology 274: 120-39

12. Bearcroft WCG, Jamieson MF (1958) An outbreak of subcutaneous tumors in rhesus monkeys. Nature 182: 195-196

13. Behrend L, Henderson G, Zwacka RM (2003) Reactive oxygen species in oncogenic transformation. Biochem Soc Trans 31: 1441-1444

14. Benhar M, Engelberg D, Levitzki A (2002) ROS, stress-activated kinases and stress signalling in cancer. EMBO Rep 3: 420-425

15. Bize IB, Oberley LW, and Morris HP (1980) Superoxide dismutase and superoxide radical in Morris haepatomas. Cancer Res 40: 3686-3693

16. Blatt NB, Glick GD (2001) Signalling pathways and effector mechanisms pre-programmed cell death. Bioorg Med Chem 9: 1371-1384

17. Brown JP, Twardzik DR, Maquardt H, Todaro GJ (1985) Vaccinia virus encodes a polypeptide homologous to epidermal growth factor and transforming growth factor. Nature 313: 491-492

18. Brown ST, Nally JF, Kraus SJ (1981) Mollucum contagiosum. Sex Transm Dis 8: 227-234

19. Bruijin LI, Houseweart MK, Kato S, Anderson KL, Anderson SD, Ohama E, Reaume AG (1998) Aggregation and motor neuron toxicity of an ALS-linked SOD1 mutant independent from wild-type SOD1. Science 281: 1851-1854

20. Buller RM, Palumbo GJ (1991) Poxvirus pathogenesis. Microbiology Review 55: 80-121

21. Burdon RH (1995) Superoxide and hydrogen peroxide in relation to mammalian cell proliferation. Free Radic Biol Med 18: 775-794

22. Burdon RH, Gill V, Rice-Evans C (1989) Cell proliferation and oxidative stress. Free Radic Res Commun 7: 149-159

23. Burdon RH, Gill V, Rice-Evans C (1990) Oxidative stress and tumor cell proliferation. Free Radic Res Commun 11: 65-76

24. Burdon RH, Rice-Evans C (1989) Free radicals and the regulation of mammalian cell proliferation. Free Radic Res Commun 6: 345-358

25. Burgering BM, Coffer PJ (1995) Protein kinase B (c-Akt) in phosphatidylinositol-3-OH kinase signal transduction. Nature 376: 599-602

26. Buttke TM, Sandstorm PA (1994) Oxidative stress as a mediator of apoptosis. Immunol Today 15: 7-10

27. Cai J, Jones DP (1998) Superoxide in apoptosis. J Biol Chem 273: 11401-11404

28. Cameron C, Hota-Mitchell S, Chen L, Barrett J, Cao JX, Macaulay C, Willer D, Evans D, McFadden G (1999) The complete DNA sequence of myxoma virus. Virology 264: 298-318

29. Cao JX, Teoh ML, Moon M, McFadden G, Evans DH (2002) Leporipoxvirus Cu-Zn superoxide dismutase homologs inhibit cellular superoxide dismutase, but are not essential for virus replication or virulence. Virology 296: 125-35

30. Cardone MH, Roy N, Stennick HR, et al (1998) Regulation of cell death protease caspase-9 b phosphorylation. Science 282: 1318-1321

31. Carmody RJ, Cotter TG (2001) Signalling apoptosis: a radical approach. Redox Rep 6: 77-90

32. Casareno RLB, Waggoner D, and Gitlin JD (1998) The copper chaperone CCS directly interacts with copper/zinc superoxide dismutase. J. Biological chemistry 273: 23625-23628

33. Cerutti PA (1985) Prooxidant states and tumor promotion. Science 227: 375-381

34. Chakraborti S, Chakraborti T (1998) Oxidant-mediated activation of mitogen activated protein kinase and nuclear transcription factors in the cardiovascular system: A brief overview. cell signaling 10: 675-683

35. Chan TO, Rittenhous SE, Tsichlis PN (1999) AKT/PKB and other D3 phosphoinositide-regulated kinases: kinase activation by phoshatide-dependent phosphorylation. Ann Rev Biochem 68: 965-1014

36. Chang W, Upton C, Hu SL, Purchio AF, McFadden G (1987) The genome of Shope fibroma virus, a tumorigenic poxvirus, contains a growth factor gene with sequence similarity to those encoding epidermal growth factor and transforming growth factor alpha. Mol cell biol 7: 535-540

37. Chu ZL, McKinsey TA, Liu L, Gentry JJ, Malim MH, Ballard DW (1997) Suppression of tumour necrosis factor-induced cell death by inhibition of apoptosis c-IAP2 is under NF-kappaB control. Proc Natl Acad Sci U S A 94: 10057-10062

38. Clement MV, Stamenkovic I (1996) superoxide is a natural inhibitor of Fas mediated cell death. Embo J 15: 216-225

39. Cluskey S, Ramsden (2001) Mechanisms of neurodegeneration in amyotrophic lateral sclerosis. J Clin Pathol 54: 386-392

40. Crapo JD, Oury T, Rabouille C, Slot JW, Chang LY (1992) Copper, zinc superoxide dismutase is primarily a cytosolic protein in human cells. Proc Natl Acad Sci U S A 89: 10405-10409

41. Crawford D, Zbinden I, Amstad P, Cerutii P (1989) Oxidant stress induces the protooncogenes c-fos and c-myc in mouse epidermal cells. Oncogene 3: 27-32

42. Culotta VC, Klomp LWJ, Strain J, Casareno RLB, Krema B, Gitlin JD (1997) The copper chaperone for superoxide dismutase. J. Biological chemistry 272: 23469-23472

43. Dales S (1990) Reciprocity in the interaction between the poxviruses and their cells. Ann Rev Microbiol 44: 173-192

44. Dandona P, Thusu K, Cook S, Snyder B, Makowski J, Armstrong D, Nicotera T, (1996) Oxidative damage to DNA in diabetes mellitus. Lancet 347: 444-445

45. Datta SR, Dudek H, Tao X (1997) Akt phosphorylation of BAD couples survival signals to the cell-intrinsic death machinery. Cell 91: 231-241

46. Dickinson DA, Forman HJ (2002) Glutathione in defense and signaling: lessons from small thiol. Ann N Y Acad Sci 973: 488

47. Digiacomo RF, Mare CJ (1994) Viral disease, 2nd edn. Academic Press, San Diego

48. Dlamini Z, Mbita Z, Zungu M (2004) Genealogy, expression, and molecular mechanisms in apoptosis. Pharm Therapeutics 101: 1-15

49. Dubochet J, Adrian M, Richter K, Garces J, Wittek R (1994) Structure of intracellular mature vaccinia virus observed by cryoelectron microscopy. J Virol 68: 1935-41

50. Easterbrook KB (1966) Controlled degradation of vaccinia virions in vitro: an electron microscopy study. J. Ultrastruct. Res. 14: 484-496

51. Essani K, Dales S (1979) Biogenesis of vaccinia: evidence for more than 200 polypeptides in the virion. Virology 95: 385-394

52. Evans HJ, Steinman HM, and Hill RL (1974) Bovine rythrocyte superoxide dismutase. Isolation and characterization of tryptic, cyanogen bromide, and maleylated tryptic peptides. J. Biological chemistry 249: 7315-7325

53. Falconi M, Iovino M, Desideri A (1999) A model for the incorporation of metal from the copper chaperone CCS into Cu,Zn superoxide dismutase. Structure 7: 903-908

54. Fang FC, DeGroote MA, Foster JW, Baumler AJ, Ochsner U, Testerman Bearson S, Giard JC, Xu, Y, Campbell G, Laessig T (1999) Virulent Salmonella typhimurium has two periplasmic Cu,Zn-superoxide dismutases. Proc Natl Acad Sci U S A 96: 7502-7507

55. Fenner F (1996) Poxviruses. Lippincott-Raven, Philadelphia

56. Finkel T (1998) Oxygen radicals and signalling. Curr opin cell biol 10: 248-253

57. Fisher CL, Cabelli DE, Tainer JA, Halliwell RA, Getzoff ED (1994) The role of arginine 143 in the electrostatics and mechanism of Cu,Zn superoxide dismutase: computational and experimental evaluation by mutational analysis. PROTEINS: Structure, Functions, and Genetics 19: 24-34

58. Floyd RA (1990) Role of oxygen free radicals in carcinogenesis and brain ischemia. Faseb J 4: 2587-2597

59. Franek WR, Horowitz S, Stansberry L, Kazzaz JA, Koo HC, Li Y (2001) Hyperoxia inhibits oxidants-induced apoptosis in lung epithelial cells. J Biol Chem 276: 569-575

60. Frank S, Kampfer H, Podda M, Kaufmann R, Pfeilshifter J (2000) Identification of copper/zinc superoxide dismutase as a nitric oxide-regulated gene in human (HaCaT) keratinocytes: implications for keratinocyte proliferation. Biochem J 346: 719-728

61. Gardner PR, Fridovich I (1991) Superoxide sensitivity of the Escherichia coli aconitase. J Biol Chem 266: 19328-33

62. Gardner PR, Fridovich I (1992) Inactivation-reactivation of aconitase in Escherichia coli. A sensitive measure of superoxide radical. J Biol Chem 267: 8757-63

63. Gaudette M, Hirano M, Siddique T (2000) Current status of SOD1 mutations in Familial amyotrophic lateral sclerosis. Amyotroph Lateral Scler Other Motor Neuron Disord 1: 83-89

64. Getzoff ED, Cabelli DE, Fisher CL, Parge HE, Viezzoli MS, Banci L, Hallewell RA (1992) Faster superoxide dismutase mutants designed by enhancing electrostatic guidance. Nature 358: 347-351

65. Glerum DM, Shtanko A, Tzagoloff A (1996) Characterization of COX17, a yeast gene involved in copper metabolism and assembly of cytochrome oxidase. J. Biological chemistry 271: 14504-14509

66. Goebel SJ, Johnson GP, Perkus ME, Davis SW, Winslow JP, Paoletti E (1990) The complete DNA sequence of vaccinia virus. Virology 179: 247-66, 517-63

67. Griendling K, Ushio-Fukai M (2000) Reactive oxygen species as mediators of angiotensin II signaling. Regultory Peptides 91: 21-27

68. Griendling KK, Minieri CA, Ollerrenshaw JD, Alexander RW (1994) Angiotensin II stimulates NADH and NADPH oxidase activity in cultured vascular smooth muscle cells. Circ Res 74: 1141-1148

69. Gupta A, Rosenberger SF, Bowden GT (1999) Increased ROS levels contribute to elevated transcription factor and MAP kinase activities in malignantly progressed mouse keratinocyte cell lines. Carcinogenesis 20: 20643-2073

70. Gurney ME, Pu H, Chiu AY, Dal Canto MC, Polchow CY, Alexander DD (1994) Motor neuron degeneration in mice that express a human Cu,Zn superoxide dismutase mutation. Science 264: 1772-1775

71. Haddad JJ (2002) The involvement of L-g-glutamyl-L-cyteinyl-glycine (glutathione/GSH) in the mechanism of redox signaling mediating $MAPK^{p38}$-dependent regulation of pro-inflammatory cytokine production. Biochem Pharmacol 63: 305-320

72. Haddad JJ (2004) Oxygen sensing and oxidant/redox-related pathways. Biochem Biophys Res Commun 316: 969-977

73. Haddad JJ (2004) Redox and oxidant-mediated regulation of apoptosis signaling patways: immuno-pharmaco-redox conception of oxidative siege versus cell death commitment. Int Immunopharmacology 4: 475-493

74. Haddad JJ, Land SC (2000) O2-voked regulation of HIF-1a and NFkB in perinatal lung epithelium requires glutathione biosynthesis. Am J Physiol, Lung Cell Mol Physiol 278: L492-503

75. Haddad JJ, Olver RE, Land SC (2000) Antioxidant/pro-oxidant equilibrium regulates HIF-1a and NFkB redox sensitivity: evidence for inhibition by glutathione oxidation in alveolar epithelial cells. J. Biological chemistry 275: 21130-21139

76. Haendeler J, Weiland U, Zeiher A, and Dimmeler S (1997) Effects of redox-related congeners of NO on apoptosis and caspase- activity. Nitric Oxide 1: 282-293

77. Hall LT, Sanchez RJ, Holloway SP, Zhu H, Stine JE, Lyons TJ, Demler B, Schirf V, Hansen JC, Nersissian AM, Valentine JS, Hart PJ (2000) X-ray crystallographic and analytical ultracentrifugation analyses of truncated and full-length yeast copper chaperone for SOD (LYS7): a dimer-dimer model of LYS7-SOD association and copper delivery. Biochem. 39: 3611-3623

78. Halliwell B, Gutteridge JM (1990) Role of radicals and catalytic metal ions in human disease: an overview. Methods Enzymol 186: 1-85

79. Halliwell B, Gutteridge JM (1999) Free Radicals in Biology and Medicine, 3 edn. Oxford University Press Inc., New York

80. Harman DJ (1956) Aging: a theory based on free radical and radiation chemistry. Gerontology 11: 298-300

81. Hastings JW (1971) Light to hide by: ventral luminescence to camouflage the silhouette. Science 173: 1016-11019

82. Hirsch T, Marzo I, Kroemer G (1997) Role of the mitochondrial permeability transition pore in apoptosis. Biosci Rep 17: 67-76

83. Hockenbery DM, Oltvai ZN, Yin XM, Milliman CL, Korsmeyer SJ (1993) Bcl-2 functions in an antioxidant pathway to prevent apoptosis. Cell 75: 241-251

84. Hokenbery DM, Oltvai ZN, Yin XM, Milliman CL, Korsmeyer SJ (1993) Bcl-2 functions in an antioxidant pathway to prevent apoptosis. cell 75: 241-251

85. Huang TT, Carlson EJ, Epstein LB, Epstein CJ (1992) The role of superoxide anions in the establishment of an interferon-a-mediated antiviral state. Free Radic Res Commun 17: 59-72

86. Ikebuchi Y, Masumoto K, Tasaka K, Koike K, Kasahara K, Miyake A, Tanizawa O (1991) Superoxide anion increases intracellular pH, intracellular free calcium and arachidonate release in human amnion cells. J Biol Chem 266: 13233-13237

87. Irani K, Xia Y, Zweier JL, Sollot SJ, Der CJ, Fearon ER, Sundaresan M, Finkel T, Goldschmidt-Ctermont PJ (1997) Mitogenic signaling mediated by oxidants in Ras-transformed fibroblasts. Science 275: 1649-1651

88. Jenner P (1994) Oxidative damage in neurodegenerative disease. Lancet 344: 796-798

89. Johnston JA, Dalton MJ, Gurney ME, Kopito RR (2000) Formation of high molecular weight complexes of mutant Cu/Zn superoxide dismutase in a mouse model for familial amyotrophic lateral sclerosis. Proc Natl Acad Sci U S A 97: 12571-12576

90. Jones RD, Hancock JT, Morice AH (2000) NADPH oxidase: a universal oxygen sensor? Free Radic Biol Med 29: 416-424

91. Kannan K, Jain SK (2000) Oxidative stress and apoptosis. Pathophysiology 7: 153-163

92. Kaufmann SH, Hengartner MO (2001) Programmed cell death: alive and well in the new millenium. Trends Cell Biol 11: 526-534

93. Kinnula VL, Crapo JD (2004) Superoxide Dismutases in malignant cells and human tumors. Free Radic Biol Med 36: 718-744

94. Klug D, Rabani J, Fridovich I (1972) A direct demonstration of the catalytic action of superoxide dismutase through the use of pulse radiolysis. J Biol Chem 247: 4839-42

95. Korshunov SS, Imlay JA (2002) A potential role for periplasmic superoxide dismutase in blocking the penetration of extenal superoxide into the cytosol of Gram-negative bacteria. Mol Microbiol 43: 95-106

96. Lamb AL, Torres AS, O'Halloran TV, Rosenzweig AC (2000) Heterodimer formation between superoxide dismutase and its copper chaperone. Biochem. 39: 14720-14727

97. Lamb AL, Torres AS, O'Halloran TV, Rosenzweig AC (2001) Heterodimeric structure of superoxide dismutase in complex with its metallochaperone. Nature 8: 751-755

98. Lamb AL, Wenimont AK, Pufahl RA, Cullota VC, O'Halloran TV, Rosenzweig AC (1999) Crystal structure of the copper chaperone for superoxide dismutase. Nat. Struct. Biol. 6: 724-729

99. Lamb AL, Wernimont AK, Pufahl RA, Cullota VC, O'Halloran TV, Rosenzweig A (2000) Crystal structure of the second domain of the human copper chaperone for superoxide dismutase. Biochem. 39: 1589-1595

100. Lang D, Mosfer SI, Shakesby A, Donaldson,F, Lewis MJ (2000) Coronary microvascular endothelial cell redox state in left ventricular hypertrophy: the role of angiotensin II. Circ Res 86: 463-469

101. Langford PR, Kroll JS (1997) Distribution, cloning, characterization and mutagenesis of sodC, a gene encoding copper/zinc superoxide dismutase, a potential determinant of virulence, in Haemophilus ducreyi. FEMS Immunol Med Microbiol 17: 235-242

102. Lee YJ, Shacter E (1999) Oxidative stress inhibits apoptosis in human lymphoma cells. J Biol Chem 274: 19792-19798

103. Leonarduzzi GAM, Basaga H, Chiarpotto E, Sevanian A, Poli G (2000) Lipid oxidation products in cell signaling. Free Radic Biol Med 28: 1370-1378

104. Li H, Yuan J (1999) Deciphering the pathways of life and death. Curr opin cell biol 11: 261-266

105. Li J, Li PF, Dietz R, von Harsdorf R (2002) Intracellular superoxide induces apoptosis in VSMCs: Role of mitochondrial membrane potential, cytochrome c and caspases. Apoptosis 7: 511-517

106. Lin SJ, Pufahl RA, Dancis A, O'Halloran TV, Cullota VC (1997) A role for the Saccharomyces cerevisae ATX1 gene in copper trafficking and iron transport. J. Biological chemistry 272: 9215-9220

107. Liu S, Lin X, Shi D, Cheng J, Wu C, Zhang Y (2002) Reactive oxygen species stimulated human hepatoma cell proliferation via cross-talk between PI3-K/PKB and JNK signalling pathways. Arch Biochem Biophys 406: 173-182

108. Lu Z, Li Y, Que Q, Kutish GF, Rock DL, Van Etten JL (1996) Analysis of 94kb of the chlorella virus PBCV-1 330-kb genome: map positions 88 to 182. Virology 216: 102-123

109. Malinowski DP, Fridovich I (1979) Chemical modification of arginine at the active site of the bovine erythrocyte superoxide dismutase. Biochem. 18: 5909-5917

110. Marklund SL, Holme E, Hellner L (1982) Superoxide dismutase in extracellular fluids. Clin Chim Acta 126: 41-51

111. Massung RF, Esposito JJ, Liu LI, Qi J, Utterback TR, Knight JC, Aubin L, Yuran TE, Parsons JM, Loparev VN, et al. (1993) Potential virulence determinants in terminal regions of variola smallpox virus genome. Nature 366: 748-51

112. McCord JM, Fridovich I (1969) Superoxide dismutase. An enzymic function for erythrocuprein (hemocuprein). J Biol Chem 244: 6049-55

113. McCord JM (1974) Free radicals and inflammation: protection of synovial fluid by superoxide dismutase. Science 185: 529-31

114. McCord JM (1993) Oxygen-derived free radicals. New Horiz 1: 70-6

115. McCord JM (2000) The evolution of free radicals and oxidative stress. Am J Med 108: 652-9

116. McCord JM, Turrens JF (1994) Mitochondrial injury by ischemia and reperfusion. Curr. Topis Bioenerg. 17: 173-195

117. McFadden G (1988). Martinus-Nijhoff Pubs., Boston

118. McNee W (2001) Oxidative stress and regulation of glutahione in lung inflammation. Eur J Pharmacol 49: 195-207

119. Meister A (1994) Glutathione, ascorbates, and cellular protection. Cancer Res 54: 1969

120. Moghal N, Sternberg PW (1999) Multiple positive and negative regulators of signalling by the EGF-receptor. Curr opin cell biol 11: 190-196

121. Moss B, Smith GL, Mackett M (1983) Use of vaccinia virus as an infectious molecular cloning and expression vector. Gene Amplif Anal 3: 201-13

122. Moss B (1996) Poxviridae: the viruses and their replication. Lippincott-Raven Press, New York

123. Moss B, Carroll MW, Wyatt LS, Bennink JR, Hirsch VM, Goldstein S, Elkins WR, Fuerst TR, Lifson JD, Piatak M, Restifo NP, Overwijk W, Chamberlain R, Rosenberg SA, Sutter G (1996) Host range restricted, non-replicating vaccinia virus vectors as vaccine candidates. Adv Exp Med Biol 397: 7-13

124. Murrell GAC, Francis MJO, Bromley L (1989) Oxygen free radicals stimulate fibroblast proliferation. Biochem Soc Trans 17: 484-484

125. Murrell GAC, Francis MJO, Bromley L (1990) Modulation of fibroblast proliferation by oxygen free radicals. Biochem J 265: 659-665

126. Nose K, Shibanuma M, Kikuchi K, Kazeyana H, Sakiyama S, Kuroki T (1991) Transcriptional activities of early response genes in a mouse osteoblastic cell line. Eur J Biochem 201: 99-106

127. Okado-Matsumoto A, Fridovich I (2001) Subcellular distribution of superoxide dismutases (SOD) in rat liver: Cu,Zn-SOD in mitochondria. J Biol Chem 276: 38388-93

128. Opgenorth A, Graham K, Nation N, Strayer D, McFadden G (1992) Deletion analysis of two tandemly arranged virulence genes in myxoma virus, M11L and myxoma growth factor. J Virol 66: 4720-31

129. Opgenorth A, Nation N, Graham K, McFadden G (1993) Transforming growth factor alpha, Shope fibroma growth factor, and vaccinia growth factor can replace myxoma growth factor in the induction of myxomatosis in rabbits. Virol. 192: 701-709

130. Papa S, Zazzeroni F, Pham CG, Bubici C, Franzoso G (2004) Linking JNK signaling to NF-kB: a key to survival. J Cell Sci 117: 5197-5208

131. Perkus ME, Goebel SJ, Davis SW, Johnson GP, Norton EK, Paoletti E (1991) Deletion of 55 open reading frames from the termini of vaccinia virus. Virology 180: 406-10

132. Pervaiz S, Clement MV (2001) A permissive apoptotic environment: function of a decrease in intracellular superoxide anion and cytosolic acidification. Biochem Biophys Res Commun 290: 1145-1150

133. Pervaiz S, Clement MV (2004) Tumor intracellular redox status and drug resistance--serendipity or a causal relationship? Curr Pharm Des 10: 1969-1977

134. Pervaiz S, Ramalingam K, Hirpara JL, Clement MV (1999) Superoxide anion inhibits drug-induced tumor cell death. FEBS Lett 459: 343-348

135. Petrone WF, English DK, Wong K, McCord JM (1980) Free radicals and inflammation: superoxide-dependent activation of a neutrophil chemotactic factor in plasma. Proc Natl Acad Sci U S A 77: 1159-63

136. Phillips JP, Cambell SD, Michaud D, Charbonneau M, Hilliker AJ (1989) Null mutation of copper/zinc superoxide dismutase in *Drosophila* confers hypersensitivity to paraquat and reduced longevity. Proc. Natl. Acad. Sci. 86: 2761-2765

137. Pogo BG, Obom KM, Haddad J, Holland JG (1989) Shope fibroma: a model system to study tumorigenesis by poxviruses. Ann N Y Acad Sci 567: 222-233

138. Poli G, Leonarduzzi G, Chiarpotto (2004) Oxidative stress and cell signalling. Curr medicinal chemistry 11: 1163-1182

139. Porter CD, Archard LC (1987) Characterization and physical mapping of Molluscum contagiosu virus DNA and location of a sequence capable of encoding a conserved domain of epidermal growth factor. J Gen Virol 68: 673-682

140. Rae TD, Schmidtt PJ, Pufahl RA, Cullota VC, O'Halloran TV (1999) Undetectable intracellular free copper: the requirement of a copper chaperone for superoxide dismutase. Science 284: 805-808

141. Rae TD, Torres AS, Pufahl RA, O'Halloran, TV (2001) Mechanism of Cu,Zn superoxide dismutase activation by the human metallochaperone CCS. J. Biological chemistry 276: 5166-5176

142. Reaume AG, Elliot JL, Hoffman EK (1996) Motor neurons in Cu/Zn superoxide dismutase-deficient mice develop normally but exhibit enhanced cell death after axonal injury. Nat Genet 13: 43-47

143. Reed JC (2000) Mechanisms of apoptosis. Am J Pathol 157: 1415-1430

144. Richardson JS, Thomas KA, Rubin BH, Richardson DC (1975) Crystal structure of bovine Cu,Zn superoxide dismutase at 3A resolution: chain tracing and metal ligands. Proc Natl Acad Sci U S A 72: 1349-1975

145. Riesen DJ, Stern DF (1998) Specificity within the EGF family/ErbB receptor family signalling network. Bioessays 20: 41-48

146. Robinson MJ, Cobb MH (1997) Mitogen-activated protein kinase pathways. Curr opin cell biol 9: 180-186

147. Ross J (1972) Myxomatosis and the rabbit. Br Vet J 128: 172-6

148. Ross J, Sanders MF (1984) The development of genetic resistance to myxomatosis in wild rabbits in Britain. J Hyg (Lond) 92: 255-61

149. Rypniewski WR, Mangani S, Bruni B, Orioli PL, Casati M, Wilson KS (1995) Crystal structure of reduced bovine erythrocyte superoxide dismutase at 1.9A resolution. J. Mol. Biol. 251: 282-296

150. Saitoh M, Nishitoh H, Fujii M, Takeda K, Tobiume K, Sawada Y et al. (1998) Mammalian thiolredoxin is a direct inhibitor of apoptosis signal-regulating kinases (ASK)-1. Embo J 17: 2596-2606

151. Sako Y, Minoghchi S, Yanagida T (2000) Single molecule imaging of EGFR signalling on the surface of living cells. Nat Cell Biol 2: 168-172

152. Schmidtt PJ, Rae TD, Pufahl RA, Hamma T, Strain J, O'Halloran TV, Cullota VC (1999) Multiple protein domains contribute to the action f the copper chaperone for superoxide dismutase. J. Biological chemistry 274: 23719-23725

153. Schreck R, Albermann K, Baeuerle PA (1992) Nuclear factor kappa B: an oxidative stress-responsive transcription factor of eukaryotic cells. Free Radic Res Commun 17: 221-237

154. Scott CB, Holdbrook R, Sell S (1981) Cell-mediated immune response to Shope fibroma virus-induced tumors in adult rabbits. J Natl Cancer Inst 66: 681-9

155. Seet BT, Johnston JB, Brunetti CR, Barrett JW, Everett H, Cameron C, Sypula J, Nazarian SH, Lucas A, McFadden G (2003) Poxviruses and immune evasion. Annu Rev Immunol 21: 377-423

156. Seet BT, McCaughan CA, Handel TM, Mercer A, Brunetti C, McFadden G, Fleming SB (2003) Analysis of an orf virus chemokine-binding protein: Shifting ligand specificities among a family of poxvirus viroceptors. Proc Natl Acad Sci U S A 100: 15137-42

157. Sell S, Scott CB (1981) An immunohistologic study of Shope fibroma virus in rabbits: tumor rejection by cellular reaction in adults and progressive systemic reticuloendothelial infection in neonates. J Natl Cancer Inst 66: 363-73

158. Sen CK (2000) Celullar thiols and redox-regulated signal transduction. Curr Top Cell Reg 36: 1-30

159. Sen CK, Roy S (2001) Redox control of caspases. Environ Toxicol Pharmacol 10: 215-220

160. Senkevich TG, Bugert JJ, Sisler JR, Koonin EV, Darai G, Moss B 1996 (1996) Genome sequence of a human tumorigenic poxvirus: prediction of specific host response-evasion genes. Science 273: 813-816

161. Shchelkunov SN, Massung RF, Esposito JJ (1995) Comparison of the genome DNA sequences of Bangladesh-1975 and India-1967 variola viruses. Virus Res 36: 107-18

162. Shchelkunov SN, Totmenin AV, Loparez VN, Safronov PF, Gutorov VV, Chizhikov VE, Knight JC, Parsons JM, Massung RF, and Esposito JJ (2000) Alastrim smallpox variola minor virus genome DNA sequences. Virology 266: 361-386

163. Shibanuma M, Kuroki T, Nose M (1988) Induction off DNA replication and expression of protooncogenes c-myc and c-fos in quiescent Balb/3T3 cells by xanthine-xanthine oxidase. Oncogene 3: 17-21

164. Shibanuma M, Kuroki T, Nose M (1988) Superoxide as a signal for increase in intracellular pH. J cell physiol 136: 379-383

165. Shibanuma M, Kuroki T, Nose M (1990) Stimulation by hydrogen peroxide of DNA synthesis competence family gene expression and phosphorylation of a specific protein in quiescent Balb/3T3 cells. Oncogene 3: 27-32

166. Shope RE (1993) A filterable virus causing a tumor-like condition in rabbits and its relationship to virus myxomatosum. J. Exp. Med. 56: 803-822

167. Sies H (1885) Oxidative stress: Introductory remarks. Academic Press, USA

168. Simon HU, Haj-Yehia A, Levi-Schaffer F (200) Role of reactive oxygen species (ROS) in apoptosis induction. Apoptosis 5: 415-418

169. Sioni Y, Kahlos K, Napankangas U, Kaarteenacho-Wiik R, Saily M, Koistinen P et al. (2001) Wide-spread expression of thiol-redoxin and thioredoxin reductase in non-small cell lung carcinoma. Clin Cancer Res 7: 1750-1757

170. Smith GL, Chan YS, Howard ST (1991) Nucleotide sequence of 42 kbp of vaccinia virus strain WR from near the right inverted terminal repeat. J Gen Virol 72 (Pt 6): 1349-76

171. Soto C (2001) Protein misfolding and disease; protein refolding and therapy. FEBS Lett 498: 204-207

172. Steinman HM (1982) Superoxide dismutases: protein chemistry and structure-function relationship. CRP Press, Inc., Florida

173. Stirpe F, Higgins T, Tazzori PL, Rosengurt E (1991) Stimulation by xanthine oxidase of 3T3 Swiss fibroblasts and human lymphocytes. Exp Cell Res 192: 635-638

174. Strasser A, O'Connor, L, Dixit VM (2000) Apoptosis signalling. Annu Rev Biochem 69: 217-245

175. Strayer DS, Cabirac G, Sell S, Leibowitz JL (1983) Malignant rabbit fibroma virus: observations on the culture and histopathologic characteristics of a new virus-induced rabbit tumor. J Natl Cancer Inst 71: 91-104

176. Sturtz LA, Diekert K, Jensen LT, Lill R, Culotta VC (2001) A fraction of yeast Cu,Zn-superoxide dismutase and its metallochaperone, CCS, localize to the intermembrane space of mitochondria. A physiological role for SOD1 in guarding against mitochondrial oxidative damage. J Biol Chem 276: 38084-9

177. Sun Y, Oberley LW, Oberley TD, Elwell JH, Sierra-Rivera E (1993) Lowered antioxidant enzymes in spontaneously transformed embryonic mouse liver cells in culture. Carcinogenesis 14: 1457-1463

178. Sundaresa M, Yu ZX, Ferrans VJ, Irani K, Finkel T (1995) Requirement for generation of H2O2 for platelet-derived growth factor signal transduction. Science 270: 296-299

179. Susin SA, Zamzami N, Castedo M, Hirsch T, Marchetti P, Macho A, Daugas E, Geuskes M, Kroemer G (1996) Bcl-2 inhibits the mitochondrial release of an apoptogenic protease. J. Exp. Med. 184: 1331-1341

180. Tan S, Sagara Y, Liu Y, Maer P, Schubert D (1998) The regulation of reactive oxygen species production during programmed cell death. J cell biol 141: 1423-1432

181. Tartaglia J, Pincus S, Paoletti E (1990) Poxvirus-based vectors as vaccine candidates. Crit Rev Immunol 10: 13-30

182. Thornberry NA, Lazebnik Y (1998) Caspases: enemies within. Science 281: 1312-1316

183. Tomalski MD, Eldridge R, Miller LK (1991) A baculovirus homolog of a Cu/Zn superoxide dismutase gene. Virology 184: 149-61

184. Tulman ER, Afonso CL, Lu Z, Zsak L, Kutish GF, Rock DL (2004) The genome of canarypox virus. J Virol 78: 353-66

185. Twardzik DR, Ranchalis JE, Moss B, Todaro GJ (1987) Vaccinia growth factor: newest member of the family of growth modulators which utilize the membrane receptor for EGF. Acta Neurochir Suppl (Wien) 41: 104-9

186. Uchida K SM, Naito Y, Torii Y, Nakamura Y, Osawa T (1999) Activation of stress signaling pathways by the end product of lipid peroxidation. 4-Hydroxy-2-nonenal is a potential inducer of intracellular peroxide production. J Biol Chem 274: 2234-2242

187. Upton C, Opgenorth A, Traktman P, McFadden G (1990) Identification and DNA sequence of the Shope fibroma virus DNA topoisomerase gene. Virology 176: 439-47

188. Upton C, Macen JL, McFadden G (1987) Mapping and sequencing of a gene from myxoma virus that is related to the encoding epidermal growth factor and transforming growth factor alpha. J virol 61: 1271-1275

189. Valentine JS, Pantoliano MW (1981). Wiley-Interscience, New York

190. Valentine SJ, Gralla EB (1997) Delivering copper inside yeast and human cells. Science 278: 817-818

191. Van Antwerp DJ, Martin SJ, Kafri T, Green DR, Verma IM (1996) Suppression of TNF-alpha-induced apoptosis by NF-kappaB. Science 274: 787-789

192. Veis DJ, Sorenson CM, Shutter JR, Korsmeyer SJ (1993) Bcl-2 deficient mice demonstrate fulminant lyphoid apoptosis, polycystic kidneys and hypopigmented hair. Cell 75: 229-240

193. Wang X, Martindale JL, Liu Y, and Holbrook NJ (1998) The cellular response to oxidative stress: influences of mitogen-activated protein kinases signalling pathways on cell survival. Biochem J 33: 291-300

194. Waskiewicz AJ, Cooper JA (1995) Mitogen and stress response pathways: MAP kinase cascades and phosphatase regulation in mammalians and yeast. Curr opin cell biol 7: 798-805

195. Weisiger RA, Fridovich I (1973) Mitochondrial superoxide dismutase: site of synthesis and intramitochondrial localization. J Biol Chem 248: 4793-4796

196. Willer DO, McFadden G, Evans DH (1999) The complete genome sequence of shope (rabbit) fibroma virus. Virology 264: 319-43

197. Xia Z, Dickns M, Raingeaud J, Davis RJ, Greenberg ME (1995) Opposing effects of ERK and JNK-p38 MAP kinases on apoptosis. Science 270: 1326-1331

198. Yamakawa H, Ito Y, Naganawa T, Banno Y, Nakashima S, Yoshimura S, Sawada M, Nishimura Y, Nozawa Y, Sakai N (2000) Activation of caspase 9 and 3 during hydrogen peroxide induced apoptosis of PC12 cells independent of ceramide formation. Neurol Res 22: 556-564

199. Zachertowska A, Brewer D, Evans DH (2004) MALDI-TOF mass spectroscopy detects the capsid structural instabilities created by deleting the myxoma virus cupro-zinc SOD1 homolog M131R. J Virol Methods 122: 63-72

200. Zimmerman R, Cerutti P (1984) Active oxygen acts as a promoter of transformation in mouse embryo C3H/10T1/2/C18 fibroblast. Proc Natl Acad Sci U S A 81: 2085-2087

201. Zoratti M, Szabo I (1995) The mitochondrial permeability transition. Biochim Biophys Acta 1241: 139-176

CHAPTER 2 – LEPORIPOXVIRUS M/S131R INHIBIT CELLULAR SOD1 BUT ARE NOT ESSENTIAL FOR VIRUS REPLICATION OR VIRULENCE *

Published in the *Virology* journal

Preface

A version of this chapter has been accepted for publication. Cao JC, Teoh MLT, Moon M, McFadden G, and Evans DHE. 2002. *Virology*. 296:125-35. The data presented in this chapter is a result of a collaboration work with Dr. Cao and Dr. McFadden from University of Western Ontario. Although I shared the first authorship with Dr. Cao, most data presented were generated by experiments carried out by me, except the construction of M131RΔ myxoma virus and the animal study, which were done by Dr. Cao. Miss M. Moon started out this project by generating the recombinant vaccinia viruses for the overexpression of S131R.

* Reprinted from *Virology*, Vol 296, Jing Xin Cao, Melissa L.T. Teoh, Mijin Moon, Grant McFadden, and David H. Evans, Leporipoxvirus Cu-Zn Superoxide Dismutase Homologs Inhibit Cellular Superoxide Dismutase, but are not Essential for Virus Replication or Virulence, pp 125-135, Copyright (2005), with permission from Elservier.

Leporipoxvirus Cu-Zn Superoxide Dismutase Homologs Inhibit Cellular Superoxide Dismutase, but are not Essential for Virus Replication or Virulence

Jing Xin Cao[1,3,4], Melissa L.T. Teoh[2,4], Mijin Moon[2], Grant McFadden[1], and David H. Evans[2]*

[1]Robarts Research Institute and Department of Microbiology
The University of Western Ontario
London, Ontario, N6G 2V4

[2]Department of Molecular Biology & Genetics
The University of Guelph
Guelph, Ontario, N1G 2W1
CANADA

Running title: Leporipoxvirus Cu-Zn Superoxide Dismutase

*Corresponding Author: Phone (519) 824-4120 ext. 2575; Fax (519) 837-2075.

Correspondent Footnote: Please address all correspondence to Dr. D. Evans, Department of Molecular Biology & Genetics, University of Guelph, Guelph, Ontario, N1G 2W1, Canada; Phone (519) 824-4120 ext. 2575; E-mail dhevans@uoguelph.ca.

[3]Present Address: National Microbiology Laboratory, 1015 Arlington Street, Winnipeg, MB, R3E 3R2.

[4]These authors contributed equally to this work.

2.1 INTRODUCTION

It has long been known that reactive oxygen species (ROS) are important components of cellular anti-microbial or anti-viral defence mechanisms. Interestingly, many viruses including poxviruses, encode genes that may play a role in regulating the redox status of infected cells. In poxviruses, examples of these genes include Orthopoxvirus and Leporipoxvirus glutaredoxin homologs, Molluscipoxvirus and Fowlpoxvirus glutathione peroxidase homologs, and widely distributed viral copper-zinc superoxide dismutase homologs (SOD1). The functional implications of these genes are still widely unclear. Some of these proteins have been shown to play a role in virus replication and assembly, while others may protect replicating viruses from harmful effects of ROS produced either endogenously or by phagocytic cells during the course of viral infection [21].

The biology of some of these genes is derived from previous biochemical and genetic investigations *in vitro*. Vaccinia encodes two glutaredoxin gene homologs (G4L and O2L) which possess thioltransferase and dehydroascorbate reductase activity, respectively [3, 15]. G4L homologs are widely distributed amongst vertebrate poxviruses but O2L-like genes are encoded by just vaccinia and variola [15, 17]. G4L serves as a redox-shuttle in a cytoplasmic disulphide bond pathway required for vaccinia virus morphogenesis [36] while O2L serves a non-essential role in nucleotide biosynthesis [25]. Glutathione peroxidase homologs (MC066L and FPV06) are encoded by Molluscum contagiosum and fowlpox viruses respectively [1, 29]. The molluscum protein is a selenoenzyme that can reduce cytotoxic peroxides and protects transfected

cells from ultraviolet light-induced hydrogen peroxide [30]. Due to a lack of a suitable viral culture system, MC066L's biological function remains unclear.

Poxviral homologs of the cellular SOD1 represent a third class of widely distributed proteins with potential redox functions. Superoxide dismutases are antioxidants that provide a first line of defence against cytotoxic ROS by catalyzing the dismutation of superoxide anion ($O_2^{\cdot-}$) into H_2O_2 and O_2 [12]. Superoxide has potential anti-viral activity, because it is the major ROS produced by activated phagocytes, although it is the hydrogen peroxide that is actually the more dangerous toxicant and a powerful apoptotic inducer. Poxvirus-encoded homologs of animal SOD1 have been identified in a variety of genomes, including the Orthopoxviruses vaccinia (A45R) and variola, the Leporipoxviruses myxoma and Shope fibroma (M131R and S131R respectively), Molluscum contagiosum virus (MC163R), and *Entomopoxviruses* (e.g. AMV255) [2, 6, 8, 9, 32, 38]. Seemingly non-essential and inactive SOD1-like genes of unknown function are also encoded by baculoviruses [35].

We are interested in the SOD1 homologs encoded by SFV and myxoma virus due to their highly conserved sequences, which suggests that the M/S131R proteins may serve a function retained by selection during the long divergence of these two evolutionarily distinct Leporipoxviruses. The same sequence conservation characterizes vaccinia and variola virus SOD1 homologs, although these viruses are clearly more recently divergent than are myxoma and SFV and the gene sequences have drifted much further from cellular SOD1 than have Leporipoxvirus genes. Almazán and colleagues have recently shown that A45R protein is a catalytically-inactive viral core component which is not required for growth in culture or virulence in mice [4]. Since there are some

in-frame deletions plus some critical mutations, it is not surprising that A45R is catalytically inactive. Their study still leaves the biological function of this gene uncertain despite providing important insights into the molecular genetic properties of A45R.

We have decided to investigate the biochemical properties of the more "SOD1-like" proteins encoded by Leporipoxviruses. Our results show that similar to the A45R, M/S131R lack catalytic activity, but interestingly, SFV and myxoma virus proteins can inhibit the activity of cellular SOD1. M131R was also shown to be dispensable in tissue culture system since viruses encoding a disrupted gene still replicate normally. It remains obscure what advantages are gained by SOD1 homologs because deleting M131R did not affect virulence in European rabbits.

2.2 MATERIALS AND METHODS

Cells, viruses, and virus culture. Baby green monkey kidney (BGMK), rabbit kidney (RK13), and spontaneously immortalized rabbit corneal fibroblast (SIRC) cells were grown in Dulbecco's modified Eagle's media (DMEM) supplemented with 10% fetal bovine serum as previously described [24]. Myxoma virus strain Lausanne, SFV strain Kasza, and vaccinia virus strain Western Reserve (WR) were obtained from the American Type Culture Collection. Vaccinia strain VTF7.5 encodes T7 phage RNA polymerase and was obtained from Dr. B. Moss (NIH). Myxoma strain MYXlac was described previously and encodes the *E. coli lacZ* gene inserted at the intergenic locus between the myxoma growth factor gene and M009L [23]. MYXlac virions were purified by sedimentation through tartrate gradients [38], except that infected cells were extracted by both sonication and Dounce homogenization and banded particles were dialyzed to remove the gradient buffer.

Growth curve analysis employed monolayers of BGMK and RK13 cells (~5 x 10^5 in a 3.5 cm dish) infected with ~5 x 10^6 virus plaque forming units of virus in 200 μL of growth medium. After incubation at 37°C for 1 hr, the cells were washed with phosphate buffered saline (PBS) and the media replaced. The infection was stopped by transferring the dish to -80°C, at the time points indicated (Figure 2.3), and the virus harvested using three rounds of freeze and thaw, followed by centrifugation at 1,500 x g for 10 minutes. Appropriate dilutions of this supernatant were plated on near confluent monolayers of

BGMK or RK13 cells, cultured three days, fixed with 3.7% formaldehyde at room temperature, stained with 0.5% crystal violet for 15 minute, and counted.

Protein labelling experiments employed monolayers of SIRC cells cultured in DMEM and 10% fetal calf serum. Following virus infection, the media was replaced with cysteine-methionine depleted DMEM (Gibco) supplemented with 10% dialyzed fetal bovine serum. Two hours prior to harvest, 200 μCi of ^{35}S labelled cysteine and methionine mix was added per 10^6 cells (ICN). The cells were harvested by washing twice with PBS and then scraped into 500 μL of RIPA lysis buffer. After fractionating the proteins by SDS-PAGE, the gel was stained with Coomassie dye, destained, dried, and exposed to X-OMAT-AR (Kodak) film.

Deletion of M131R. Myxoma strain MYX_M131RΔ was constructed using homologous recombination (Figure 2.2). The targeting plasmid, pJXC100, was constructed by PCR amplifying 542 bp of DNA located upstream of M131R [primers M131R-FLF (5'-ATCTCGAGTGCGTATATTATACACGGCC-3') and M131R-FLR (5'-GGGATATCCATTTATAGTATTACTAAACG-3')] plus 509 bp downstream [primers M131R-FRF (5'-GGACTAGTTAAATAACCTCGCTAAAATG-3') and M131R-FRR (5'-TAGAGCTCGGGAATCTACTCTACTGTT-3')], and then inserting these fragments into *Eco*RV/*Xho*I and *Spe*I/*Sac*I sites in pBluescript KS+. A cassette encoding the *E. coli gpt* gene driven by a vaccinia early/late p7.5 promoter [11] was subsequently inserted at the *SmaI* site. DNA sequencing confirmed the absence of PCR-induced mutations. Plasmid pJXC100 was transfected into BGMK cells infected with wild-type myxoma virus, strain Lausanne, and strain MYX_M131RΔ isolated using three

rounds of blind passage in the presence of mycophenolic acid (25 μg/mL) followed by three rounds of plaque purification without selection.

Cloning and purification of recombinant S131R – The PCR and two primers [sSOD5' (5'-AAGCTTAGGATCCATGAATAATAGAGCGTG-3') and sSOD3' (5'-AAGAATTCTTAAGCAACTCCTATAATC-3')] were used to amplify a 500 bp DNA fragment encoding the S131R open reading frame. The PCR product was cloned using a pCR2.1 Topo cloning kit (Invitrogen), sequenced, and recloned in *Bam*HI/*Eco*RI-cut pGEX2T vector producing pDE422. The recombinant fusion protein was extracted from *E. coli* strain DH5α/pDE422 following isopropyl-β-d-galactopyranoside induction, and affinity purified using a glutathione resin as directed by the suppliers of these reagents (Pharmacia). The fusion protein was treated with human thrombin (~1 cleavage unit of thrombin per 100μg protein, Sigma) to release the sfvSOD domain.

Recombinant sfvSOD was also produced using a hybrid vaccinia virus-T7 RNA polymerase expression system [14]. The PCR and two primers [sSOD/*Nco*I (5'-CCATGGATAATAGAGCGTGTC-3') and sSOD 3' (above)] were used to amplify a 500 bp DNA fragment encoding the S131R open reading frame. The PCR product was cloned using a pCR2.1 Topo cloning kit (Invitrogen), sequenced, and recloned into *Nco*I and *Xho*I sites in a pTM3 targeting vector, producing pMM103. pMM103 was transfected into vaccinia virus infected cells, and recombinant isolates recovered using mycophenolic acid (25 μg/mL), xanthine (250 μg/mL), and hypoxanthine (15 μg/mL) selection. The structure of putative recombinants was confirmed by Southern blotting. SfvSOD expression was obtained by co-infecting BSC-40 cells with recombinant viruses (VMM1.5 or VMM5.2) plus VTF7.5 at a multiplicity of infection of 2 of each virus.

Monoclonal antibody preparation. Recombinant sfvSOD fusion protein was purified from *E. coli* and 4 x 30 μg injections were used to immunize Balb/C mice over a two week period. Spleen cells were recovered, fused to SP2/0 myeloma cells using polyethylene glycol, and hybridoma lines isolated using RPMI selection media containing 20% fetal bovine serum plus hypoxanthine, aminopterin, and thymidine [19]. Clone P115.27.R2 was shown, using enzyme-linked immunosorbent assays and Western blots, to produce antibodies that strongly reacted with sfvSOD but not glutathione-S-transferase. It was subcloned twice by the method of limiting dilution and then stored frozen in liquid nitrogen. Antibodies were subsequently purified from serum free culture supernatants by protein G affinity chromatography (Biorad). Several cell lines, producing antibodies which recognized the GST fusion partner, were also identified in this screen. One (P115.21.R2) was retained as a source of GST-specific IgG.

Cu-Zn SOD assays. *In situ* gel assays utilized the method of Beauchamp and Fridovich [7]. However, in experiments designed to detect sfvSOD and myxSOD activity, we omitted the chloroform/ethanol extraction step because it is uncertain whether viral SOD1 homologs, like cellular SOD1, would resist this treatment. This step was retained in spectrophotometric experiments designed to detect changes in cellular SOD1 activity, because it removes Mn and Fe SOD. SIRC or BGMK cell monolayers were infected with virus at a multiplicity of infection of 10, and then harvested with a plastic scraper in a buffer containing 39 mM Na_2HPO_4, 11 mM NaH_2PO_4, 0.1 mM EDTA, pH 7.4. After sonication and clarification by centrifugation at 16,000 x g, the

protein concentration was determined using a Bradford dye (Biorad), ~30 μg of protein was mixed with one volume of 2x loading buffer (without sodium dodecyl sulfate or reducing agent), and then fractionated by electrophoresis on a 10% native polyacrylamide gel. SOD activity was detected by soaking the gel in a solution containing 2.5 mM nitroblue tetrazolium (Sigma) for 20 minutes at 20°C, followed by soaking 15 min in a solution containing 28 mM tetramethylethylenediamine (Biorad), 28 μM riboflavin (Sigma), and 36 mM potassium phosphate, pH 7.8. The gel was then exposed to bright white light on a transilluminator for 20 min. The stain was replaced with water and the exposure continued until maximal contrast was obtained between the achromatic zone, marking SOD1 activity, and the blue background (~1 hr). Positive controls used commercial bovine SOD1 (Sigma).

Spectrophotometric assays measured SOD interference in the reduction of 6-hydroxydopamine [16]. Briefly, 60 μg of sample was added to 0.45 mL of 50 mM sodium phosphate, 0.1 mM EDTA, pH 7.4 in a spectrophotometer cuvette equilibrated at 37°C, and the reaction started by adding 5 μL of 10 mM 6-[10]hydroxydopamine hydrobromide (ICN). The sample was mixed quickly and the rate of change of the absorbance monitored for 30 sec at 490 nm.

SDS-PAGE and Western blot analysis. SDS-PAGE (12%) was performed as described previously [39] and the proteins then electrophoretically transferred to a PVDF membrane (Millipore). In some experiments N-ethylmaleimide (Sigma) was added to a final concentration of 40 mM in all extraction and loading buffers [37]. The membrane was blocked overnight at 4°C in PBST (phosphate-buffered saline containing 0.1%

Tween) and 5% blocking agent (Amersham) and then incubated with 1:1,000 diluted monoclonal antibody for 1 hr at 20°C. After six washes with PBST buffer, the membrane was probed with 1:20,000 diluted horseradish peroxidase conjugated anti-mouse IgG (BioRad), washed again six times with PBST, and immunoreactive material detected using a chemiluminescent detection kit (Pierce).

Electron microscopy. A suspension of 200 nm diameter polystyrene beads (10^9 particles per mL, Duke Scientific) was diluted 1:10 with a sample of gradient purified and dialyzed virus particles, applied to the surface of a 200 mesh Formvar-coated copper grid and negatively stained with 1.5% uranyl acetate. The sample was imaged with a LEO 912AB microscope, imaged digitally, and 11,000x magnification prints prepared showing random fields of virus and beads. The ratio of beads to virus particles, in conjunction with the bead concentration, provided an estimate of virus titer.

Pathogenesis studies. The experimental procedure was essentially identical to one previously described [20], except that each rabbit was injected with 3000 plaque forming units of virus.

2.3 RESULTS

Structural features of Leporipoxvirus SOD homologs - The S131R and M131R genes of SFV and myxoma viruses encode proteins of masses 17,775 and 17,786 Da, respectively with ~94% amino acid identity. BLAST searches [5] readily detected other viral protein homologs as well as numerous cellular homologs. A Macaw alignment of a selection of these proteins including SOD1-like proteins encoded by vaccinia and variola viruses, homologs encoded by other representative DNA viruses, and also cytosolic rabbit (*Oryctolagus cuniculus*) [26] and bovine (*Bos taurus*) SOD1s [33] is shown in Figure 2.1. The crystal structure of the bovine enzyme [27, 34] provides insights into the properties of the homologous viral proteins and illustrates several intriguing features of the poxvirus proteins. In comparison to the *Orthopoxvirus* proteins, Leporipoxvirus proteins are more closely resemble their cellular homologs, although not as closely as do other viral proteins. For example, SFV and myxoma proteins retain all four of the Zn binding residues and three out of four Cu coordinating residues, while point mutations and deletions in the variola and vaccinia genes have clearly eliminated all metal binding residues but one of the Cu coordinating residues. Nevertheless, as a result of an R-to-V substitution at the catalytic site, the SFV and myxoma proteins would still be predicted to be catalytically inactive (Figure 2.1). Beside, an intrastrand disulphide bond would also be disrupted in the Leporipoxvirus proteins by a C-to-W substitution near the protein C-terminus. The Leporipoxvirus proteins have a unique feature with relatively long N-terminal extensions in comparison to other protein homologs. Since there is a highly conserved "KAVC" motif immediately upstream of M_{22}, M_1 should be

favoured rather than M_{22} as the translational start site. It is also noteworthy that the majority of glycines and other small hydrophobic residues comprising the SOD1 homodimer interface have been retained over the course of evolution by all of these proteins, indicating that myxoma and SFV SOD1 homologs should still be capable of forming homodimers as do cytosolic SOD1s.

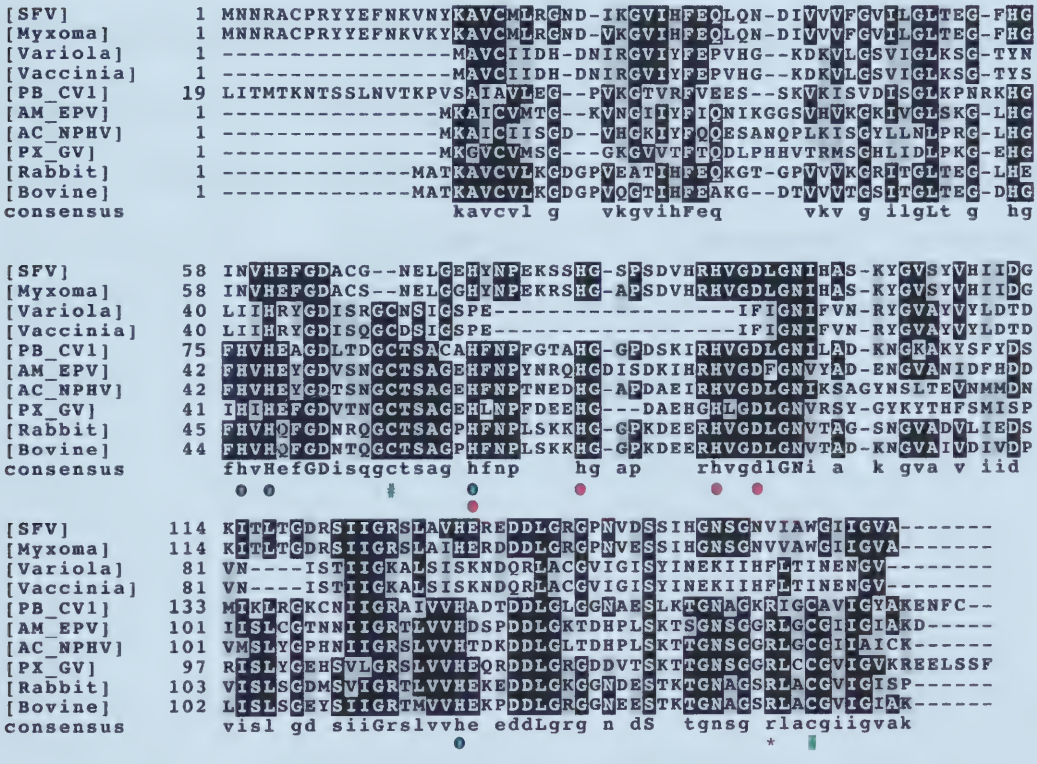

Figure 2.1. Multiple sequence alignment illustrating viral and cellular SOD1 homologs. Protein sequences were aligned using Macaw and the Figure prepared using Boxshade 3.21 (www.isrec.isb-sib.ch:8080/software). Based upon the crystal structure of bovine SOD1, the symbols located beneath the consensus sequence indicate: o- Cu-binding residues; • Zn-binding residues; # - intrastrand disulphide cross-linked cysteines; * - catalytic arginine. Genbank accession numbers are SFV (strain Kasza, NP_052020), myxoma virus (strain Lausanne, NP_051845), variola major virus (strain India-1967, NP_042201), vaccinia virus (strain WR, P26669), PB_CV1 (*Paramecium bursaria* chlorella virus 1, NP_048593), AM_EPV (*Amsacta moorei* entomopoxvirus, NP_065037), AC_NPHV (*Autographa californica* nucleopolyhedrovirus, NP_054060), PX_GV (*Plutella xylostella* granulovirus, NP_067786), rabbit (*Oryctolagus cuniculus*, P09212), and bovine (*Bos taurus*, P00442) SOD1s.

Recombinational inactivation of myxoma M131R – A recombinant virus with a deletion in M131R gene was generated to determine whether these genes encode an essential function. We used homologous recombination to construct a mutant virus in which the M131R gene was entirely replaced by a *gpt* cassette [11] while leaving intact the flanking genes (Figure 2.2A). The structure of the resulting virus, MYX_M131RΔ was confirmed by using PCR analysis (Figure 2.2B). Although there is no deleterious effect of the mutation upon growth of MYX_M131RΔ virus in culture, single step growth analysis showed that mutant viruses seem to grow better than do wild-type viruses (Figure 3). When plated on either RK13 or BGMK cells at a multiplicity of infection of ten, virus titers were reproducibly ~10-fold higher for the mutant virus versus the wild type myxoma virus. We concluded that the M131R gene is not essential for growth of myxoma virus in culture and may, paradoxically, inhibit virus production.

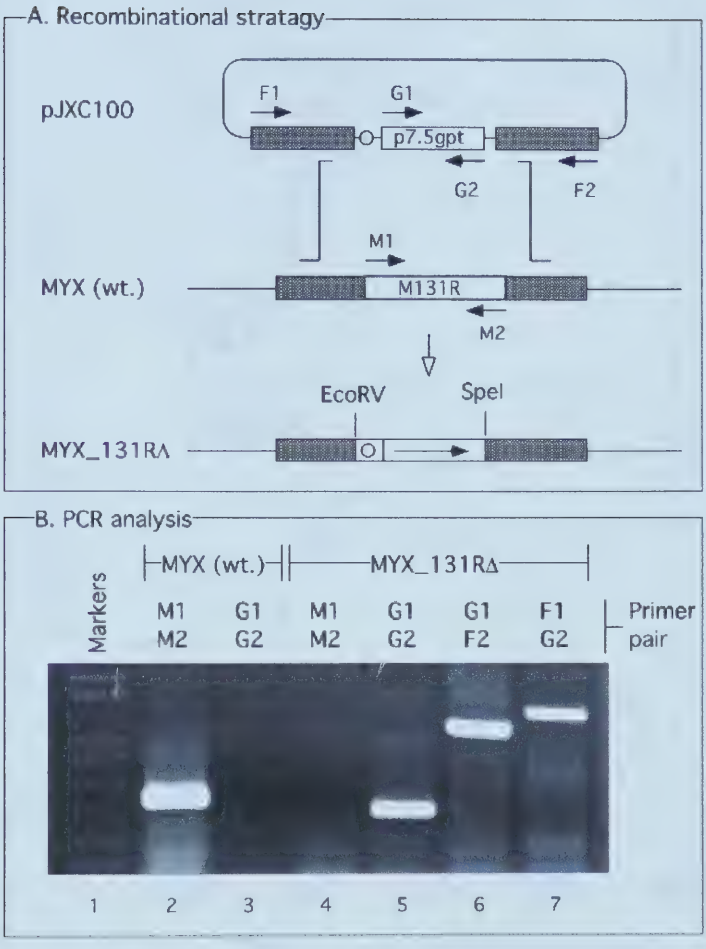

Figure 2.2. Insertional inactivation of myxoma virus M131R. Panel A. Plasmid pJXC100 was assembled using the PCR and encodes the *E. coli gpt* gene flanked by sequences also flanking the M131R gene. This plasmid was transfected into myxoma virus infected cells and recombinant viruses isolated based upon the resulting resistance to mycophenolic acid. Flanking genes M130R and M132L are unaffected by this deletion. Panel B. PCR analysis of recombinant virus lacking M131R. Primers designed to amplify the M131R open reading frame (lane 2) do not detect M131R sequences in MYX_M131RΔ (lane 4). However, primers targeting the N-terminal or C-terminal portions of the *E. coli gpt* gene, permit amplification of sequences encoding the *gpt* and flanking genes (lanes 6 and 7).

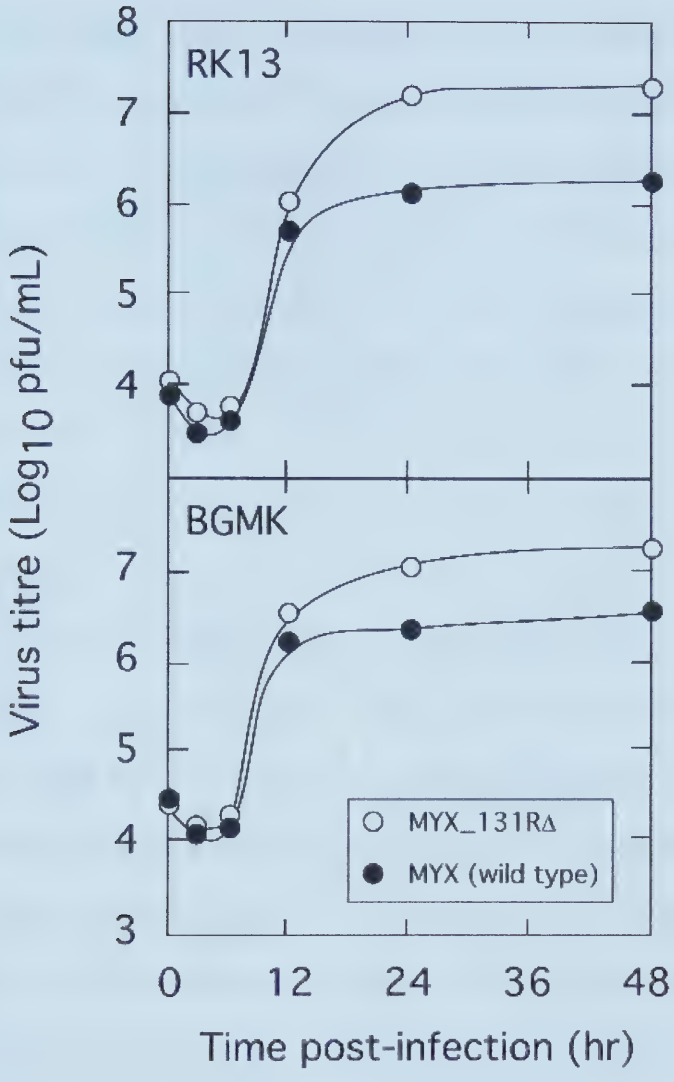

Figure 2.3. Effect of an M131R deletion mutation on virus growth. RK13 and BGMK cells were infected with either wild-type myxoma virus or the MYX_M131RΔ deletion mutant virus at a multiplicity of infection of ten. Virus samples were harvested by freeze-thaw at the indicated times post-infection, and virus titers were determined on BGMK cell monolayers in triplicate.

Expression of Leporipoxvirus SODs. M/S131R are predicted to be late gene products since both genes encode 5'-TAAATG-3' motifs typical of poxviral late promoters. Western blot analyses and ^{35}S-labeling were hence performed. Figure 2.4 shows an analysis of the ^{35}S-labeled proteins that were recovered from myxoma-infected cells at various times following infection in the presence of ^{35}S-labeled cysteine and methionine. An 18 kDa protein was first detected in wild type myxoma virus infected extracts about 12 hr post-infection which then accumulated to high levels by 24 hr post-infection (Figure 2.4A). That this protein is M131R was suggested by the fact that it cannot be detected in mock-infected cells or in cells infected with the MYX_M131RΔ deletion virus (Figure 2.4A, lanes 1 and 7). In addition to these experiments we also performed a Western blot analysis using a monoclonal antibody raised against recombinant S131R. This antibody reacts equally well with both SFV and myxoma proteins and in this experiment first detected the expression of an 18 kDa antigen in wild type myxoma-infected cells about 12 hr post infection. The 18 kDa protein continued to accumulate in wild-type extracts through 24 hr post-infection and was again not present in mock- or MYX_M131RΔ-infected cells (Figure 2.4B). Analysis of the proteins present in the culture media surrounding virus-infected cells showed that these proteins were not secreted (data not shown). These data show that M131R (and S131R, although not shown) are intracellular proteins expressed with kinetics typical of Leporipoxvirus late gene products. That these are late gene products was confirmed by the fact that Ara-C blocks the M131R protein expression in myxoma-infected BGMK cells (data not shown).

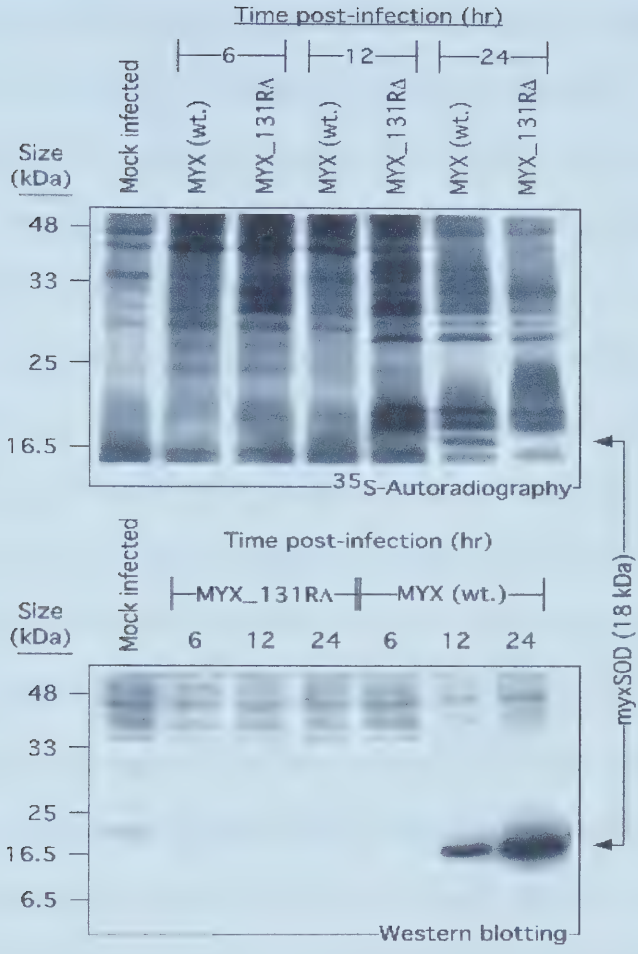

Figure 2.4. Kinetics of M131R protein expression determined by ^{35}S-labeling and western blot analysis. Upper panel. BGMK cells were infected with either wild-type myxoma virus, or the MYX_M131RΔ deletion mutant virus, at a multiplicity of infection of 20. The media was supplemented with ^{35}S cysteine and methionine to label any proteins synthesized following infection. The cells were washed and harvested at the times indicated and 80 μg of protein loaded per lane using a loading buffer containing both sodium dodecyl sulfate and β-mercaptoethanol. Autoradiography was used to identify proteins expressed during virus infection. An ~18 kDa protein was first detected in cells infected with wild-type virus about 12 hour post infection and by 24 hr post-infection it was one of the most abundant labeled molecules in these extracts. This protein is not seen in cells infected with MYX_M131RΔ. We often noted more labeled virus proteins in samples extracted from MYX_M131RΔ-infected cells at 12 hr post-infection. This may reflect the somewhat better growth of mutant viruses (Figure 2.3). Lower panel. Proteins were extracted from virus-infected BGMK cells at the indicated times, fractionated using SDS-PAGE, and western blotted using a monoclonal antibody raised against recombinant sfvSOD. An ~18 kDa late protein is also detected by this method, again only in cells infected with wild-type virus.

The fact that M131R can be readily detected in cell free extracts using ^{35}S-labeling, suggested that this is an abundantly expressed viral protein. To investigate whether these proteins are structural components like the A45R of the vaccinia virus, we purified myxoma virus particles using tartrate gradients, and used Western blotting to confirm that both SFV and myxoma virus incorporate the proteins into virions (data not shown). We then estimated the quantity of the protein being incorporated by the virus into the virion using a combination of semi-quantitative Western blotting and virus particle counts. Recombinant S131R protein was purified from *E. coli* (see below), cleaved with thrombin, and known amounts of this protein were Western blotted alongside of proteins extracted from gradient-purified myxoma virus particles. We chose to determine the numbers of virus particles by electron microscopy rather than by plaque assay since purification of myxoma often inactivates some uncertain fraction of the virus, and thus creates uncertainties regarding the ratio of particle to plaque forming units (see Methods and Material) By assuming that the two nearly identical viral proteins are equally immunoreactive, these experiments suggested that 4.7×10^7 virions contain ~2 ng of M131R, or about 1400 protein molecules per particle. This is admittedly only a crude estimate of the ratio of protein to particle, but it is still clear that large quantities of protein are incorporated into Leporipoxvirions.

Catalytic activities of Leporipoxvirus SOD1 homologs - To determine whether these proteins were catalytically active, we prepared recombinant S131R and assayed the protein for SOD1 activity using an *in situ* gel assay. The SFV S131R gene was amplified using the PCR and cloned into an *E. coli* pGEX2T expression vector. A fusion protein was then produced in bearing S131R fused to glutathione-S-transferase (GST) [31]. The recombinant protein was affinity purified and the GST domain was removed by using thrombin cleavage. The fusion protein was also used to prepare a mouse monoclonal antibody with the assistance of Dr. M. Suresh (Univ. of Alberta). After digestion with thrombin, these protein preparations contained the released GST domain plus three or four ~18 kDa S131R polypeptides that all reacted with the antibody (data not shown). The purified recombinant protein was then subjected to native gel electrophoresis and assayed for SOD1 activity using an *in situ* gel assay. This assay detects SOD1 activity as a clear band on a blue-stained gel. The background colour was formed from a reduction activity of nitroblue tetrazolium to formazan by superoxide radical. This assay indirectly indicates SOD1 activity which is a result of the dismutase interfering in the reduction of superoxide [7]. While these assays readily detected less than 10 ng of bovine SOD1, no activity was seen using up to 2 μg of S131R fusion protein (Figure 2.5). When protein purity and mass differences are taken into account, this result suggested that if S131R does retain catalytic activity, the dismutase activity is substantially less than 0.5% of that exhibited by bovine SOD1 under these reaction conditions.

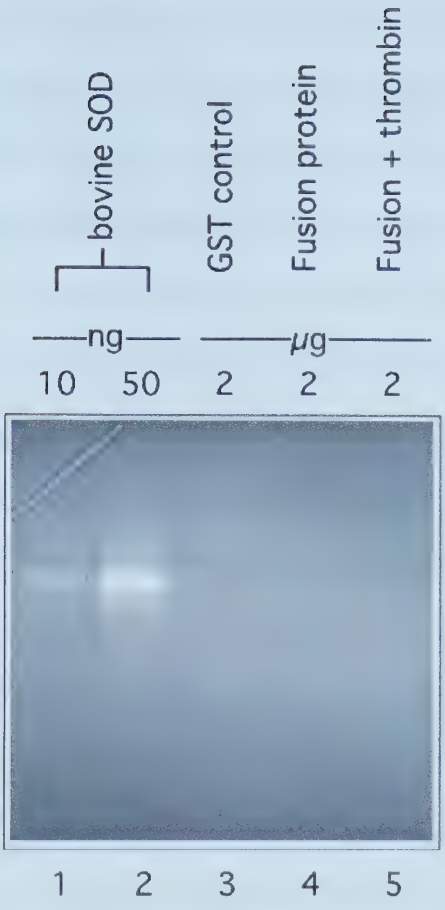

Figure 2.5. Recombinant sfvSOD does not catalyze superoxide dismutase reactions. The indicated quantities of purified protein were separated on a 10% native polyacrylamide gel and the gel stained for SOD activity. This *in situ* assay readily detected the activity associated with ≤10 ng of bovine SOD1 (lane 1), but neither the GST-sfvSOD fusion protein (lane 4), nor thrombin-treated fusion protein (lane 5), displayed any detectable activity.

We also used *in situ* gel assays to screen extracts prepared from mammalian cells infected with SFV or myxoma virus to rule out the possibility that bacterial expression systems might be incapable of folding or incorporating metals into the SFV protein, and again found no evidence to suggest that virus infection induced expression of a novel SOD activity. We also examined whether active protein could be produced using a hybrid vaccinia virus/T7 expression system [13]. Recombinant vaccinia viruses were constructed encoding the native S131R gene product under control of a T7 promoter (VMM1.5 and VMM5.2) and coinfected into cells along with a helper virus expressing T7 RNA polymerase (VTF7.5). Sufficient amounts of protein were recovered 24 hr post-infection for it to be easily visible as an 18 kDa protein band on a Coomassie stained gel and comprising perhaps 2% of SIRC cell protein extracts (data not shown). Western blots confirmed the identity of the protein. However, we still saw no new or enhanced SOD1 activity when ~60 μg of the whole cell extract was assayed for activity using the dye reduction assay (data not shown). Endogenous cellular Cu-Zn superoxide dismutase was easily detected under these conditions, showing that the assay and extraction methods were working properly. Experiments using myxoma virus and vaccinia expressed recombinant M131R similarly failed to detect any novel dismutase activities. While it is difficult to accurately derive a minimal estimate of catalytic activity using these different alternate experimental approaches, we found no evidence to suggest the Leporipoxviral proteins retain any catalytic capacity as superoxide dismutases.

Leporipoxvirus SOD1 homologs form disulphide cross-linked dimers. We noticed that depending upon whether samples were denatured under oxidizing or reducing conditions prior to electrophoresis, M/S131R exhibited different molecular weights, as shown on Figure 2.6 using extracts prepared from cells co-infected with vaccinia virus strains VTF7.5 and VMM5.2. Western blotting with the monoclonal antibody detected a recombinant S131R protein exhibiting a mass of ~18 kDa in cell extracts treated with reducing agents, sodium dodecyl sulfate and β-mercaptoethanol, whereas a predominant species exhibiting a mass closer to ~35 kDa was detected in unreduced extracts (Figure 2.6, lanes 1 and 3). M131R exhibited identical behavior in BGMK cell extracts as did purified S131R expressed in *E. coli* (data not shown). Since disulphide bonds can be easily oxidized during protein extraction, we repeated the experiment adding 40 mM N-ethyl maleimide to all of the extraction and gel loading buffers. This treatment alkylates free sulfhydryl residues and indeed prevented formation of dimers and higher order complexes (Figure 2.6, lane 2). These experiments show that unlike cellular SOD1s, which bear *intra*strand disulphide bonds [34], Leporipoxviral proteins can form homodimers linked in solution by *inter*strand disulphide bonds. However, formation of dimers and other complexes requires more oxidizing conditions than those found in the cytoplasm of infected cells, indicating that M/S131R are expressed as monomer *in vivo*.

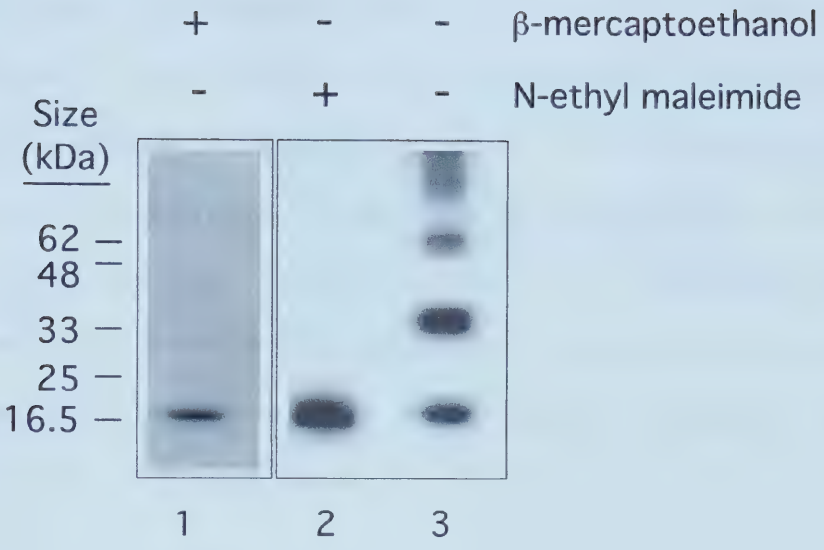

Figure 2.6. SfvSOD can form disulphide-crosslinked dimers. Proteins were extracted 24 hr post-infection from SIRC cells infected with VMM5.2 plus VTF7.5 at a multiplicity of infection of 20. Protein samples were extracted by boiling in a loading buffer containing 2% sodium dodecyl sulfate with or without 2% β-mercaptoethanol, separated by SDS-PAGE, and western blotted using an anti-sfvSOD monoclonal antibody. In the absence of reducing agent, the sfvSOD protein forms variable amounts of aggregates with a prominent species migrating as a 34.5 kDa dimer (lane 3). This is halved to about 18 kDa by β-mercaptoethanol treatment (lane 1). When proteins were extracted in the presence of 40 mM N-ethylmaleimide, alkylation of free sulfhydryl groups similarily prevented formation of high molecular weight complexes (lane 2).

Effect of virus infection on cellular SOD1 activity. As indicated previously, we were unable to detect any novel superoxide dismutase activities induced during the course of SFV or myxoma infection from a number of experiments. Rather, virus infection clearly caused a time-dependent reduction in the activity of endogenous SOD1 as shown in Figure. 2.7. Cells infected with SFV at a multiplicity of infection of ten, resulted in a 60% reduction in cellular SOD1 levels over a 40 hour time period as determined using an *in situ* gel assay. The effect was very reproducible being observed three times in three independent experiments. However, these experiments cannot differentiate gene-specific effects from the non-specific effects that might be caused by virus inhibition of cellular gene expression, so we repeated the experiments using MYX_M131RΔ virus as well (data not shown).

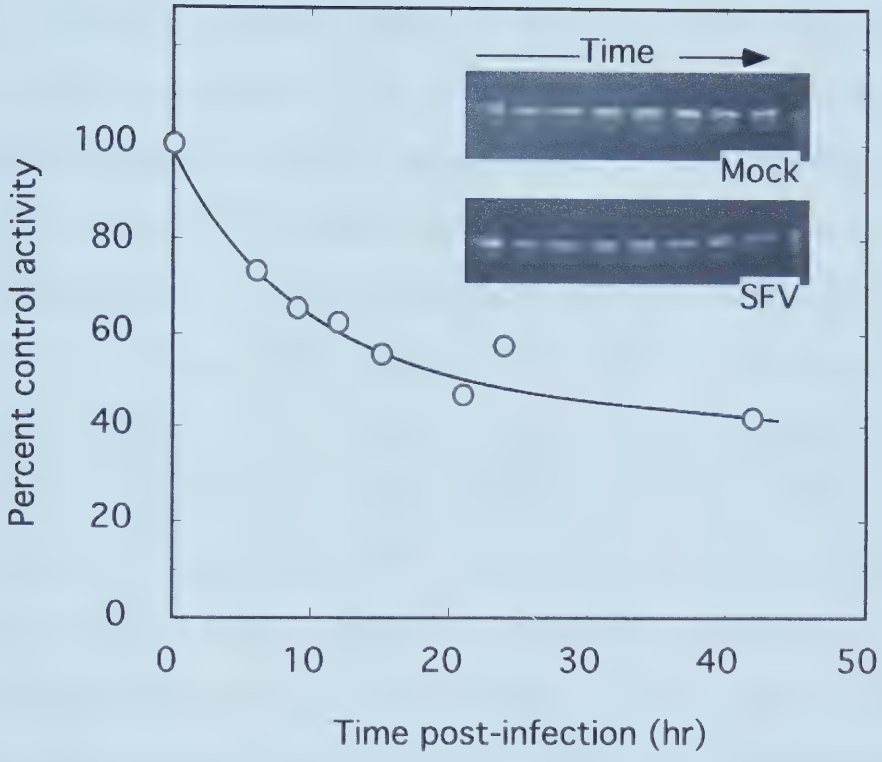

Figure 2.7. Cellular SOD1 activity declines during SFV infection. SIRC cells were infected (or mock infected) with SFV at a multiplicity of infection of 10 and the infection terminated by freezing the cells at the time points indicated. Proteins were recovered and extracted with chloroform and ethanol and 30 μg of protein applied to each lane of a native polyacrylamide gel. After electrophoresis, SOD1 activity was detected by *in situ* staining (see Methods and Materials). Two major isoforms of rabbit cellular SOD1 were detected in these assays, while at least three major SOD1 isoforms are seen in this preparation of commercial bovine control protein (right-most lanes). Densitometry (using NIH Image1.6.1) showed that the combined activity of both rabbit isoforms declined nearly 60% over the course of 42 hr in SFV-infected cells, relative to the amount of SOD1 activity detected at parallel time points in mock-infected cells.

Since the gel assay is an indirect measurement of SOD1 activity, we have decided to use another assay to confirm the finding as well as to quantitate the loss of the cellular SOD1 activity by a spectrophotometric method. This assay detects SOD1 activity by its ability to inhibit an autoxidation reaction of 6-hydroxydopamine, which produces superoxide radical in solution [16]. We extracted protein samples from virus-infected mammalian cells with chloroform and methanol to remove SOD2 and thus ensure the assay detects only SOD1. The results of one such experiment are shown in Figure 2.8. This spectrophotometric assay further confirmed the gel-based data (Figure 2.7), with SFV infections causing a ~60% reduction in SOD1 activity over 42 hr in both experiments. A similar reduction in SOD1 activity was also seen in myxoma-infected cells and in cells infected with recombinant vaccinia viruses expressing S131R. In the latter case it is noteworthy that the vaccinia virus expression vectors probably express 10-to-100-fold more protein than is produced by wild-type SFV or myxoma viruses, and suggests that M/S131R protein concentrations probably do not limit the rate of inhibition of cellular SOD1 in ordinary infections. Most importantly, there was only limited change in SOD1 activity in MYX_M131RΔ infected cells, relative to mock-infected cells, until very late in infection and at about the time where significant cytopathic effects start to be seen. We concluded that although the Leporipoxvirus M131R and S131R gene products are catalytically inactive, their expressions were accompanied by a reduction in the activity of cellular SOD1.

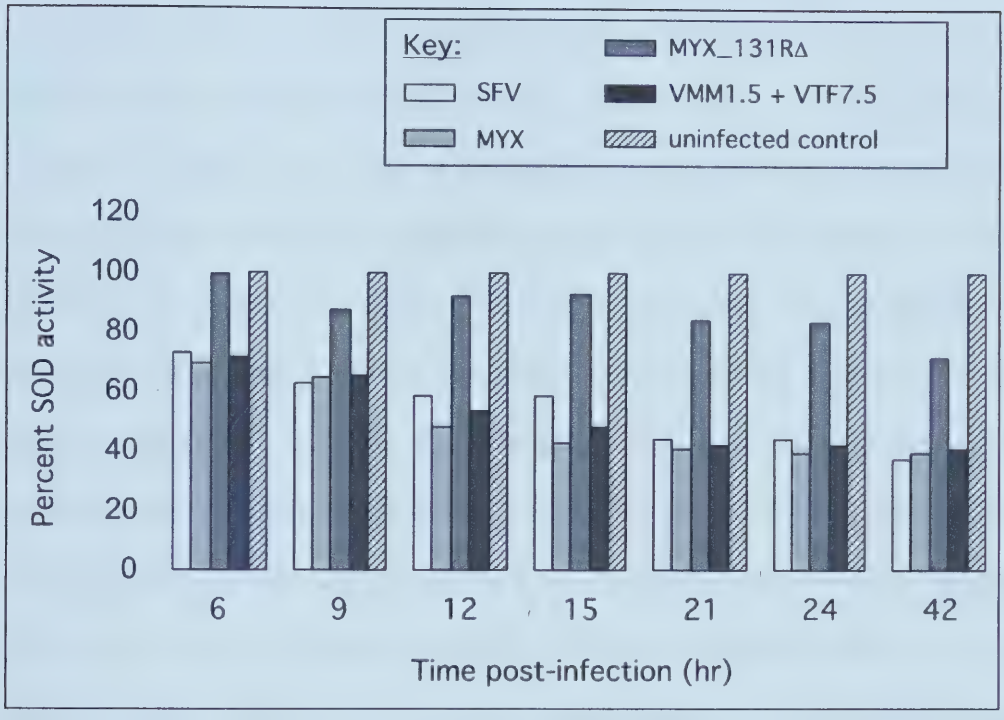

Figure 2.8. Changes in cellular SOD1 activity monitored by hydroxydopamine assays. SIRC cells were infected with the indicated viruses at a multiplicity of infection of 10 and SOD1 activity assayed spectrophotometrically as described in the Materials and Methods. The amount of SOD1 activity in infected cells was normalized relative to the amount detected in mock-infected cells at each time point, and each measurement was determined in triplicate. The absolute amount of SOD1 activity measured in mock-infected cells ranged from 14 U/mg at time t = 0 hr to 16 U/mg at time t = 42 hr.

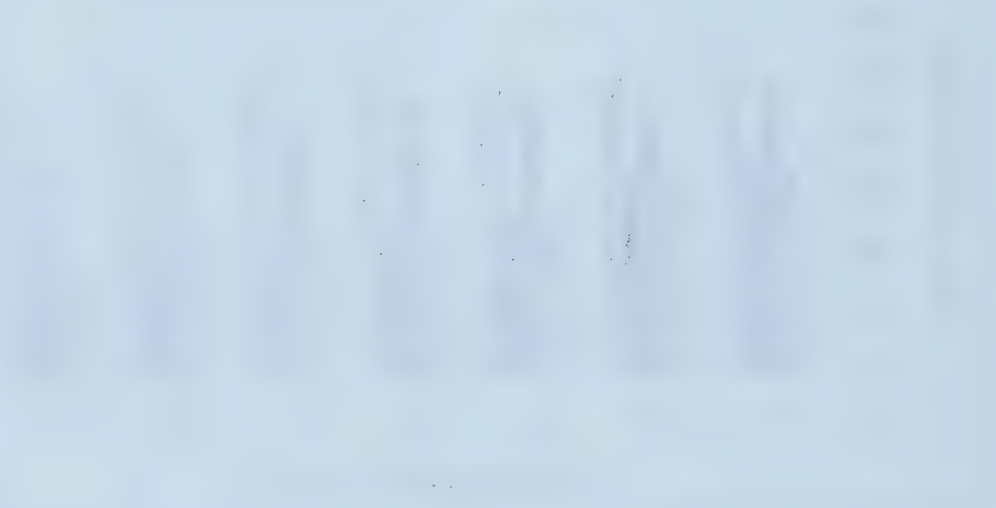

Virulence of MYX_M131RΔ in European rabbits. To investigate the role of the M131R gene product in virus pathogenicity, six European rabbits were inoculated with the MYX_M131RΔ virus and the clinical manifestations were compared with infections caused by the parental myxoma virus strain Lausanne. We examined such disease features as the primary lesion, secondary lesions, secondary bacterial infections, and disease outcome. The results of this study are summarized in Table 2.1. In overall, M131R-deleted viruses caused a form of myxomatosis disease very similar to that caused by wild-type viruses. However, two modest differences were observed. First, MYX_M131RΔ caused a primary lesion that appeared one day later than did lesions caused by the parental virus (day three versus day two post inoculation), and the growth of these primary lesions lagged behind those produced by wild-type viruses. Second, MYX_M131RΔ viruses resulted in more localized tumour-like nodules, rather than spreading to form the secondary lesions seen in wild-type infections. Instead, the ears of rabbits infected with the mutant virus bore lesions exhibiting a more generalized inflamed appearance. Although these observations suggest that mutating M131R affects lesion morphology, it was clear that deleting the gene in no way affects the profound immunosuppression and subsequent bacteremia so characteristic of myxomatosis [18, 22]. All animals showed evidence of secondary bacterial infection by six-day post infection and all had to be euthanized by days 10 or 11 due to the severity of the symptoms. Post-mortem examination of the internal tissues, including various lymph nodes, showed no significant differences in gross pathology.

TABLE 2.1. Pathogenicity of M131R-deficient viruses in European rabbits

	Phenotype and timing (days post-inoculation)	
Feature	Myxoma virus (MYX_M131RΔ)[1]	Myxoma virus (wildtype)[2]
Primary lesion	Day 3 - First appearance. Day 4 - Diameter 1 to 1.5 cm	Day 2 - First appearance. Day 4 - Diameter 3 cm with multiple satellite lesions surrounding inoculation site
Secondary lesions	Day 6 - First appearance Day 7 - Generalized ear inflammation more evident.	Day 5 - Multiple secondary lesions (nodules) on ears, nose and eyelids.
Bacteremia	Day 6 - First appearance, heavy discharge from nose and eyes, laboured breathing.	Day 6 - First appearance, heavy discharge from nose and eyes, laboured breathing.
Termination	Days 10 and 11 - Euthanized due to difficulties eating, drinking and breathing.	Days 10 and 11 - Euthanized due to difficulties eating, drinking and breathing.

[1] Six rabbits, 3000 pfu intradermally.

[2] Two rabbits, 3000 pfu intradermally.

2.4 DISCUSSION

Poxviruses have been known to encode a wide spectrum of proteins to target immune molecules of an infected host (review in [28]). These viral proteins include those that subvert the cytokine and chemokine networks as well as anti-apoptotic genes that inhibit the programmed cell suicide death, and the list is growing as we learn more from the studies investigating poxviral genes with potential immunomodulatory functions. Based on the virus genomic sequence data, it has been known for quite some time that poxviruses contain several open reading frames that may play roles in regulation of the redox status of the infected cells. We are interested in investigating whether the Leporipoxviral "redox gene", M/S131R could be another candidate that helps the virus to counteract the host anti-viral defence responses. Here, we reported the characterization of the S131R and M131R, the SOD1 homologs encoded by SFV and myxoma virus respectively. We found a reduction in the activity of their cellular homolog as these proteins were expressed *in vivo*, but what advantage is gained by the virus is something that requires further investigation.

Amino acid sequence analysis of SFV and myxoma SOD1 homologs in relative to the sequence and structure of catalytically active bovine SOD1 has revealed some mutations in the viral genes that provide reasons for the lack of enzymatic activity. In particular an R-to-V substitution would be expected to block the catalysis by preventing the interactions that stabilize superoxide anion within the active site (V_{154} in M/S131R appears to replace R_{142} in bovine SOD1). A further reduction in activity might be expected from the substitution of T_{136} and H_{45} in bovine SOD1 by H_{148} and N_{59} in

M/S131R, respectively. These substitutions could impede the formation of the Cu binding cleft, hence interfering with superoxide gaining access to the metal. Molecular modeling also provides an explanation for why these proteins can form dimers linked by interstrand disulphide bonds (Figure 2.6). The ability to form intrastrand disulphide bonds, as seen in the bovine SOD1 protein structure, would be blocked in the viral proteins by a C-to-W_{157} substitution near the M/S131R C-termini (Figure 2.1). Instead, this mutation, plus a small deletion located near M/S131R residue C_{67} in one protein subunit, would place C_{67} within cross-linking distance of a highly conserved cysteine on the second chain (C_{21} in M131R and S131R, C_7 in bovine SOD1). Symmetry considerations suggest that two chains could be held together as dimers by two such interstrand disulphide bonds, although data presented in Figure 2.6 suggests that other heterologous disulphide bonding arrangements are possible. Collectively these mutations readily explain the observed biochemical properties of Leporipoxvirus SOD homologs, but they leave unanswered the intriguing question of why the proteins have conserved all of the Zn and most of the Cu binding residues. In this regard these proteins are different from Orthopoxvirus SOD homologs, where substitutions and deletions have eliminated the Zn-binding domain (Figure 2.1), rearranged the cysteines that block interstrand crosslinks, and radically altered other portions of the protein.

Leporipoxvirus SOD1 homologs resemble their Orthopoxvirus homologs in being expressed late in infection and packaged into virions. We estimated that abundant amounts, ~1400 molecules of M131R are packaged per virion. Although Almazan *et al.* did not try to quantitate the amounts of A45R protein packaged in their studies, the efficiency of their immunogold labelling is consistent with it also being an abundant

vaccinia capsid protein [4]. It is thus surprising that M/S131R, like A45R, is not required for growth in culture, considering them being one of the major virion structural components. In fact MYX_M131RΔ virus grew to 10-fold higher titers than did wild-type virus under conditions involving either a multiplicity of infection of ten (Figure 2.3), or following plating at a multiplicity of infection of <0.001 (data not shown). Replacing the M131R with the selection marker *gpt* gene should not affect this rather puzzling phenotype since earlier studies showed that insertion and expression of the *gpt* gene in myxoma M001R/L had no effect on virus replication in BGMK and RK13 cells [20]. In this regard myxoma virus behaves differently from vaccinia virus as deleting A45R has no obvious effects on viral growth. One explanation might be that this selection pressure long ago introduced advantageous deletion mutation(s) into Orthopoxviral A45R homologs, and that deleting the rest of the gene gains vaccinia no further growth advantages.

It remains a mystery why a virus lacking an abundant capsid protein would grow better than the wild-type parent. It is also not clear whether this phenotype is associated with the reduction of cellular SOD1 activity (Figure 2.7 and 2.8). One possible explanation concerns a hypothetical competition for intracellular Cu and/or Zn. The interfacial amino acid residues that participate in docking SOD1 monomers to cellular copper chaperones were conserved in the Poxviral SOD1 homologs. If the viral proteins were to compete successfully with the cellular homolog for binding to the chaperone, slow inhibition of cellular SOD1 might occur as a result of preventing proper addition of metals to an accumulating apo-SOD1 protein. In addition, Zn is a co-factor in many proteins, including the transcription machinery, and may play a role in regulating

apoptosis [10]. Since both M/S131R have retained their Zn binding residues, they might sequester sufficient amounts of the metal to modulate such Zn-dependent processes. [In this regard it is notable that A45R protein lacks most of the amino acids involved in Zn binding (Figure 2.1) and so a model involving competition for Zn could also explain why deleting A45R had no effect on vaccinia growth.] Finally, inhibition of the cellular SOD1 activity could be achieved by M/S131R through formation of inhibitory complexes with the cellular proteins. Although we have yet to demonstrate the heterodimer formation experimentally, there is no reason to doubt the possibility simply from the structural modeling as well as from the sequence analysis. However, it is not obvious why complex formation should inhibit the functional subunit at this point. Any of these schemes would, of course, require a lot of the viral protein. This may not be an issue given the amount of M/S131R that could be released into the cytoplasm following uncoating or which is synthesized late in infection. We noted that cellular SOD1 activity levels start to decline before the onset of late gene expression (Figure 2.7 and 2.8), and this process may reflect the impact of virion-associated proteins released during virus uncoating.

Despite the better growth rate of MYX_M131RΔ virus in culture in relative to the wild-type virus, M131R is not a contributing factor to the virulence of myxoma virus in European rabbits. Both wild type and deletion mutant viruses caused nearly identical disease courses and mortality, with the only modest difference noted being a slight delay in the rate of initial disease progression in MYX_M131RΔ-infected animals (Table 2.1). A similar lack of effect, associated with deleting A45R from vaccinia virus, was also noted previously using mouse and rabbit infection models [4].

In summary, this report has revealed that the properties of SFV and myxoma M/S131R gene products, like vaccinia A45R protein, are paradoxical in which the abundant virion structural proteins are clearly not essential for virus viability and deletion mutations have no apparent effect on virulence in animals. We are left to speculate that these proteins may play a role in virus transmission, perhaps protecting virions from natural environmental insults not encountered in laboratory conditions. Alternatively the functions of the genes might have been masked by the virulent disease observed in *Oryctolagus* species. In other words, they may serve a function required in their natural hosts, the *Sylvilagus* rabbits but clearly, novel experimental protocols will be required to confirm or refute this hypothesis.

2.5 REFERENCES

1. Afonso CL, Tulman ER, Lu Z, Zsak L, Kutish GF, Rock DL (2000) The genome of fowlpox virus. J Virol 74: 3815-31

2. Aguado B, Selmes IP, Smith GL (1992) Nucleotide sequence of 21.8 kbp of variola major virus strain Harvey and comparison with vaccinia virus. J Gen Virol 73 (Pt 11): 2887-902

3. Ahn BY, Moss B (1992) Glutaredoxin homolog encoded by vaccinia virus is a virion-associated enzyme with thioltransferase and dehydroascorbate reductase activities. Proc Natl Acad Sci U S A 89: 7060-4

4. Almazan F, Tscharke DC, Smith GL (2001) The vaccinia virus superoxide dismutase-like protein (A45R) is a virion component that is nonessential for virus replication. J Virol 75: 7018-29

5. Altschul SF, Madden, T.L., Schaffer, A.A., Zhang, J., Zhang, Z., Miller, W., and Lipman, D.J. (1997) Gapped BLAST and PSI-BLAST: a new generation of protein database search prorams. Nucleic Acids Res 25: 3389-3402

6. Bawden AL, Glassberg KJ, Diggans J, Shaw R, Farmerie W, Moyer RW (2000) Complete genomic sequence of the Amsacta moorei entomopoxvirus: analysis and comparison with other poxviruses. Virology 274: 120-39

7. Beauchamp C, Fridovich I (1971) Superoxide dismutase: improved assays and an assay applicable to acrylamide gels. Anal Biochem 44: 276-87

8. Blasco R, Cole NB, Moss B (1991) Sequence analysis, expression, and deletion of a vaccinia virus gene encoding a homolog of profilin, a eukaryotic actin-binding protein. J Virol 65: 4598-608

9. Cameron C, Hota-Mitchell S, Chen L, Barrett J, Cao JX, Macaulay C, Willer D, Evans D, McFadden G (1999) The complete DNA sequence of myxoma virus. Virology 264: 298-318

10. Chai F, Truong-Tran, A.Q., Ho, L.H., and Zalewski, P.D. (1999) Regulation of caspase activation and apoptosis by cellular zinc fluxes and zinc deprivation: A review. Immunol Cell Biol 77: 272-278

11. Falkner FG, Moss B (1988) Escherichia coli gpt gene provides dominant selection for vaccinia virus open reading frame expression vectors. J Virol 62: 1849-54

12. Fridovich I (1997) Superoxide anion radical (O2-.), superoxide dismutases, and related matters. J Biol Chem 272: 18515-7

13. Fuerst TR, Niles EG, Studier FW, Moss B (1986) Eukaryotic transient-expression system based on recombinant vaccinia virus that synthesizes bacteriophage T7 RNA polymerase. Proc Natl Acad Sci U S A 83: 8122-6

14. Fuerst TR, Earl PL, Moss B (1987) Use of a hybrid vaccinia virus-T7 RNA polymerase system for expression of target genes. Mol Cell Biol 7: 2538-44

15. Gvakharia BO, Koonin EK, Mathews CK (1996) Vaccinia virus G4L gene encodes a second glutaredoxin. Virology 226: 408-11

16. Heikkila RE (1985) Autooxidation of 6-hydroxydopamine. CRS Press, Boca Raton, FL

17. Johnson GP, Goebel SJ, Perkus ME, Davis SW, Winslow JP, Paoletti E (1991) Vaccinia virus encodes a protein with similarity to glutaredoxins. Virology 181: 378-81

18. Kerr PJ, Best SM (1998) Myxoma virus in rabbits. Rev Sci Tech 17: 256-68

19. Kohler G, and Milstein, C. (1975) Continuous cultures of fused cells secreting antibody of predefined specificity. Nature 256: 495-497

20. Lalani AS, Masters J, Graham K, Liu L, Lucas A, McFadden G (1999) Role of the myxoma virus soluble CC-chemokine inhibitor glycoprotein, M-T1, during myxoma virus pathogenesis. Virology 256: 233-45

21. McFadden G (1998) Even viruses can learn to cope with stress. Science 279: 40-1

22. Nash P, Barrett J, Cao JX, Hota-Mitchell S, Lalani AS, Everett H, Xu XM, Robichaud J, Hnatiuk S, Ainslie C, Seet BT, McFadden G (1999) Immunomodulation by viruses: the myxoma virus story. Immunol Rev 168: 103-20

23. Opgenorth A, Strayer D, Upton C, McFadden G (1992) Deletion of the growth factor gene related to EGF and TGF alpha reduces virulence of malignant rabbit fibroma virus. Virology 186: 175-91

24. Parks RJ, Evans DH (1991) Enhanced recombination associated with the presence of insertion and deletion mutations in poxvirus-infected cells. Virology 184: 299-309

25. Rajagopal I, Ahn BY, Moss B, Mathews CK (1995) Roles of vaccinia virus ribonucleotide reductase and glutaredoxin in DNA precursor biosynthesis. J Biol Chem 270: 27415-8

26. Reinecke K, Wolf, B., Michelson, A.M., Puget, K., Steffens, G.J., and Flohe, L. (1988) The amino-acid sequence of rabbit Cu-Zn superoxide dismutase. Biol chem Hoppe-Seyler 369: 715-725

27. Rypniewski WR, Mangani, S., Bruni, B., Orioli, P.L., Casati, M., and Wilson,K.S. (1995) Crystal structure of reduced bovine erythrocyte superoxide dismutase at 1.9A resolution. J. Mol. Biol. 251: 282-296

28. Seet BT, Johnston JB, Brunetti CR, Barrett JW, Everett H, Cameron C, Sypula J, Nazarian SH, Lucas A, McFadden G (2003) Poxviruses and immune evasion. Annu Rev Immunol 21: 377-423

29. Senkevich TG, Bugert, J.J., Sisler, J.R., Koonin, E.V., Darai, G., and Moss, B. 1996 (1996) Genome sequence of a human tumorigenic poxvirus: prediction of specific host response-evasion genes. Science 273: 813-816

30. Shisler JL, Senkevich TG, Berry MJ, Moss B (1998) Ultraviolet-induced cell death blocked by a selenoprotein from a human dermatotropic poxvirus. Science 279: 102-5

31. Smith DB, and Johnson KS (1988) Single-step purification of polypeptide expressed in *Echerichia coli* as fusions with glutathione-S-transferase. Gene 67: 31-40

32. Smith GL, Chan YS, Howard ST (1991) Nucleotide sequence of 42 kbp of vaccinia virus strain WR from near the right inverted terminal repeat. J Gen Virol 72 (Pt 6): 1349-76

33. Steinman HM, Naik VR, Abernethy JL, and Hill RL (1974) Bovine erythrocyte superoxide dismutase. Complete amino acid sequence. J Biol Chem 249: 7326-7338

34. Tainer JA, Getzoff, E.D., Beem, K.M., Richardson, J.S., and Richardon, D.C. (1982) Determination and analysis of the 2 A-structure of copper, zinc superoxide dismutase. J Mol Biol 160: 181-217

35. Tomalski MD, Eldridge R, Miller LK (1991) A baculovirus homolog of a Cu/Zn superoxide dismutase gene. Virology 184: 149-61

36. White CL, Weisberg AS, Moss B (2000) A glutaredoxin, encoded by the G4L gene of vaccinia virus, is essential for virion morphogenesis. J Virol 74: 9175-83

37. White CL, Senkevich TG, Moss B (2002) Vaccinia virus G4L glutaredoxin is an essential intermediate of a cytoplasmic disulphide bond pathway required for virion assembly. J Virol 76: 467-72

38. Willer DO, McFadden G, Evans DH (1999) The complete genome sequence of shope (rabbit) fibroma virus. Virology 264: 319-43

39. Zhang W, Evans DH (1993) DNA strand exchange catalyzed by proteins from vaccinia virus-infected cells. J Virol 67: 204-12

CHAPTER 3 – LEPORIPOXVIRUS SOD1 HOMOLOGS ARE CATALYTICALLY INERT DECOY PROTEINS THAT BIND COPPER CHAPERONE FOR SOD1 (CCS) *

Published in *Journal of Biological Chemistry*

Preface

A version of this chapter has been accepted for publication. Teoh MLT, Walasek PJ, and Evans DHE. 2003. *Journal of Biological Chemistry*. 278:33175-33184. The data presented in all figures was generated solely by me with the help of Miss Walasek in performing site-directed mutagenesis to generate the GST-S131R mutants. I wrote the first draft of the manuscript but the final version of this paper was edited by my supervisor, Dr. David Evans.

* Reprinted from Journal of Biological Chemistry, Vol. 278, Melissa L. T. Teoh, Paula J. Walasek, and David H. Evans, pp33175-84, Copyright (2003), with permission from American Society for Biochemistry and Molecular Biology.

Leporipoxvirus Cu-Zn superoxide dismutase homologs are catalytically inert decoy proteins that bind copper chaperone for SOD (CCS)*

By Melissa L. T. Teoh, Paula J. Walasek§, and David H. Evans¶

Running title: Poxvirus Cu-Zn SOD homologs

Department of Molecular Biology & Genetics

University of Guelph

Guelph, ON, N1G 2W1,

Canada

*This work was supported by operating and equipment grants from NSERC and the CIHR. The costs of publication of this article were defrayed in part by the payment of page charges. This article must therefore be hereby marked "*advertisement*" in accordance with 18 U.S.C. Section 1734 solely to indicate this fact.

§Current address: Dept. of Chemistry, University of Waterloo, 200 University Avenue West, Waterloo, ON, N2L 3G1.

¶To whom correspondence should be addressed: Dept. of Molecular Biology & Genetics, University of Guelph, Guelph, ON, N1G 2W1, Canada. Tel: 519-824-4120 (ext. 2575); Fax: 519-837-2075; E-mail: dhevans@uoguelph.ca.

3.1 INTRODUCTION

Cytosolic Cu-Zn superoxide dismutase (SOD1) is a homodimeric enzyme that catalyzes the dismutation of superoxide radical [15]. This activity protects cells from oxidative stress and the importance of the enzyme is illustrated by the effects of SOD1 expression levels on aging [18] and the association of SOD1 mutations with cases of human familial amyotrophic lateral sclerosis [21]. Superoxide dismutases are also expected to serve some role in modulating innate immunity since $O_2^{\cdot-}$ is one of several toxicants employed by the cellular arm of the immune system to kill bacteria and virus-infected cells [16, 31]. SOD1s are metalloproteins that depend upon a zinc atom for the maintenance of their structural integrity [14] and employ a copper atom as a catalytic cofactor [12]. The zinc atom is probably acquired by passive diffusion *in vivo*, but the copper atom is delivered by a "copper chaperone for SOD1" (CCS) using a switch-like translocation mechanism [11, 23] in a process requiring the formation of a SOD1-CCS heterodimer [13, 30].

Intriguingly, many large DNA viruses encode SOD1 homologs including Chordopoxviruses [1, 2, 4, 5, 32], Entomopoxviruses [3], and Baculoviruses [29]. Most of the poxvirus-encoded SOD1 homologs belong to one of two well conserved structural classes comprising either the Orthopoxvirus genes, which seem to have undergone an extensive process of deletional mutagenesis during the course of viral evolution [26], or proteins like those encoded by Leporipoxviruses which more closely resemble their cellular homologs [32]. The biological function(s) of the poxvirus-encoded enzymes are still largely unknown. It is noteworthy that all of the poxviral SOD1 homologs

characterized to date are catalytically inactive and a number of mutations might be responsible for this phenotype [2, 5]. Mutations in the protein sequence do not prevent homodimer formation under oxidizing conditions [5], but might be expected to delete some or all of the metal binding domains in these proteins. The proteins encoded by Leporipoxviruses (Shope fibroma virus [SFV] and myxoma virus [MYX]) and by the Orthopoxvirus vaccinia are also abundant virion components. It was thus very surprising to discover that despite the retention of these genes by many viruses, deleting either the vaccinia A45L or the MYX virus M131R genes seemed to have little effect on growth in culture or on virulence in animal disease models [2, 5]. The only biological effect that has been noted is that Leporipoxvirus SOD1 homologs ("SFV SOD" and "MYX SOD") inhibit the activity of endogenous cellular SOD1 activities *in vivo* [5]. This behaviour is unique to Leporipoxvirus SOD homologs, but how and why the MYX or SFV proteins might modulate the activity of cellular Cu-Zn SOD is unclear.

These observations raise several questions concerning poxviral SOD1 homologs that might, if answered, provide insights into the function of these intriguing proteins. First, these genes have clearly undergone an extensive process of mutagenesis and this has had a particular effect of producing a catalytically inactive protein. What are the multiple mutations responsible for this genetic feature? The answer to this question would establish whether encoding a functional superoxide dismutase has, at any time in the recent evolutionary past, been of some selective advantage for these viruses. Second, it is unclear from a comparison of the protein sequences of viral and cellular SOD1 homologs, what effect the many amino acid substitutions and small deletions have had on the metal binding properties of these proteins. Do the viral enzymes retain the capacity to

bind metals and thus perhaps function as Zn and/or Cu chelators? Finally, poxviral SOD1s conserve many of the amino acids that form the interface between cellular SOD1 homodimers and between SOD1 and CCS heterodimers (Figure 3.1). If these poxviral proteins have retained the capacity to associate with cellular SOD1 and/or CCS, this would provide a possible mechanism by which Leporipoxviruses could perturb the level of cellular superoxide dismutase activity.

In the studies that follow we show that Leporipoxvirus SOD1 homologs have lost the capacity to bind copper but retain the capacity to bind the copper chaperone and bind zinc. These biochemical properties suggest a novel way in which myxoma and Shope fibroma viruses might be using SOD1 homologs to manipulate intracellular concentrations of $O_2^{\cdot-}$ and thus promote the growth of virus-infected cells.

3.2 MATERIALS AND METHODS

Virus and virus culture. All cell lines (BSC40, BGMK, SIRC) were cultured in Dulbecco's modified Eagle's media (DMEM) supplemented with 10% fetal bovine serum [5]. Myxoma virus (strain Lausanne) and vaccinia virus (strain WR) were obtained originally from the American type culture collection and a vaccinia strain encoding T7 RNA polymerase (VTF7.5) obtained from Dr. P. Traktman (University of Wisconsin). The construction of a recombinant myxoma virus encoding a deletion of MYX SOD1 (myxΔM131R) and a vaccinia virus encoding SFV SOD1 under the regulation of a T7 promoter (VMM5.2) is described elsewhere [5]. Viruses were routinely passaged on BGMK or SIRC cells. Expression of recombinant SFV SOD1 in mammalian cells was accomplished by co-infecting BSC40 or BGMK cells with vaccinia VMM5.2 plus VTF7.5 at a multiplicity of two of each virus [5].

Plasmids and site-directed mutagenesis. Plasmid pDE422 [5] encodes the SFV SOD1 open-reading frame (S131R) fused in-frame with glutathione-S-transferase (GST) in pGEX2T (Amersham Pharmacia Biotech.). A standard PCR-based mutagenesis technique and mutagenic PCR primers were used to sequentially introduce amino acid substitutions into the SOD1 domain of the fusion protein. Table 1 illustrates the primers used and the resulting amino acid substitutions. Multiple amino acid substitutions were introduced in the order H148T→N59H→W157C→V157R creating mutant proteins designated S131R-T, S131R-TH, S131R-THC, and S131R-THCR, respectively. The W157C substitution mutation was also introduced separately into the cloned SFV S131R gene, creating a protein designated S131R-C. All plasmids were sequenced to confirm

the presence of the introduced substitution mutations and to ensure that no additional mutations were present. A plasmid encoding a protein comprising GST fused to full-length human copper chaperone for SOD1 (CCS) in pGEX4T was obtained from Dr. J. Gitlin (Washington University School of Medicine) [6]. Protein expression studies used *Escherichia coli* strain BL21.

Expression and purification of GST-tagged proteins. GST-tagged proteins were prepared following a modified commercial protocol (Amersham-Pharmacia). Bacterial cultures were grown to an optical density of one at 30° C in the presence of 50 μg/mL ampicillin and induced with 0.2 mM IPTG. $CuSO_4$ and $ZnSO_4$ were added to final concentrations of 0.1 mM, 30 min later, and the cells harvested by centrifugation two hours post-induction. The cell pellet was washed with phosphate buffered saline (PBS), frozen and thawed, and broken with a Dounce homogenizer in PBS containing 1 mM phenylmethylsulfonyl fluoride, 10mM EDTA, 75 μg/mL lysozyme, 5 mM dithiothreitol (DTT), and 1% Triton-X100. The debris was removed by centrifugation and GST-tagged proteins recovered by chromatography using a GSTrap column. Proteins were eluted with 10 mM reduced glutathione in 50 mM Tris-HCl (pH 8.0). Where indicated, GST-tagged proteins were cleaved overnight at room temperature in Tris-HCl with one cleavage unit of thrombin (Sigma) per 100 μg of fusion protein.

Metal analysis. Affinity purified GST fusion proteins were dialyzed extensively against 2000 volumes of Chelex-100 treated 25 mM phosphate buffer (pH 7.8) at 4° C. Protein concentration was determined using a dye-binding assay (Biorad) and a bovine serum albumin protein standard and the copper and zinc contents determined using a Varian 3000 graphite furnace atomic absorption spectrometer. Dialyzed bovine Cu-Zn

SOD (Sigma) was used as a control and reference for metal content. The metal content of GST was also measured and we detected <0.2 mol of zinc and no detectible copper per mol of GST protein.

Cu-Zn SOD assays. Superoxide dismutase activity was measured by monitoring the inhibition of reduction of ferricytochrome C by hypoxanthine/xanthine oxidase [20]. A solution containing the test sample and 12 mU/mL xanthine oxidase in 0.25 mL of PBS, was added to 0.25 mL of PBS containing 120 U/mL catalase, 0.2 mM hypoxanthine and 0.1 mM ferricytochrome C. The sample was incubated for five minutes at room temperature and ΔA_{550} monitored over two more minutes. One unit of activity is the amount of protein required to inhibit the reduction of cytochrome C by 50%.

Protein binding assays. GST "pull-down" assays used extracts prepared from bacteria expressing a GST-hCCS fusion protein. About 50 μL of 50% v/v glutathione-Sepharose beads (Sigma) were added to 1.0 mL of clarified bacterial lysate containing ~80 μg of fusion protein and incubated at 4° C for one hour. The beads were recovered by centrifugation, washed three times with PBS and then incubated with ~0.9 mg of mammalian cell protein in 0.2 mL of PBS at 4° C for two hours. The beads were washed extensively with PBS, and the protein complexes released by adding 0.1 mL of SDS-PAGE loading buffer containing 0.1 M DTT, plus 2% β-mercaptoethanol, and heating at 100° C for five minutes. Human SOD1 was used as a positive control (Sigma).

Immunoprecipitation assays used extracts isolated from virus-infected BGMK cells. The cells were harvested 15-24 hr post-infection by lysis with a buffer containing 1% NP-40, 0.1 mM phenylmethylsulfonyl fluoride, 1 μM aprotinin, and 1 μg/mL leupeptin and the insoluble material removed by centrifugation. The supernatant (~600

μL) was incubated overnight at 4° C with 1:500 diluted preimmune rabbit serum and ~50 μL (packed volume) of protein A beads (Sigma) and pre-cleared by centrifugation. The protein content of the supernatant was determined and 1 mg of protein extract (~600 μL) mixed with 5 μg of rabbit αCCS or murine αSFV S131R antibody and incubated at 4° C for two hours. Protein A beads were used to retrieve the complexes that were then washed three times with NP-40 lysis buffer. Proteins were released from the beads by boiling them for 5 min in 0.2 mL of SDS-PAGE loading buffer containing 0.1 M DTT. These interaction assays were repeated three times with similar results.

SDS-PAGE and Western blot analysis. Proteins were size fractionated using 12% SDS-PAGE [33] and transferred to a PVDF support as directed by the manufacturer of the membrane (Millipore). The membrane was treated with 5% blocking agent (Amersham) in PBST (PBS containing 0.1% Tween-20) and then incubated with either monoclonal αSFV SOD antibody (diluted 1:1000) or polyclonal αCCS antibodies (1:5000) in PBST for one hour at room temperature. The blot was washed six times with PBST and incubated with 1:50,000 diluted secondary antibody conjugated to horseradish peroxidase in PBST for one hour at room temperature. The membranes were washed extensively and horseradish peroxidase detected using a chemiluminescent substrate (Pierce) and Kodak OMAT-AR film. The monoclonal mouse αSFV S131R antibody detects both MYX and SFV SOD1 homologs, but not cellular SOD1 [5]. The polyclonal rabbit αCCS antibodies were kindly provided by Dr. J. Gitlin [6]. They target human CCS domains I and III [23] and thus do not cross-react with cellular SOD1. A polyclonal sheep α-human SOD1 antibody was purchased from Biodesign and also did not cross-react with viral SOD1 homologs (data not shown).

Confocal fluorescence microscopy. A Leica TCS SP2 confocal microscope was used to investigate the distribution of MYX SOD1 antigen. BGMK cells were seeded on glass cover slips, infected (or mock infected) with myxoma virus at a multiplicity of infection of 20, and cultured overnight. Next day (24 hr post-infection) "MitoTracker" Red CMXRos dye (Molecular Probes) was added to the media at 0.25 μM final concentration, and the incubation continued for 45 min at 37° C. The cells were washed, fixed for 15 min with 3.7% formaldehyde in fresh pre-warmed media, washed with PBS, and permeabilized by a 5 min treatment at room temperature with 0.2% Triton X-100 in PBS. Thereafter all incubations and washes were performed at room temperature solutions containing PBS. The cells were washed, "blocked" for 30 min with 5% non-immune goat serum (Molecular Probes), and then incubated for 1 hr with a solution containing 1:40 diluted αSFV/MYX SOD1 monoclonal antibody plus 2% goat serum. The cells were washed and incubated for 30 min with a solution containing 1:400 diluted Alexafluor 488-labelled goat-α–mouse IgG (Molecular Probes) plus 2% goat serum, then washed again and mounted in a PBS solution containing 50% glycerol.

Isolation and purification of mitochondria. SIRC cells were infected with virus, at a multiplicity of infection of two, and cultured 24 hr. Fifteen millilitres of ice-cold homogenization buffer (10 mM Tris·HCl at pH 7.4, 1 mM EDTA, 0.2 M mannitol, 50 mM sucrose, 1x Roche complete protease inhibitor cocktail) was added to each 30 x 150 mm dish and the cells broken with a Dounce homogenizer on ice. Three different cell fractions were then isolated by a series of centrifugation steps and each fraction washed three times with homogenization buffer. These were a crude nuclear fraction (1,000 x g, 10 min), a crude heavy mitochondrial fraction (3,000 x g, 10 min), and a

crude light mitochondrial fraction (20,000 x g, 20 min). The remaining material was designated the post-mitochondrial supernatant.

Mitochondria were further gradient purified using the method of Okado-Matsumoto and Fridovich [17] as suggested by Nycomed Pharma. A 50% (w/v) stock solution of Nycodenz, (in 10 mM Tris·HCl, 1 mM EDTA, pH 7.4) was diluted with 0.25 M sucrose, in the same buffer, to produce solutions containing 20-34% Nycodenz. Discontinuous density gradients were then prepared by layering 1.5 mL of 34%, 2.5 mL of 30%, 2.5 mL of 23% and finally 1 mL of 20% Nicodenz in 11 mL centrifuge tubes. The crude heavy mitochondrial pellet was resuspended in 3 mL of 25% Nycodenz, layered over this gradient, and centrifuged at 19,900 rpm for 90 min at 4°C in a Beckman SW28 Ti rotor. Four distinct bands formed at the gradient boundaries and 0.6 mL of mitochondria removed from the 25/30% interface by side puncture [17]. The purity of these fractions was judged by Western blotting. Actin was used as a cytosolic marker (1/5,000 diluted α-β-actin monoclonal antibody, Sigma), GRP78 as a microsomal marker (1/1,000 diluted α-GRP78 rabbit polyclonal antibody, Santa Cruz), catalase as a peroxisome marker (1/5,000 diluted α-catalase monoclonal antibody, Sigma), and cytochrome C oxidase as a mitochondrial marker (1/1,000 α-COX subunit IV monoclonal antibody, Molecular Probes). Manganese SOD (mSOD) was detected using an α-mSOD rabbit polyclonal antibody diluted 1/5,000 and purchased from Stress Gene.

3.3 RESULTS

Structural features of SFV and other poxvirus SOD1 homologs. Figure 3.1 shows a comparison of the amino acid sequences of the SOD1-like proteins encoded by poxviruses with the homologous sequences of bovine SOD1 and the SOD-like domain II of human CCS (hCCS). This multiple sequence alignment illustrates the multiple deletions in the gene that seem to have occurred during the evolution of Orthopoxviruses like ectromelia, vaccinia and variola. These deletions would be expected to delete all the residues shown from crystallographic analysis of bovine SOD1 [22] to form the zinc binding domain (Figure 3.1, "●") and results in this family of virus genes segregating to a different branch of a SOD-based "relatedness" tree (Figure 3.1, lower panel). In contrast the SFV S131R gene product, and similar "non-orthopoxvirus" proteins, seems to have retained many of the structural features of SOD1s including the amino acids that form the interface between SOD homodimers (Figure 3.1, "*"). SFV SOD1 has also retained homologs of the amino acids which in the yeast CCS-SOD1 heterodimeric structure [13] form key interactions between CCS and SOD1 (Figure 3.1, "o"). The residues responsible for binding zinc have also been conserved in SFV SOD1, but an H→N substitution would delete at least one of the copper coordinating residues (Figure 3.1, "○"). The capacity to form an intrastrand cross-link also seems to have been impaired by a C→W substitution, and possibly by the displacement of the cysteine partner, and an R→V substitution is expected to delete an arginine involved in catalysis [22]. Similar sequence changes characterize the gene encoded by myxoma virus, and to viruses belonging to the Capripoxvirus family, while the protein encoded by *Amsacta*

moorei entomopoxvirus is sufficiently similar to cellular SOD1 orthologs to account for it being catalytically active (R. Moyer and M. Becker, personal communication).

Interestingly, Lamb *et al.* [13] noted that forming a SOD1-CCS heterodimer leads to an exchange of disulphide bonds. A intrastrand bond between C57 and C146, seen in the yeast SOD1 homodimer, is replaced in the SOD1-CCS complex by an interstrand disulphide bond between the SOD1 monomer and domain III of yeast CCS (SOD1 C57 and CCS C229). Molecular modelling suggests that amino acid C67 in the Leporipoxvirus SOD1 homologs occupies a position very similar to that of C57 in yeast SOD, within loop 4 and corresponding to the S-S subloop region of the cellular enzymes. Viral SOD homologs don't encode a second homologous cysteine that would be well positioned to form an intrastrand disulphide bond with viral residue C67. Instead, this residue would be predicted to protrude outwards and facing the surface of the protein where it would be well positioned to form an intermolecular disulphide bond with CCS C229.

Figure 3.1. Multiple sequence alignment of cellular and viral SOD1 homologs. Clustal W [28] was used to align the indicated protein sequences and this alignment used to generate an average distance tree. *Orthopoxvirus* SOD1 homologs are encoded by ectromelia (EVM-144), cowpox (CPXV-187), camelpox (CMLV-165), variola (VAR_Bang-A45R), vaccinia strain MVA (VV_MVA-158R), rabbitpox (RPV-157), vaccinia strain Copenhagen (VV_Cop-A45R), and monkeypox (MPV-Zar-A46R) viruses. *Capripoxviruses* include sheeppox (ShPV_TU-126), lumpy skin disease virus (LSDV-131), and swinepox (SPV-129) viruses. *Leporipoxviruses* are myxoma (MYX-M131R) and Shope fibroma (SFV-S131R) viruses. The alignment also includes an *Amsacta moorei* entomopoxvirus gene (AmEPV-255), bovine SOD1 (SODC_BOVINE) and residues 71-235 from domain II of human CCS (CCS_HUMAN). The figure also shows residues found from X-ray structures to form the SOD1:SOD1 and SOD1:CCS interface [13]. It should be noted that other alignments are also possible. In particular, RLACG motif in orthpoxvirus SOD1 genes (position 124-128) might be better aligned with functional SOD gene (position 142-146 in bovine SOD1). The alignment also shows that orthopoxvirus SOD1 genes seem to be divergent with some small in-frame deletions (indicated as gap in the alignment). However, this feature could be an artifact of the scoring system. Closer examination indicates that the orthopoxvirus genes could be originated from either CCS/SOD but one can't really differentiate these two possible origins from the tree. The positions of the four amino acid substitutions that were introduced into SFV S131R in an attempt to restore catalytic activity are also noted (N59H, H148T, V154R, and W157C).

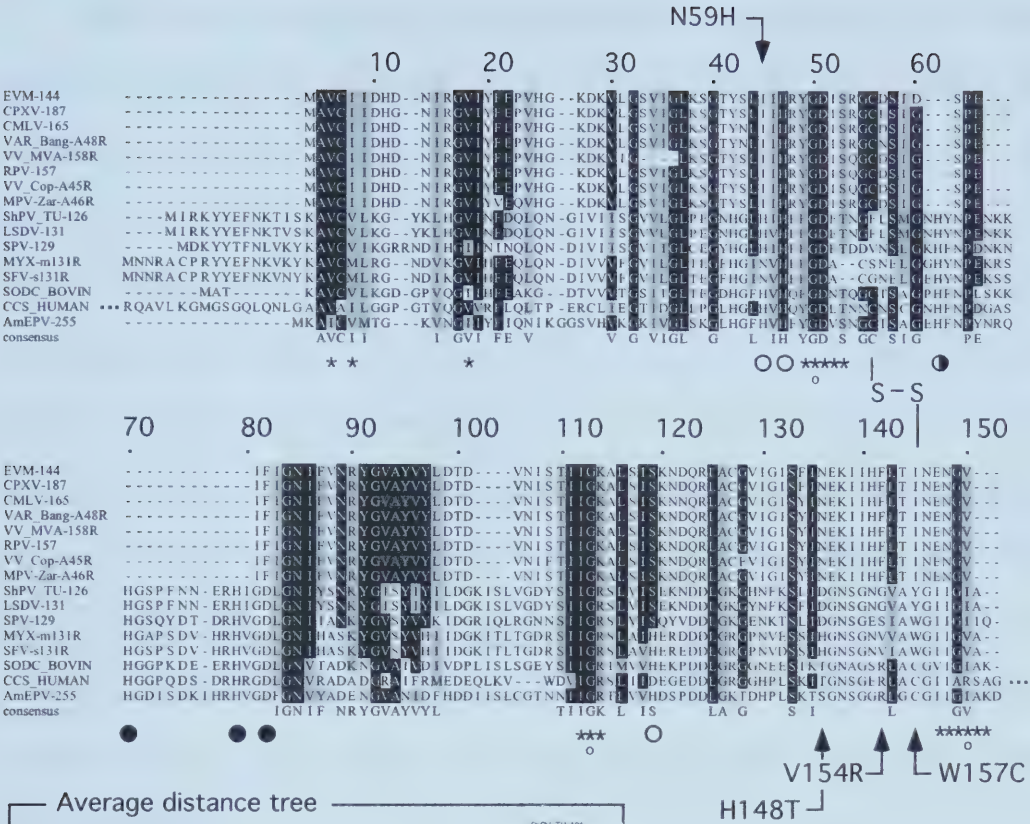

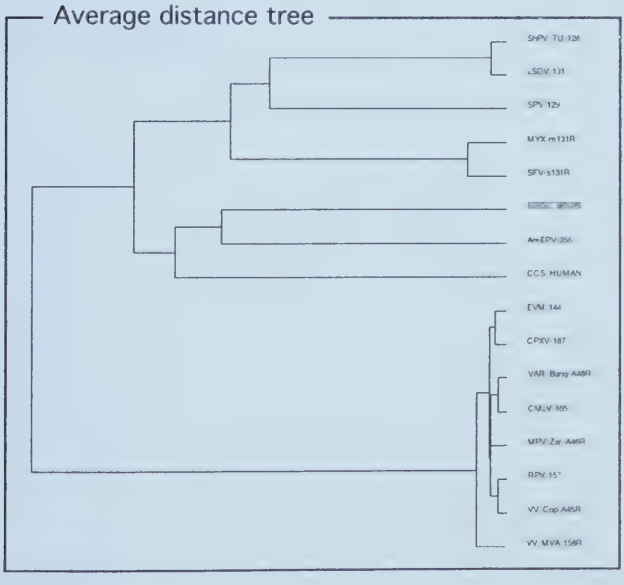

Key

- ○ Cu-binding residue
- ● Zn-binding residue
- * SOD-SOD interface
- ◦ CCS-SOD interface

Site directed mutagenesis and purification of recombinant SFV S131R protein. In order to gain some insights into the impact of these different amino acid substitutions upon the enzymatic and metal-binding properties of SFV S131R, we introduced a series of amino acid substitution mutations into the SFV S131R gene, in an attempt to return the sequence to something more closely resembling a catalytically active superoxide dismutase. The sequence alterations are shown in Table 3.1. The W157C mutation (numbering refers to the SFV S131R gene) was introduced to restore some potential for forming an intrastrand disulphide bond with the semi conserved cysteine at S131R position 67. Based upon molecular modelling of the structure of the copper binding cleft in SFV S131R, the two H148T and N59H substitutions were expected to restore the original copper-coordinating domain, and the V154R mutation was introduced to restore a highly conserved arginine that comprises part of the bovine SOD1 catalytic site.

Table 3.1. Mutant forms of S131R proteins generated by sequential rounds of site directed mutagenesis. Mutations were introduced in the order H148T→N59H→W157C→V157R as well as W157C separately. The quadruple mutant S131R-THCR might be expected to restore the copper-coordinating domain (H148T+N59H), an intrastrand disulphide bond (W157C) and a catalytic arginine (V154R).

Mutant	Oligonucleotides (5'-3')	Amino acid substitution(s)
S131R-C	ACGTTATCGCCTGTGGGATTATAGGAGTTGCT ATCCCACAGGCGATAACGTTACCGGAATTACC	W157C
S131R-T	AGTTCGATAACCGGTAATTCCGGTAATGTT GAATTACCGGTTATCGAACTGTCTACGTT	H148T
S131R-TH	CACGGTATACATGTTCATGAGTTTGGAGAT TCATGAACATGTATACCGTGAAATCCTTCA	H148T+N59H
S131R-THC	ACGTTATCGCCTGTGGGATTATAGGAGTTGCT ATCCCACAGGCGATAACGTTACCGGAATTACC	H148T+N59H+W157C
S131R-THCR	AGGCGATGCGGTTTCCGGAATTACCGGTTAT GGAAACCGCATCGCCTGTGGGATTATAGGAGTT	H148T+N59H+W157C+V154R

These S131R mutant proteins, along with the wild type protein, were expressed in *E. coli* as GST-fusion proteins, purified using affinity chromatography (see Materials and Methods) and digested with thrombin to release the 18 kDa S131R proteins (Figure 3.2). These proteins were all readily expressed as GST fusion proteins in *E. coli* and for the most part caused no obvious toxicity. The growth of bacterial strains encoding the quadruple mutant S131R-THCR was slowed significantly upon inducing the expression of this particular polypeptide, but this effect was overcome by adding $CuSO_4$ and $ZnSO_4$ to the media.

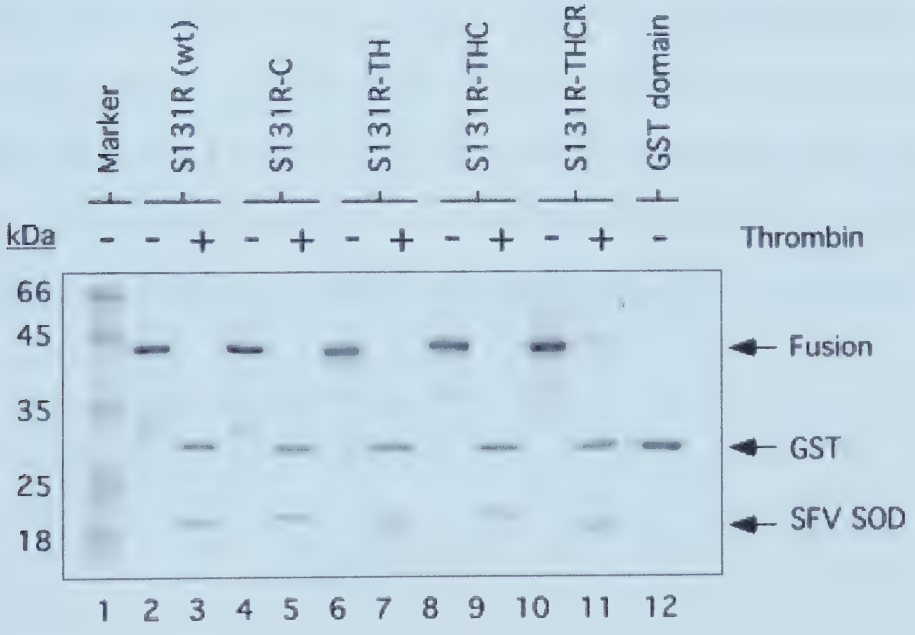

Figure 3.2. SDS-PAGE analysis of recombinant forms of SFV SOD protein. GST-tagged proteins were prepared in *E. coli*, affinity purified, and digested where indicated with thrombin. About 200 ng of each protein was then size-fractionated using a 12% SDS-PAGE gel and visualized by staining with GelCode Blue dye (Pierce). Up to four amino acid substitutions were introduced into the protein (S131R-THCR) with little apparent effect on yield or purity.

Multiple mutations prevent SFV SOD from behaving as a superoxide dismutase. Despite introducing up to four potentially restorative amino acid substitution mutations into SFV SOD, we were unable to restore any significant additional dismutase activity to the protein. Our previous work had used a semi-quantitative *in situ* gel staining method to show that the native protein exhibited less than one percent of the activity of bovine or human Cu-Zn SOD [5]. Using a more quantitative cytochrome-c-based spectrophotometric method, we observed that the wild-type protein retains almost exactly 1% of the activity of the purified bovine enzyme (Figure 3.3). No significant changes in this level of activity were obtained with the introduction of any of the amino acid substitutions, even in the quadruple S131R-THCR mutant protein. It also made no difference to the level of activity whether, or not, SFV SOD was cleaved from the GST fusion protein (Figure 3.3) and incubating the proteins beforehand with metal salts had no effect on the activity (data not shown). We concluded that at least four, and probably more, mutations have accumulated over the evolution of the SFV S131R gene and these multiple mutations render the encoded polypeptide inactive as a superoxide dismutase.

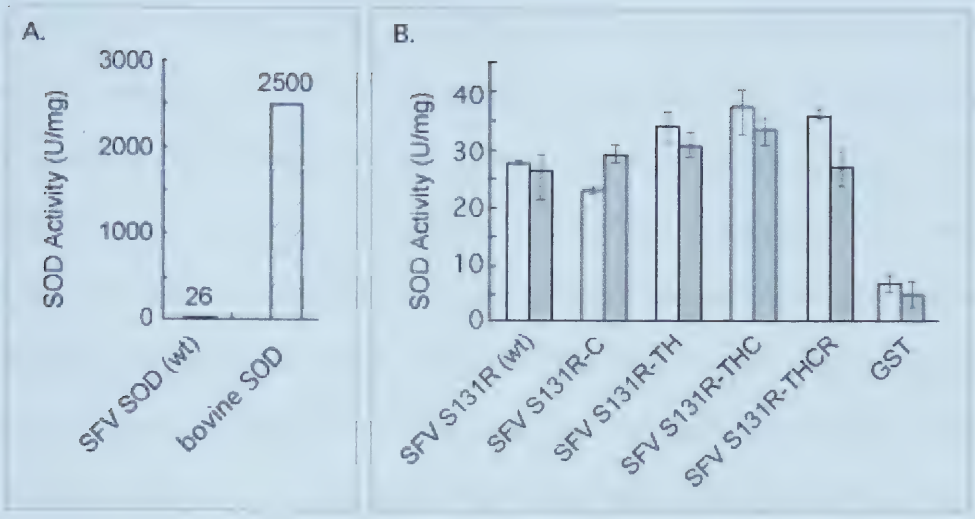

Figure 3.3. Superoxide dismutase activity of wild-type and mutant forms of S131R protein. SOD1 activity was determined by measuring the enzymatic interference in the reduction of cytochrome-C in a reaction containing hypoxanthine and xanthine oxidase. Panel A shows a comparison of the activities of wild-type SFV SOD protein and bovine SOD1. The S131R gene product displays only ~1% of the SOD1 activity of a *bona fide* cellular SOD1. Panel B shows that introducing up to four amino acid substitutions into S131R still does not restore SOD1 activity. Both intact (open bars) and thrombin-cleaved (grey bars) GST fusion proteins were assayed to show that removing the GST domain did not alter the activity.

SFV SOD homolog binds zinc but not copper. Graphite furnace atomic absorption spectroscopy was used to analyze the copper and zinc content of the purified recombinant proteins (Figure 3.4). These experiments can be complicated by the presence of trace levels of adventitious metals, so care was taken to exhaustively dialyse the recombinant proteins against metal-free buffers and thus eliminate any weakly associated copper or zinc. In addition, controls were performed which readily detected ~1 mol each of Cu and Zn per mol of dialyzed bovine SOD1 and we found there was no significant contribution to the metal content from the GST domain (cleaved or not). It should be noted that we also explored several alternative methods of sample preparation including varying the copper and zinc content of the bacterial media. The metal content of the SFV proteins seemed quite insensitive to such experimental perturbations and this gives us some confidence that the results reported are not especially sensitive to vagaries in the method of protein preparation. These studies showed that wild-type SFV S131R bound ~1.3 mol of zinc per mol of SOD1 polypeptide and this quantity of metal was largely unaffected by introducing S131R-T, S131R-TH, and S131R-THC substitutions into the polypeptide. In contrast to the bovine SOD1 control, the Leporipoxvirus proteins bound significantly less copper than zinc, with the most of the protein forms binding $\leq$ 0.2 mol of copper per mol of protein. Although the poor affinity for copper could readily explain why most of these protein species lacked dismutase activity (Figure 3.3), it is notable that the S131R-THCR protein also lacked activity even though a significant portion of the protein was seemingly isolated in a Cu-Zn metallated form. The S131R-THCR protein bound both metals although, unlike bovine SOD1, it bound less than stoichiometric quantities of each. We detected ~0.35 mol of zinc and ~0.4 mol of copper

per mol of protein (Figure 3.4). An attractive explanation for these properties of the quadruple mutant protein is that copper may still not be incorporated properly into the active site. Instead it could be displacing zinc from the zinc-binding site and this anomalous binding could explain the lack of activity.

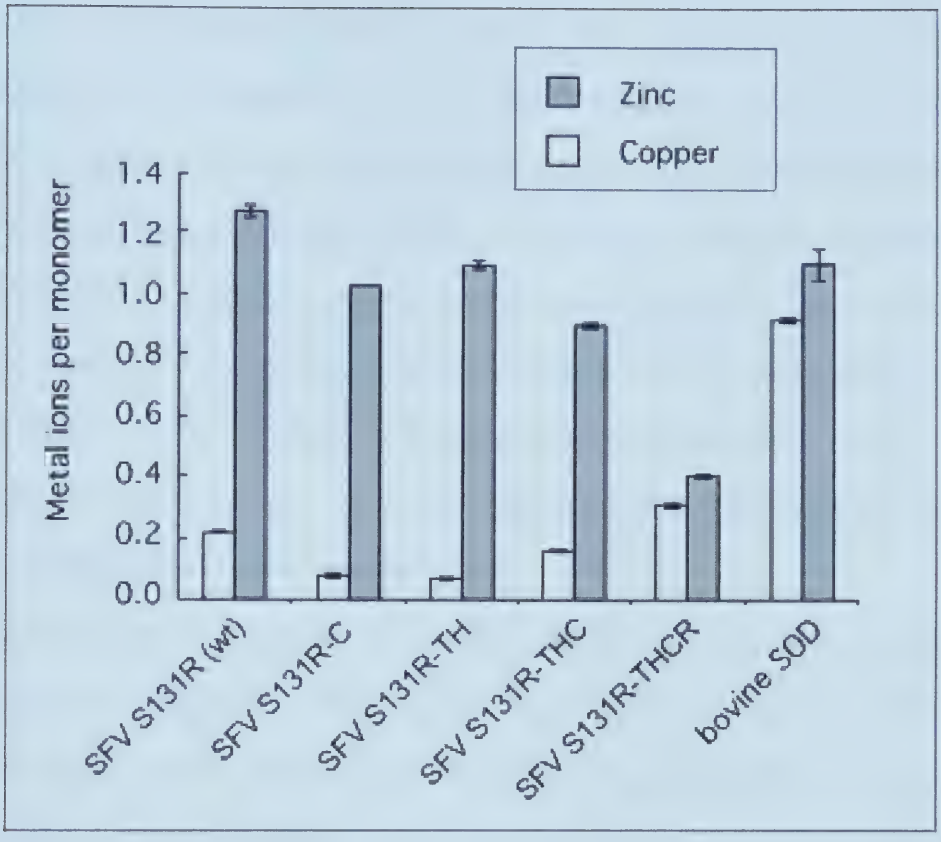

Figure 3.4. Metal content of wild-type and mutant forms of SFV SOD. Affinity purified GST fusion proteins were dialyzed extensively at 4° C against a Chelex-treated 2.5 mM phosphate buffer prior to metal analysis. Except for the SOD-THCR mutant, the zinc contents of the other forms of SFV S131R are comparable to that of bovine SOD1. None of the SFV S131R species bound copper with a stoichiometry comparable to bovine SOD1.

Leporipoxviruses Cu-Zn SOD homologs form stable complexes with cellular CCS. The experiments described above showed that Leporipoxvirus SOD1 homologs have retained the zinc-binding property of cellular SOD1s. MYX and SFV SOD1-like proteins can also form homodimers [5] much like their cellular counterparts. These observations suggested that the poxvirus proteins might have partially conserved the metal and protein-binding properties of SOD1s even though they may not have retained the catalytic activity over the course of viral evolution. We were thus curious to determine whether SFV and MYX proteins shared a third property of cellular SOD1s; the capacity to form stable complexes with copper chaperones for SOD1 (CCS). A combination of "GST-pull-down" and co-immunoprecipitation studies showed that CCS is another binding partner both *in vivo* and *in vitro*.

In the first set of experiments we co-infected BGMK cells with two recombinant vaccinia viruses and prepared a cell-free extract. Vaccinia strain VMM5.2 encoded the SFV S131R gene under the regulation of a T7 promoter and, in the presence of a helper virus encoding T7 RNA polymerase (VTF7.5) caused the expression of large quantities of native SFV S131R [5]. Extracts were prepared from these cells and incubated with a fusion protein consisting of GST-linked to CCS and immobilized on glutathione-Sepharose beads. The bound protein was eluted with reduced glutathione, separated using SDS-PAGE and a Western blot performed using a monoclonal antibody specific for SFV S131R (Figure 3.5). The GST-tagged CCS readily extracted an 18 kDa SFV SOD from vaccinia-infected cell lysates. No trace of the 18 kDa polypeptide was recovered from mock infected cell extracts, nor did GST alone bind to SFV S131R. SFV S131R thus appeared to form complexes with CCS.

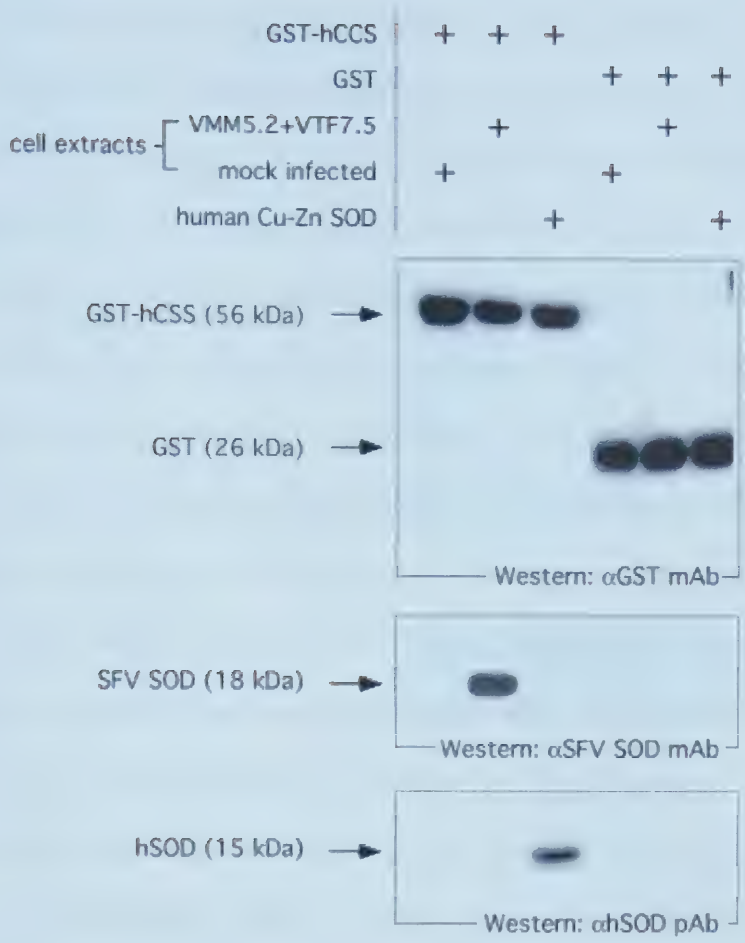

Figure 3.5. ***In vitro*** **interactions between SFV SOD and human CCS.** Recombinant SFV SOD was produced by infecting BSC-40 cells with a mixture of two vaccinia viruses encoding a T7 promoter regulated copy of the SFV S131R gene (VMM5.2) plus T7 RNA polymerase (VTF7.5). A cell free extract was then prepared and incubated with a GST-hCCS fusion protein attached to glutathione Sepharose beads. The beads were recovered, washed and the bound proteins eluted and size-fractionated using a 12% SDS-PAGE gel. Western blots were then used to detect either the GST domain (top panel) or SFV S131R (middle panel). Controls included extracts isolated from mock-infected cells and beads coated with just GST protein. Only the GST-hCCS fusion protein precipitated recombinant SFV S131R. Another control (bottom panel) illustrates the interaction between GST-hCCS and human SOD1 (10 μg per reaction).

To further investigate the specificity of this interaction, polyclonal antisera directed against CCS domains I and III, or monoclonal antibodies directed against SFV SOD1, were immobilized on protein A-agarose beads and incubated with vaccinia-infected BGMK cell lysates containing recombinant SFV SOD1. Any bound proteins were eluted from the beads, separated by SDS-PAGE and a Western blot performed using different antibodies. Although BGMK cells have a monkey origin, the α-human CCS antibodies immunoprecipitated an appropriately sized monkey CCS peptide from both mock and virus-infected cell extracts (Figure 3.6, middle panel). The αCCS antibodies co-immunoprecipitated SFV SOD1 from a virus-infected cell extract, but not from mock-infected cell extracts (Figure 3.6, top). In the reciprocal experiment, the αSFV SOD monoclonal antibody immunoprecipitated SFV SOD1 from virus-infected cell extracts (Figure 3.6, top) and co-immunoprecipitated the 30 kDa monkey CCS from the same sample (Figure 3.6A, middle). BGMK cell CCS was not detected in precipitates obtained from mock-infected cell extracts, thus demonstrating the specificity of the αSFV S131R monoclonal antibody. Oddly, more CCS was detected in virus-infected cells than in mock-infected cells (compare lanes 1 and 2). We do not know the explanation for this observation, but it seemed to be a reproducible feature of vaccinia virus infection.

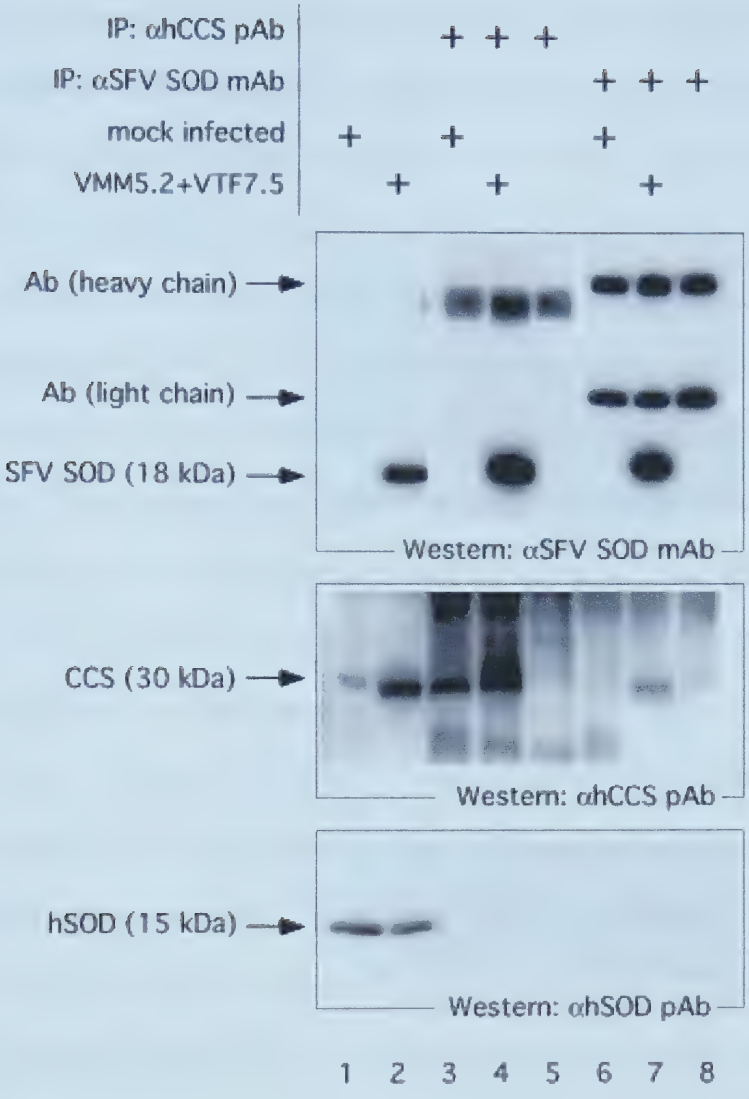

Figure 3.6. Co-immunoprecipitation of SFV SOD1 and cellular CCS. Extracts were prepared from either mock-infected cells or cells infected with a mixture of two recombinant vaccinia viruses (VMM5.2 plus VTF7.5). These extracts with incubated with antibodies directed against either CCS or SFV SOD1, the proteins immunoprecipitated and size fractionated using an SDS-PAGE gel, and a Western blot analysis performed using the indicated reagents. Cell-free extracts were also applied directly to the SDS-PAGE gel omitting the precipitation step. CCS precipitated both SFV SOD1 (top panel) and CCS (middle panel), but only in cell extracts where recombinant SFV SOD1 was being expressed. SFV SOD1 precipitated SFV SOD11 (top panel) and CCS (middle panel), but again only in cell extracts where recombinant SFV SOD was being expressed. Neither antibody co-immunoprecipitated cellular SOD1 even though it is present in the extracts (bottom panel). Protein samples were replaced with buffer in lanes 5 and 8). These controls identify the backgrounds produced by the precipitating antibodies.

Several controls served to validate these methods. The recombinant SFV SOD1 is highly expressed using T7-based vaccinia vectors, so to exclude the possibility that we were observing a non-specific binding reaction we substituted an αGST monoclonal antibody for the αCCS antibody and observed no recovery of SFV SOD1 or CCS (data not shown). We also looked for an interaction in cells infected with myxoma virus where the level of expression of MYX SOD1 is expected to more closely resemble a normal infection. We chose to use myxoma virus for these studies because MYX SOD1 is nearly identical to SFV SOD1 (the two proteins share 94% amino acid identity) and a myxoma ΔM131R knockout virus [5] was available for use as a control. The αSFV S131R monoclonal antibody cross-reacted with MYX SOD1 in myxoma-infected cells (Figure 3.7, top) and the antibody co-immunoprecipitated monkey cell CCS from the sample (Figure 3.7, bottom). The same αSFV S131R antibody did not precipitate CCS from cells infected with MYX_M131RΔ deletion virus. In the reciprocal experiment, the αCCS antibodies immunoprecipitated CCS from all of the samples (Figure 3.7, bottom), but only retrieved MYX SOD1 from cells infected with wild-type virus (Figure 3.7, top). Collectively, these data clearly show that Leporipoxvirus SOD1 homologs form strong and stable interactions with cellular CCS even in normal infections.

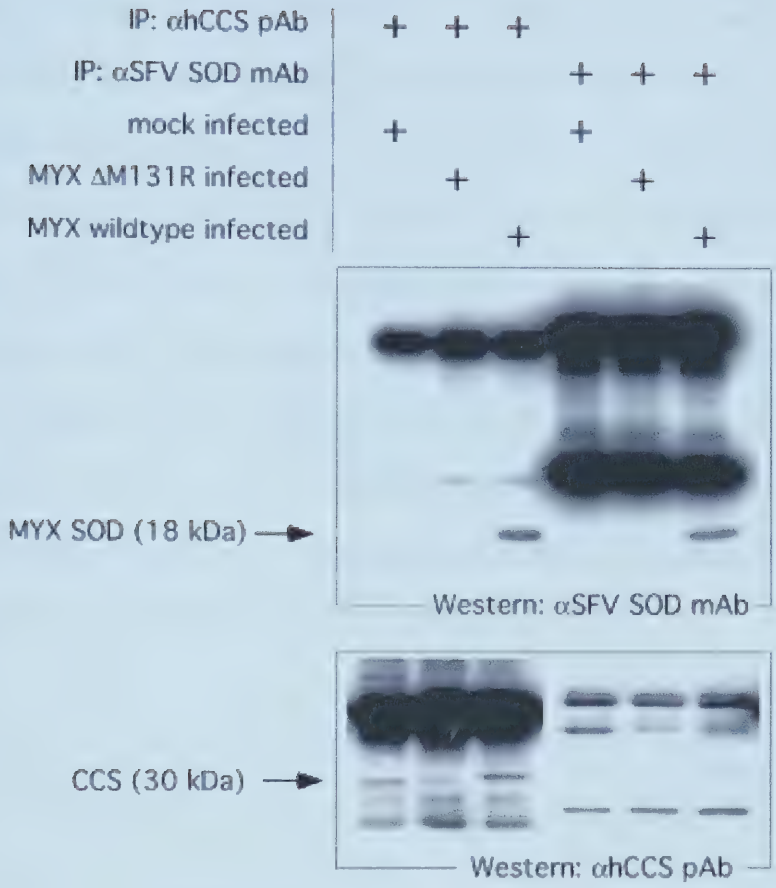

Figure 3.7. Co-immunoprecipitation of MYX SOD1 and cellular CCS in myxoma-infected cells. Extracts were prepared from mock-infected BGMK cells, or cells infected with either wild-type myxoma virus or a virus encoding a deletion of MYX SOD1 (ΔM131R). These extracts with incubated with antibodies directed against either CCS or SFV SOD1, the proteins were immunoprecipitated and size fractionated using an SDS-PAGE gel, and a Western blot analysis performed using the indicated reagents. CCS precipitated both MYX SOD1 (top panel) and CCS (bottom panel), but MYX SOD1 was only co-immunoprecipitated from cells infected with wild-type myxoma virus. An αSFV SOD1 antibody precipitated MYX SOD1 (top panel) and CCS (bottom panel), but CCS was only co-immunoprecipitated from cells infected by wild-type myxoma virus. Note that the αSFV SOD1 mAb used in these experiments cross-reacts with both myxoma and SFV SOD1 homologs since the two proteins are nearly identical (Figure 3.1).

Leporipoxvirus SOD1s do not bind cellular SOD1 or affect the levels of this protein. If MYX and SFV SOD1s have conserved sufficient sequence to still bind human and monkey CCS it raises the question whether these proteins can also form stable heterodimers with cellular SOD1. We were unable to detect any complexes formed between SFV SOD1 and cellular SOD1 as judged by immunoprecipitation studies (Figure 3.6, bottom panel). We also noted that virus infection caused no obvious change in the level of SOD1 protein (Figure 3.8) despite the fact that infection is associated with a ~60% decline in the *activity* of cellular SOD1 [5]. We concluded that if these interactions do occur, they are either too weak to disrupt preformed cellular SOD1 homodimers or cannot survive the precipitation reactions. Nor do these viruses affect the quantity of SOD1 protein present in an infected cell.

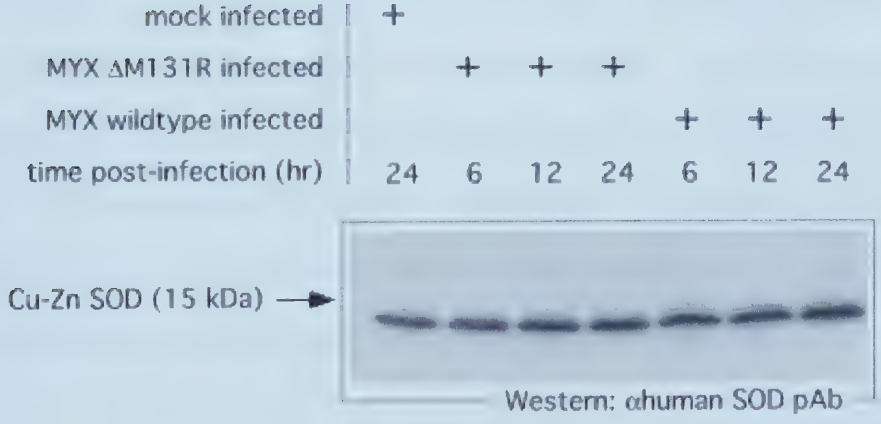

Figure 3.8. Stability of cellular SOD1 in virus-infected cells. BGMK cells were infected with wild-type or ΔM131R myxoma virus and the level of cellular SOD1 determined by Western blotting. Myxoma SOD1 is a late gene product that is first detected ~12 hr post-infection [5].

Distribution of Leporipoxvirus SOD1 homologs in infected cells. These experiments raise questions regarding where viral SOD1 homologs might be exerting their effects on the copper chaperone. The distribution of the myxoma protein was investigated using confocal immunofluorescence microscopy and the αSFV/MYX SOD1 monoclonal antibody. Preliminary experiments (not shown) detected a speckled staining pattern suggestive of mitochondrial involvement. This was confirmed using a double-labelling strategy where infected cells were stained with both the αSFV/MYX SOD1 monoclonal antibody and a mitochondrial-specific dye (Figure 3.9). Although some MYX SOD1 antigen was distributed throughout the cell by 24 hr post-infection, a substantial portion of the Alexfluor (green) αMYX SOD1 label was seen to overlap with the MitoTracker (red) mitochondrial label (Figure 3.9) and this co-localization was observed throughout the cross-sections imaged (data not shown). No SOD1 antigen was detected in cells infected with the ΔM131R knockout virus or in mock-infected cells. We also attempted to localize cellular CCS using the αCCS polyclonal antibody. Unfortunately this antigen-antibody combination produced a weak signal and high background in BGMK cells and the high gain needed to detect the signal, rendered suspect the interpretation of double-labelling experiments (data not show). Nevertheless it was clear that the interactions characterized above, between viral SOD1 homologs and cellular CCS, could potentially occur in organelles like the mitochondria.

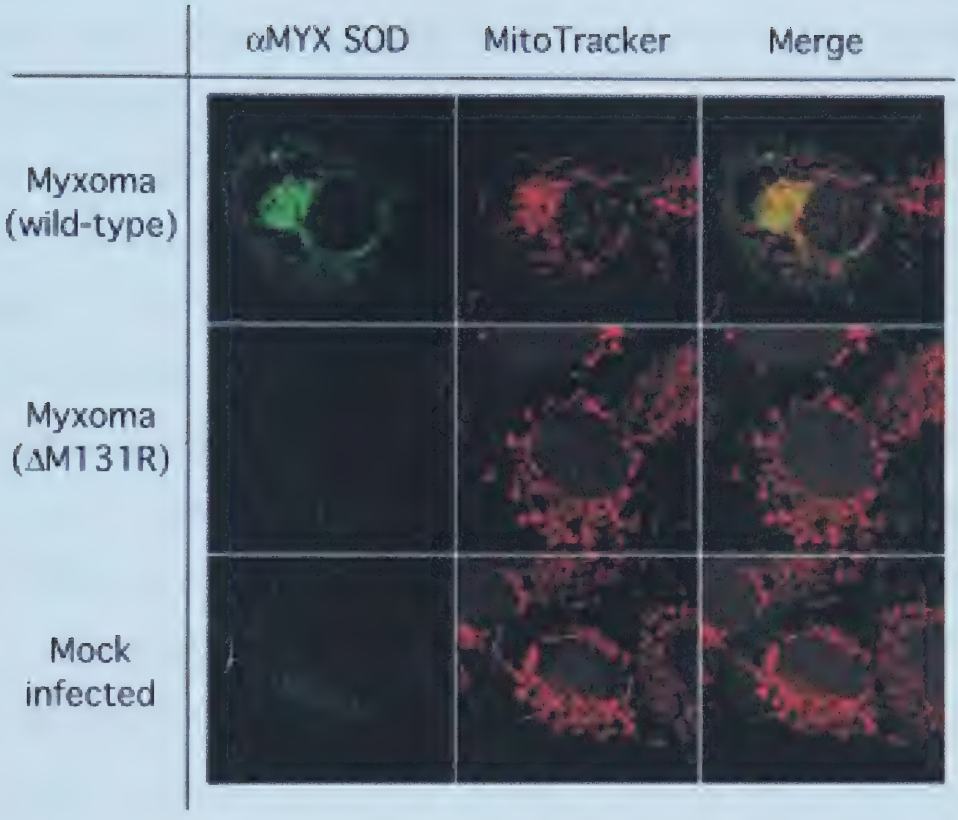

Figure 3.9. Intracellular localization of myxoma virus SOD1. BGMK cells were infected with either wild-type myxoma virus (top panels), myxoma virus encoding a deletion of MYX SOD1 (ΔM131R) (middle panels), or mock infected (bottom panels) and cultured overnight. The distribution of viral SOD antigen was then determined by immunostaining with αSFV/MYX SOD1 mAb antibody and Alexafluor 488-labelled goat-α-mouse secondary antibody (green). Mitochondria were located using MitoTracker CMXRos fluor (red). Much of the MYX SOD1 antigen co-localized with the mitochondria and produced a yellow signal in the merged image. No MYX SOD1 antigen was detected in ΔM131R- or mock-infected cells (lower panels).

Purified mitochondria also contain MYX SOD1. To further investigate the distribution of viral SOD in infected cells, we used cell fractionation methods and Nycodenz density gradient centrifugation to isolate different organelle fractions including highly purified mitochondria [17]. Mitochondria obtained from the 25/30% Nycodenz interface were shown, using Western blots and appropriate protein markers, to be substantially free of contamination by cytosolic, microsomal, and peroxisomal debris (Figure 3.10). The α-S131R monoclonal antibody still detected similar amounts of the MYX-SOD antigen in all of the fractions isolated from wild-type virus infected cells. Using these methods it is difficult to be certain that proteins aren't lost through diffusion from organelles during their fractionation. However, considering the relative amounts of each fraction recovered from the cells and loaded on these gels, we estimated that about 2% of the viral SOD1 was present in the mitochondrial fractions. No MYX SOD1 was detected in cells infected with the ΔM131R virus, while the presence or absence of MYX SOD1 had no obvious effect on the amount of cellular SOD1 detected in the mitochondria isolated from cells infected with wild-type or ΔM131R knockout viruses.

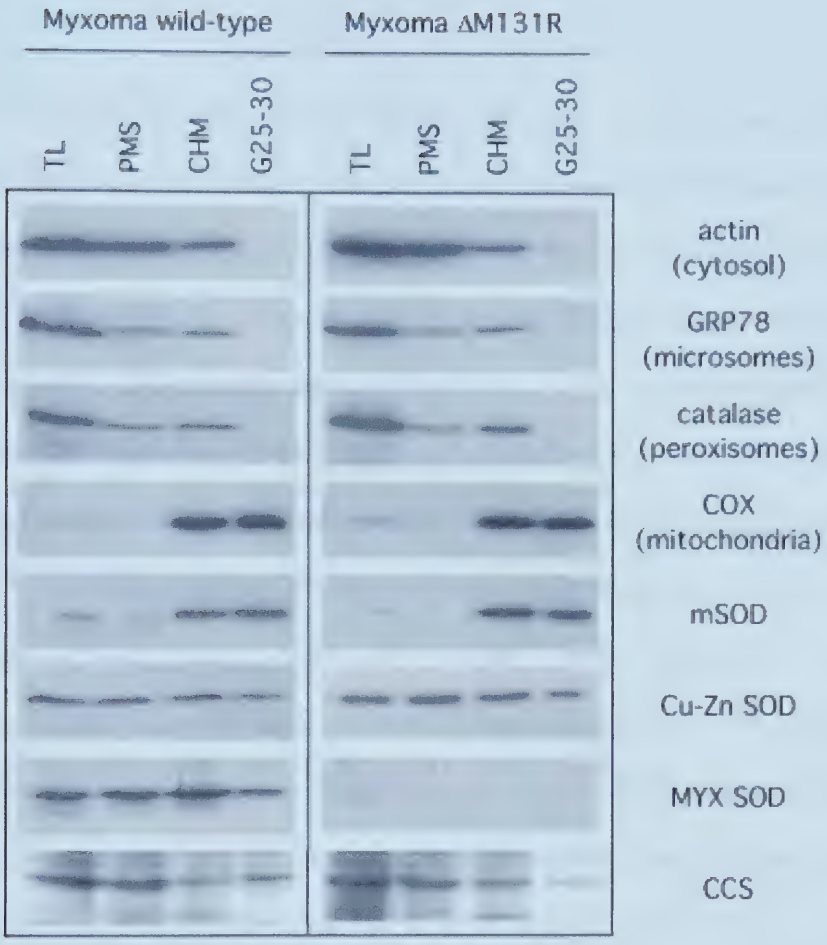

Figure 3.10. Density gradient fractionation of mitochondria from virus-infected cells. SIRC cells were infected with either wild-type myxoma virus, or a virus encoding a deletion of the SOD gene (ΔM131R). Twenty-four hours post-infection, the cells were fractionated by centrifugation and mitochondria purified using Nycodenz gradients as described in the Materials and Methods. A 50-fold cell equivalent excess of both the crude heavy mitochondria (CHM) and gradient-purified mitochondria (G25-30) were applied to the gel compared with the total lysate (TL) and post-mitochondrial supernatant (PMS). Western blots were used to verify the identity and purity of the fractions using the indicated protein markers. Additional Western blot analyses were used to detect manganese SOD (mSOD), cellular SOD1 (Cu-Zn SOD), and myxoma SOD1 (MYX SOD). About 2% of the MYX SOD1 antigen was detected in mitochondria extracted from cells infected with wild-type virus infected cells, very similar to the fraction of cellular SOD1 localized in the mitochondria.

3.4 DISCUSSION

Poxviruses encode a variety of proteins that serve to inhibit the activities of host antiviral defences. Interestingly, many of these virus genes encode homologs of cellular proteins and understanding what feature(s) of these cellular orthologs have been retained by the viral protein often provides insights into its function. A good example are the many truncated TNF-receptor mimics encoded by poxviruses, which typically retain the TNF-binding properties of their cellular homologs, but lack the signalling and transmembrane domains [9]. These proteins function as decoys, interfering in the TNF-mediated signalling that can kill infected cells. Poxviruses also encode a number of chemokine binding proteins which, by binding a wide assortment of chemokines, interfere in the migration of leukocytes to sites of infection or inflammation [25]. Leukocytes and macrophage use reactive oxygen species (ROS) to prime apoptosis or to kill infected cells out-right, and it is thus not too surprising that poxviruses might encode homologs of the SOD1s that play a key role in ROS-metabolism.

Poxviruses are rather genetically stable pathogens in part because they encode proof-reading DNA polymerases [7]. Yet this work and other data [2, 5] show that while divergent evolutionary processes may have retained two remarkably conserved forms of SOD1 homologs amongst several genera of poxviruses (Figure 3.1), these processes have not favoured retention of the dismutase function. Indeed, at least four (and probably more) amino acid substitutions have long rendered SFV and MYX SOD1 homologs catalytically inert. These mutations include substitutions that interfere in copper binding (Figure 3.4) and this would be expected to have a significant effect on activity given the

role of Cu(I)-Cu(II) redox reactions in catalysis. That these are not the only catalytically inactivating mutations is suggested by the fact that, although the Cu-binding deficiency can be partially overcome in multiply modified forms of the protein (Figure 3.4), this alteration does not restore any catalytic activity (Figure 3.3). SFV SOD1 *was* observed to retain the Zn-binding properties of its cellular homologs (Figure 3.4), while all of the Orthopoxvirus SOD1 homologs have almost certainly deleted the Zn-binding domain (Figure 3.1). We suggest that the zinc atom most likely serves the same non-essential structural role in stabilizing SFV SOD1 as it does stabilizing cellular SOD1 and that this feature was lost at some point in the evolution of the Orthopoxvirus proteins.

For what purpose might a poxvirus encode such peculiar modified forms of SOD1? SFV and MYX SOD1 homologs don't form heterodimeric complexes with cellular SOD1s (Figure 3.6) or affect the level of protein (Figure 3.8), but they do share with their cellular SOD1 homologs the capacity to bind cellular copper chaperone for SOD (Figures 3.5-3.7). We suggest that poxvirus SOD1 homologs are protein decoys that have retained a selective capacity to bind to cellular CCS, and in this way can interfere with CCS-catalyzed metallation reactions. This competition between virus and cellular SOD1s for CCS would decrease the intracellular pool of fully metallated SOD1 and hence cause a decline in dismutase activity even though levels of SOD1 antigen remain static (Figure 3.8). Viral SOD1 homologs are produced and packaged in the virion in abundance [2, 5] and so if SOD1 activity is slowly turning over in virus-infected cells, such a model could explain why one sees a gradual, M/S131R-dependent, reduction in the activity of SOD1 over the course of viral infection [5]. The peculiar structures of poxvirus SOD1 homologs are also compatible with this model. When one looks at the

structure of SFV and MYX SOD1s (Figure 3.1) it is noteworthy that many amino acids are conserved which in the homologous yeast protein mediate an interaction with yeast CCS. Moreover, cysteine C67 is remarkably well positioned to participate in the formation of an intermolecular disulphide bond bridging a viral SOD1 homolog to the CCS [13]. Although this disulphide bond is probably not essential for stable complex formation [13], the presence of this residue may be one more factor favouring formation of dead-end complexes at the expense of properly metallated cellular SOD1.

The fact that Leporipoxvirus SOD1 homologs cannot bind copper would not preclude formation of these heterodimeric complexes, since several studies have observed interactions between Cu-deficient mutant SOD1 proteins and CCS [6, 30]. Indeed, the inability to incorporate copper in the viral partner may be another important stabilizing factor that effectively traps the two proteins in an inactive state and it is noteworthy that the complexes involving viral SOD1 homologs are seemingly more stable than are those formed between CCS and cellular SOD1. [We observed that CCS can be used to co-immunoprecipitate SFV SOD1, but not cellular SOD1 (Figure 3.5 and 3.6). Such a regulatory model is not entirely new. Several years ago, Schmidt *et al.* proposed that cells could regulate the level of superoxide dismutase activity by having that activity depend upon a coordinated interaction between two separate proteins [24]. Poxviruses may simply have interposed a SOD1 mimic into this normal cellular process and we are currently generating a system that can directly measure the effect of S131R on the chaperone activity of CCS.

The inhibitory properties of these proteins suggest that Leporipoxviruses gain some benefits from interfering with the dismutation of superoxide radical and disrupting

cellular redox homeostasis. How might increasing the intracellular concentration of $O_2^{\cdot-}$ benefit a virus? One can imagine several advantages, however the most attractive explanation relates to the fibroxanthosarcoma-like tumours formed by MYX and SFV in natural infections [10]. Superoxide can have subtle effects on cells depending upon the concentration, but it is noteworthy that decreasing $O_2^{\cdot-}$ concentrations can create a "pro-apoptotic" environment, while increasing the concentration of superoxide anion can inhibit Fas-mediated apoptosis and stimulate proliferation [8, 19]. In this regard it is especially striking that some portion of the MYX SOD1 protein co-localizes with the mitochondrial compartment. It has been speculated that it is the unmetallated form of cellular SOD1 that is transported into the mitochondrial intermembrane space where it is then trapped by a CCS-catalyzed copper transfer reaction [27]. If this is correct, then targeting a competing viral SOD1 homolog to the same location might be expected to significantly alter the concentration of active SOD1 within the mitochondrial compartment and perhaps have dramatic effects on apoptotic processes originating in the mitochondria. It thus makes perfect biological sense for these viruses to encode a protein capable of increasing $O_2^{\cdot-}$ concentrations in virus-infected cells, since that would help promote the extensive cellular proliferation so characteristic of Leporipoxvirus infections. It should be noted that we could not previously detect any obvious effects of deleting M131R on the virulence of myxoma virus [5], but a gene promoting tumour growth might not have been amenable to study using this animal model. Myxomatosis is a disease peculiar to domestic rabbits (*Oryctolagus cuniculus*) and causes a rapidly lethal systemic infection and bacteraemia associated with profound immunosuppression. However, in its natural host (*Sylvilagus spp.*) myxoma causes a very different self-

limiting disease associated with large tumour-like growths [10] and only under these disease conditions might the subtle effects of a gene affecting tumourigenesis be seen. SFV causes a self-limiting disease in domestic rabbits that much more closely replicates the natural disease course in its host, *Sylvilagus floridanus,* and we are currently investigating the prediction that SFV S131R plays a role in virus-induced tumourigenesis using this alternative animal model.

3.5 REFERENCES

1. Aguado B, Selmes IP, Smith GL (1992) Nucleotide sequence of 21.8 kbp of variola major virus strain Harvey and comparison with vaccinia virus. J Gen Virol 73: 2887-902

2. Almazan F, Tscharke DC, Smith GL (2001) The vaccinia virus superoxide dismutase-like protein (A45R) is a virion component that is nonessential for virus replication. J Virol 75: 7018-29.

3. Bawden AL, Glassberg KJ, Diggans J, Shaw R, Farmerie W, Moyer RW (2000) Complete genomic sequence of the Amsacta moorei entomopoxvirus: analysis and comparison with other poxviruses. Virology 274: 120-39.

4. Cameron C, Hota-Mitchell S, Chen L, Barrett J, Cao JX, Macaulay C, Willer D, Evans D, McFadden G (1999) The complete DNA sequence of myxoma virus. Virology 264: 298-318

5. Cao JX, Teoh ML, Moon M, McFadden G, Evans DH (2002) Leporipoxvirus Cu-Zn superoxide dismutase homologs inhibit cellular superoxide dismutase, but are not essential for virus replication or virulence. Virology 296: 125-35

6. Casareno RL, Waggoner D, Gitlin JD (1998) The copper chaperone CCS directly interacts with copper/zinc superoxide dismutase. J Biol Chem 273: 23625-8

7. Challberg MD, Englund PT (1979) Purification and properties of the deoxyribonucleic acid polymerase induced by vaccinia virus. J Biol Chem 254: 7812-9

8. Clement MV, Stamenkovic I (1996) Superoxide anion is a natural inhibitor of FAS-mediated cell death. Embo J 15: 216-25

9. Cunnion KM (1999) Tumor necrosis factor receptors encoded by poxviruses. Mol Genet Metab 67: 278-82

10. Digiacomo RF, Mare CJ (1994) Viral disease. In: Manning PJ (ed) The biology of the laboratory rabbit. Academic Press, San Diego, pp 171-197

11. Hall LT, Sanchez RJ, Holloway SP, Zhu H, Stine JE, Lyons TJ, Demeler B, Schirf V, Hansen JC, Nersissian AM, Valentine JS, Hart PJ (2000) X-ray crystallographic and analytical ultracentrifugation analyses of truncated and full-length yeast copper chaperones for SOD (LYS7): a dimer-dimer model of LYS7-SOD association and copper delivery. Biochemistry 39: 3611-23

12. Klug D, Rabani J, Fridovich I (1972) A direct demonstration of the catalytic action of superoxide dismutase through the use of pulse radiolysis. J Biol Chem 247: 4839-42

13. Lamb AL, Torres AS, O'Halloran TV, Rosenzweig AC (2001) Heterodimeric structure of superoxide dismutase in complex with its metallochaperone. Nat Struct Biol 8: 751-5

14. Marmocchi F, Caulini G, Venardi G, Cocco D, Calabrese L, Rotilio G (1975) The effect of the presence of the metal prosthetic groups on the subunit structure of bovine superoxide dismutase in sodium dodecyl sulfate. Physiol Chem Phys 7: 465-71

15. McCord JM, Fridovich I (1969) Superoxide dismutase. An enzymic function for erythrocuprein (hemocuprein). J Biol Chem 244: 6049-55

16. Mills EL, Debets-Ossenkopp Y, Verbrugh HA, Verhoef J (1981) Initiation of the respiratory burst of human neutrophils by influenza virus. Infect Immun 32: 1200-5

17. Okado-Matsumoto A, Fridovich I (2001) Subcellular distribution of superoxide dismutases (SOD) in rat liver: Cu,Zn-SOD in mitochondria. J Biol Chem 276: 38388-93

18. Parkes TL, Elia AJ, Dickinson D, Hilliker AJ, Phillips JP, Boulianne GL (1998) Extension of Drosophila lifespan by overexpression of human SOD1 in motorneurons. Nat Genet 19: 171-4

19. Pervaiz S, Clement MV (2002) A permissive apoptotic environment: function of a decrease in intracellular superoxide anion and cytosolic acidification. Biochem Biophys Res Commun 290: 1145-50

20. Quick KL, Hardt JI, Dugan LL (2000) Rapid microplate assay for superoxide scavenging efficiency. J Neurosci Methods 97: 139-44

21. Rosen DR, Siddique T, Patterson D, Figlewicz DA, Sapp P, Hentati A, Donaldson D, Goto J, O'Regan JP, Deng HX, et al. (1993) Mutations in Cu/Zn superoxide dismutase gene are associated with familial amyotrophic lateral sclerosis. Nature 362: 59-62

22. Rypniewski WR, Mangani S, Bruni B, Orioli PL, Casati M, Wilson KS (1995) Crystal structure of reduced bovine erythrocyte superoxide dismutase at 1.9 A resolution. J Mol Biol 251: 282-96

23. Schmidt PJ, Rae TD, Pufahl RA, Hamma T, Strain J, O'Halloran TV, Culotta VC (1999) Multiple protein domains contribute to the action of the copper chaperone for superoxide dismutase. J Biol Chem 274: 23719-25

24. Schmidt PJ, Ramos-Gomez M, Culotta VC (1999) A gain of superoxide dismutase (SOD) activity obtained with CCS, the copper metallochaperone for SOD1. J Biol Chem 274: 36952-6

25. Seet BT, McFadden G (2002) Viral chemokine-binding proteins. J Leukoc Biol 72: 24-34

26. Smith GL, Chan YS, Howard ST (1991) Nucleotide sequence of 42 kbp of vaccinia virus strain WR from near the right inverted terminal repeat. J Gen Virol 72: 1349-76

27. Sturtz LA, Diekert K, Jensen LT, Lill R, Culotta VC (2001) A fraction of yeast Cu,Zn-superoxide dismutase and its metallochaperone, CCS, localize to the intermembrane space of mitochondria. A physiological role for SOD1 in guarding against mitochondrial oxidative damage. J Biol Chem 276: 38084-9

28. Thompson JD, Higgins DG, Gibson TJ (1994) CLUSTAL W: improving the sensitivity of progressive multiple sequence alignment through sequence weighting, position-specific gap penalties and weight matrix choice. Nucleic Acids Res 22: 4673-80

29. Tomalski MD, Eldridge R, Miller LK (1991) A baculovirus homolog of a Cu/Zn superoxide dismutase gene. Virology 184: 149-61.

30. Torres AS, Petri V, Rae TD, O'Halloran TV (2001) Copper stabilizes a heterodimer of the yCCS metallochaperone and its target superoxide dismutase. J Biol Chem 276: 38410-6

31. Weiss SJ, King GW, LoBuglio AF (1978) Superoxide generation by human monocytes and macrophages. Am J Hematol 4: 1-8

32. Willer DO, McFadden G, Evans DH (1999) The complete genome sequence of shope (rabbit) fibroma virus. Virology 264: 319-43

33. Zhang W, Evans DH (1993) DNA strand exchange catalyzed by proteins from vaccinia virus-infected cells. J Virol 67: 204-12

CHAPTER 4 – TUMOURIGENIC LEPORIPOXVIRUSES UPREGULATE INTRACELLULAR SUPEROXIDE TO INHIBIT APOPTOSIS AND PROMOTE CELL PROLIFERATION *

In Press in the *Journal of Virology*

Preface

A version of this chapter has been accepted for publication. Teoh MLT, Turner PV, and Evans DHE 2005. *Journal of Virology*. 79:5799-811. Dr. Turner performed the tumour biopsy on the infected rabbits hence generated the histological staining photographs of the tumour tissues, but the rest of the data presented were generated by me. I wrote the first draft of the manuscript and the final version of the paper was generated with the editorial contribution from my supervisor, Dr. David Evans.

* Reprinted from *Journal of Virology*, Vol. 79, Melissa L. T. Teoh, Patricia V. Turner, and David H. Evans, pp. 5799-811,Tumourigenic poxviruses up-regulate intracellular superoxide to inhibit apoptosis and promote cell proliferation, copyright (2005), with permission from American Society for Microbiology.

Title: Tumourigenic poxviruses up-regulate intracellular superoxide to inhibit apoptosis and promote cell proliferation

Running title: Poxvirus perturbation of superoxide homeostasis

Authors: Melissa L. T. Teoh[1], Patricia V. Turner[2], and David H. Evans[1,*]

Affiliation: [1]Dept. of Medical Microbiology & Immunology
Faculty of Medicine and Dentistry
The University of Alberta
Edmonton, AB, T6G 2H7, CANADA

[2]Dept. of Pathobiology, Ontario Veterinary College
The University of Guelph
Guelph, ON, N1G 2W1, CANADA

Manuscript number: JVI02501-04 REVISED

*Corresponding author: Please address all correspondence to Dr. Evans at the University of Alberta. E-mail devans@ualberta.ca; Tel. (780) 492-2308; Fax (780) 492-7521

4.1 INTRODUCTION

Redox phenomena serve a critical function in numerous biological and biochemical processes. Reactive oxygen species (ROS) are generated during normal cellular metabolism as well as by activated phagocytes in response to infection [16, 22, 28]. Since the intracellular accumulation of toxicants like superoxide radical ($O_2\cdot^-$), hydrogen peroxide, and hydroxyl radical is undesirable, ROS levels are usually tightly limited by multiple cellular mechanisms. They are also closely regulated because superoxide plays an important role as a secondary messenger in mediating inflammation, stimulating cell proliferation, and regulating apoptosis [reviewed by [4, 5, 29]]. This has led to the widely accepted premise that the regulation of redox homeostasis is important in determining when cells rest, proliferate, or die.

One of the key enzymes involved in maintaining this regulatory net is Cu-Zn superoxide dismutase 1 (SOD1), an enzyme that catalyzes the removal of superoxide radicals though their chemical dismutation [16, 17]. Mutations in SOD1 have been causally linked to the familial form of human amyotrophic lateral sclerosis [35], but there have been many persistent reports that tumour cells also exhibit deficiencies in SOD1 activity along with elevated levels of $O_2\cdot^-$ and other ROS [7, 19, 46]. The significance of these observations is hard to judge given the genetic diversity of transformed cells and the sometimes contradictory evidence [reviewed in [25]]. However, gene transfection methods have been used more recently to directly manipulate SOD1 activity in transformed cells and this has been seen to alter the growth rate, tumour-forming, and metastatic potential of these cells [15, 48, 59]. These and other observations have led to

the suggestion that increasing the concentration of intracellular superoxide can promote tumour growth and survival. One of the most plausible mechanisms by which ROS can do this arises from the observation that superoxide (or its metabolite H_2O_2), can stimulate the activity of mitogen-activated kinases. This can in turn promote cellular transformation, proliferation, and metastasis [4, 5].

Interestingly, many large DNA viruses encode SOD1 homologs including baculoviruses and poxviruses. The first of the SOD1-like poxvirus genes to be discovered was the A45R gene encoded by the *Orthopoxvirus* vaccinia [2, 44], but sequencing later showed that *Leporipoxviruses* encode similar genes which even more closely resemble cellular SOD1, and which have been designated M131R and S131R in myxoma virus (MYX) and Shope fibroma virus (SFV), respectively [10, 56]. MYX and SFV are sometime called "tumourigenic" poxviruses because they produce fibroxantho-sarcoma-like tumour growths when infecting their natural hosts (new world hares). These growths are relatively benign in adult animals and regress over 3-4 weeks due to a combined humoral and cell-mediated immune response [38, 45]. We have been using MYX and SFV to elucidate the biological function of these enigmatic genes.

M131R and S131R encode 96% identical, catalytically *inactive,* late proteins. They are non-essential proteins that are nevertheless packaged in large quantities in virus particles and promote a gradual reduction in SOD1 activity in virus-infected cells [10]. These proteins cannot bind copper, which is essential for dismutase activity, but they have retained the zinc-binding properties of their cellular homolog and similarly form stable heterodimeric complexes with the cellular copper chaperone for SOD1 [50]. Copper chaperone for SOD1 (CCS) serves the essential purpose of cuprolating SOD1

[26, 36]. These observations led us to hypothesize that M131R and S131R gene products are protein "decoys", which compete with SOD1 for CCS activity and thus deplete the copper supply to the cellular enzyme [50]. In doing this, SFV and MYX (and possibly other poxviruses) may be exploiting the fact that CCS seems to serve a critical role in regulating SOD1 activity [13].

Studying what role these genes might play in virus pathogenesis requires a careful choice of animal model. Myxoma virus causes myxomatosis in European laboratory rabbits (*Oryctolagus cuniculus*), but the high mortality, rapid systemic spread, and profound immunodeficiency characteristic of myxomatosis is very different from the benign infections MYX causes in *Sylvilagus* hares. Perhaps consequentially we could not detect any obvious requirement for M131R gene function using this virulent disease model, beyond a slight delay in the appearance and spread of the primary lesion [10]. In contrast, SFV naturally lacks several genes essential for MYX pathogenesis [9] and produces a disease in rabbits that more closely recapitulates the disease course seen in *Sylvilagus* hares. Using this infection model we show here that SFV mutant viruses lacking the S131R gene produce much smaller and faster-regressing tumours than do wild type virus. S131R-deficient virus is also unable to up-regulate superoxide levels or suppress Fas-mediated apoptotic induction like wild type SFV. These studies illustrate a novel mechanism of viral pathogenesis, wherein tumourigenic poxviruses manipulate intracellular superoxide concentrations to promote infected cell growth and immune evasion, and may ultimately provide insights into the role ROS and redox status play in regulating other forms of tumour growth and metastasis.

4.2 MATERIALS AND METHODS

Cells and viruses. Rabbit corneal fibroblast cells (SIRC cells) were grown in Dulbecco's modified Eagles media (DMEM) supplemented with 10% fetal bovine serum as previously described [32]. Shope fibroma virus (SFV) strain Kasza and myxoma virus (MYX) strain Lausanne were originally obtained from the American Type Culture Collection. The construction of a MYX virus lacking the M131R gene (MYX M131RΔ) was described previously [10] and encodes an *E. coli gpt* cassette replacing the M131R gene. Viruses were purified by sucrose density gradient ultracentrifugation, diluted in phosphate buffered saline (PBS), and titered on SIRC cells before use in animals. Human T-cell lymphoma Jurkat cells were obtained from Dr. M. Barry (University of Alberta) and grown in RPMI 1640 medium supplemented with 10% fetal bovine serum [54].

Construction of recombinant viruses. An SFV strain lacking S131R was constructed as outlined in Figure 4.1. Plasmid pMLT601 comprises 515 bp of SFV DNA located upstream, and 455 bp downstream of the S131R gene. These flanking sequences were prepared using the polymerase chain reaction and primers S131R-LFF plus S131R-LFR2 and S131R-RFF2 and S131R-RFR (Table 4.1). A tri-partite recombinational cloning reaction was then used to join the two flanking fragments to *Not*I-digested pBluescript KS+ DNA, directed by sequences homologous to the vector and common to the PCR fragments (Table 4.1, underlined) as described [57]. The resulting plasmid (pMLT601) was then digested with *Pac*I, dephosphorylated, and ligated to an *E. coli gpt* gene regulated by a vaccinia virus P7.5 promoter [6]. This plasmid was transfected into SIRC cells infected with wild type SFV, and the VMLT1.6 virus isolated by three rounds

of passage in the presence of 25 μg/mL mycophenolic acid followed by three rounds of plaque purification without the selection.

An S131R^{+} revertant virus was prepared by returning S131R gene sequences to VMLT1.6. Primers S131R-LFF and S131R-RFR (Table 4.1) and the PCR were used to amplify a 1.5 kb DNA fragment encoding the S131R gene and flanking sequences, and the DNA cloned into pBluescript KS+ as described above. The resulting plasmid (pMLT701) was then transfected into VMLT1.6-infected cells, progeny virus harvested five days later, and these viruses plated without mycophenolic acid selection on SIRC cells under an agar overlay. About 100 of these plaque-purified virus isolates were then screened for sensitivity to mycophenolic acid. The drug-sensitive virus that was isolated using this method, was then plaque purified two more times and designated R-S131R.

MYX virus encoding M131R linked to the enhanced green fluorescent protein (EGFP) were prepared using a combination of PCR and PCR fusion methods to assemble of gene targeting cassette, and homologous recombination to generate the virus. Briefly primers C/N1F plus C1R and primers C2F and C5R were used to prepare PCR fragments encoding a portion of M130R plus M131R (using a cloned MYX DNA template) and EGFP (using a pEGFP-C3 template, BD/Clontech) respectively. These were then linked into a single DNA fragment using a PCR fusion reaction and primers C/N1F and C5R. Similarly, primers C4F plus C4R and C6F plus C/N3R were used to prepare PCR fragments encoding the *E. coli gpt* gene (using pTM3 template [6]) and M132L (using a MYX DNA template), respectively. These were linked into a single DNA fragment using a PCR fusion reaction and primers C4F and C/N3R. These two fragments were then joined using another fusion reaction and primers C/N1F and C/N3R. This 3.9 kbp

DNA was transfected into MYX-infected cells and virus resistant to mycophenolic acid isolated and plaque purified. The structure of the resulting virus is illustrated in FIG 4.8.

TABLE 4.1. Sequences of the oligonucleotides used in this study

Designation	Sequence (5'-to-3')
S131R-LFF	ACTAGTTCTAGAGCGGCCATTACGTACCCTCTAGAACCCATAGG
S131R-LFR2	CGAAGAACGTTAATTAAAGTACGCTACATTATAGATAACTAAA-CGATAAATAAGCG
S131R-RFF2	TAGCGTACTTTAATTAACGTTCTTCGGGAGTTGCTTAAATAATT-TTGCTAAAATATATAAG
S131R-RFR	AGCTCACCGCGGTGGCGGCCCTACTCTACTGTTGCTTTGTCGTT
C/N1F	ACTAGTTCTAGAGCGGCCGGATCCTGCGTATATTATACACGGCC
C1R	TCCTCGCCCTTGCTCACCATGGCGCCAGCAACTCCTATAATCCC CCAG
C2F	CTGGGGGATTATAGGAGTTGCTGGCGCCATGGTGAGCAAGGGC-GAGGA
C4F	GCATGGACGAGCTGTACAAGTAACTAAACGGGTCTTGAGGGGT
C5R	ACCCCTCAAGACCCGTTTAGTTACTTGTACAGCTCGTCCATGC
C4R	ATACATTTTAGCGAGGTTATGATGGCATTTCTTCTGAGCA
C6F	TGCTCAGAAGAAATGCCATCATAACCTCGCTAAAATCTAT
C/N3R	GCTCCACCGCGGTGGCGGCCTCTAGAGGGGGAATCTACTCTAC TGTT

Growth curve analysis. Confluent monolayers of SIRC cells were infected with each virus at a multiplicity of infection of 0.1. After 1 hour at 37˚C, the cells were washed and overlaid with fresh media. Virus were harvested over the next two days (Figure 4.2) and stored frozen at –80˚C. The virus were released by three rounds of freeze-thaw, clarified by centrifugation at 1,500 x g for 5 min and plated on SIRC cell. The cells were cultured for five days at 37˚C and plaques visualized using a 15 min incubation with crystal violet stain (2% formaldehyde, 2% acetic acid, 20% ethanol, and 0.5% crystal violet in PBS) followed by a rinse with PBS.

Southern and western blot analysis. DNA was extracted from virus-infected cells, cleaved with *Xba*I, fractionated using a 0.8% agarose gel, and transferred to a nylon membrane (Bio-Rad). PCR amplified DNAs, [α-^{32}P] dCTP and a random-prime labelling kit were used to prepare radioactive probes as directed by the kit supplier (Boehringer Mannheim). For western blot analysis cells were infected with virus at a multiplicity of infection of 10 and cell extracts prepared 24 hr post-infection as described [10]. Proteins were fractionated by sodium dodecyl sulfate – polyacrylamide gel electrophoresis (SDS-PAGE) and transferred electrophoretically to a PVDF membrane as recommended by the manufacturer (Millipore). Western blotting was performed as described previously [10] using a 1:2,000 dilution of a monoclonal antibody that reacts with both the MYX and SFV M/S131R gene products. The primary antibody was detected using a 1:20,000 diluted goat anti-mouse horseradish peroxidase-conjugate and a chemiluminescent detection kit (Pierce).

Confocal microscopy. SIRC cells were cultured on glass coverslips and infected with virus at a multiplicity of infection of twenty. Next day (24 hr post-infection) the

cells were washed with PBS, and incubated in fresh medium containing 5 μM hydroethidine (Molecular Probes) at 37°C for 20 minutes. The cells were washed with PBS and then further stained with 1 μg/mL DAPI (Molecular Probes) for 5 minute at room temperature, washed again, and the coverslips mounted in PBS containing 75% (v/v) glycerol. To stain cells for SFV antigens we used the method described in [10]. A duplicate set of virus-infected cells were fixed and incubated with a primary antibody (1:50 diluted anti-SFV antiserum) followed by a secondary reagent consisting of a 1:400 diluted goat-anti-rabbit antibody conjugated with AlexaFluor 488 (Molecular Probes). These cells were subsequently also stained with DAPI as described above.

Viral pathogenesis. Young adult female New Zealand white rabbits (three virus groups times six animals per group) were injected intradermally with 50 μL of PBS containing 10^5 plaque-forming units of sterile virus in the shaved skin of the back. The rabbits were observed daily for any symptoms of stress, temperature changes, and tumour size. Tumour appearance was documented by digital photography. Tumour volumes were subsequently calculated using the formula $V = [(\pi/24) \times \text{length} \times (\text{width}+\text{height})^2]$ [1]. On days 7, 10, and 13, one rabbit from each treatment group was sedated with acepromazine (0.2 mg/kg) and butorphanol (0.2 mg/kg) intramuscularly, and tumours biopsied using a 6 mm punch. The tissues were fixed, sectioned, and stained with hematoxylin and eosin for light microscopy. A pathologist blinded as to treatment groups scored the histological appearance on a 0 to 3 scale (maximum total score = 12) for each of the following changes: edema (abnormal fluid accumulation), inflammation (influx of inflammatory cells), necrosis (destruction of normal tissue components and architecture), and fibromatous cell proliferation (proliferative changes characteristic of SFV infection).

All procedures were reviewed, approved, and supervised by the University of Guelph Animal Care Committee operating under the mandate of the Canadian Council for Animal Care.

Aconitase assays. BGMK or SIRC cells were infected with the indicated viruses at a multiplicity of infection of twenty. Next day (24 hr post-infection) the cells were washed with PBS and harvested by centrifugation at 16,000 × *g* for 5 minutes at 4° C. The method of Gardner and Fridovich was used to measure aconitase activity [20]. Briefly, each cell pellet was resuspended in ice-cold lysis buffer containing 50mM Tris·HCl (pH 7.4), 0.6 mM $MnCl_2$, and 20 μM fluorocitrate. The cells were broken by sonication on ice (3 × 1 min) and clarified by centrifugation at 16,000 × *g* for 5 min at 4° C. Aliquots of this supernatant were immediately assayed for aconitase activity by following ΔA_{340} in a 500 μl reaction mixture containing 50 mM Tris·HCl (pH 7.4), 30 mM sodium citrate, 0.6 mM $MnCl_2$, 0.2 mM $NADP^+$, and 1 unit/ml of isocitrate dehydrogenase (Sigma-Aldrich). Reactions were incubated for 1 hr at 20°C with automated absorbance measurements at 5 min intervals. Relative changes in the $[O_2{\cdot}^-]$ were calculated from equation (3) in reference [21] and assumed that, in cells infected with M/S131R-deficient viruses, background levels of superoxide will have reversibly inactivated 14% of the aconitase.

Apoptosis. Jurkat cells were infected, or mock infected, with virus for 24 hours at a multiplicity of infection of ten. Apoptosis was induced by adding either 2 μM staurosporine (Sigma-Aldrich), or 250 ng/mL anti-Fas antibody (Upstate Biotechnology) to the culture media. As a negative control, we added 20 μM of the caspase inhibitor zVAD.fmk (Promega) to the media prior to inducing apoptosis. The cells were

harvested 3 and 10 hr post-treatment with staurosporine and anti-Fas antibody, respectively, and assayed for apoptotic induction as follows.

DNA laddering patterns were evaluated by agarose gel electrophoresis [24]. Briefly, 10^6 cells from each sample were harvested by centrifugation and the cell pellets incubated for one minute in 0.1 mL of ice-cold lysis buffer (50 mM Tris·HCl [pH 7.5], 1 % NP-40, 20 mM EDTA). Each sample was centrifuged for 1,600 x g for 5 min, the supernatant recovered, and SDS and ribonuclease A added to final concentrations of 1% and 10 mg/mL, respectively. The samples were incubated for 1 hr at 50°C, proteinase K added to a final concentration of 2 mg/mL and further incubated at 37°C overnight. The DNA was ethanol precipitated and fractionated by electrophoresis using a 1.5% agarose gel. Alternatively, we used a Roche Diagnostics TUNEL (terminal transferase-mediated dUTP-fluorescein nick end labelling) assay kit to detect apoptotic DNA cleavage. Again, 10^6 cells were collected by centrifugation and the cell pellets were washed with PBSF (PBS containing 1% fetal calf serum). The cells were fixed with 2% paraformaldehyde in PBS for 30 min at room temperature, washed with PBSF, and then permeabilized with 0.1% sodium citrate containing 0.1% Triton X-100 on ice for 2 min. The cells were again washed twice with PBSF, resuspended in 50 µL of a solution containing 45 µl of TUNEL label and 5 µl of TUNEL enzyme, and incubated at 37°C for 1 hr. The unincorporated label was removed by washing with PBSF and the cell pellets finally resuspended in 0.4 mL of PBSF. A Becton Dickinson FACScan was used to determine the distribution of the TUNEL label using at least 10,000 cells per sample.

To detect caspase-3 activation, whole cell lysates were prepared by boiling 10^3 infected cells in 50 µL of SDS-PAGE loading buffer (containing 2% mercaptoethanol)

for five minutes. Ten microliters of each extract were then subjected to western blot analysis, as described above, using a 12% SDS-PAGE gel and a 1:5,000 diluted polyclonal rabbit anti-caspase 3 with chemiluminescent detection.

4.3 RESULTS

Construction and characterization of S131R-deficient Shope fibroma viruses. Homologous recombination was used as outlined in the Materials and Methods to replace the entire S131R open reading frame with sequences encoding an *E. coli gpt* gene as a positive selection marker (Figure 4.1A). After plaque purification, the PCR was used to identify potential recombinants and then Southern blots were used to confirm the expected presence of a ~2.6 kbp *Xba*I recombinant fragment in all of the mycophenolic acid resistant virus genomes (Figure 4.1B). The resulting S131R-deleted virus was designated VMLT1.6. A second round of recombination was then used to restore the S131R gene to VMLT1.6. This produce a wild-type revertant virus, designated R-S131R, which was used as a control to ensure that only the S131R gene was disrupted during construction of VMLT1.6. R-S131R genomic DNA was digested with *Xba*I and Southern blots were used to detect the presence of a ~1.5 kbp restriction fragment which is diagnostic of the restoration of the S131R gene (Figure 4.1B, middle). Western blots were subsequently used to monitor expression of S131R protein. The 17.8 kDa S131R protein was detected in SIRC cells infected by wild-type SFV and R-S131R virus, using a monoclonal antibody, but absent in extracts prepared from cells infected with S131R-deficient virus (Figure 4.1B, bottom). Collectively, these data showed that the recombinant viruses have the predicted genome structure and gene expression patterns.

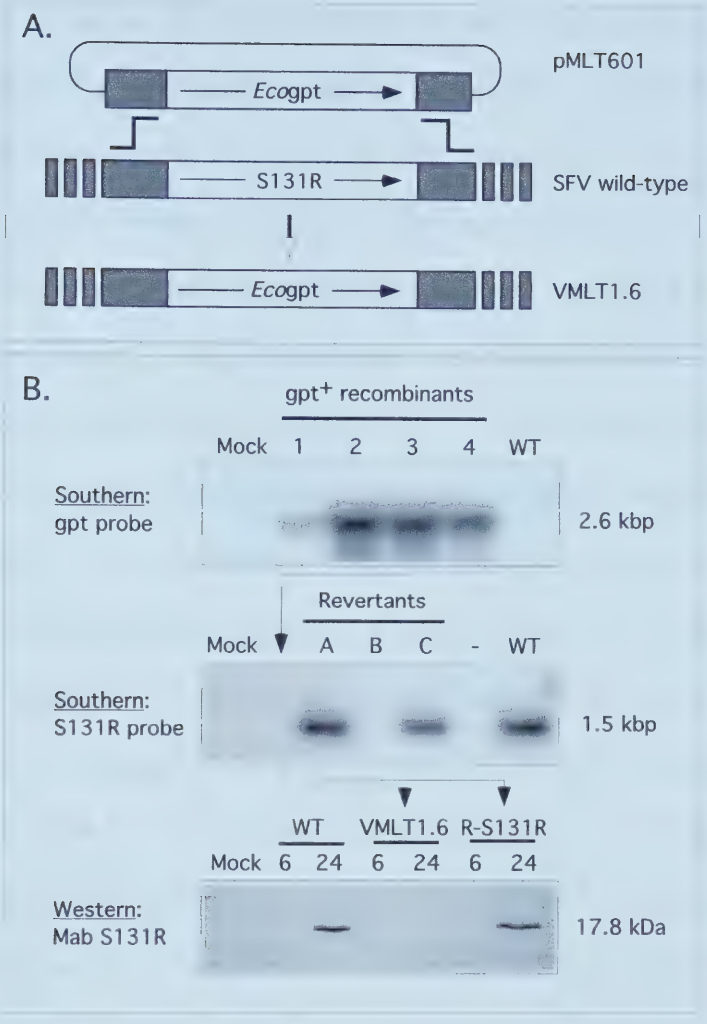

Figure 4.1. Construction and characterization of recombinant SFV strains. Plasmid pMLT601 was transfected into wild-type SFV infected SIRC cells by the calcium phosphate method and mycophenolic acid-resistant recombinants isolated as outlined in materials and methods. This replaces the S131R gene and its promoter with an *E. coli gpt* cassette. (Panel A). Digestion of these virus DNAs with *Xba*I followed by Southern blotting detected a 2.6kb fragment in several independently isolated clones, which hybridized with an *E. coli gpt* probe (Panel B, top). Virus isolate #3 was designated VMLT1.6 and retained for use as an S131R-deficient virus. The S131R gene was restored to VMLT1.6 using a second round of transfection and recombination using wild type SFV DNA encoding the S131R gene and flanking sequence homology. Digestion of these revertant virus with *Xba*I followed by Southern blotting with an S131R gene probe detected a 1.5 kb fragment diagnostic of wild type S131R gene structure (Panel B, middle). Virus isolate "A" was designated R-S131R. A western blot showed that this revertant virus expressed normal levels of S131R gene product with normal (late) expression kinetics, however no S131R protein was detected in cells infected with the VMLT1.6 virus (Panel B, bottom).

Growth properties of S131R-deficient viruses. The phenotypic properties of S131R-deficient SFV strains closely resembled the properties of M131R-deleted MYX strains [10]. The gene is clearly dispensable for virus replication in tissue culture and, like M131R-deficient MYX strains, the size and morphology of the foci formed by VMLT1.6 virus on SIRC cells were indistinguishable from those of the SFV-WT and R-S131R strains (data not shown). The S131R-deficient SFV virions also shared with mutant MYX strains some thermolability at elevated (55° C) temperatures [58]. Perhaps the most interesting property of these viruses, and one that again characterizes M131RΔ MYX virus [10], is that deleting the S131R gene enhances the yield of SFV. This is illustrated by the single-step growth curve shown in Figure 4.2. Starting with a low multiplicity of infection (0.1), all three viruses exhibited the same growth characteristics during the first 12 hours post-infection. However, the VMLT1.6 infection ultimately produced about 10-fold more infectious particles than either the wild type or R-131R strains. Even though SFV and MYX appear to be evolutionarily distinct viruses [9, 56], these results illustrate the apparent biological equivalence of the two orthologous genes.

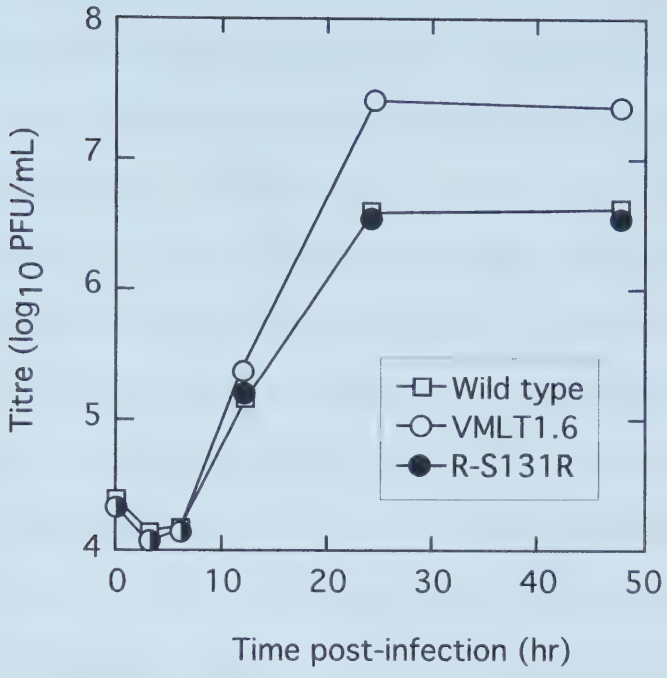

Figure 4.2. Single-step growth properties of an S131R-deficient SFV strain. SIRC cells were infected the indicated virus isolates at a multiplicity of infection of 0.1. Virus were harvested at the indicated times, titered on SIRC cells, and plaques detected with a crystal violet stain. Although each virus sample was titered in triplicate, the calculated standard error bars are about the size of the data points and have thus not been plotted. All three virus exhibit similar growth kinetics, but like M131R-deficient MYX strains [10], the S131R mutant viruses grow significantly better in culture.

The S131R gene product perturbs intracellular superoxide concentrations. To test whether the S131R protein plays any role in regulating intracellular superoxide concentrations, we examined the effect of virus infection on the fluorescent properties of hydroethidine dye (HE). Hydroethidine reacts with superoxide to produce a compound resembling ethidium bromide, which then forms a red fluorescent product [60]. This product can be detected by confocal fluorescent microscopy using cells infected with different SFV strains and stained with HE dye (Figure 4.3). Our analysis showed that cells infected with wild type SFV contained higher concentrations of intracellular superoxide, relative to mock-infected cells, as judged by the stronger staining in SFV-infected cells. Mock-infected cells showed only a low level of HE staining, detecting a low basal level of production of $O_2^{\cdot -}$ by cellular metabolism. This phenotype was clearly dependent upon S131R gene function, since deleting S131R produced only a background level of HE staining in VMLT1.6-infected cells, while cells infected with R-S131R revertant virus exhibited wild-type levels of superoxide-dependent HE fluorescence.

A high multiplicity of infection was used in these experiments to ensure that all cells were infected with SFV (20 plaque-forming units [PFU] per cell), however these studies could have been confounded by the failure of VMLT1.6 virus to infect the majority of cells being imaged. To show that these cells were all more or less equally infected with virus, we also stained the cells with convalescent antibodies recovered from rabbits that had been experimentally infected with wild type SFV (see below). This immunolabelling of SFV antigens was done in parallel with hydroethidine staining, because HE staining must be conducted in live cells while immunolabelling required a fixation step. The convalescent serum contained high level of anti-SFV IgG antibodies

and detected the presence of cytoplasmic SFV antigens in essentially all of the cells in these infected monolayers (Figure 4.3, bottom panel). No cross-reactive antigens were detected in mock-infected cells. This result showed that variations in infection efficiency do not explain the effects different viruses have on cellular superoxide levels.

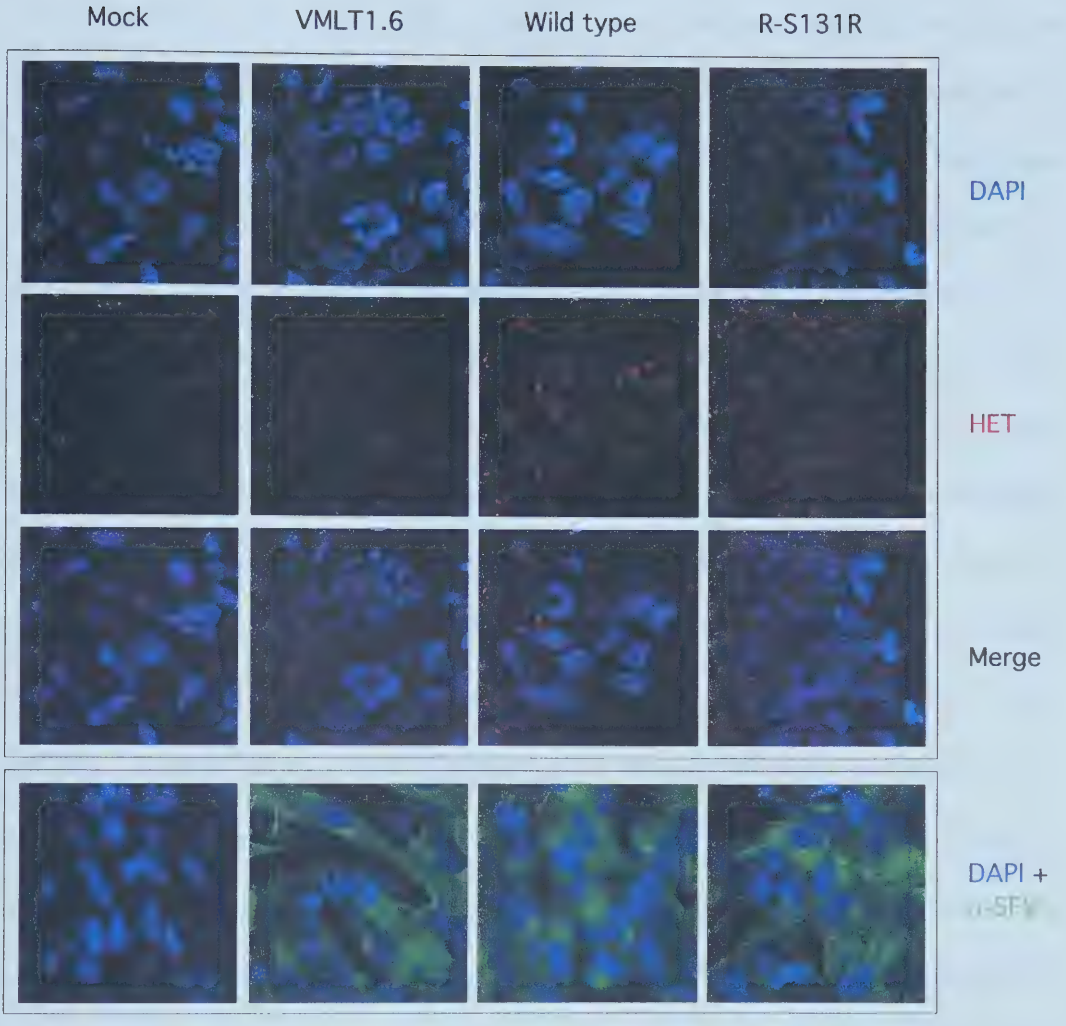

Figure 4.3. The S131R gene promotes an increase in the concentration of intracellular superoxide radical in SFV-infected cells. SIRC cells were infected, or mock-infected, with the indicated virus and then stained with hydroethidine (HE) and DAPI to detect superoxide or DNA respectively. A background level of superoxide is detected in mock-infected cells, which does not appear to be altered by infection with the VMLT1.6 virus (columns 1 and 2). Elevated levels of superoxide are detected in cells infected with wild type and R-S131R revertant virus infected cells, as judged by an increase in the amount of HE fluorescence (columns 3 and 4). As an infection control, a parallel set of infected, or mock-infected, cells were labeled with a polyclonal antisera obtained from an SFV-infected rabbit, followed by detection with a secondary antibody conjugated with horse-radish peroxidase. SFV antigens were detected in all of the infected specimens. Note that superoxide converts HE into a fluorescent intercalating dye of imperfectly understood structure and this is detected by the subsequent staining of nucleic acids [60]. The distribution of HE stain thus does not reflect the original cellular distribution of superoxide.

Although hydroethidine is recognized as one of the better reagents available for detecting superoxide, the method can underestimate the rate of $O_2^{\cdot -}$ production due to HE-catalyzed superoxide dismutation [49]. Another well-validated method is based upon the observation that superoxide can reversibly strip the metal from [4Fe-4S] clusters and thus inhibits iron-sulfur enzymes like aconitase. We used a photometric method [20] to assay aconitase activity in extracts prepared from SFV-infected cells, and the data obtained using this method were in full agreement with results obtained using HE. These results are presented in Figure 4.4. Infection caused a general reduction in aconitase levels, relative to mock-infected cells, but superimposed upon this cytopathic effect was the observation that extracts from cells infected with SFV wild type and R-S131R viruses contained 12-15% less aconitase than did extracts prepared from cells infected with the VMLT1.6 S131RΔ virus. These differences were seen in both rabbit and monkey cells and were clearly statistically significant ($p \leq 0.005$ for SFV wild type versus VMLT1.6 viruses [Student's two-tail *t*-test for n=3]). The same effects were also seen using cells infected with mutant and wild type myxoma viruses (Figure 4.4). Based upon using these two independent approaches for detecting intracellular superoxide, we concluded that the M/S131R genes serve a role in up-regulating superoxide levels in virus-infected cells.

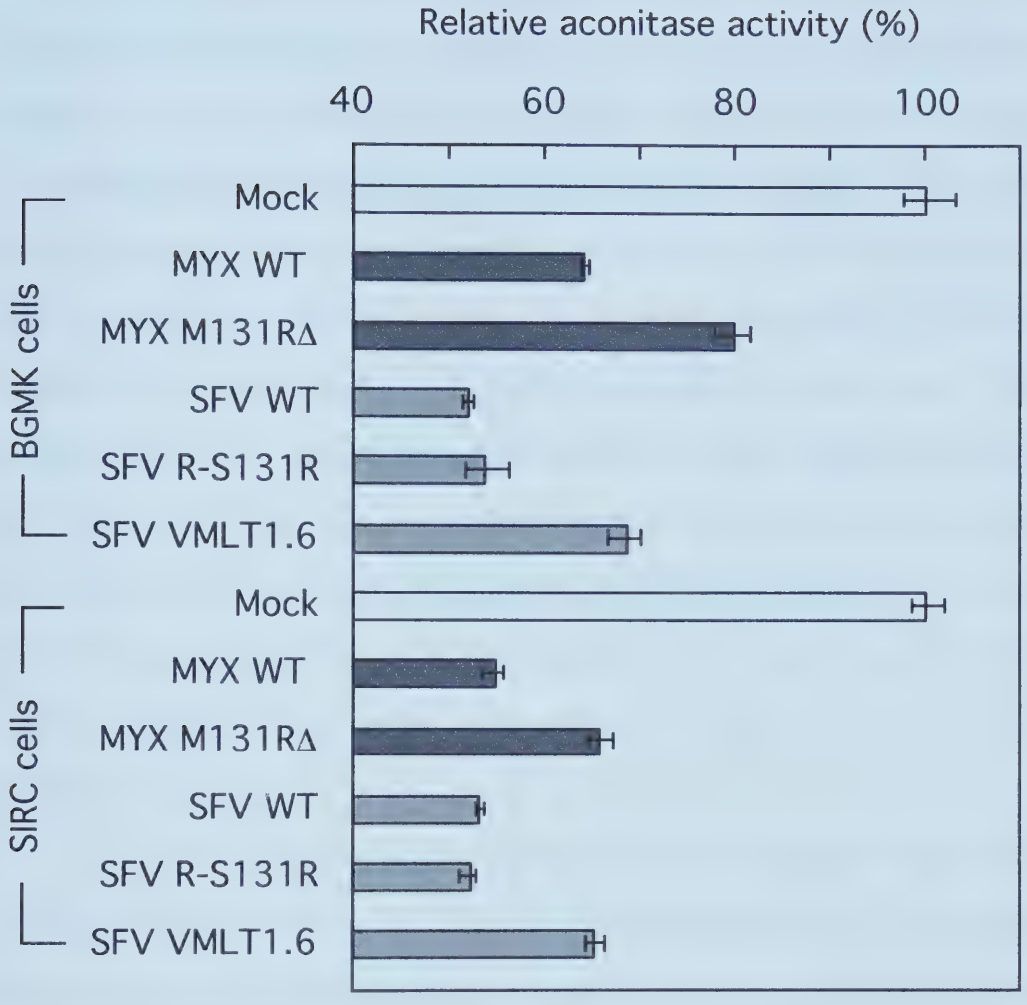

Figure 4.4. Detection of intracellular superoxide using an aconitase inhibition assay. A spectrophotometric method was used to measure the activity of the superoxide-sensitive enzyme aconitase in extracts prepared from virus-infected cells. Infection caused a non-specific reduction in cytosolic aconitase activity relative to the activity detected in mock-infected BGMK and SIRC cells. In addition to this effect, any virus encoding M131R or S131R caused an additional 12-15% reduction in aconitase activity relative to cells infected with mutant viruses lacking these genes.

S131R is a virulence factor that promotes tumourigenesis in rabbits. To examine whether the S131R gene serves any role in modulating SFV pathogenicity, we inoculated young adult female New Zealand white rabbits with VMLT1.6 virus and compared the clinical manifestations of the disease with those induced by wild type and R-S131R revertant virus. Before initiating these experiments, the wild type virus was used in a small pilot experiment to determine the infectious properties of our SFV laboratory stock (strain Kasza) and to identify an appropriate infectious dose. Three different doses of virus were injected intradermally into nine New Zealand white rabbits (10^4, 10^5, and 10^6 PFU per animal, in triplicate) and the kinetics of tumour induction was then followed over three-weeks. We identified 10^5 PFU as an appropriate innoculum, since a 10-fold higher dose produced no further effects on the disease progression, while 10^4 PFU per rabbit caused smaller growths and a less synchronized rate of tumour induction (data not shown).

Our wild type Shope fibroma virus produced the classical fibroxanthosarcomatous tumours in rabbits that have been described in the literature [33, 42]. These tumours were limited to the site of innoculation (the rear flank) with no evidence of systemic spread to other sites in these animals. Photographs were taken daily to monitor the course of the infection and Figure 4.5A (top) shows the pattern of tumour growth and recession following the inoculation of one representative rabbit with wild type virus. Lesions began to appear on day three post-infection, and the tumour-like growths reached a maximum size by about day ten. The lesion became hemorrhagic and then necrotic by day thirteen at which point tumour regression also began to be noted. The tumours continued shrinking and the thick scalp caused by the necrosis eventually sloughed off,

leaving in a small residual scar. The infection was completely resolved by day 28 post-infection. Wild type and R-S131R virus produced indistinguishable disease progressions. In contrast, although VMLT1.6 virus still established an infection, the size of the tumour formed by this virus was greatly reduced by deleting the S131R gene (Figure 4.5A, bottom). These tumour-like growths appeared with about the same kinetics as in wild type infections, but the tumours were much smaller and reached a maximum size at an earlier time point (day 7 instead of day 10). It is also noteworthy that the hemorrhagic and necrotic phases were less extensive in VMLT1.6-infected animals, with virtually no dark necrotic scars. Tumour regression was rapid and these animals completely resolved the infection by day 18 post-innoculation.

Tumour size measurements were also determined in parallel with these visual studies and are presented in Figure 4.5B. A total of six animals per group were followed, although as a biopsy was taken at different time points from each of three animals in each group (see below), that animal was removed from further calculations of tumour volume. Tumours from all three groups grew at a similar rate during the first five days after inoculation and those produced by wild type and R-S131R virus continued to grow rapidly until they reached essentially identical maximum sizes of 1,070 ± 80 mm^3 and 1,080 ± 60 mm^3 (for wild type and R-131R viruses, respectively) by day ten post-infection. In contrast the growth rate of tumours produced by S131R-deficient virus started to slow by day five post-infection and reached a maximum size only half that of the wild type virus (500 ± 40 mm^3) by day seven post-infection. These smaller tumours also cleared in half the time compared with those seen in wild type and R-131R infections. Thus S131R-deficient virus produce significantly smaller tumours than do

wild type or R-S131R virus ($p = 3x10^{-4}$ and $4x10^{-3}$, respectively, at day 7 versus day 10 [Student's two-tail *t*-test for n=4]).

Figure 4.5. Deleting the S131R gene attenuates SFV-induced disease in rabbits. New Zealand white rabbits were inoculated intradermally with 10^5 plaque-forming units of wild type, VMLT1.6, or R-S131R revertant virus on a shaved area at the back of each animal. The resulting tumours were monitored daily and recorded with a digital camera (Panel A) and the tumour volume determined with a digital calliper (Panel B). Virus lacking the SFV S131R gene produced smaller tumours, which regressed much faster than those produced by wild type and revertant viruses (Panel B). There was also less inflammation, haemorrhaging, and necrosis accompanying the resolution of infections caused by mutant virus relative to wild type infections (Panel A). Note that a total of six animals were used in each group, but as one animal from each group was biopsied on days 7, 10, and 13, that animal was excluded from further measurements of tumour progression. R-S131R virus produced tumour-like growths identical to wild type SFV, and these images have therefore been omitted from Panel A.

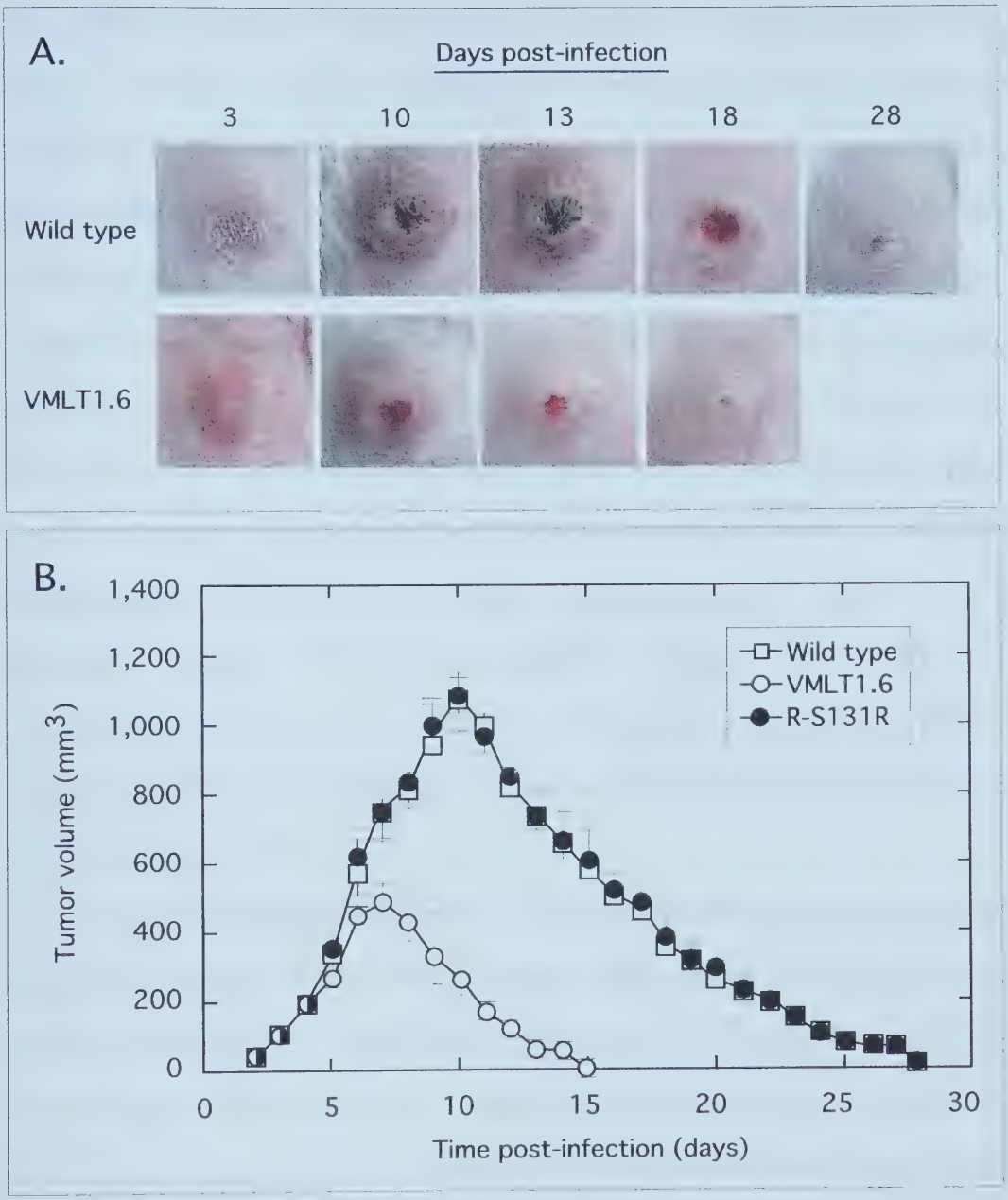
A.
Days post-infection
3
10
13
18
28
Wild type
VMLT1.6
B.
Tumor volume (mm3)
1,400
1,200
1,000
800
600
400
200
0
0
5
10
15
20
25
30
Time post-infection (days)
Wild type
VMLT1.6
R-S131R

Histologic studies on tumour biopsies. To observe the cellular response to virus infection, tumour biopsies were performed at different time points and subjected to microscopic evaluation. A lesion scoring system was established (see Materials and Methods) that provided a semi-quantitative measure of the extent of pathology at time-points permitted by our animal utilization protocol. By day 7 post-infection, all three treatment groups exhibited identical lesion scores (score = 6) consistent with there being no obvious microscopic differences in the appearance of the tumours (Figure 4.6A, B, and C). We saw ulcerated skin masses overlying the injection sites and this correlated histologically with a locally extensive full thickness epithelial necrosis. All three specimens had an overlying crust consisting of necrotic cell debris mixed within a proteinaceous exudate. The subcutis subtending this area was edematous with marked perivascular and periadnexal mixed leukocytic infiltrates (Figure 4.6J). These infiltrates comprised a mixture of heterophils, macrophages and lesser numbers of lymphocytes and plasma cells (Figure 4.6H).

By day 10 post-infection, we started to see obvious histologic differences between the specimen obtained from a VMLT1.6-infected animal (lesion score = 6) and those obtained from the other two control animals (lesion scores = 8) (Figure 4.6D, E and F). Little change was seen in the necrotic epithelial lesion produced by the VMLT1.6 virus, beyond a mild increase in dermal necrosis and a decrease in perivascular edema. There was no evidence of fibromatous cell proliferation. In the other two groups the lesions had continued to progress. In addition to a superficial epithelial necrosis, extensive areas of superficial and deep dermal inflammation with dense mononuclear cell infiltrates were observed. These were associated with the disruption and loss of hair follicles and adnexal

structures, and dermal necrosis admixed with hemorrhage and edema. Additionally, there were scattered areas of deep dermal fibromatous cell proliferation (Figure 4.6L) and mesenchymal cell disorganization within a classical myxoid tumour stroma.

By day 13, the tumours from animals in the VMLT1.6 group were resolving and regressing histologically (lesion score = 4) with abnormalities limited to residual mononuclear leukocytic infiltrates in superficial areas of the biopsied section (Figure 4.6G). In contrast specimens obtained from the wild type and R-S131R groups showed evidence of continued disease progression with pending tissue rejection and subsequent sloughing (lesions scores = 9 and 10 for R-S131R and wild type infections, respectively) (Figure 4.6H and I). We also noted extensive and well-demarcated areas of superficial and deep dermal necrosis with marked mononuclear cell infiltrates, dermal fibrosis and scarring, occasional vascular thromboses, and marked fibromatous proliferation in these sections. Collectively these observations show that infections initiated by S131R-deficient virus are more rapidly cleared by a cell-mediated immune response and this occurs before the appearance of myxoid stroma and the fibromatous cell proliferation that characterizes wild type SFV infections.

Figure 4.6. Histologic analysis of tumours induced by wild type, VMLT1.6, and R-S131R viruses. Tumours were biopsied on the days indicated and stained with hematoxylin and eosin for light microscopy. Specimens have been oriented to place the ulcerated epithelium (thick red crust) on the top (A, B, C arrow) and the deeper dermal layers at the bottom (J, deep dermis delineated by 'd'). The pale, clear areas throughout the tissue sections represent areas of edema (A, C, J asterisks) while the more basophilic areas (dark purple/blue areas) represent areas of mixed leukocytic infiltration. On day 7 post-infection no differences were noted in tumour appearance between any of the treatment groups. Rare eosinophilic intranuclear inclusion bodies were noted in perifollicular cells of animals infected with wild type virus (K, arrow). On day 10, the necrotic epithelial lesion was relatively unchanged in VMLT1.6-infected animals (D) beyond a mild increase in dermal necrosis and a decrease in perivascular edema. We saw no evidence of fibromatous cell proliferation. In contrast, these lesions had continued to progress in tissues infected with either the wild type and revertant viruses (E and F, respectively). In addition to superficial epithelial necrosis, extensive areas of superficial and deep dermal inflammation with dense mononuclear cell infiltrates were observed (J, open arrows denote perivascular infiltrates), with continued disruption and loss of hair follicles and adnexal structures (B, C, arrowheads mark loss of follicular structures), and dermal necrosis admixed with hemorrhage and edema. By day 13 post-infection, specimens taken from wild-type and revertant virus infections still showed extensive areas of inflammation, necrosis (H and I, necrotic areas delineated by white arrows), and proliferation at the site of injection (L), whereas tumours from animals in the VMLT1.6 group were resolving and regressing back to a near normal state (G).

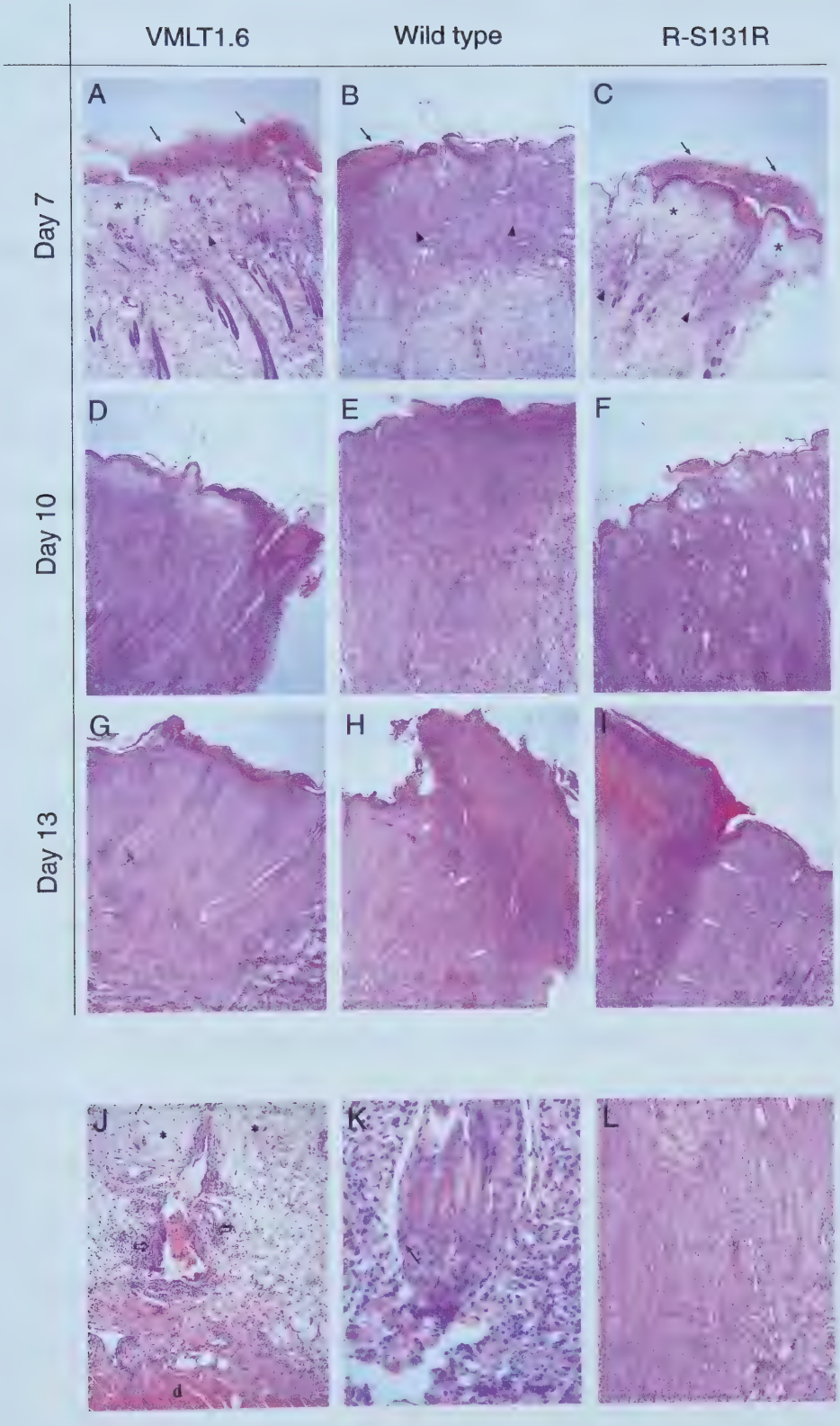
VMLT1.6
Wild type
R-S131R
Day 7
Day 10
Day 13
A
B
C
D
E
F
G
H
I
J
K
L

M131R inhibits both mitochondria-mediated and anti-Fas induced apoptosis in virus-infected cells. The results outlined above could be explained by the hypothesis that cells infected with S131R-deficient viruses cannot mount an effective defense against a cell-mediated immune response. This response often targets virus-infected cells for killing by apoptotic processes and the superoxide anion that is up-regulated during virus infection (Figure 4.3) is known to suppress apoptosis triggered though the Fas receptor pathway [11, 12]. Therefore we decided to test whether Leporipoxvirus SOD1 homologs might serve an anti-apoptotic function in virus-infected cells. These experiments were performed using human T-lymphocyte Jurkat cells and MYX instead of SFV virus. Jurkat cells provide a well-characterized model for studying apoptotic processes and suitable reagents are widely available for use with human cells. MYX virus was used because Jurkat cells can support MYX growth, but not that of SFV. As noted above the genetic and biochemical properties of the MYX and SFV M/S131R homologs seem to be identical and we also confirmed that MYX infection of Jurkat cells up-regulates superoxide concentrations in an M131R-dependent manner (Figure 4.9).

Jurkat cells were treated with either staurosporine or anti-Fas antibodies to induce either the mitochondrial or death-receptor mediated pathways of apoptosis, respectively. Both treatments efficiently induced apoptosis as illustrated by the fragmentation of chromosomal DNA into nucleosome-sized fragments and the subsequent detection of this "apoptotic ladder" by agarose gel electrophoresis (Figure 4.7A). In contrast, when cells were infected with wild type MYX for 24 hours prior to the induction of apoptosis, no DNA fragmentation was observed following either treatment. Most importantly, this effect seemed to be dependent upon M131R function

since deleting the gene permitted near normal levels of staurosporine-induced apoptosis and normal levels of Fas-mediated apoptosis (Figure 4.7A). Control experiments showed that neither mutant nor wild type virus infection could trigger apoptosis in Jurkat cells in the absence of an apoptotic inducer. We also treated these cells with a broad-spectrum caspase inhibitor, zVAD.fmk, and this compound blocked the appearance of an apoptotic DNA ladder in samples treated with the apoptotic stimulants (Figure 4.7B).

To investigate more closely the impact of M131R on this process, we examined the fate of caspase-3 by Western blot analysis. Caspase-3 is one of the key downstream effector molecules in the proteolytic cascade. Treating mock-infected Jurkat cells with 2 μM staurosporine or 250 ng/ml of anti-Fas antibody resulted in the cleavage and activation of caspase-3 as revealed by the conversion of the 32 kDa pro-enzyme into a 19 kDa product (Figure 4.7C). Caspase-3 activation was also seen in cells infected by M131RΔ virus, but blocked in cells infected by wild type MYX. To prove that wild type virus were establishing a productive infection we also performed a Western blot looking for expression of the M131R late gene product. The protein was readily detected, but as expected only in cells infected with wild type virus (Figure 4.7D). These observations suggest that Leporipoxvirus SOD1 homologs interfere with apoptotic signaling events at some point upstream of caspase-3 activation.

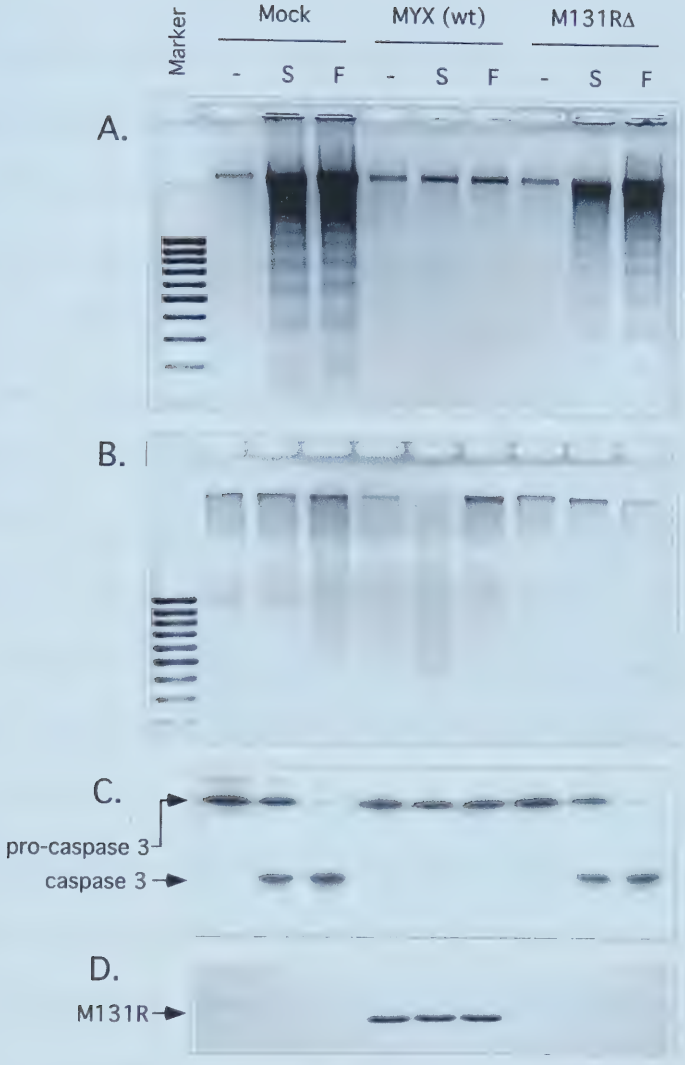

Figure 4.7. The MYX M131R gene product protects infected cells from Fas- and staurosporine-induced apoptosis. Jurkat cells were infected for 24 hr with wild type or M131R-deleted MYX virus and then exposed to staurosporine (S) or anti-Fas antibody (F) for 3 h or 10 h, respectively. Fragmented cellular DNA was extracted, fractionated by agarose gel electrophoresis, and visualized with ethidium bromide. In mock-infected cells, both staurosporine and anti-Fas treatments produced a classical 200bp nucleosomal ladder indicative of apoptotic induction (a 100 bp size marker is indicated). Wild type MYX protected Jurkat cells from these effects, but this protection depends upon M131R gene function and was not seen in cells infected with M131RΔ virus (Panel A). As a control we added the caspase inhibitor zVAD.fmk, and this drug completely prevented DNA laddering (Panel B). Western blot analysis showed that DNA laddering correlated with caspase 3 activation and that the M131R-deleted virus cannot prevent cleavage of pro-caspase 3 (Panel C). Another western blot control, showed that the M131R protein was expressed only in cells infected with wild type MYX virus (Panel D).

To further confirm the anti-apoptotic function of M131R as well as gain some more quantitative insights into the effectiveness of this immunomodulatory pathway, we performed TUNEL labelling of virus-infected cells followed by FACS analysis. Control experiments showed that treating mock-infected Jurkat cells with anti-Fas antibody for 10 hr resulted in 38% of cells becoming TUNEL-positive whereas a 3 hr exposure to staurosporine resulted in 29% TUNEL-positive cells (Figure 4.8, top). The effectiveness of anti-apoptotic MYX gene products is illustrated by the fact that only background levels of TUNEL-positive cells were detected when these cells were first infected with wild type virus prior to either treatment (Figure 4.8, middle). Interestingly, using this assay it can be seen that deleting the M131R gene rendered virus-infected cells partially and perhaps differentially sensitive to both of these exogenous stimuli (Figure 4.8, bottom). In the absence of M131R gene function, mutant MYX virus still appeared able to mount a partial defense against staurosporine-triggered apoptosis (~70% of wild type) and a less-effective response to Fas-triggered apoptosis (~40% of wild type). These observations suggest that Leporipoxvirus SOD1 homologs can protect Type II Jurkat T-cells from both mitochondrial and Fas/FasL-mediated apoptotic pathways. However, M/S131R gene function likely acts in concert with the activity of other previously characterized anti-apoptotic gene products such as M11L [14].

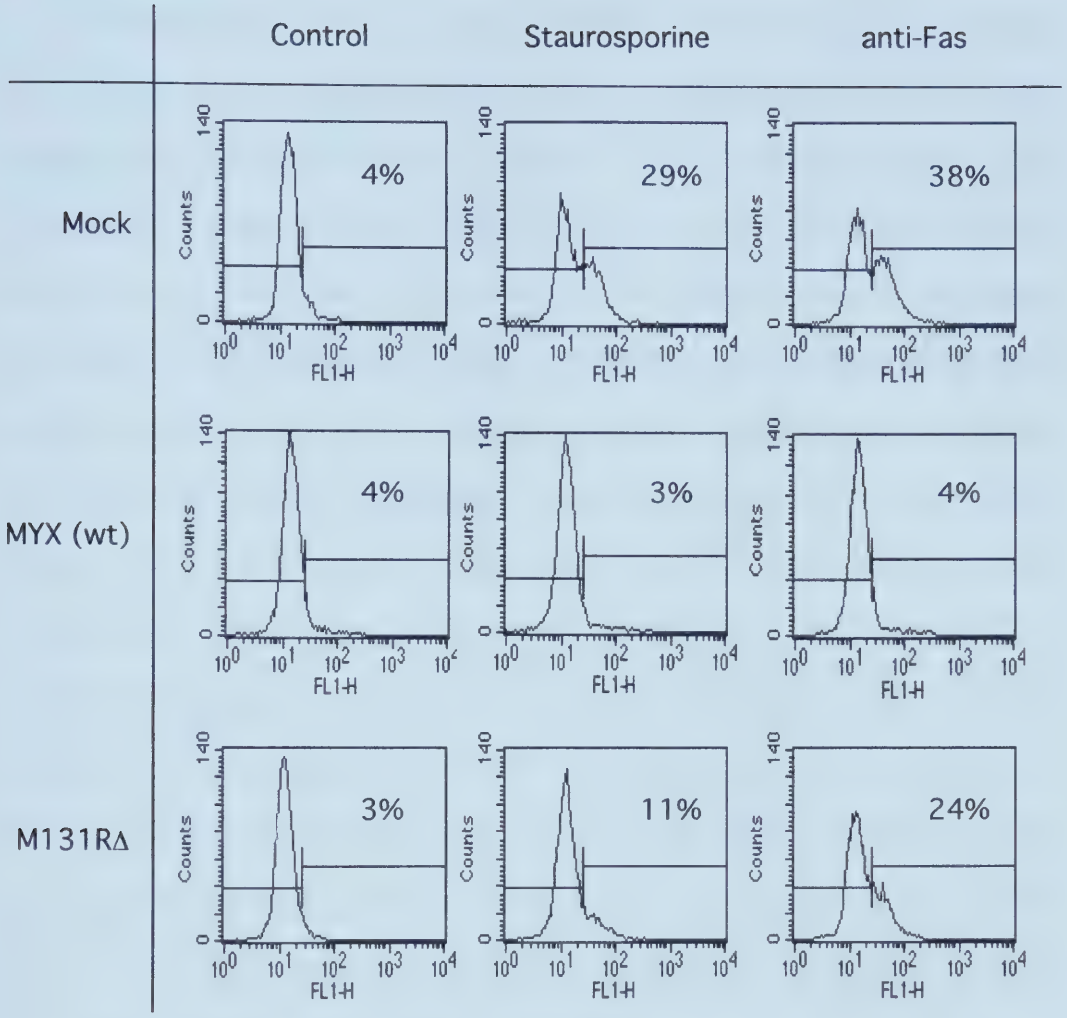

Figure 4.8. FACS detection of apoptosis in MYX-infected cells. Jurkat cells were infected, or mock-infected, with the indicated viruses and treated with staurosporine or anti-Fas antibodies as described in FIGURE 4.7. A TUNEL labelling kit and FACS analysis were then used to identify the percentage of cells undergoing apoptosis. Wild type MYX infection completely suppressed apoptosis induced by either agent, whereas the deletion of M131R gene function rendered the cells partially susceptible to both stimuli. The M131R gene appeared to play a greater role in protecting cells from anti-Fas treatment as judged by the relatively greater proportion (24%) of apoptotic cells detected in M131RΔ-infected cells treated with anti-FAS antibody.

M131R is abundantly expressed and widely distributed throughout infected cells. Finally, in order to gain some insights into where, when, and how M131R might be exerting these anti-apoptotic effects, we prepared a recombinant MYX virus encoding enhanced green fluorescent protein (EGFP) fused to the C-terminus of M131R (Figure 4.9A). This M131R-EGFP virus was then used to directly monitor the intracellular distribution of M131R without the necessity of fixing and immunostaining the protein as we have had to do previously [50]. The fusion protein was easily detected by Western blot analysis and exhibited a late gene expression pattern identical to native M131R protein. The fusion protein also co-sedimented with MYX virions though a sucrose density gradient as does the native protein (data not shown). To test whether the fusion protein was functional, we infected Jurkat cells with the M131R-EGFP virus and stained the cells 24 hr post-infection with hyrdoethidine. The dye detected an increase in the superoxide concentration in $EGFP^+$ cells relative to the background HE signal detected in mock and M131RΔ virus infected cells (Figure 4.9B). In these experiments the EGFP signal was also seen distributed throughout the cell cytoplasm, but Jurkat cells are not well suited to localization studies due to their small size.

SIRC cells provided a better model for a distribution analysis. We still could not detect the faint signal that might be expected from delivery of virus-encapsidated M131R-EGFP protein to infected cells, but we could easily detect the late expression of the protein starting 10-12 hr post-infection. By 24 hr post-infection, confocal fluorescence microscopy detected very high levels of a fluorescent protein distributed throughout all parts of the cytosol of infected cells (Figure 4.9C). This distribution included the nucleus, a site not well visualized by our previous studies using fluorescent

antibody methods [50]. We also compared the distribution of the protein with the distribution of mitochondria, since we had previously noted some evidence that a portion of the M131R protein might localize to mitochondrial compartments [50]. Our results confirmed that some M131R protein does co-localize with the mitochondrial stain mitotracker red, but the broad distribution of the EGFP fluorescence suggested that no one part of the cell is a special target for this protein. SOD1-like Leporipoxvirus proteins are produced in abundance during virus infection and based on these studies can act at sites distributed throughout the cell.

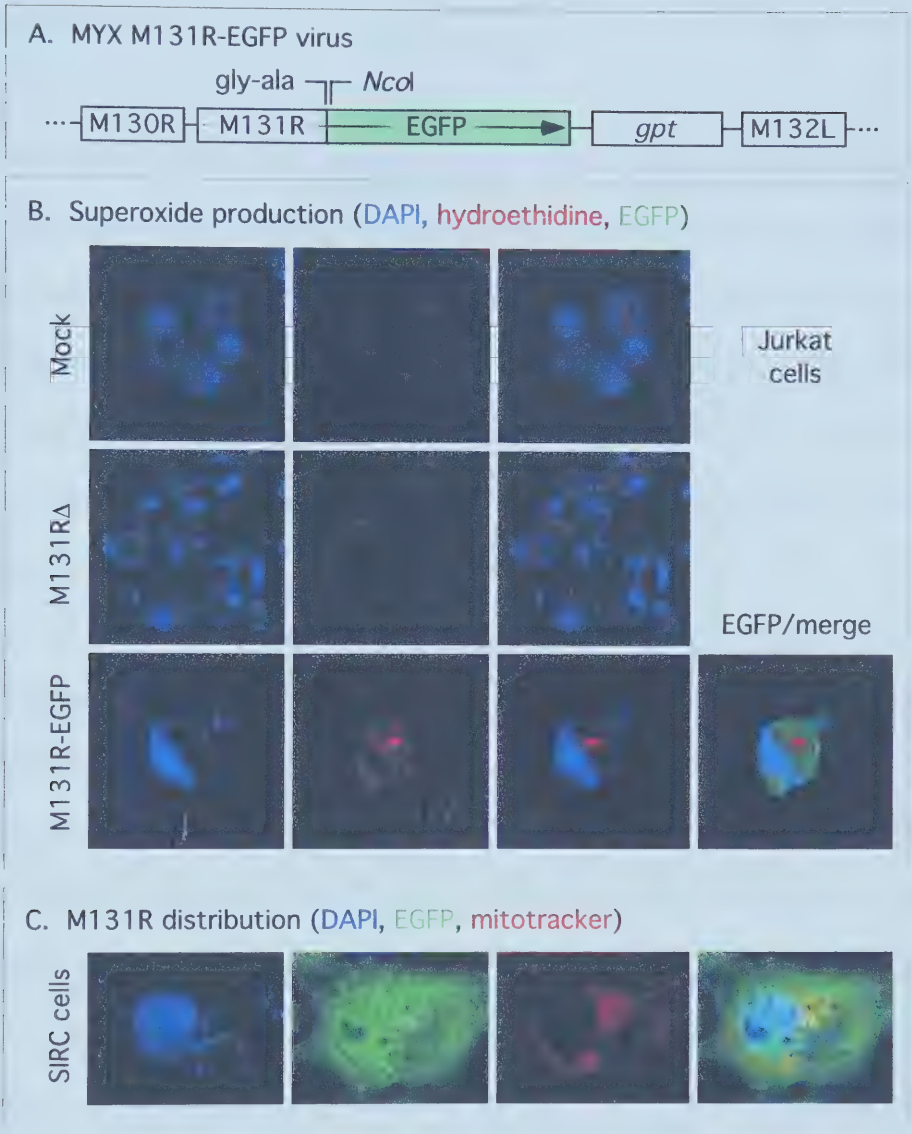

Figure 4.9. Distribution of EGFP-tagged M131R protein in virus-infected cells. Panel A illustrates the MYX M131R-EGFP virus used in these studies. The virus encodes a C-terminal fusion of EGFP to M131R and a *gpt* selectable marker separating the gene encoding the fusion protein from M132L. The M131R-EGFP fusion protein continues to be expressed from the M131R promoter. These MYX virus were used to infect Jurkat cells at a multiplicity of infection of ten for 24 hr and then these cells were stained with DAPI or hydroethidine to visualize the nucleus and measure the amount of superoxide generated over a 20 min incubation period (Panel B). Note the elevated level of HE dye product seen in cells infected with M131R-EGFP virus. M131R-EGFP fusion protein is also detected in this cell. Panel C compares the distribution of M131R-EGFP fusion protein relative to the locations of the nucleus (DAPI) and mitochondria (mitotracker red). EGFP-tagged M131R appears to be distributed widely in the cell.

4.4 DISCUSSION

Poxviruses encode many genes that are not essential for replication in culture, but which are important determinants of pathogenicity *in vivo* [reviewed in [39]]. A characteristic feature of many of these gene products is that they complex with signaling molecules (e.g. cytokines, double-stranded RNAs, or regulatory proteins) and thus interfere directly in the activation of critical anti-viral defense pathways. In the current study, we have investigated the biological function of Leporipoxvirus SOD1 homologs. We have shown that these genes are not required for virus growth, indeed M/S131R-deficient viruses actually grow better than do wild type virus. This cannot be attributed to the presence of the *gpt* marker since, as long as they are not exposed to ultraviolet light, MYX viruses encoding the same *gpt* cassette replacing the M127L photolyase gene, grow equally well as wild type MYX [6, 55]. We suspect that the phenomenon reflects a role served by the protein in stabilizing the capsid against environmental stressors like desiccation and heat. Such a function is not required under laboratory growth and infection conditions and might conceivably have detrimental effects on virus yields [58]. We have also shown that deleting the SFV S131R gene renders SFV less "tumourigenic" in rabbits and that these gene products play a role in suppressing Fas and staurosporine-triggered apoptosis in cultured cells. Concurrently, we have shown that wild type MYX and SFV infections normally cause increases in the intracellular concentration of superoxide anion, and that this effect is dependent upon M/S131R gene function. Superoxide anion has been shown to exert both pro-proliferative and anti-apoptotic effects on cells under some circumstances (see below), and our data suggest that

tumourigenic poxviruses can gain advantages from these effects by using Cu-Zn SOD1 homologs to indirectly manipulate the concentration of $O_2\cdot^-$ in virus-infected cells.

How $O_2\cdot^-$ affects such diverse phenomena as cell growth, apoptosis, and inflammation is complicated by the "Goldilocks effect" in that either too much *or* too little superoxide will have deleterious effects on cells, and that an optimal growth environment requires a redox state that is "just right". These biphasic effects of redox stress on cellular metabolism, coupled with the genetic diversity of cultured cells, can provide an explanation for the sometimes paradoxical data in the literature [23]. It is now generally understood that the activation of cellular receptors by growth factors or cytokines leads to ROS production, and that this can trigger a signal transduction cascade in which ROS-sensitive mitogen-activated kinases activate the AP-1 transcription factor via phosphorylation of its c-*jun* and c-*fos* subunits [4, 5, 47]. Leporipoxviruses, like most other Chordopoxviruses, express functional epidermal growth factor homologs [30, 31]. These proteins promote a proliferative response in infected cells and are expected to signal through the ErbB pathway. The pro-proliferative effects of these viral growth factors would be potentiated by inhibiting cellular SOD1 (and thus stabilizing $O_2\cdot^-$) and account for the reduced fibromatous cell proliferation seen in animals infected with S131R-deficient viruses (Figure 4.6). The activity of this gene product would also explain why deleting MYX and malignant rabbit virus growth factor genes doesn't entirely prevent virus-induced tumour formation.

How ROS might regulate apoptosis is less well understood at the molecular level and is further complicated in poxvirus-infected cells where additional anti-apoptotic gene products are also expressed. It is clear that overproduction of superoxide beyond the

detoxification capacities of a cell can induce apoptosis or necrosis [8]. However it is unlikely that the increase in $[O_2\cdot^-]$ that is detected using HE staining is very large (Figure 4.3), given that virus infection caused just a 60% drop in the amount of Cu-Zn SOD1 activity [10] and only a modest (10-20%) decrease in the activity of the superoxide-sensitive cellular enzyme aconitase (Figure 4.4). The difference in aconitase activity in cells infected with mutant versus wild-type viruses, permits the calculation [21] that M/S131R activity changes the steady-state $[O_2\cdot^-]$ only 2.5- or 3.0-fold in SIRC and BGMK cells, respectively, and shows that SFV and MYX infections create only a mildly pro-oxidative state in virus-infected cells. Under these conditions there have still been a number of reports showing that superoxide has anti-apoptotic effects. For example treating cells with either paraquat or the SOD1 inhibitor diethyldithiocarbamate caused a two-to-three-fold increase in intracellular $[O_2\cdot^-]$ that completely suppressed Fas-mediated apoptotic killing of human melanoma cells [11]. More recently the ROS produced following exposure to growth factors has also been shown to have anti-apoptotic effects in pancreatic cancer cells [51]. How this effect is accomplished is still controversial. Vaquero *et al.* showed that growth factor signaling can activate soluble non-mitochondrial NAD(P)H oxidases to produce superoxide and suggested that this ROS might then activate anti-apoptotic genes regulated by NF-κB. NF-κB also activates SOD1 gene expression [34] so this makes sense from a regulatory perspective. However, this is unlikely to be the whole story because the AP-1 constituent c-*fos* is an NF-κB regulated gene [18] and thus the two ROS-sensitive pathways are interlinked at the transcriptional level. SFV and MYX are presumably perturbing this network of

exquisitely redox-sensitive systems to their advantage, but our current understanding of these networks suggests that there are many molecular targets.

We also noted that deleting M131R seemed to differentially affect myxoma virus's capacity to suppress both of the mitochondrial and Fas-mediated apoptotic pathways. Wild type virus inhibited apoptosis in the presence of both agents, but cells infected with M131R-deficient virus retained a greater degree of resistance to apoptosis following staurosporine treatment than was seen following treatment with anti-Fas antibodies. This suggests that M/S131R may serve a relatively more important role in suppressing extrinsic apoptotic signaling. Jurkat cells are type II cells, in which both Fas-mediated and staurosporine-induced apoptosis depend upon the activation of the mitochondrial pathway, so our data suggest that changes in the $[O_2 \cdot^-]$ are exerting pleiotropic, but relatively greater, effects on upstream events linking aggregation of the Fas receptor to Bak activation. Caspase 8 activity is ROS sensitive and thus represents at least one possible enzymatic target within this cascade [43]. The fact that inactivating M131R does not completely abrogate either response is not surprising given that the MYX M11L gene product targets the mitochondrial voltage-gated ion channel and protects virus-infected cells from apoptotic signals mediated by Bak [14, 52]. Interestingly, these authors also noted that M11L-deficient virus were still capable of providing significant protection against Fas-mediated apoptosis [14], demonstrating the existence of other MYX-encoded anti-apoptotic genes. What this residual defense might be is not explained by the known biological properties of other MYX apoptotic modifiers (M-T2, M-T4 and M-T5) and could be explained by the existence of M131R.

M131R and S131R are not the only known poxvirus gene products that can alter the redox state of infected cells. For example the molluscum contagiosum MC066L gene encodes a glutathione peroxidase that protects cells expressing the protein from the pro-apoptotic peroxides generated by ultraviolet light [41]. Poxviruses also catalyze the oxidation of disulphide bonds in virus proteins using a network of redox active proteins [40]. Whether other poxvirus SOD1 homologs all serve the same function as M/S131R is doubtful since the SOD1 homolog encoded by *Amsacta moorei* entomopoxvirus is catalytically active and likely serves an entirely different function in virus-infected insects [3]. Many other virus infections have also been reported to disrupt cellular ROS homeostasis, but in few cases have any insights into the mechanism been elucidated [37]. It is striking that the hepatitis B virus x (Hbx) protein has been suggested to interfere with the activity of the mitochondrial permeability pore, thus generating ROS with effects not unlike those we see in Leporipoxvirus infections [53]. In particular this ROS has also been proposed to activate transcriptomes regulated by NF-κB and STAT-3 transcription factors and which, in cells constitutively expressing Hbx, might account for some of the pathological features of hepatocellular carcinomas [27].

In conclusion, the information that we have gathered from the study of Leporipoxviruses SOD1 homologs leads to the discovery of a novel poxvirus immunoevasion pathway that promotes virus-induced tumourigenesis. We suggest that these viral SOD1 homologs promote an increase in the intracellular superoxide concentration, which both stimulates cellular proliferation and inhibits apoptosis. Future work will focus on resolving where this ROS stress might be exerting its effect(s) on a complex chain of interlinked signal transduction cascades.

4.5 REFERENCES

1. Addison CL BT, Ralston R, Muller WJ, Gauldie J, Graham FL (1995) Intratumoral injection of an adenovirus expressing interleukin 2 induces regression and immunity in a murine breast cancer model. Proc Natl Acad Sci U S A 92: 8522-8526

2. Almazan F, Tscharke DC, Smith GL (2001) The vaccinia virus superoxide dismutase-like protein (A45R) is a virion component that is nonessential for virus replication. J Virol 75: 7018-29.

3. Becker MN, Greenleaf WB, Ostrov DA, Moyer RW (2004) Amsacta moorei Entomopoxvirus Expresses an Active Superoxide Dismutase. J Virol 78: 10265-75

4. Behrend L, Henderson G, Zwacka RM (2003) Reactive oxygen species in oncogenic transformation. Biochem Soc Trans 31: 1441-4

5. Benhar M, Engelberg D, Levitzki A (2002) ROS, stress-activated kinases and stress signaling in cancer. EMBO Rep 3: 420-5

6. Bennett CJ, Webb M, Willer DO, Evans DH (2003) Genetic and phylogenetic characterization of the type II cyclobutane pyrimidine dimer photolyases encoded by Leporipoxviruses. Virology 315: 10-9

7. Bize IB, Oberley LW, Morris HP (1980) Superoxide dismutase and superoxide radical in Morris hepatomas. Cancer Res 40: 3686-93

8. Buttke TM, Sandstrom PA (1994) Oxidative stress as a mediator of apoptosis. Immunol Today 15: 7-10

9. Cameron C, Hota-Mitchell S, Chen L, Barrett J, Cao JX, Macaulay C, Willer D, Evans D, McFadden G (1999) The complete DNA sequence of myxoma virus. Virology 264: 298-318

10. Cao JX, Teoh ML, Moon M, McFadden G, Evans DH (2002) Leporipoxvirus Cu-Zn superoxide dismutase homologs inhibit cellular superoxide dismutase, but are not essential for virus replication or virulence. Virology 296: 125-35

11. Clement MV, Stamenkovic I (1996) Superoxide anion is a natural inhibitor of FAS-mediated cell death. Embo J 15: 216-25

12. Clement MV, Pervaiz S (1999) Reactive oxygen intermediates regulate cellular response to apoptotic stimuli: an hypothesis. Free Radic Res 30: 247-52

13. Culotta VC, Klomp LW, Strain J, Casareno RL, Krems B, Gitlin JD (1997) The copper chaperone for superoxide dismutase. J Biol Chem 272: 23469-72

14. Everett H, Barry M, Sun X, Lee SF, Frantz C, Berthiaume LG, McFadden G, Bleackley RC (2002) The myxoma poxvirus protein, M11L, prevents apoptosis by direct interaction with the mitochondrial permeability transition pore. J Exp Med 196: 1127-39

15. Frank S, Kampfer H, Podda M, Kaufmann R, Pfeilschifter J (2000) Identification of copper/zinc superoxide dismutase as a nitric oxide-regulated gene in human (HaCaT) keratinocytes: implications for keratinocyte proliferation. Biochem J 346 Pt 3: 719-28

16. Fridovich I (1978) The biology of oxygen radicals. Science 201: 875-80

17. Fridovich I (1997) Superoxide anion radical (O2-.), superoxide dismutases, and related matters. J Biol Chem 272: 18515-7

18. Fujioka S, Niu J, Schmidt C, Sclabas GM, Peng B, Uwagawa T, Li Z, Evans DB, Abbruzzese JL, Chiao PJ (2004) NF-kappaB and AP-1 connection: mechanism of NF-kappaB-dependent regulation of AP-1 activity. Mol Cell Biol 24: 7806-19

19. Galeotti T, Wohlrab H, Borrello S, De Leo ME (1989) Messenger RNA for manganese and copper-zinc superoxide dismutases in hepatomas: correlation with degree of differentiation. Biochem Biophys Res Commun 165: 581-9

20. Gardner PR, Fridovich I (1992) Inactivation-reactivation of aconitase in Escherichia coli. A sensitive measure of superoxide radical. J Biol Chem 267: 8757-63

21. Gardner PR, Raineri I, Epstein LB, White CW (1995) Superoxide radical and iron modulate aconitase activity in mammalian cells. J Biol Chem 270: 13399-405

22. Halliwell B, Gutteridge JMC (1999) Free radicals in biology and medicine, 3rd edn. Oxford University Press, New York

23. Hernandez-Saavedra D, McCord JM (2003) Paradoxical effects of thiol reagents on Jurkat cells and a new thiol-sensitive mutant form of human mitochondrial superoxide dismutase. Cancer Res 63: 159-63

24. Herrmann M, Lorenz HM, Voll R, Grunke M, Woith W, Kalden JR (1994) A rapid and simple method for the isolation of apoptotic DNA fragments. Nucleic Acids Res 22: 5506-7

25. Kinnula VL, Crapo JD (2004) Superoxide dismutases in malignant cells and human tumors. Free Radic Biol Med 36: 718-44

26. Lamb AL, Torres AS, O'Halloran TV, Rosenzweig AC (2001) Heterodimeric structure of superoxide dismutase in complex with its metallochaperone. Nat Struct Biol 8: 751-5

27. Lee YI, Hwang JM, Im JH, Kim NS, Kim DG, Yu DY, Moon HB, Park SK (2004) Human hepatitis B virus-X protein alters mitochondrial function and physiology in human liver cells. J Biol Chem 279: 15460-71

28. Malmstrom BG (1982) Enzymology of oxygen. Annu Rev Biochem 51: 21-59

29. McCord JM (2000) The evolution of free radicals and oxidative stress. Am J Med 108: 652-9

30. Opgenorth A, Strayer D, Upton C, McFadden G (1992) Deletion of the growth factor gene related to EGF and TGF alpha reduces virulence of malignant rabbit fibroma virus. Virology 186: 175-91

31. Opgenorth A, Nation N, Graham K, McFadden G (1993) Transforming growth factor alpha, Shope fibroma growth factor, and vaccinia growth factor can replace myxoma growth factor in the induction of myxomatosis in rabbits. Virology 192: 701-9

32. Parks RJ, Evans DH (1991) Effect of marker distance and orientation on recombinant formation in poxvirus-infected cells. J Virol 65: 1263-72

33. Prose PH, Friedman-Kien AE, Vilcek J (1971) Morphogenesis of rabbit fibroma virus. Correlation with pathogenesis of the skin lesion. Am J Pathol 64: 467-78

34. Rojo AI, Salinas M, Martin D, Perona R, Cuadrado A (2004) Regulation of Cu/Zn-superoxide dismutase expression via the phosphatidylinositol 3 kinase/Akt pathway and nuclear factor-kappaB. J Neurosci 24: 9324-34

35. Rosen DR, Siddique T, Patterson D, Figlewicz DA, Sapp P, Hentati A, Donaldson D, Goto J, O'Regan JP, Deng HX, et al. (1993) Mutations in Cu/Zn superoxide dismutase gene are associated with familial amyotrophic lateral sclerosis. Nature 362: 59-62

36. Schmidt PJ, Rae TD, Pufahl RA, Hamma T, Strain J, O'Halloran TV, Culotta VC (1999) Multiple protein domains contribute to the action of the copper chaperone for superoxide dismutase. J Biol Chem 274: 23719-25

37. Schwarz KB (1996) Oxidative stress during viral infection: a review. Free Radic Biol Med 21: 641-9

38. Scott CB, Holdbrook R, Sell S (1981) Cell-mediated immune response to Shope fibroma virus-induced tumors in adult rabbits. J Natl Cancer Inst 66: 681-9

39. Seet BT, Johnston JB, Brunetti CR, Barrett JW, Everett H, Cameron C, Sypula J, Nazarian SH, Lucas A, McFadden G (2003) Poxviruses and immune evasion. Annu Rev Immunol 21: 377-423

40. Senkevich TG, White CL, Koonin EV, Moss B (2002) Complete pathway for protein disulfide bond formation encoded by poxviruses. Proc Natl Acad Sci U S A 99: 6667-72

41. Shisler JL, Senkevich TG, Berry MJ, Moss B (1998) Ultraviolet-induced cell death blocked by a selenoprotein from a human dermatotropic poxvirus [see comments]. Science 279: 102-5

42. Shope RE (1932) A transmissible tumor-like condition of rabbits. J. Exp. Med. 56: 793-802

43. Smith GK, Barrett DG, Blackburn K, Cory M, Dallas WS, Davis R, Hassler D, McConnell R, Moyer M, Weaver K (2002) Expression, preparation, and high-throughput screening of caspase-8: discovery of redox-based and steroid diacid inhibition. Arch Biochem Biophys 399: 195-205

44. Smith GL, Chan YS, Howard ST (1991) Nucleotide sequence of 42 kbp of vaccinia virus strain WR from near the right inverted terminal repeat. J Gen Virol 72: 1349-76

45. Smith JW, Tevethia SS, Levy BM, Rawls WE (1973) Comparative studies on host responses to Shope fibroma virus in adult and newborn rabbits. J Natl Cancer Inst 50: 1529-39

46. Sun Y, Oberley LW, Oberley TD, Elwell JH, Sierra-Rivera E (1993) Lowered antioxidant enzymes in spontaneously transformed embryonic mouse liver cells in culture. Carcinogenesis 14: 1457-63

47. Sundaresan M, Yu ZX, Ferrans VJ, Sulciner DJ, Gutkind JS, Irani K, Goldschmidt-Clermont PJ, Finkel T (1996) Regulation of reactive-oxygen-species generation in fibroblasts by Rac1. Biochem J 318 (Pt 2): 379-82

48. Tanaka M, Kogawa K, Nishihori Y, Kuribayashi K, Nakamura K, Muramatsu H, Koike K, Sakamaki S, Niitsu Y (1997) Suppression of intracellular Cu-Zn SOD results in enhanced motility and metastasis of Meth A sarcoma cells. Int J Cancer 73: 187-92

49. Tarpey MM, Fridovich I (2001) Methods of detection of vascular reactive species: nitric oxide, superoxide, hydrogen peroxide, and peroxynitrite. Circ Res 89: 224-36

50. Teoh ML, Walasek PJ, Evans DH (2003) Leporipoxvirus Cu,Zn-superoxide dismutase (SOD) homologs are catalytically inert decoy proteins that bind copper chaperone for SOD. J Biol Chem 278: 33175-84

51. Vaquero EC, Edderkaoui M, Pandol SJ, Gukovsky I, Gukovskaya AS (2004) Reactive oxygen species produced by NAD(P)H oxidase inhibit apoptosis in pancreatic cancer cells. J Biol Chem 279: 34643-54

52. Wang G, Barrett JW, Nazarian SH, Everett H, Gao X, Bleackley C, Colwill K, Moran MF, McFadden G (2004) Myxoma virus M11L prevents apoptosis through constitutive interaction with Bak. J Virol 78: 7097-111

53. Waris G, Huh KW, Siddiqui A (2001) Mitochondrially associated hepatitis B virus X protein constitutively activates transcription factors STAT-3 and NF-kappa B via oxidative stress. Mol Cell Biol 21: 7721-30

54. Wasilenko ST, Meyers AF, Vander Helm K, Barry M (2001) Vaccinia virus infection disarms the mitochondrion-mediated pathway of the apoptotic cascade by modulating the permeability transition pore. J Virol 75: 11437-48

55. Webb MAM (2004) An investigation of factors affecting poxvirus genetic stability. National Library of Canada = Bibliothèque nationale du Canada, Ottawa

56. Willer DO, McFadden G, Evans DH (1999) The complete genome sequence of shope (rabbit) fibroma virus. Virology 264: 319-43

57. Willer DO, Yao XD, Mann MJ, Evans DH (2000) In vitro concatemer formation catalyzed by vaccinia virus DNA polymerase. Virology 278: 562-569

58. Zachertowska A, Brewer D, Evans DH (2004) Maldi-tof mass spectroscopy detects the capsid structural instabilities created by deleting the myxoma virus cupro-zinc SOD1 homolog M131R. J Virol Met (in press)

59. Zhang Y, Zhao W, Zhang HJ, Domann FE, Oberley LW (2002) Overexpression of copper zinc superoxide dismutase suppresses human glioma cell growth. Cancer Res 62: 1205-12

60. Zhao H, Kalivendi S, Zhang H, Joseph J, Nithipatikom K, Vasquez-Vivar J, Kalyanaraman B (2003) Superoxide reacts with hydroethidine but forms a fluorescent product that is distinctly different from ethidium: potential implications in intracellular fluorescence detection of superoxide. Free Radic Biol Med 34: 1359-68

CHAPTER 5 – DISCUSSION AND FUTURE DIRECTIONS

5.1 Discussion

When the SODs were first discovered, it was assumed that their roles were primarily to provide defence against the cytotoxic metabolite, superoxide radical. More recently, however, it has become apparent that superoxide serves a rather wider range of metabolic regulatory roles, even in perfectly healthy cells. The pleiotropic effects of ROS have expanded our understanding of the importance of SODs in maintaining a specific redox state at a particular stage of cellular development. In fact, the redox status of infected cells is so crucial that Leporipoxviruses have developed a system to disrupt this regulation by encoding an inactive SOD1 mimic, by the M/S131R genes. Our studies on viral SOD1 homologs have not only provided insights into mechanisms of virus virulence but also provided further evidence of the importance of these cellular redox homeostatic systems.

Not much was known about virus encoded SOD1 homologs prior to 2001, except that due to sequencing efforts, many members of the poxvirus family were found to encode SOD1-like genes [1, 5, 43, 46, 48], including Leporipoxviruses [10, 56]. Geoffrey Smith's group was the first to characterize one of these proteins, the A45R gene product encoded by vaccinia virus [2]. Like M/S131R (Chapter 1.9), A45R was found to be inactive as a dismutase and despite the fact that this gene is highly conserved among 12 strains of vaccinia virus, cowpox virus, elephantpox virus, and camelpox virus (94 to 100% amino acid identity), they found that A45R is nonessential for virus replication or for virulence in both murine and rabbit models. Almazan *et al.* also showed that A45R is

a core virion component that rather surprisingly seemed to serve no obvious effect on virus replication or virulence.

Around the same time, we were investigating the biochemical properties of the more "SOD1-like" (Chapter 1.9) M/S131R genes encoded by Leporipoxviruses. Our study revealed some similarities between M/S131R and A45R as well as some important differences. Like A45R, M/S131R were found to be abundantly expressed late gene products which are incorporated into mature virions (Figure 2.4 and [57]). However, deleting M/S131R not only did not compromise virus replication, but actually promoted virus growth compared with wild-type viruses (Figure 2.3 and 4.2, respectively). This phenomenon is interesting and yet puzzling, since we have also determined that SFV packages at least 1,000 molecules of S131R per mature virion (Chapter 1.2). Moreover, deleting these genes rendered myxoma virus and SFV sensitive to elevated temperature, suggesting that the proteins play a role in maintaining virion structural stability [57]. We have no explanation for why we see enhanced virus yields when such an abundant virion structural protein is deleted, although perhaps, there is a "trade-off" associated with encoding inhibitors of cellular SOD1 wherein promoting a prooxidant state in wild type virus infected cells somehow interferes with virus replication or limits the virus yield per cell. Alternatively, there exists some kind of trade-off between stability and infectivity wherein factors that stabilize virions against environmental stresses (like dessication) may not always favour infectivity [57].

Although M/S131R are catalytically inactive (Figure 2.5), they are able to down-regulate cellular SOD1 activity (Figure 2.7 and 2.8). This inhibitory behaviour seems to be unique amongst poxviral SOD1 homologs. We have detected a strong interaction

between M/S131R and cellular CCS (Figure 3.5-3.7), which suggests that M/S131R can act by depleting the copper supply to endogenous SOD1, and thus down-regulate its activity. However, since CCS exists in a much lower concentration than SOD1 and most SOD1 already exists in fully metallated active state at any given time, competing for CCS simply cannot explain how Leporipoxviral M/S131R could inhibit cellular SOD1 activity so soon after infection (Figure 2.7 and 2.8). Besides, if M/S131R can form complexes with CCS, it seems likely that they should also still be able to interact with cellular SOD1 using the conserved dimer interacting interfaces (Chapter 1.9 and 2.2). I have examined this issue and found some evidence that S131R can indeed interact with cellular SOD1, although the interaction is much weaker than that seen in M/S131R:CCS complexes (Appendix Figure A.3). Therefore, I would suggest that Leporipoxviral M/S131R cause a decline in cellular SOD1 activity by two routes. First, these viral proteins can form inactivating complexes with cellular SOD1. Second, they can also sequester CCS, preventing further activation of cellular SOD1. However, we have not proven that these complexes are necessarily enzymatically inactive and this is an area of investigation that requires further research.

By whatever means that it is accomplished, inhibiting cellular SOD1 activity caused the expected increase in intracellular superoxide level (Figure 4.3). This increase in the radical level will create an oxidative stress in infected cells. As reviewed in Chapter 1, ROS, particularly superoxide and hydrogen peroxide, are major regulators of the cell signalling pathways affecting cell proliferation, differentiation, and cell death by apoptosis or necrosis [12, 19, 37]. Our data suggests that these virus SOD1 homologs are designed to tip the oxidant/antioxidant balance towards the former state in infected cells

and this should induce cellular proliferation. As predicted, tumour cell proliferation was less pronounced in rabbits infected with SFV_S131RΔ virus (Figure 4.5 A and B). Deleting S131R gene did not completely abolish tumour formation, but of course these viruses also encode gene(s) that regulate proliferation by the epidermal growth factor pathway using SFGF in SFV and MGF in myxoma virus-infected cells. SFGF and MGF tap into cellular signalling pathways to induce proliferation by binding to the ErbB family of receptors [53], and while the deletion of MGF attenuates the disease symptoms, viruses lacking MGF can still induce tumour formation in European rabbits. Recently, Sabourdy *et al.* [40] has provided evidence showing that SFGF is critical for the proliferative phenotype associated with SFV infection in European rabbits. However, the viral growth factor cannot explain all the morphological aberrations in infected tissues since mutant SFV with SFGF gene deletion can still induce small tumour formation. This has led the authors to conclude that factors other than SFGF influence the SFV-induced tumourigenisis. We have shown through our studies that S131R is likely one of the factors that influence the proliferative property of SFV. It would be interesting to see whether a mutant virus with deletion of both the S131R and SFGF genes still show a proliferative phenotype.

Our studies also provide insights into the importance of choosing a disease model that reflects the natural biology of a viral disease. The original study showed that deleting M131R did not affect the overall course of myxomatosis, although we did notice a small delay in the appearance of the primary lesion and a more localized lesion in rabbits inoculated with the mutant virus [11] at least during the earlier stages of infection. We suspect that the effects of M131R on cellular proliferation may have been overlooked

using the virulent disease caused by myxoma virus in European rabbits (*Oryctolagus cuniculus*). The European rabbit is a well established model that has been used to study the functions of myxoma virus-encoded immunosuppresive genes [29] but it does not reflect the natural course of infection in its natural host (*Sylvilagus* hares). By using the same animal host, European rabbits, but infected with SFV, we were able to show the association of S131R with virus tumourigenesis.

This link between S131R and cellular proliferation provides a good *in vivo* support for the hypothesis that mild oxidative stress provides a driving force for cellular proliferation. In fact, a great deal of evidence has accumulated linking ROS and cancer over the last three decades. Most significantly, the observation that cancer cells are nearly always low in SOD2 (MnSOD) and usually low in SOD1 activity [32] has led Oberley and Buettner [31] to first suggest that the loss of SOD activity is important in tumour cell phenotype due to the subsequent increase in steady-state levels of superoxide. Their pioneering hypothesis that replacement of the lost SOD activity could result in reversal of malignant cancer phenotype has opened a promising door towards cancer treatment. Oberley's group has shown that overexpression of both SOD1 and SOD2 can inhibit the growth of many cancer cell types [30, 58] and the tumour suppressive effect of SOD is likely due to a decrease in superoxide and the subsequent increase of hydrogen peroxide from the dismutase reaction [39].

Although overproduction of superoxide beyond the detoxification capacities of endogenous cellular antioxidants will induce apoptosis [9], low levels of this radical will prevent apoptosis [15, 24, 34, 35]. Using a well-established apoptosis model consisting of myxoma virus-infected human T-lymphocyte Jurkat cells, myxoma virus M131R

clearly inhibited apoptosis in those cells (Figure 4.7 and 4.8). Moreover, M131R seems to provide more protection against Fas-mediated apoptosis than it did against apoptosis triggered by intrinsic mitochondrial-mediated pathway. This is consistent with the work of Clement *et al.*[15] who reported that superoxide is an effective inhibitor of Fas-mediated apoptosis. Although we have shown that the inhibitory effects of M131R function upstream of caspase 3 cleavage (Figure 4.7C), details of where this apoptosis pathway is blocked remain to be elucidated. However, M/S131R exhibited anti-apoptotic functions are unlikely to be exerted within the mitochondria. Only a small fraction of these proteins were detected in the mitochondria of infected cells (~ 2%) (Chapter 3), and there is no leader sequence encoded by M/S131R that would direct their localization to the organelle. The presence of these proteins in the mitochondria may be explained by the fact that approximately 2% of both cellular SOD1 and CCS reside in the mitochondrial intermembrane space [33] and an interaction between these viral and cellular proteins could simply recruit M/S131R to the same compartment.

However, it should be noted that the confocal images on Figure 3.9 showed that much more than 2% of M131R colocalize with mitochondria, which are different than those images obtained latter (Figure 4.9). This could be explained by the fact that different cell lines (BGMK versus Jurkat cells, respectively) were used for those experiments. As well, different techniques were used in which M131R was visualized by immunofluorescent staining in Figure 3.9 whereas latter images (Figure 4.9) were acquired using an EGFP tag. This can be done without fixing and staining the cells. Finally, those studies were performed at different institutes with different confocal microscopes which possess different sensitivities. Therefore, the distribution of

M/S131R should be further carefully investigated. For example, sequential serial sections of the confocal images could be obtained to confirm or refute the mitochondria localization.

This work serves to identify another in a continually growing list of poxviral anti-apoptotic strategies. Previously, at least five other myxoma-encoded genes have been shown to have anti-apoptotic properties. These anti-apoptotic genes all act on different pathways to prevent an abortive infection and they include M-T2 (M002L/R), M-T4 (M004L/R), M-T5 (M005L/R), M11L, and SERP-2 (M151R) [4]. M-T2 associates with TNF receptors to prevent the TNF-α-mediated apoptosis [42], M-T4 localizes to the ER and inhibits apoptosis by interfering with the assembly of pro-apoptotic complex [20], M11L interacts with pro-apoptotic protein Bak at the mitochondria to prevent activation of mitochondrial-mediated apoptotic signalling [55], SERP-2 functions as a weak inhibitor of caspase 1 and prevents apoptosis of lymphoid cells in rabbits [25], and M-T5 promotes cell survival [27] by interacting with cellular regulatory proteins (cullin-1 and Akt) that participate in cellular responses to stress stimuli [21]. The addition of M131R to this long list of proteins further illustrates the importance of subverting this innate host response against virus infection, as well as showing the remarkable manner in which myxoma virus has evolved systems capable of targeting numerous key regulatory routes in apoptotic pathway. One notable difference is that all these proteins are viral early gene products except for M/S131R. Although these are late gene products, they are still expected to be available soon after infection, since they are abundant structural components which would be released after viral uncoating. Besides M/S131R, another poxviral protein that has been shown to prevent cell death triggered by oxidative stress

signals is that encoded by the molluscum contagiosum virus MC066 gene. MC066 protein is a glutathione peroxidase that depletes infected cells of toxic hydrogen peroxide [47]. The SFV RING finger protein, N1R is also believed to provide protection against hydrogen peroxide mediated oxidative stress [7], but how it does this remains to be established.

What is perhaps surprising about these observations is that Leporipoxviruses can achieve a redox state ideally suited for promoting cellular proliferation and viral growth. The effects of the redox status on cellular homeostasis and proliferation are postulated to be bimodal [23] which is illustrated in Figure 5.1. Small changes in the redox environment, say towards a mild oxidative state, can stimulate a variety of factors that support greater cell proliferation. In contrast, when the oxidative stress is pushed beyond the cellular "threshold" level capable of detoxifying the damaging effects of ROS, cellular proliferation decreases followed by induction of cell death by apoptosis. Damage beyond that level leads to necrotic death. This concept of a progression of behaviour from "proliferation to apoptosis to necrosis", linked to an increased rate of oxidation has recently gained prominent recognition in the redox field, as it provides a good explanation for the seemingly contradictory literature on the effects of redox state on cellular biology (Chapter 1.12). Although different cell types may possess different "threshold" levels for different responses, each operates within quite a narrow range of redox states [8, 18, 22, 23, 44]. This has led us to wonder how Leporipoxviruses can identify the "window of opportunity" that promotes proliferation while suppressing apoptosis. Confocal microscopy revealed that M/S131R are distributed widely throughout infected cells in much the same manner as is the cellular SOD1 [14, 45].

Despite the abundance expression of M/S131R, cellular SOD1 activity is only partially inhibited by this protein (Figure 2.7 and 2.8). This is perhaps not unexpected because cellular SOD1 activity could not be completely inhibited as this would lead to severe oxidative damage and trigger cell death. We suspect that Leporipoxviruses are using M/S131R to create a level of superoxide anion that is often referred to as "mild oxidative stress", but which is never defined in the literature. This is because it is difficult to quantify the concentrations of transiently-existed superoxide radical and because the level of significance probably varies in different cell types. The best evidence showing that M/S131R produce only "mild oxidative stress" comes from the fact that cellular superoxide-sensitive aconitase activities in cells infected with wild type Leporipoxviruses are only decreased ~12-15% in comparison to cells infected with M/S131RΔ viruses (Figure 4.4). These levels of inactivated aconitase correspond to ~2-3 fold increase in intracellular superoxide level (Chapter 4). These conditions (chemically induce either exogeneously or endogeneously, or genetic manipulation of SOD levels) have been shown by others to be pro-proliferative [8, 22] and antiapoptotic [15].

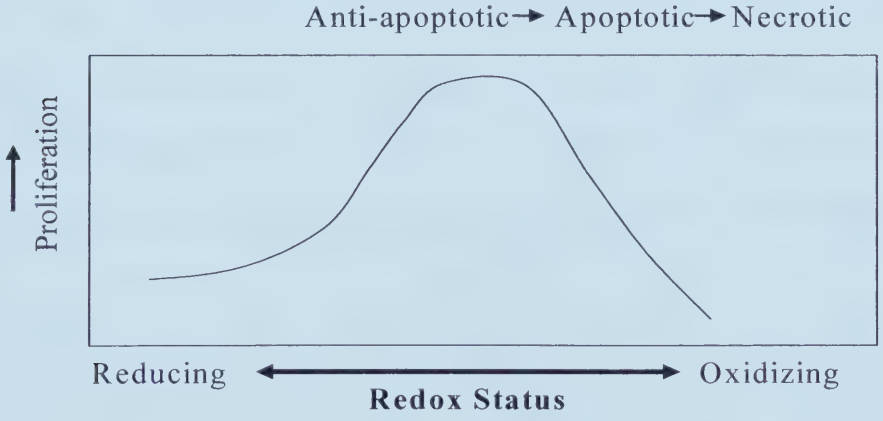

Figure 5.1. Postulated impact of redox status on cellular progression from proliferation to apoptosis to necrosis. Modified from Kinnula *et al.* [23].

What might be the molecular mechanism by which M/S131R affect the cellular signalling cascades that lead to the observed proliferative and anti-apoptotic behaviour? There are many possible mechanisms, considering the complex biological effects of superoxide [8, 17, 23] discussed in Chapter 1. The MAPK signalling pathway is likely important, since when cells are stimulated by ROS, signals are transduced through the same signalling pathways as those triggered by growth factors [19, 37]. The most probable mechanism may involve oxidation of cysteine residues in redox-sensitive regulatory molecules. The formation of intra- or inter-molecular disulfide bonds is sometimes associated with changes in enzymatic activities, or can potentially stabilize protein-protein interactions through disulfide linkages. Not much is known about how superoxide inhibits apoptosis except that some caspase activities are sensitive to oxidative modification [50] and transcription factors such as NF-κB, which transactivates apoptosis inhibitors such as Gadd45β and IAP, is itself activated by ROS [16]. A model summarizing mechanisms by which Leporipoxviral M/S131R could induce proliferative and anti-apoptotic functions is shown on Figure 5.2. I suggest that M/S131R manipulate the control of signalling events by oxidative modification of cell "sensory" receptor molecules, or signal transduction proteins, by causing an intracellular accumulation of superoxide radical as shown on Figure 5.2. The outcomes of these events are cell proliferation and survival and could aid Leporipoxvirus growth and replication.

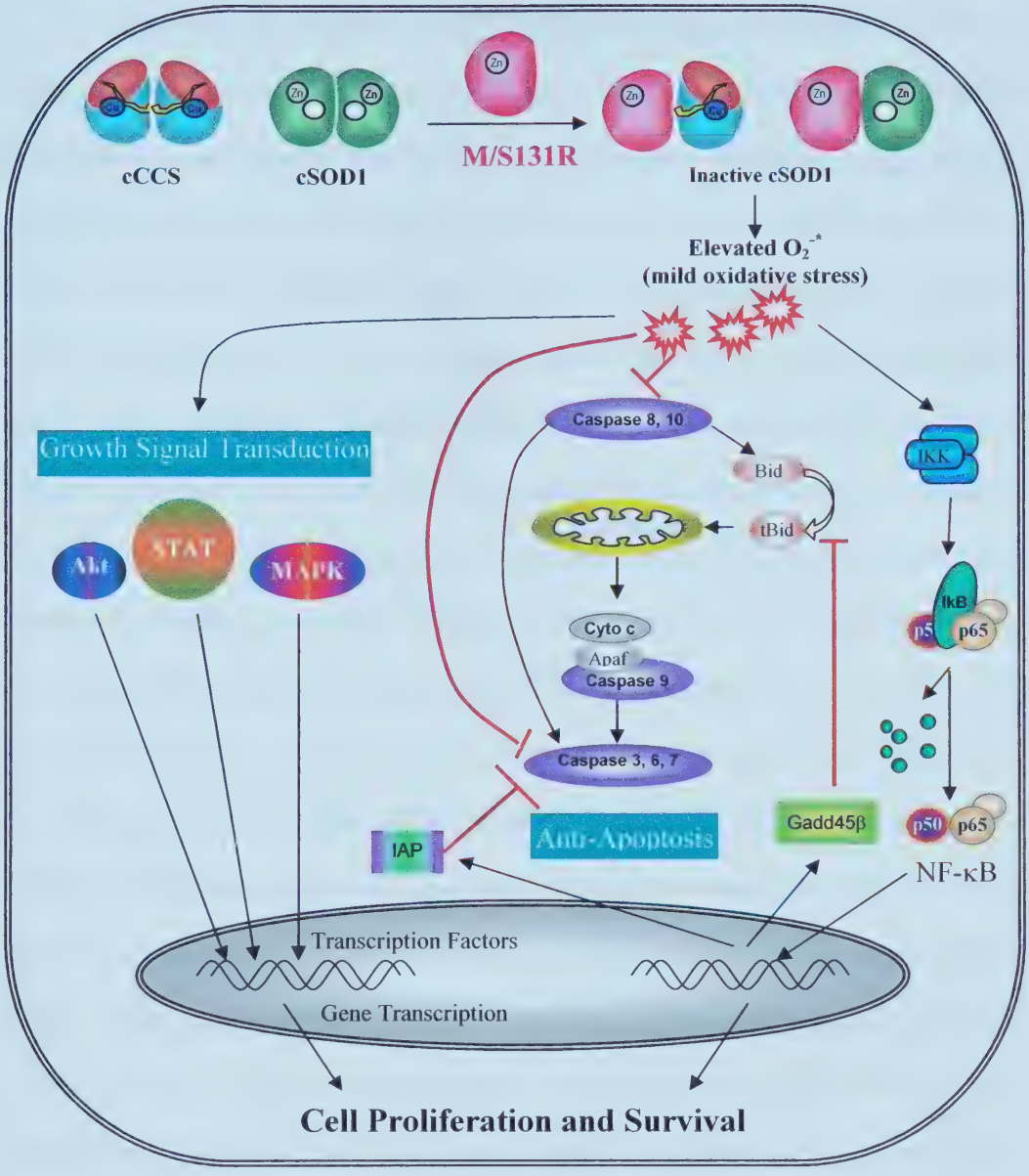

Figure 5.2. A model summarizing ways in which Leporipoxviral M/S131R could promote cell proliferation and survival. M/S131R interact with both cellular CCS and SOD1, resulting in inhibition of cSOD1 dismutation activity. Intracellular superoxide radicals accumulate as a consequence, leading to mild oxidative stress, which in turn, stimulates cell proliferation through growth signal transduction pathways. Superoxide could also prevent apoptosis by inhibiting caspase activity as well as by activating apoptosis inhibitors.

To date, there have been only a handful of other studies concerning virus-encoded SOD1 homologs. The *Autographa californica* nuclear polyhedrosis virus (ACMNPV) encoded SOD1 gene was the first one reported more than a decade ago [51]. Although this baculovirus homolog is predicted to be fully active, as it encodes conserved metal binding residues and the catalytic arginine residue, no dismutase activity was detected [51]. The importance of this "theoretically active" protein for baculovirus infection remains unclear to date. What other studies have been conducted on these proteins all focus on poxviruses. The reports concerning vaccinia virus A45R [2] and our studies on Leporipoxviral M/S131R [11, 49], have recently been extended by studies concerning an *Entomopoxvirus, Amsacta moorei* (AmEPV) SOD1 homolog [6]. This insect poxvirus encodes a SOD1 homolog designated AMV255 but the function of this catalytically active viral protein is unclear since it is not required for virus growth or virulence [6]. These findings reveal some interesting differences between the SOD1 homologs encoded by the vertebrate poxviruses, and those encoded by insect viruses. All SOD1 homologs encoded by *Chordopoxviruses* are abundantly expressed but inactive (from reported studies or from sequence prediction) while *Amsacta moorei* (and possibly baculovirus) encode seemingly active SOD1 homologs. This presence of active SOD1 in insect poxviruses may reflect a function required in insect hosts that might have been adapted for other purposes during the evolution of vertebrate poxviruses.

Whether Orthopoxvirus SOD1 homologs serve the same function as the Leporipoxvirus proteins is unclear. Almazan *et al.* [2] have shown that deleting vaccinia virus A45R had no effect on virus virulence in either a murine or a rabbit intradermal model. This led them to conclude that A45R is nonessential for virulence. However,

they did notice that deleting A45R caused a slight increase in virulence during an early stage of infection in a murine intranasal model. In view of the fact that vaccinia virus's natural host is unknown [26], it is possible that, like myxoma virus M131R, A45R could served a function in its natural host that is not detected using those murine and rabbit models. Certainly considering the abundance of its expression in infected cells, its incorporation into mature virion particles, as well as the high conservation of sequence between four strains of vaccinia virus and four strains of variola virus (96% amino acid identity), it is logical to speculate that these viral SOD1 homologs must provide some benefits. Perhaps, A45R can be compensated by other viral proteins [2], or it is only required during certain environmental stresses not seen in the laboratory conditions.

Although no other viruses encode SOD1 homologs, evidence is starting to accumulate suggesting a role for ROS in the pathogenesis of many other virus infections. In particular the increased generation of ROS seems to be a common theme in cells infected by Hepatitis C virus (HCV) [38], human immunodeficiency virus (HIV) [28, 44], influenza viruses and paramyxoviruses [36], and Hepatitis B virus [54, 3]. However, there are no direct links between any specific viral genes and these effects. Alterations in redox state characterize many virus infections, but it remains unclear whether the effects are a direct or indirect consequence of infection.

In conclusion, the information that we have gathered from studying Leporipoxvirus SOD1 homologs has led to the discovery of a novel poxvirus pathway for regulating tumourigenesis. We suggest that Leporipoxviral M/S131R promote an increase in intracellular superoxide levels, which stimulate cellular proliferation and inhibits apoptosis in virus-infected cells. However, a number of important details remain

to be investigated if we are to fully understand the intricate networks linking virus infection, host immune responses, and oxidative stress to viral pathogenesis. Such an understanding may help devise new therapies for treating viral diseases. These studies might also broaden our understanding of the links between oxidative stress, cellular proliferation, and apoptosis.

5.2 Future Directions

Although much progress has been made towards understanding the biochemical properties of Leporipoxviral M/S131R proteins and their biological functions *in vitro* and *in vivo*, more questions remained to be answered regarding their molecular mechanisms of action. Future experiments will need to more closely examine the activities of proteins involved in transducing growth and apoptosis signals. For instance, changes in the level of activated NF-κB of phosphorylated MAPK kinases in Leporipoxvirus-infected cells should be analyzed. We also need to know more about whether M/S131R can still function in promoting proliferation and inhibiting apoptosis outside the context of virus infection. This could be achieved by overexpressing these proteins in cells in culture, ideally under the conditional regulation of a tet (or other) regulated promoter.

It will also be important (and informative) to determine whether M/S131R inhibit primarily the Fas- or on mitochondria-mediated apoptotic pathway, or both. The Jurkat cells that we used in our apoptosis assays are classified as type II cells, in which Fas-mediated apoptosis event is mostly dependent on the activation of mitochondrial pathways. This is due to the limited cleavage of caspase 8 by death inducing signalling complex [41]. In view of this cross-talk between the two pathways, it is difficult to distinguish the route of inhibition in Jurkat cells, especially when the Fas-mediated pathway is involved. Therefore, we need to perform apoptosis assay in type I cells where both pathways operate independently of the other. Unfortunately myxoma virus and SFV have narrow host ranges, which create some experimental challenges in finding the right cell lines and reagents.

A high resolution structure for M/S131R would also greatly help us understand how these proteins interact with cellular SOD1 and/or CCS. Solving the crystal structure of M/S131R in complex with a eukaryotic CCS is of particular interest since several studies have described strong and stable interactions between Cu-deficient mutant SOD1 proteins and CCS [13, 52]. Indeed, the inability to transfer copper to the viral partner may be an important stabilizing factor that effectively traps the two proteins in an inactive state. If this is true of poxvirus SOD1 homologs, a high resolution structure would be of much interest to the larger research community studying ROS and SOD1 biology.

Finally, the effects of M/S131R on the intracellular ROS pool needs to be studied in great details. We have only focused on the selective effects of M/S131R on superoxide radicals, while ignoring the downstream effects on compounds such as hydrogen peroxide and peroxynitrite. Both of these compounds have also been shown to be important signal species. Since hydrogen peroxide is the product of superoxide dismutation reaction, the effects of M/S131R on viral pathogenesis might not have simply come from the accumulation of superoxide radical, but could also be due to a suppressive effect on hydrogen peroxide generation. Hydrogen peroxide, like superoxide, participates in cell proliferation, apoptosis, and necrosis signalling pathways in a dose-dependant manner, in which high levels are cytotoxic [8, 17]. Therefore, M/S131R-mediated inhibition of cellular SOD1 activity could aid in preventing hydrogen peroxide to reach cytotoxic levels, hence protecting cells from apoptosis. These studies could be performed using confocal microscopy and compounds that fluoresce upon reaction with hydrogen peroxide or peroxynitrite. The result would clarify whether it is

increase levels of superoxide, increased peroxynitrite, or decreased hydrogen peroxide concentrations that are mediating the activities of M/S131R.

5.3 References

1. Aguado B, Selmes IP, Smith GL (1992) Nucleotide sequence of 21.8 kbp of variola major virus strain Harvey and comparison with vaccinia virus. J Gen Virol 73 (Pt 11): 2887-902

2. Almazan F, Tscharke DC, Smith GL (2001) The vaccinia virus superoxide dismutase-like protein (A45R) is a virion component that is nonessential for virus replication. J Virol 75: 7018-29

3. Bannister WH, Federici G, Heath JK, and Bannister JV (1986) Antioxidant systems in tumor cells: The levels of antioxidant enzymes, ferritin, and total iron in a human hepatoma cell line. Free Radic Res Commun 1: 361-367

4. Barrett JW, Cao JJ, Hota-Mitchell S, and McFadden G (2001) Immunomodulatory proteins of poxviruses. Seminar in Immunol. 13: 73-84

5. Bawden AL, Glassberg KJ, Diggans J, Shaw R, Farmerie W, Moyer RW (2000) Complete genomic sequence of the Amsacta moorei entomopoxvirus: analysis and comparison with other poxviruses. Virology 274: 120-39

6. Becker MN, Greenleaf WB, Ostrov DA, Moyer RW (2004) Amsacta moorei Entomopoxvirus Expresses an Active Superoxide Dismutase. J Virol 78: 10265-75

7. Brick DJ, Burke RD, Schiff L, Upton C (1998) Shope fibroma virus RING finger protein N1R binds DNA and inhibits apoptosis. Virology 249: 42-51

8. Burdon RH (1995) Superoxide and hydrogen peroxide in relation to mammalian cell proliferation. Free Radic Biol Med 18: 775-794

9. Buttke TM, and Sandstorm PA (1994) Oxidative stress as a mediator of apoptosis. Immunol Today 15: 7-10

10. Cameron C, Hota-Mitchell S, Chen L, Barrett J, Cao JX, Macaulay C, Willer D, Evans D, McFadden G (1999) The complete DNA sequence of myxoma virus. Virology 264: 298-318

11. Cao JX, Teoh ML, Moon M, McFadden G, Evans DH (2002) Leporipoxvirus Cu-Zn superoxide dismutase homologs inhibit cellular superoxide dismutase, but are not essential for virus replication or virulence. Virology 296: 125-35

12. Carmody RJ, and Cotter TG (2001) Signalling apoptosis: a radical approach. Redox Rep 6: 77-90

13. Casareno RL, Waggoner D, and Gitlin JD (1998) The copper chaperone CCS directly interacts with copper/zinc superoxide dismutase. J Biol Chem 273: 23625-8

14. Casareno RLB, Waggoner D, and Gitlin JD (1998) The copper chaperone CCS directly interacts with copper/zinc superoxide dismutase. J. Biological chemistry 273: 23625-23628

15. Clement MV, and Stamenkovic I (1996) superoxide is a natural inhibitor of Fas mediated cell death. Embo J 15: 216-225

16. Franek WR, Horowitz S, Stansberry L, Kazzaz JA, Koo HC, and Li Y (2001) Hyperoxia inhibit oxidants-induced apoptosis in lung epithelial cells. J Biol Chem 276: 569-575

17. Haddad JJ (2004) Redox and oxidant-mediated regulation of apoptosis signaling pathways: immuno-pharmaco-redox conception of oxidative siege versus cell death commitment. Int Immunopharmacology 4: 475-493

18. Hernandez-Saavedra D, McCord JM (2003) Paradoxical effects of thiol reagents on Jurkat cells and a new thiol-sensitive mutant form of human mitochondrial superoxide dismutase. Cancer Res 63: 159-63

19. Herrlich P, and Bohmer FD (2000) Redox regulation of signal transduction n mammalian cells. Biochem Pharmacol 59: 35-41

20. Hnatiuk S, Barry M, Zeng W, Liu L, Lucas A, Percy D, McFadden G (1999) Role of the C-terminal RDEL motif of the myxoma virus M-T4 protein in terms of apoptosis regulation and viral pathogenesis. Virology 263: 290-306

21. Johnston JB WG, Nazarian SH, Barrett J, and McFadden G (2004) Myxoma virus M-T5 is a cell cycle regulator that protects poxvirus-infected cells from stress stimuli. In: XVth International Poxvirus and Iridovirus Conference, Oxford, England, pp 54

22. Kang J, Zheng R (2004) Dose-dependent regulation of superoxide anion on the proliferation, differentiation, apoptosis and necrosis of human hepatoma cells: the role of intracellular Ca 2+. Redox Rep 9: 37-48

23. Kinnula VL, and Crapo JD (2004) Superoxide Dismutases in malignant cells and human tumors. Free Radic Biol Med 36: 718-744

24. Lee YJ, and Shacter E (1999) Oxidative stress inhibits apoptosis in human lymphoma cells. J Biol Chem 274: 19792-19798

25. Messud-Petit F, Gelfi J, Delverdier M, Amardeilh MF, Py R, Sutter G, Bertagnoli S (1998) Serp2, an inhibitor of the interleukin-1beta-converting enzyme, is critical in the pathobiology of myxoma virus. J Virol 72: 7830-9

26. Moss B (1996) Poxviridae: the viruses and their replication. Lippincott-Raven Press, New York

27. Mossman K, Lee SF, Barry M, Boshkov L, McFadden G (1996) Disruption of M-T5, a novel myxoma virus gene member of poxvirus host range superfamily, results in dramatic attenuation of myxomatosis in infected European rabbits. J Virol 70: 4394-410

28. Muller F (1992) Reactive oxygen intermediates and human immunodeficiency virus (HIV) infection. Free Radic Biol Med 13: 651-657

29. Nash P, Barrett J, Cao JX, Hota-Mitchell S, Lalani AS, Everett H, Xu XM, Robichaud J, Hnatiuk S, Ainslie C, Seet BT, McFadden G (1999) Immunomodulation by viruses: the myxoma virus story. Immunol Rev 168: 103-20

30. Oberley L (2001) Anticancer therapy by overexpression of superoxide dismutase. antioxid redox signal 3: 461-472

31. Oberley L, and Buettner GR (1979) Role of superoxide dismutase in cancer: a review. Cancer Res 39: 1141-1149

32. Oberley TD, and Oberley LW (1997) Antioxidant enzyme levels in cancer. Histol Histopathol 12: 525-535

33. Okado-Matsumoto A, and Fridovich I (2001) Subcellular distribution of superoxide dismutases (SOD) in rat liver: Cu,Zn-SOD in mitochondria. J Biol Chem 276: 38388-93

34. Pervaiz S, and Clement MV (2004) Tumor intracellular redox status and drug resistance--serentipity or a causal relationship? Curr Pharm Des 10: 1969-1977

35. Pervaiz S, Ramalingam K, Hirpara JL, and Clement MV (1999) Superoxide anion inhibits drug-induced tumor cell death. FEBS Lett 459: 343-348

36. Peterhan E, Grob M, Burge T, and Zanoni R (1987) Virus-induced formation of reactive oxygen intermediates in phagocytic cells. Free Radic Res Commun 3: 39-46

37. Poli G, Leonarduzzi G, and Chiarpotto (2004) Oxidative stress and cell signalling. Curr medicinal chemistry 11: 1163-1182

38. Qadri I, Iwahashi M, Capasso JM, Hopkin MW, Flores S, Schaack J, and Simon FR (2004) Induced oxidative stress and activated expression of manganese superoxide dismutase during hepatitis C virus replication: role of JNK, p38 MAPK and Ap-1. Biochem J 378: 919-928

39. Ridnour L, Oberley TD, and Oberley LW (2004) Tumour suppressive effects of MnSOD overexpression may involve imbalance in peroxide generation versus peroxide removal. antioxid redox signal 6: 501-512

40. Sabourdy F, Casteignau A, Gelfi J, Deceroi S, Delverdier M, and Messud-petit F (2004) Tumorigenic poxviruses: growth factors in a viral context? J Gen Virol 85: 3597-3606

41. Scaffidi C, Fulda A, Srinivasan S, Friesen C, Li F, Tomaselli KJ, Debatin KM, Krammer PH, and Peter ME (1998) Two CD95 (APO-1/Fas) signaling pathways. Embo J 17: 1675-1687

42. Schreiber M, Sedger L, McFadden G (1997) Distinct domains of M-T2, the myxoma virus tumor necrosis factor (TNF) receptor homolog, mediate extracellular TNF binding and intracellular apoptosis inhibition. J Virol 71: 2171-81

43. Senkevich TG, Bugert JJ, Sisler JR, Koonin EV, Darai G, Moss B (1996) Genome sequence of a human tumorigenic poxvirus: prediction of specific host response-evasion genes. Science 273: 813-6

44. Seve M, Favier A, Osman M, Hernandez D, Vaitaitis G, Flores NC, McCord JM, Flores SC (1999) The human immunodeficiency virus-1 Tat protein increases cell proliferation, alters sensitivity to zinc chelator-induced apoptosis, and changes Sp1 DNA binding in HeLa cells. Arch Biochem Biophys 361: 165-72

45. Shaw PJ, Chinnery RM, Thagesen H, Borthwick GM, Ince PG (1997) Immunocytochemical study of the distribution of the free radical scavenging enzymes Cu/Zn superoxide dismutase (SOD1); MN superoxide dismutase (MN SOD) and catalase in the normal human spinal cord and in motor neuron disease. J Neurol Sci 147: 115-25

46. Shchelkunov SN, Totmenin AV, Loparev VN, Safronov PF, Gutorov VV, Chizhikov VE, Knight JC, Parsons JM, Massung RF, Esposito JJ (2000) Alastrim smallpox variola minor virus genome DNA sequences. Virology 266: 361-86

47. Shisler JL, Senkevich TG, Berry MJ, Moss B (1998) Ultraviolet-induced cell death blocked by a selenoprotein from a human dermatotropic poxvirus. Science 279: 102-5

48. Smith GL, Chan YS, Howard ST (1991) Nucleotide sequence of 42 kbp of vaccinia virus strain WR from near the right inverted terminal repeat. J Gen Virol 72 (Pt 6): 1349-76

49. Teoh ML, Walasek PJ, Evans DH (2003) Leporipoxvirus Cu,Zn-superoxide dismutase (SOD) homologs are catalytically inert decoy proteins that bind copper chaperone for SOD. J Biol Chem 278: 33175-84

50. Thornberry NA, and Lazebnik Y (1998) Caspases: enemies within. Science 281: 1312-1316

51. Tomalski MD, Eldridge R, Miller LK (1991) A baculovirus homolog of a Cu/Zn superoxide dismutase gene. Virology 184: 149-61

52. Torres AS, Petri V, Rae TD, O'Halloran TV (2001) Copper stabilizes a heterodimer of the yCCS metallochaperone and its target superoxide dismutase. J Biol Chem 276: 38410-6

53. Tzahar E, Moyer JD, Waterman H, Barbacci EG, Bao J, Levkowitz G, Shelly M, Strano S, Pinkas-Kramarski R, Pierce JH, Andrews GC, Yarden Y (1998) Pathogenic poxviruses reveal viral strategies to exploit the ErbB signaling network. Embo J 17: 5948-63

54. Vierucci A, DeMartino M, Graziani E, Rossi E, London WT, and Blumberg BS (1983) A mechanism for live cell injury in viral hepatitis: Effects of hepatitis B virus on neutrophil function in vitro and in children with chronic active hepatitis. Pediatr Res 10: 814-820

55. Wang G, Barrett JW, Nazarian SH, Everett H, Gao X, Bleackley C, Colwill K, Moran MF, McFadden G (2004) Myxoma virus M11L prevents apoptosis through constitutive interaction with Bak. J Virol 78: 7097-111

56. Willer DO, McFadden G, Evans DH (1999) The complete genome sequence of shope (rabbit) fibroma virus. Virology 264: 319-43

57. Zachertowska A, Brewer D, and Evans DH (2004) MALDI-TOF mass spectroscopy detects the capsid structural instabilities created by deleting the myxoma virus cupro-zinc SOD1 homolog M131R. J Virol Methods 122: 63-72

58. Zhang Y, Zhao W, Zhang HJ, Domann FE, and Oberley LW (2002) Overexpression of copper zinc superoxide dismutase suppresses human glioma cell growth. Cancer Res 62: 1205-1212

APPENDIX A – SUPPORTING METHODS AND DATA

A.1 SFV S131R is regulated as a late gene product

The kinetics of SFV S131R mRNA transcription was monitored by Northern blot analysis. Total RNA was isolated from SFV-infected SIRC cells (m.o.i= 10), at selected times post infection, by using Trizol reagent (GibcoBRL) as described by the manufacturer. Twenty microgram of total RNA from each sample were then denatured, fractionated through 1.5% formaldehyde agarose gels, and transferred to Zeta-probe membrane (Bio-Rad, CA). A hybridization probe was prepared by using Ready-To-Go DNA Labelling Beads from Amersham Pharmacia, in which S131R encoding DNA, excised from *Bam*HI and *Eco*RI digestion of pGEX-2T-S131R plasmid DNA, was labeled with [^{32}P]-dCTP. The S131R transcript was detected by hybridization at 43^{o}C overnight with radiolabelled probe followed by autoradiography on Kodak film.

The Northern blot revealed two viral-specific SOD1 transcripts (Figure A1). These RNAs were not found in mock-infected cells or early in infection (i.e., 6 h p.i.). Synthesis of the transcripts was first detected at 12 h p.i. and continued to 24 h p.i. in SFV-infected cells. This indicates that the viral S131R is regulated as a late gene.

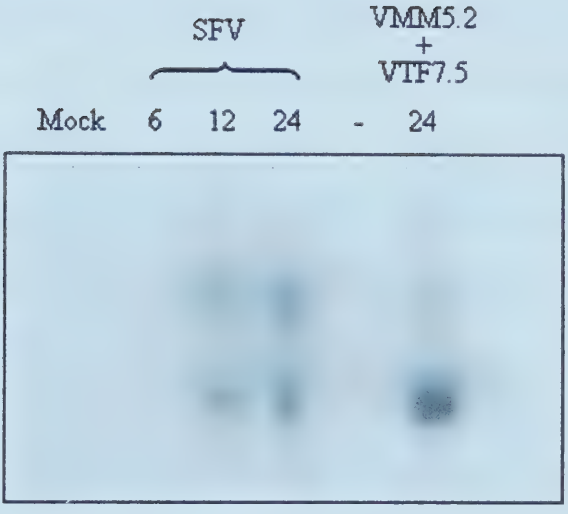

Figure A.1. Northern blot analysis of S131R transcription. Total RNA was isolated from mock-infected SIRC cells (Mock); SFV-infected cells at 0, 6, 12, and 24 hours post infection; or cells infected with recombinant vaccinia virus encoding S131R as positive control.

A.2 Leporipoxviral M/S131R are virion structural components

Poxvirus viral late gene products are often packaged into virions. These proteins are either virion structural components or proteins essential for successful subsequent infection [3]. To test whether M/S131R, like vaccinia A45R [1], are virion proteins, we used a Western blot analysis. A potassium tartrate gradient was used to purify the wild type myxoma virus, M131RΔ virus, wild type vaccinia virus, or a mixture of the recombinant vaccinia viruses (VMM5.2 and VTF7.5) as described in Chapter 2.3. Purified virus particles were then fractionated using SDS-PAGE in a reducing sample buffer. Proteins were transferred to a PVDF membrane and probed for the presence of M/S131R using a monoclonal antibodies directed against S131R as previously described (Chapter 2.3) [2].

As shown on Figure A.2, the 18 kDa M131R was detected in purified wild type myxoma virus, but absent from purified M131RΔ virus. Recombinant vaccinia viruses purified from cells co-infected with VMM5.2 and VTF7.5, also contain S131R. These results indicate that the Leporipoxviral M/S131R are virion structural components and they are cross-compatible with vaccinia packaging system.

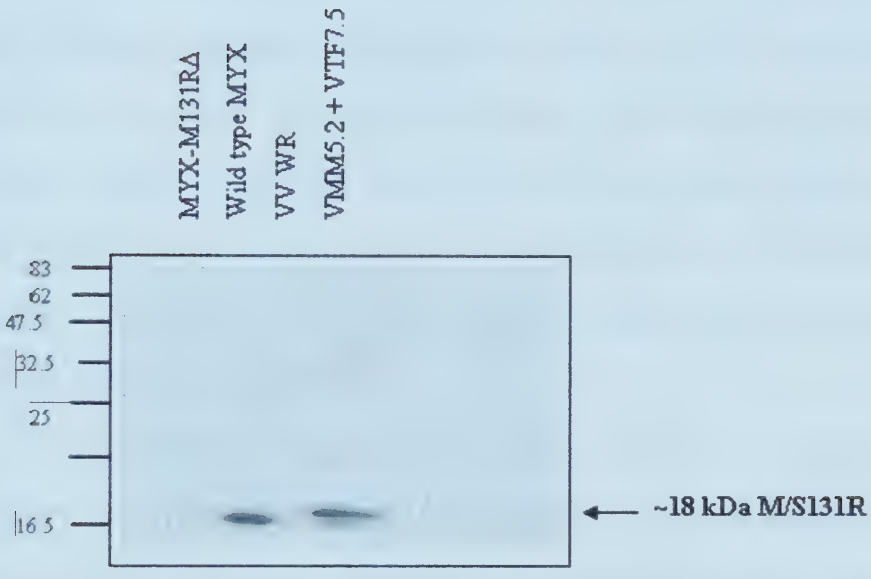

Figure A.2. M131R is packaged into myxoma virion particles. Western blot was used to detect the 18 kDa M131R protein in gradient purified myxoma viruses. The SFV protein was also produced and packaged by recombinant vaccinia viruses (VMM5.2 and VTF 7.5) designed to overexpress S131R.

A.3 S131R interacts with cellular SOD1

The M/S131R protein sequences predict that these viral proteins could form complexes with both cellular proteins (SOD1 and CCS). However, previous experiments only detected interactions between M/S131R and cellular CCS. No interactions between these viral proteins and cellular SOD1 were detected (Chapter 3) [4]. However, we also failed to detect an interaction between cellular SOD1 and CCS, suggesting that our original protocols might have been too stringent. That is only strong and stable interaction, like the S131R:CCS interaction, were detected while weaker complexes might have been washed off during the immunoprecipitation and GST pull down assays. Therefore, we reexamined these interaction issues by using purified GST-S131R as bait under less stringent wash conditions.

SIRC, and BGMK cell lysates were prepared as described in Chapter 3.4. About 50 μL of a solution containing 50% (v/v) glutathione-Sepharose beads (Sigma) was added to 1.0 mL of solution containing 80 μg of purified GST fusion protein, or just GST, and incubated at 4° C for one hour. The beads were recovered by centrifugation, washed three times with PBS, and then incubated with ~0.9 mg of the cell lysates in 0.2 mL of PBS (containing protease inhibitor) at 4° C for two hours. The beads were washed gently three times with PBS, and the protein complexes released by adding 0.1 mL of SDS-PAGE loading buffer containing 0.1 M DTT, plus 2% β-mercaptoethanol, and heating at 100° C for five minutes. Proteins were size fractionated using 12% SDS-PAGE [5] and transferred to a PVDF support as directed by the manufacturer of the membrane (Millipore). The membrane was treated with 1% blocking agent (Amersham) in PBST (PBS containing 0.1% Tween-20) and then incubated with either a monoclonal

αGST antibodies (1:1000) or a polyclonal αhSOD1 (1:1000) in PBST for one hour at room temperature. The blot was washed six times with PBST and incubated with 1:50,000 diluted secondary antibody conjugated to horseradish peroxidase in PBST for one hour at room temperature. The membranes were washed extensively and horseradish peroxidase detected using a chemiluminescent substrate (Pierce) and Kodak OMAT-AR film.

As shown on the Western blot (Figure A.3), the αhSOD1 antibody can detect both SIRC and BGMK SOD1s (lane 1 and 2, respectively). The GST-tagged hCCS also readily retrieved the cellular SOD1 from both cell lysates (lane 5 and 6). Most importantly, the cellular SOD1 was also detected in the samples retrieved using GST-S131R fusion protein (lane 7 and 8). GST alone did not bind the cellular SOD1 (lane 3 and 4), indicating that the interactions were specific to hCCS and S131R. This experiment shows that the SFV SOD1 homolog (S131R) can interact with both cellular CCS and SOD1.

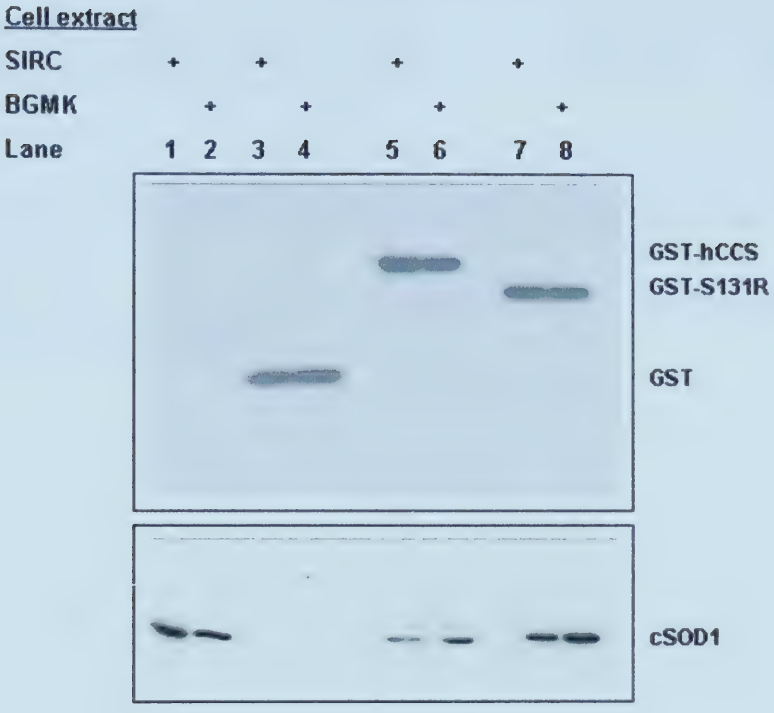

Figure A.3. GST-S131R protein forms complexes with cellular SOD1. Cell lysates were incubated with purified GST, GST-hCCS, or GST-S131R fusion proteins. Protein complexes were recovered using glutathione-Sepharose beads, eluted, and analyzed for the presence of cellular SOD1 by Western blotting with αhSOD1 (bottom). GST and GST fusion proteins were also detected by Western blotting with an αGST monoclonal antibody (top). Approximately $1/5^{th}$ of the cell extracts were loaded in lanes 1 and 2 to illustrate the amount of SOD1 present in these extracts.

A.4 References

1. Almazan F, Tscharke DC, Smith GL (2001) The vaccinia virus superoxide dismutase-like protein (A45R) is a virion component that is nonessential for virus replication. J Virol 75: 7018-29

2. Cao JX, Teoh ML, Moon M, McFadden G, Evans DH (2002) Leporipoxvirus Cu-Zn superoxide dismutase homologs inhibit cellular superoxide dismutase, but are not essential for virus replication or virulence. Virology 296: 125-35

3. Moss B (1996) Poxviridae: the viruses and their replication. Lippincott-Raven Press, New York

4. Teoh ML, Walasek PJ, Evans DH (2003) Leporipoxvirus Cu,Zn-superoxide dismutase (SOD) homologs are catalytically inert decoy proteins that bind copper chaperone for SOD. J Biol Chem 278: 33175-84

5. Zhang W, Evans DH (1993) DNA strand exchange catalyzed by proteins from vaccinia virus-infected cells. J Virol 67: 204-12

University of Alberta Library
0 1620 2041 8545
B45774